

# Production of Sleptons in $e^-e^-$ -Collisions

Dissertation zur Erlangung des  
naturwissenschaftlichen Doktorgrades  
der Julius-Maximilians-Universität  
Würzburg

vorgelegt von

Alexander Wagner

aus Würzburg

Würzburg 2008

Eingereicht am: 15.04.2008  
bei der Fakultät für Physik und Astronomie

1. Gutachter: Prof. Dr. H. Fraas  
2. Gutachter: Prof. Dr. A. Bartl  
der Dissertation

1. Prüfer: Prof. Dr. H. Fraas  
2. Prüfer: Prof. Dr. A. Bartl  
3. Prüfer: Prof. Dr. K. Brunner  
im Promotionskolloquium

Tag des Promotionskolloquiums: .....

Doktorurkunde ausgehändigt am: .....

**Production of  
Sleptons in  
 $e^-e^-$ -Collisions**

**Wagner, Alexander:**

Production of Sleptons in  $e^-e^-$ -Collisions/ vorgelegt von Alexander Wagner. -  
Würzburg, 2008. 182 S., graph. Darst., Literaturverz. S. 137-162  
Zugl.: Würzburg, Univ., Diss., 2008

*Schlagworte (SWD):* Supersymmetrie, Tesla <Teilchenbeschleuniger>, ILC,  
Teilchenspektrum, CP-Parität, Flavourmischung

*Schlagworte (frei):* Selektion, Slepton, Leptonflavourverletzung, CP-  
Verletzung, MSSM, Linearbeschleuniger, Elektron-  
Elektron-Streuung, Strahlpolarisation

*RVK:* UO 6490, UN 6130

*Für Hans*



# Contents

<b>1</b>	<b>Introduction</b>	<b>7</b>
<b>2</b>	<b>Supersymmetry</b>	<b>9</b>
2.1	Why Supersymmetry? . . . . .	9
2.1.1	Problems of the SM... . . . . .	9
2.1.2	...and Supersymmetric Solutions . . . . .	10
2.2	The MSSM . . . . .	11
2.2.1	SUSY Breaking . . . . .	12
2.2.2	Neutralinomixing . . . . .	14
2.3	Slepton Mixing . . . . .	16
2.3.1	Left-Right Mixing . . . . .	16
2.3.2	Lepton Flavour Violation . . . . .	17
2.3.3	Analytical Approximations . . . . .	20
2.4	Sources of $CP$ -Violation . . . . .	22
<b>3</b>	<b>Production Process</b>	<b>25</b>
3.1	Feynman Graphs and Amplitudes . . . . .	25
3.2	Squared Amplitude . . . . .	27
3.2.1	Exchange Terms . . . . .	29
■	Longitudinal $\otimes$ Longitudinal Polarisation . . . . .	29
■	Longitudinal $\otimes$ Transverse Polarisation . . . . .	29
■	Transverse $\otimes$ Transverse Polarisation . . . . .	31
3.2.2	Interference Terms . . . . .	32
■	Longitudinal $\otimes$ Longitudinal Polarisation . . . . .	32
■	Longitudinal $\otimes$ Transverse Polarisation . . . . .	33
■	Transverse $\otimes$ Transverse Polarisation . . . . .	34
<b>4</b>	<b>Scenarios</b>	<b>37</b>
4.1	Gaugino-like mSUGRA: SPS 1a' . . . . .	39

4.2	Small $ \mu $ : Mixed SPS . . . . .	43
4.3	Higgsino-like GUT: Scenario A . . . . .	46
4.4	Higgsino-like non-GUT: Scenario B . . . . .	49
4.5	Pure $\tilde{H}_a^0$ and $\tilde{H}_b^0$ : Scenario C . . . . .	52
4.6	Gaugino-like, $\tilde{G}$ LSP: Point $\varepsilon$ . . . . .	55
4.7	GMSB, $\tilde{G}$ -LSP: SPS 7 . . . . .	60
<b>5</b>	<b><i>CP</i> Violation</b> . . . . .	<b>63</b>
5.1	Squared Amplitude . . . . .	64
5.2	Definition of the Observables . . . . .	65
5.2.1	<i>CP</i> -Even Observables . . . . .	65
5.2.2	<i>CP</i> -Sensitive Observables . . . . .	66
5.3	Numerical Results for <i>CP</i> -Violation . . . . .	68
5.3.1	General Features . . . . .	68
	■ GUT-Scenarios . . . . .	68
	■ Non-GUT-Scenarios . . . . .	70
	■ Dependence on $\tan\beta$ and $\phi_\mu$ . . . . .	70
5.3.2	SPS 1a' . . . . .	72
5.3.3	Mixed SPS . . . . .	75
5.3.4	Scenario A . . . . .	78
5.3.5	Scenario B . . . . .	81
5.3.6	Scenario C . . . . .	84
<b>6</b>	<b>Lepton Flavour Violation</b> . . . . .	<b>87</b>
6.1	Parametrisation . . . . .	88
6.1.1	Experimental Signatures . . . . .	89
6.1.2	Bounds for LFV . . . . .	90
6.2	Observables . . . . .	91
6.3	Slepton Mixing . . . . .	92
6.4	Numerical Results for LFV . . . . .	95
6.4.1	SPS 1a' . . . . .	95
6.4.2	Point $\varepsilon$ . . . . .	100
6.4.3	SPS 7 . . . . .	105
<b>7</b>	<b>Muon Colliders: <math>\mu^-\mu^-</math></b> . . . . .	<b>109</b>
7.1	<i>CP</i> Violation . . . . .	110
7.2	LFV . . . . .	111
7.3	$\mu^-\mu^-$ versus $e^-e^-$ . . . . .	112
<b>8</b>	<b>Background</b> . . . . .	<b>115</b>
8.1	Standard Model Background . . . . .	116
8.1.1	Flavour Conserving Case . . . . .	116
8.1.2	Flavour Violating Case . . . . .	118
8.1.3	Numerical Results . . . . .	120



---

8.2 SUSY-Background . . . . .	122
<b>9 Summary</b>	<b>125</b>
<b>10 Zusammenfassung</b>	<b>127</b>
<b>A Conventions and Definitions</b>	<b>131</b>
<b>B Laboratory Sytem</b>	<b>133</b>
B.1 Exchange Terms . . . . .	133
B.1.1 Longitudinal $\otimes$ Longitudinal Polarisation . . . . .	133
B.1.2 Longitudinal $\otimes$ Transverse Polarisation . . . . .	134
B.1.3 Transverse $\otimes$ Transverse Polarisation . . . . .	134
B.2 Interference Terms . . . . .	135
B.2.1 Longitudinal $\otimes$ Longitudinal Polarisation . . . . .	135
B.2.2 Longitudinal $\otimes$ Transverse Polarisation . . . . .	135
B.2.3 Transverse $\otimes$ Transverse Polarisation . . . . .	136
<b>C Bibliography</b>	<b>137</b>
<b>D List of Tables</b>	<b>162</b>
<b>E List of Figures</b>	<b>165</b>
<b>F Index</b>	<b>167</b>
<b>G Publications</b>	<b>179</b>



---

# Chapter 1

## Introduction

The *Standard Model* (SM) of elementary particle physics [1–3] describes with great success the known elementary particles and their strong and electroweak interactions in the framework of quantum field theory. The discovery of *neutrino oscillations* is the first experimental signal that can not be described in the framework of the SM (for a review see e.g. [4]).

The SM is a gauge theory built on the gauge groups  $SU(3)_C \times SU(2)_L \times U(1)_Y$ , which, however, at low energies, is spontaneously broken to  $SU(3)_C \times U(1)_{EM}$ . A currently favoured mechanism for this spontaneous symmetry breaking is the Higgs mechanism [5–7]. It introduces a new fundamental scalar field with non-vanishing vacuum expectation value, the Higgs field, whose associated boson is expected to be established experimentally at the *Large Hadron Collider* (LHC).

However, even if the Higgs boson is discovered it seems clear that the SM is not the fundamental theory [8, 9]. *Supersymmetry* (SUSY) is one of the most promising concepts for new physics with the SM as the low energy limit. It introduces a whole set of new particles and interactions, which will be the subject of detailed studies at future colliders. In fact, the search for new physics, and especially supersymmetric particles, is an important topic at the LHC which is projected to start operation in 2008. SUSY is also an important topic in the planning process for the next  $e^+e^-$  collider, the *International Linear Collider*, ILC [10]. Here, beam polarisation is considered to be of significant value in the precise study of the properties of new particles [11].

Earlier works showed that the  $e^-e^-$  mode may offer some advantages compared to the  $e^+e^-$  mode, especially for the study of the selectron properties [12–21]. However, these works either did not consider all polarisation options, especially transverse polarisation, or lacked the effects from slepton mixing and Lepton Flavour Violation (LFV).

This work is based on the most general form of slepton production at the ILC including all possible polarisation modes,  $CP$  violation from both the slepton sector as well as the neutralino sector and the possible flavour violating effects in the slepton sector. It is organised as follows: First, a short introduction to SUSY

centred on the relevant features for this work is given in chapter 2. This includes the mixing in the neutralino and slepton sector for complex parameters as well as analytical approximations for a three generation mixing in the slepton sector.

The slepton pair production process  $e^-e^- \rightarrow \tilde{\ell}_a\tilde{\ell}_b$  is introduced in chapter 3 including all possible polarisation modes. There, already some interesting features of this process mediated by the exchange of heavy Majorana fermions, the neutralinos, are revealed. This also justifies the general approach to the, at first sight seemingly, simple process. In chapter 4 some scenarios are discussed. The selection of these points in the SUSY parameter space is based mainly on previous studies done for the evaluation of the potential of the ILC. Some of the scenarios are of special interest for the discussion of  $CP$  violation while at others the  $e^-e^-$  mode would offer good chances to establish LFV.

After this general part, numerical studies on the possibilities of measuring  $CP$ -sensitive observables are made in chapter 5. First, the production cross section is studied as a  $CP$ -even observable. Contrary to earlier works [22], the full neutralino mixing is taken into account. Then a  $CP$ -sensitive observable based on transverse polarisation is constructed and evaluated.

The effect of LFV is considered in chapter 6. In some scenarios a background free measurement is possible in the  $e^-e^-$  mode [23]. This is a clear advantage compared to the  $e^+e^-$  mode. In this context, a numerical study of the actual slepton composition in the case of full three generation mixing is presented. This extends earlier studies done via random parameter scans [24–28]. An important result is that obeying the stringent experimental bounds from the branching ratios of  $\ell_a \rightarrow \ell_b\nu\bar{\nu}$  as well as  $\ell_a \rightarrow \ell_b\gamma$  (table 6.1), large flavour violating cross sections are possible.

It is shown, that the analytical approximations derived for the three generation slepton mixing are in very good agreement to the numerical results within the current experimental bounds. Within these bounds, sleptons with nearly equal selectron and smuon components are possible.

Similar studies of  $CP$  violation and LFV as in  $e^-e^-$  are also possible at a muon collider in the  $\mu^-\mu^-$  mode. A short comparison of these two modes is given in chapter 7.

The SM and SUSY background is considered in chapter 8 and numerically estimated in the SPS 1a' scenario as an example.

A summary and conclusions are given in chapter 9.

# Supersymmetry

## 2.1 Why Supersymmetry?

*This section gives a brief overview for the motivation of Supersymmetry based on the problems of the SM.*

Although the SM offers a good description of nearly all known non gravitational phenomena, there are some theoretical and phenomenological problems partly associated with the Higgs boson [8,9]. For this reason, today it is believed, that the SM can not be the fundamental theory of the elementary particles and their interactions, but is the low energy limit of a more fundamental theory. Some problems and their possible solutions in a supersymmetric framework will be discussed in this section.

### 2.1.1 Problems of the SM...

Some of the most important problems of the SM are

- *Gauge coupling unification.* The appealing idea of a *Grand Unified Theory* (GUT) that unifies all forces at a certain high energy scale is not realised within the SM [29–31].
- *Hierarchy* problem [32, 33]. This problem is also related to *fine-tuning* and the Higgs mechanism. To describe the electroweak symmetry breaking correctly by this mechanism, the mass of the Higgs scalar has to be of  $\mathcal{O}(100)$  GeV. However, as there is no symmetry protecting scalars from higher order contributions to their mass, the “natural” mass of the Higgs boson would have to be  $\mathcal{O}(10^{16})$  GeV.
- *Family structure* and *fermion masses.* There is no explanation of the existence of exactly three generations.

- *Neutrino masses.* Within the SM, neutrinos are massless and strictly left-handed particles. For this reason the observed neutrino oscillations [34–36] already give a clue that new physics exist beyond the SM.
- *Cosmology.* The SM offers no explanation for the baryon asymmetry of the universe, nor a good candidate for the cold dark matter (CDM). Additionally, embedding gravity within the standard model does not seem possible.

## 2.1.2 ...and Supersymmetric Solutions

Many of the problems mentioned in the previous subsection can be solved by SUSY:

- *Gauge coupling unification.* It was shown [37, 38] that the *Minimal Supersymmetric Standard Model* (MSSM) allows gauge coupling unification, if the supersymmetric particles have masses of  $\mathcal{O}(1)$  TeV. As can be seen in figure 2.1 this leads to a unification scale of  $\Lambda \approx 10^{16}$  GeV [29–31, 39].
- *Fine-tuning* problem [32, 33]. As bosonic and fermionic loop contributions to the Higgs mass enter with a different sign, this would result in exact cancellation of all loop contributions to the Higgs masses in case of exact SUSY.

For broken SUSY though, this cancellation is not exact; the loop corrections are much smaller than in the SM, actually of the order of the mass splitting between the SM particles and their supersymmetric partners.

- *Cosmology.* If R-Parity is conserved, the lightest supersymmetric particle (*LSP*) is stable and provides a good candidate for cold dark matter (CDM). Typical candidates are the lightest neutralino or the gravitino [32, 40, 41].
- Local SUSY offers a way to integrate gravity into the theory. This results in the so called SUGRA models.

Additionally, there are also some indirect hints that nature might be supersymmetric:

- SUSY predicted in the early 1980s a heavy top quark as necessary ingredient for the electroweak symmetry breaking. [42, 43].
- SUSY-GUTs predicted the presently measured value of  $\sin^2 \theta_w$ , e. g. [37, 38, 43].
- SUSY prefers a light Higgs boson [44, 45] as it is also preferred by electroweak precision data and the latest results from *LEP* [46–50].
- Most string theories, which are believed to describe physics at the high scale, require supersymmetry.

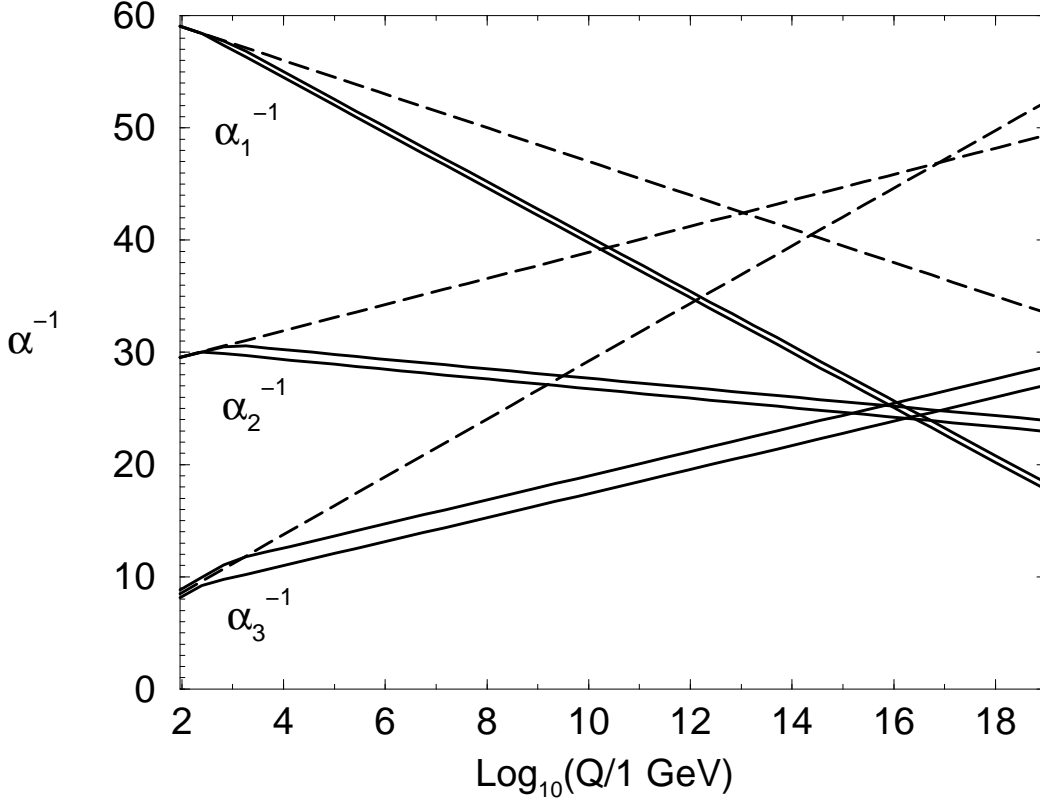


**Figure 2.1:** RG evolution of the inverse gauge couplings  $\alpha_a^{-1}(Q)$  in the SM (dashed) and the MSSM (solid). In the MSSM case the sparticle mass thresholds are varied between 250 GeV and 1 TeV, and  $\alpha_3(m_Z)$  between 0.113 and 0.123. Two-loop effects are included. [32]

## 2.2 The MSSM

*This section gives a short introduction to the MSSM. Without going into details, some common schemes for SUSY breaking are shortly introduced. The relevant parts of the SUSY breaking Lagrangian as well as the particle spectrum of the MSSM are given and the neutralino mixing is discussed.*

The MSSM [32, 51–53] has the same gauge structure  $SU(3)_C \times SU(2)_L \times U(1)_Y$  as the SM and introduces a minimal set of superfields and interactions. That is, each chiral fermion field is replaced by a chiral superfield and each gauge field is replaced by a vector superfield. Each of these superfields now contains the SM particles as well as their proper superpartners. From this procedure follows that each fermion in the SM has its spin zero superpartner, the *sfermion* ( $\tilde{f}$ ), and each

gauge boson has its spin- $\frac{1}{2}$  superpartner, the *gaugino*.

Additionally, one has to extend the Higgs sector of the SM. Besides the presence of the Higgs superpartners, the spin- $\frac{1}{2}$  higgsinos, a second Higgs doublet is required to give masses to up- and down-type chiral fermions [51, 52]. This results in the particle spectrum shown in table 2.1. The mass eigenstates shown will be discussed in greater detail in section 2.2.2 and section 2.3. This procedure and the resulting supersymmetric lagrangian can be found in the literature e. g. [32, 51–55].

SM particle	SUSY-Partner	
	interaction eigenstate	mass eigenstate
Leptons: $\ell = e, \mu, \tau$	Sleptons: $\tilde{\ell}_R, \tilde{\ell}_L$	Sleptons: $\tilde{\ell}_1, \tilde{\ell}_2$
Neutrinos: $\nu = \nu_e, \nu_\mu, \nu_\tau$	Sneutrinos: $\tilde{\nu}$	Sneutrinos: $\tilde{\nu}$
Quarks: $q = u, d, s, c, b, t$	Squarks: $\tilde{q}_L, \tilde{q}_R$	Squarks: $\tilde{q}_1, \tilde{q}_2$
W-boson: $W^\pm$	Wino: $\tilde{W}^\pm$	Chargino: $\tilde{\chi}_j^\pm$ ( $j = 1, 2$ )
Higgs boson: $H_1^-$	Higgsino: $\tilde{H}_1^-$	
Higgs boson: $H_2^+$	Higgsino: $\tilde{H}_2^+$	
Photon: $\gamma$	Photino: $\tilde{\gamma}$	Neutralino: $\tilde{\chi}_j^0$ ( $j = 1, \dots, 4$ )
Z-boson: $Z$	Zino: $\tilde{Z}$	
Higgs boson: $H_1^0$	Higgsino: $\tilde{H}_1^0$	
Higgs boson: $H_2^0$	Higgsino: $\tilde{H}_2^0$	
Gluon: $g$	Gluino: $\tilde{g}$	Gluino: $\tilde{g}$

**Table 2.1:** Particle spectrum of the MSSM

## 2.2.1 SUSY Breaking

In a supersymmetric world one would observe an exact mass degeneracy between supersymmetric particles and their SM counterparts. As no supersymmetric particles have yet been observed [56], supersymmetry has to be broken at some higher energy scale. This breaking can be mediated by several mechanisms, the most popular being gravity, which leads to the so-called *minimal supergravity models* (mSUGRA). The inclusion of gravity establishes a connection between local and global supersymmetry.

However, the ordinary gauge interactions can also be responsible for supersymmetry breaking. In this so-called *gauge mediated supersymmetry breaking* (GMSB) some new chiral supermultiplets called messengers are introduced, which couple to the source of SUSY breaking in a hidden sector as well as the (s)particles and higgsinos through ordinary  $SU(3)_C \times SU(2)_L \times U(1)_Y$  gauge boson and gaugino interactions. The still existing gravitational couplings between the MSSM and the



hidden sector are negligible compared to the gauge interaction effects, and the models can be understood mainly in terms of loop effects.

The last large class commonly considered is the so-called anomaly mediated supersymmetry breaking (AMSB). This mechanism often involves extra dimensions that are suggested by string theory.

As the actual breaking mechanisms at the high scale are not relevant for this study, they will not be further discussed. A description of these various SUSY breaking mechanisms can be found in the literature, e. g. [8, 32, 57]. Those parts of the soft SUSY breaking Lagrangian (i. e. that keep the theory renormalisable) relevant here are found to be [32]:

$$\begin{aligned}
\mathcal{L}_{\text{SSB}} = & -\frac{1}{2}(M_1\tilde{B}\tilde{B} + M_2\tilde{W}\tilde{W} + h.c.) \\
& -\tilde{\ell}_L^\dagger m_L^2 \tilde{\ell}_L - \tilde{\ell}_R m_R^2 \tilde{\ell}_R^\dagger + h.c. \\
& -\tilde{\ell}_R A \tilde{\ell}_L H_1 + h.c. \\
& -m_{H_1}^2 H_1^\dagger H_1 - m_{H_2}^2 H_2^\dagger H_2 - (B\mu H_1 H_2 + h.c.)
\end{aligned} \tag{2.1}$$

The  $\tilde{B}$  is the supersymmetric partner of the  $B$ -boson of the SM, which, together with the  $W^0$ , forms the photon and  $Z$ -boson.  $M_1$  is the  $U(1)_Y$ - and  $M_2$  the  $SU(2)_L$ - gaugino mass parameter. By redefinition of the fields, one of these (conventionally  $M_2$ ) can be made real, whereas the other ( $M_1$ ) can have a  $CP$  violating phase. This will be subject of the studies concerning  $CP$  violation (see section 2.4 and chapter 5). The complex  $3 \times 3$  matrix  $A$  describes the trilinear couplings of the scalar fields. The parameters  $m_{H_1}$  and  $m_{H_2}$  are the soft SUSY breaking contributions to the Higgs masses and  $B\mu H_1 H_2$  is a mass term, parametrising the mixing of the Higgs bosons.

$\mathcal{L}_{\text{SSB}}$  contains contributions to the slepton masses given by hermitian  $3 \times 3$  matrices:  $m_L$  for the left sleptons and  $m_R$  for the right ones. The sleptons are then given by two triples:  $(\tilde{e}, \tilde{\mu}, \tilde{\tau})_L$  for the left sector and  $(\tilde{e}, \tilde{\mu}, \tilde{\tau})_R$  for the right one. The matrices  $A$  are again the matrices of the trilinear couplings. These couplings contain a source for  $CP$  violation in the slepton sector and are also relevant for the mixing of left and right sleptons (see also section 2.3). The latter is only of some importance in the  $\tilde{\tau}$ -sector as it is proportional to the corresponding lepton mass.

The final important parameter is the higgsino mass parameter  $\mu$ . This parameter is found in the following part of the MSSM Lagrangian  $\mathcal{L}_{\text{MSSM}}$

$$\begin{aligned}
\mathcal{L}_{\text{MSSM}} \supset & -\mu(\tilde{H}_2^+ \tilde{H}_1^- + \tilde{H}_2^0 \tilde{H}_1^0) + h.c. \\
& -|\mu|^2 \left( |\tilde{H}_1^0|^2 + |\tilde{H}_1^-|^2 + |\tilde{H}_2^0|^2 + |\tilde{H}_2^-|^2 \right) + h.c. \\
& +\mu^* \left( \tilde{\ell}_R^\dagger y \tilde{\ell}_L H_2^0 + \tilde{\ell}_L^\dagger y \tilde{\nu} H_2^{+*} \right) + h.c.
\end{aligned} \tag{2.2}$$

This part contains the higgsino mass terms, again contributions to the Higgs masses and the Yukawa couplings of the sleptons by means of the  $y$ -matrix.

## 2.2.2 Neutralinomixing

If SUSY was exact, the mass and interaction eigenstates of the new particles would coincide. As a result of supersymmetry breaking, however, the interaction eigenstates mix to mass eigenstates. The partners of the W-boson (the winos) together with the charged higgsinos form the charginos, whereas the partners of the neutral gauge bosons (the Bino  $\tilde{B}$  and Zino  $\tilde{Z}$ ) together with the neutral higgsinos form the *neutralinos* (see table 2.1).

The mixing matrix of the partners of the gauge bosons to the neutralinos as mass eigenstates can be parametrised [53, 58, 59] by the

- $U(1)_Y$ -Gaugino mass parameter:  $M_1$
- $SU(2)_L$ -gaugino mass parameter:  $M_2$
- higgsino mass parameter:  $\mu$
- Ratio of the Higgs vacuum expectation values

$$\tan \beta = \frac{\langle H_2^0 \rangle}{\langle H_1^0 \rangle} = \frac{v_2}{v_1}. \quad (2.3)$$

In case of  $CP$  conservation the parameters  $M_1, M_2$  and  $\mu$  are real and  $M_{1,2} > 0$  is conventionally chosen. If GUT relations are assumed,  $M_1$  and  $M_2$  are found to be related due to gaugino mass unification by

$$\frac{M_1}{M_2} = \frac{5}{3} \tan^2 \theta_w. \quad (2.4)$$

However, there is no strict requirement that gauge coupling unification can be achieved only together with mass unification. Mass unification merely avoids problems that might arise with flavour changing and  $CP$  violating effects [32]. When dropping the restriction of mass unification other relations between  $M_1$  and  $M_2$  are possible. It may even happen that both of them are free parameters of the theory. In most scenarios it is assumed  $M_1 < M_2$  giving the lightest neutralino a larger bino contribution. Nevertheless, the lightest neutralino can also have a more wino-like character if  $M_1 > M_2$ .

The character of the neutralinos is also influenced by the relation of  $\mu$  to  $M_2$ . The relations of table 2.2 can be found as a rule of thumb for this interplay. Additionally, increasing values of  $\tan \beta$  lead to a stronger mixing, e. g. for  $M_2 > \mu$  the lighter two neutralinos get a stronger gaugino component with increasing  $\tan \beta$ .

One refers to a gaugino-(higgsino-)like scenario in case the lighter two neutralinos are mainly gauginos (higgsinos) and the heavier two are then higgsino-(gaugino)-like.

	Character of $\tilde{\chi}_1^0, \tilde{\chi}_2^0$
$M_2 > \mu$	higgsino-like
$M_2 \approx \mu$	mixed, i. e. no dominating character
$M_2 < \mu$	gaugino-like

**Table 2.2:** Effect of the relation between the higgsino mass parameter  $\mu$  and the gaugino mass parameter  $M_2$  on the mixing of the neutralinos.

From the SUSY Lagrangian the mass term of the neutralinos are thus obtained [59, 60]:

$$\mathcal{L}_{\text{mass}}^0 = -\frac{1}{2}\psi_i^0 Y'_{ij} \psi_j^0 + h.c., \quad j = 1..4 \quad (2.5)$$

with the Weyl spinors

$$\psi_j^0 = (-i\lambda_\gamma, -i\lambda_Z, \psi_H^a, \psi_H^b), \quad j = 1..4 \quad (2.6)$$

in the photino-zino  $(\lambda_\gamma, \lambda_Z, \psi_H^a, \psi_H^b)$  basis.

The neutralino mass matrix is found in this basis [59]

$$Y = \begin{pmatrix} M_2 s_w^2 + M_1 c_w^2 & (M_2 - M_1) s_w c_w & 0 & 0 \\ (M_2 - M_1) s_w c_w & M_2 c_w^2 s_w^2 & m_Z & 0 \\ 0 & m_Z & \mu s_{2\beta} & -\mu c_{2\beta} \\ 0 & 0 & -\mu c_{2\beta} & -\mu s_{2\beta} \end{pmatrix}, \quad (2.7)$$

where  $s_w = \sin \theta_w$ ,  $c_w = \cos \theta_w$ ,  $s_{2\beta} = \sin 2\beta$  and  $c_{2\beta} = \cos 2\beta$ .

$Y$  can be diagonalised by a unitary matrix  $N$ :

$$N^* Y N^{-1} = M_D^0. \quad (2.8)$$

It was shown, even in the presence of  $CP$  violating phases, that this diagonalisation can be done analytically [61], but for practical purposes numerical methods are more feasible. The mass eigenstates can be written as

$$\chi_i^0 = N_{ij} \psi_j^0, \quad (2.9)$$

where  $i, j = 1..4$ . If the Majorana spinors are introduced

$$\tilde{\chi}_i^0 = \begin{pmatrix} \chi_i^0 \\ \chi_i^0 \end{pmatrix} \quad (2.10)$$

one finds for the *lepton-slepton-neutralino interaction* [51–53]

$$\mathcal{L}_{\ell\tilde{\ell}_i\tilde{\chi}_k^0} = g f_{lk}^L \bar{\ell} P_R \tilde{\chi}_k^0 \tilde{\ell}_L + g f_{lk}^R \bar{\ell} P_L \tilde{\chi}_k^0 \tilde{\ell}_R + h.c., \quad (2.11)$$

where the relevant couplings are given by

$$f_{lk}^L = \sqrt{2} \left[ \left( \frac{1}{\sin 2\theta_w} - \tan \theta_w \right) N_{i2} + N_{i1} \right] \quad (2.12)$$

and

$$f_{lk}^R = \sqrt{2} [\tan \theta_w N_{i2} - N_{i1}]. \quad (2.13)$$

These forms of the couplings remain as the building blocks even in the presence of left-right or flavour mixing in the slepton sector.

## 2.3 Slepton Mixing

*In this section the mixing of the slepton interaction eigenstates to the mass eigenstates is discussed in the framework of pure LR mixing and the more general LFV. Finally, analytical formulae are derived that allow to estimate the composition of the slepton mass eigenstates in the limit of small LR mixing.*

Apart from the mixing of the partners of the gauge and Higgs bosons to neutralinos and charginos there is in general also a mixing of the other sfermions. In most models though, the mixing of left and right sleptons is proportional to the associated lepton mass and thus is ignored for the lighter two generations. It can, however, be important for the  $\tilde{\tau}$  sector. Slepton mixing within the left or right sector plays in any case a crucial role in the presence of LFV.

In supersymmetric extensions of the SM there is no symmetry enforcing that the mass matrices for the superpartners are diagonal in the same basis as those for the SM particles [62]. For this reason, there is generally a mixing between the sleptons. The most general form of the slepton mass matrix squared can be written as

$$M_{\tilde{\ell}}^2 = \begin{pmatrix} M_{LL}^2 & M_{RL}^{2\dagger} \\ M_{RL}^2 & M_{RR}^2 \end{pmatrix}, \quad (2.14)$$

where the  $M_{ij}$  ( $i, j = R, L$ ) are  $3 \times 3$  submatrices that are diagonal in the absence of flavour violation. The  $M_{RL}^2$  entries account for LR mixing, which will be discussed in section 2.3.1. However, one has to keep in mind that off-diagonal entries in  $M_{RL}^2$  would also induce flavour violation as off diagonal entries in  $M_{RR}^2$  or  $M_{LL}^2$  do.

### 2.3.1 Left-Right Mixing

In the case of flavour and LR mixing the matrices  $M_{RL}^2$  are in general complex  $3 \times 3$  matrices connecting the left and right sleptons of various generations. In

mSUGRA scenarios however, the entries  $M_{RL}^2$  of the general slepton mass matrix conserve flavour and  $M_{RL}^2$  (2.14) can be written as

$$M_{RL}^2 = \begin{pmatrix} m_e(A_e - \mu \tan \beta) & 0 & 0 \\ 0 & m_\mu(A_\mu - \mu \tan \beta) & 0 \\ 0 & 0 & m_\tau(A_\tau - \mu \tan \beta) \end{pmatrix}, \quad (2.15)$$

where  $m_l$  is the lepton mass and  $A_l$  the trilinear coupling ( $l = e, \mu, \tau$ ). Due to the smallness of the electron and muon mass,  $m_e$  and  $m_\mu$ , respectively, sizeable LR mixing is only to be expected in the stau sector.

On the other hand this also means that any signature of LR mixing in the production of selectrons is a clear hint for physics beyond mSUGRA. Therefore in general, it should not be ruled out entirely, but regarded as a test for the model. In the absence of flavour violation in  $M_{RL}^2$  (i. e. if this matrix is diagonal as well as the  $M_{LL}^2$  and  $M_{RR}^2$  being diagonal) the slepton LR mixing can be parametrised by a mixing angle  $\theta_{\tilde{\ell}}$  for each generation of sleptons [20, 63, 64]:

$$\begin{pmatrix} \tilde{\ell}_1 \\ \tilde{\ell}_2 \end{pmatrix} = \begin{pmatrix} \cos \theta_{\tilde{\ell}} & \sin \theta_{\tilde{\ell}} \\ -\sin \theta_{\tilde{\ell}} & \cos \theta_{\tilde{\ell}} \end{pmatrix} \begin{pmatrix} \tilde{\ell}_L \\ \tilde{\ell}_R \end{pmatrix}, \quad (2.16)$$

which is a simple rotation.

Then the general lepton-slepton-neutralino interaction Lagrangian (2.11) in the presence of LR mixing becomes

$$\mathcal{L}_{\ell\tilde{\ell}\tilde{\chi}_i^0} = g\bar{\ell}(a_{ik}P_R + b_{ik}P_L)\tilde{\chi}_i^0\tilde{\ell}_k + \text{h.c.} \quad (2.17)$$

with the new couplings

$$a_{i1} = f_i^L \cos \theta_{\tilde{\ell}}, \quad a_{i2} = -f_i^L \sin \theta_{\tilde{\ell}}, \quad (2.18)$$

$$b_{i1} = f_i^R \sin \theta_{\tilde{\ell}}, \quad \text{and} \quad b_{i2} = f_i^R \cos \theta_{\tilde{\ell}}. \quad (2.19)$$

The introduction of these rotations is a convenient way to parametrise LR mixing if it only concerns one generation. In a more general framework including flavour mixing (that is off-diagonal entries in  $M_{RL}^2$  and especially in  $M_{LL}^2$  and  $M_{RR}^2$ ) as well as LR mixing, however, the introduction of several subsequent rotations is necessary to parametrise the full mixing of the sleptons. Here, it turns out to be better to stick to the form of (2.15) for phenomenological analysis and to parametrise LR mixing by the insertion of suitable off-diagonal elements in  $M_{RL}$ . This parametrisation of the slepton mass matrix is also used for the study of LFV.

## 2.3.2 Lepton Flavour Violation

The recent discovery of neutrino oscillations [34–36] gives evidence for finite neutrino masses and is the first clear hint for physics beyond the SM. One approach

to explain the smallness of the neutrino masses is provided by the seesaw mechanism [65–67] which leads to lepton flavour violating entries in the slepton mass matrix. Signals of this mechanism have been extensively studied, e. g. [68–76]. A bottom-up approach to reconstruct the seesaw scenario and the SUSY parameters involved is given in [77].

All these studies, however, start out with a specific scenario to create LFV and relate this to a single source, namely the neutrino sector. Having the advantage of being quite predictive, this approach has the drawback of assuming a somewhat specialised scenario, whereas lepton flavour is typically violated in any supersymmetric extension to the SM, because the slepton mass matrices do not have to be diagonal in the same basis as those of the leptons [62]. Thus SUSY generally predicts quite large flavour violating effects which can be circumvented by mass unification at the GUT-scale. This is, however, an ad hoc assumption [32].

Not knowing what is actually realised in nature, it might be instructive not to rely on such a detailed model, but to use just the restrictions on the size of flavour violating effects determined by other processes like rare decays and electric and magnetic dipole moments. Following this approach, even by implementing all current experimental constraints [78–82], there are allowed areas in the parameter space with rather large flavour violation in the slepton sector [24–28]. These scenarios all feature full three generation mixing, thus allowing for cancellations among the flavour changing contributions.

Although first results may already be obtained at LHC [27] and be improved in the cleaner environment of the ILC, in certain cases it might be worthwhile to check if the  $e^-e^-$  option of this collider does offers advantages. As the background plays an important role in these processes, one might expect to gain from the  $e^-e^-$  mode, because there, the total background is generally reduced compared to  $e^+e^-$ . In certain scenarios, namely when  $\tilde{\tau}_1$  is the NLSP, even a background free measurement may be possible at an  $e^-e^-$ -collider [23].

LFV can be observed in  $e^-e^-$  collisions by means of the following processes:

- Selectron production with flavour violating decay: this corresponds to a flavour conserving production process with rather high cross sections. The selectrons then decay leptonically: one flavour conserving to an electron and a neutralino, the other to a  $\mu^-$  or  $\tau^-$  and a neutralino. This process thus contains one flavour violating vertex. The decay to the lighter chargino  $\tilde{\chi}_1^+\nu_e$  is suppressed in the scenarios considered here.
- Flavour violating slepton production with flavour conserving decay: this implies flavour violation already in the production process. Both sleptons then decay leptonically and flavour conserving, thus again, one flavour violating vertex is included.
- Flavour violating slepton production with flavour violating decays: The strong suppression can be verified numerically, as such processes contain

at least two flavour violating vertices (one in the production and another one in the decay).

Technically, one can approach LFV the same way as LR mixing, where the rotation matrix can be parametrised similarly to the *Cabbibo-Kobayashi-Maskawa-Matrix* [83–85] in the SM. Disregarding LR mixing, the left and the right sector decouple and one gets two independent CKM-type rotation matrices. As in the case of the CKM-matrix there may also exist additional *CP* phases. The general rotation matrix in this case reads [62]

$$R_i = \begin{pmatrix} c_{\phi_{12}^i} c_{\phi_{13}^i} & s_{\phi_{12}^i} c_{\phi_{13}^i} & s_{\phi_{13}^i} e^{-i\eta_i} \\ -s_{\phi_{12}^i} c_{\phi_{23}^i} - c_{\phi_{12}^i} s_{\phi_{23}^i} s_{\phi_{13}^i} e^{i\eta_i} & c_{\phi_{12}^i} c_{\phi_{23}^i} - s_{\phi_{12}^i} s_{\phi_{23}^i} s_{\phi_{13}^i} e^{i\eta_i} & s_{\phi_{13}^i} c_{\phi_{13}^i} \\ s_{\phi_{12}^i} s_{\phi_{23}^i} - c_{\phi_{12}^i} c_{\phi_{23}^i} s_{\phi_{13}^i} e^{i\eta_i} & -c_{\phi_{12}^i} s_{\phi_{23}^i} - s_{\phi_{12}^i} c_{\phi_{23}^i} s_{\phi_{13}^i} e^{i\eta_i} & c_{\phi_{23}^i} c_{\phi_{12}^i} \end{pmatrix}, \quad (2.20)$$

where  $i = L, R$ .  $\phi_{12}^i, \phi_{23}^i, \phi_{13}^i$  are the mixing angles,  $\eta_i$  is the *CP* phase for the left and right sector, respectively,  $s_{\phi_{ij}} = \sin \phi_{ij}$ , and  $c_{\phi_{ij}} = \cos \phi_{ij}$ . Unfortunately, this procedure gives quite complicated formulae for the off-diagonal entries of the mass matrix, especially, if LR mixing is taken into account.

Assuming no *CP* violation is introduced via the slepton mass matrix, this matrix can be diagonalised by a single unitary matrix  $W_{L/R}$ :

$$m_{L/R}^2 = W_{L/R}^* m_{D,L/R}^2 W_{L/R}. \quad (2.21)$$

From this, the interaction Lagrangian for the sleptons (to simplify the notation, only the left sector is given explicitly) is obtained:

$$\begin{aligned} \mathcal{L}_{\tilde{\ell}\tilde{\chi}_i^0}^W &= g f_{l,k}^L W_{L,i\alpha}^* \bar{\ell}_\alpha P_R \tilde{\chi}_k^0 \tilde{\ell}_{L,i} + g f_{l,k}^{L*} W_{L,i\alpha} \tilde{\ell}_{L,i}^* \tilde{\chi}_k^0 P_L \ell_\alpha \\ &+ (L \rightarrow R). \end{aligned} \quad (2.22)$$

The case of *CP* violation can be treated equivalently, but then two unitary matrices to diagonalise the slepton mass matrix are needed:

$$m_L^2 = U_L^\dagger m_{D,L}^2 V_L. \quad (2.23)$$

The resulting interaction Lagrangian now reads

$$\begin{aligned} \mathcal{L}_{\tilde{\ell}\tilde{\chi}_i^0}^W &= g f_{l,k}^L V_{L,i\alpha}^* \bar{\ell}_\alpha P_R \tilde{\chi}_k^0 \tilde{\ell}_{L,i} + g f_{l,k}^{L*} U_{L,i\alpha} \tilde{\ell}_{L,i}^* \tilde{\chi}_k^0 P_L \ell_\alpha \\ &+ (L \rightarrow R). \end{aligned} \quad (2.24)$$

For convenience, the new couplings  $a$  and  $b$ , are introduced in analogy to [20]:

$$a_{ik} = f_{l,k}^L V_{L,ik}^*, \quad a_{ik}^* = f_{l,k}^{L*} U_{L,ik}, \quad (2.25)$$

and

$$b_{ik} = f_{l,k}^R V_{R,ik}^*, \quad b_{ik}^* = f_{l,k}^{R*} U_{R,ik}. \quad (2.26)$$

Resulting from the diagonalisation of the slepton mass matrix, these couplings include the full mixing of the sleptons, i. e. flavour and LR mixing, as well as  $CP$  violation. Here, LR mixing can formally be seen as just a special case of LFV.

Parametrising the slepton mass matrix and inserting off-diagonal elements  $\hat{\delta}_{ij}$  turns out to be a more viable approach for phenomenological studies of slepton mixing [86, 87]. This avoids dealing with a complex and complicated  $6 \times 6$  rotation. As the diagonalisation of the mass matrix is done numerically, this does not make a difference in practise.

In the case of LR mixing, it has been pointed out that this violation of chiral symmetry might yield large effects when using *transverse beam polarisation* [88]. From the formalism it is clear that the violation of chiral symmetry is formally related to flavour violation, so one might expect large effects from transverse polarisation there as well. This motivates the examination of the process under consideration, including the full slepton mixing, as well as all possible polarisation configurations. Additional support for this approach comes from the investigation of  $CP$  violation as stated in section 2.4.

### 2.3.3 Analytical Approximations

As the full slepton mass matrix is a (in general even complex)  $6 \times 6$  matrix, it is difficult to estimate the effect of full three generation mixing. However, if one neglects the LR mixing, this matrix separates into two  $3 \times 3$  submatrices for the left and the right sector, respectively. Keep in mind that this is already an approximation which may not be justified, especially in the  $\tilde{\tau}$  sector. With this approximation the submatrices  $M_{ii}^2$  ( $i = R, L$ ) can now be treated analytically and one finds that there might be a sizeable mixing between the selectrons and smuons even for vanishing direct mixing, i. e.  $\hat{\delta}_{12} = 0$ .

Starting out, e. g., with the right submatrix

$$M_{RR}^2 = \begin{pmatrix} m_1^2 & \hat{\delta}_{12} & \hat{\delta}_{13} \\ \hat{\delta}_{12}^* & m_2^2 & \hat{\delta}_{23} \\ \hat{\delta}_{13}^* & \hat{\delta}_{23}^* & m_3^2 \end{pmatrix} \quad (2.27)$$

where  $m_i$  are the mass parameters for the sleptons and the flavour mixing parameters  $\hat{\delta}_{ij}$ , one arrives at the eigenvalue equation

$$\begin{aligned} 0 &= \begin{vmatrix} m_1^2 - \lambda & \hat{\delta}_{12} & \hat{\delta}_{13} \\ \hat{\delta}_{12}^* & m_2^2 - \lambda & \hat{\delta}_{23} \\ \hat{\delta}_{13}^* & \hat{\delta}_{23}^* & m_3^2 - \lambda \end{vmatrix} \\ &= (m_1^2 - \lambda)(m_2^2 - \lambda)(m_3^2 - \lambda) \\ &\quad - |\hat{\delta}_{23}|^2(m_1^2 - \lambda) - |\hat{\delta}_{13}|^2(m_2^2 - \lambda) - |\hat{\delta}_{12}|^2(m_3^2 - \lambda) \\ &\quad + 2\Re \left\{ \hat{\delta}_{12}\hat{\delta}_{23}\hat{\delta}_{13}^* \right\} \end{aligned} \quad (2.28)$$



$$\begin{aligned}
&= (m_1^2 - \lambda) \left[ \lambda^2 + \lambda(a + b - 2m_1^2) - m_1^2(a + b - m_1^2) + ab \right. \\
&\quad \left. - |\hat{\delta}_{23}|^2 - |\hat{\delta}_{13}|^2 - |\hat{\delta}_{12}|^2 \right] \\
&\quad - |\hat{\delta}_{13}|^2 a - |\hat{\delta}_{12}|^2 b - 2\Re \left\{ \hat{\delta}_{12} \hat{\delta}_{23} \hat{\delta}_{13}^* \right\}
\end{aligned} \tag{2.29}$$

with the mass squared differences  $a = m_1^2 - m_2^2$  and  $b = m_1^2 - m_3^2$ . Considering current experimental limits,  $\hat{\delta}_{12}$  has to be small. Setting  $\hat{\delta}_{12} = 0$  as a first approximation simplifies the calculation significantly and thus seems justified. Still, it can check numerically that the following results are a good approximation for  $\hat{\delta}_{12} \neq 0$  up to the current experimental bound.

As parameter  $a$  measures the mass difference between the lighter two sleptons, it should also be small, since in most scenarios  $\tilde{e}$  and  $\tilde{\mu}$  are nearly degenerated in mass. This degeneration is especially valid if mass unification at a higher scale is assumed. Neglecting thus  $a|\hat{\delta}_{13}|^2$  the simplified eigenvalue equation reads

$$\begin{aligned}
0 &= (m_1^2 - \lambda) \\
&\quad \times \left[ \lambda^2 + \lambda(a + b - 2m_1^2) + m_1^2(a + b - m_1^2) \right. \\
&\quad \left. - |\hat{\delta}_{23}|^2 - |\hat{\delta}_{13}|^2 + ab \right]
\end{aligned} \tag{2.30}$$

immediately yielding

$$\lambda_2 = m_1^2. \tag{2.31}$$

It has been checked numerically that this is a very good approximation in the scenarios considered.

For the other two eigenvalues the following approximation

$$\lambda_{1,3} = \frac{1}{2} \left[ 2m_1^2 - a - b \pm \sqrt{(a - b)^2 - 4(|\hat{\delta}_{13}|^2) + |\hat{\delta}_{23}|^2} \right]. \tag{2.32}$$

is leading to the hierarchy  $\lambda_1 < \lambda_2 < \lambda_3$ . Numerical checks reveal, that the two eigenvalues  $\lambda_1$  and  $\lambda_3$  are not reproduced as accurately as  $\lambda_2$ . However, as LR mixing is neglected entirely, it is obvious that very precise results cannot be expected as soon as staus are involved.

In the analytical approximation, the associated normalised eigenvector to  $\lambda_2$  is

$$\vec{\eta}_2 = \frac{\hat{\delta}_{13}}{\sqrt{|\hat{\delta}_{23}|^2 + |\hat{\delta}_{13}|^2}} \begin{pmatrix} -\frac{\hat{\delta}_{23}}{\hat{\delta}_{13}} \\ 1 \\ 0 \end{pmatrix}. \tag{2.33}$$

This eigenvector shows a nearly equal  $\tilde{e}$  and  $\tilde{\mu}$  contribution to  $\tilde{\ell}_2$  once  $\hat{\delta}_{23} \approx \hat{\delta}_{13}$ . This is especially noteworthy as the direct mixing of these two components via  $\hat{\delta}_{12}$  was set to zero in this approximation. Additionally, one can see that the

slepton associated with  $\eta_2$  has no  $\tilde{\tau}$  admixture. As an immediate consequence the flavour violating decay of this particle to  $\tau + \tilde{\chi}^0$  will be forbidden, even if kinematically accessible, due to the vanishing coupling to the  $\tau$ . Finally, one can qualitatively understand the numerical result of nearly equal mixing of  $\tilde{e}$  and  $\tilde{\mu}$  in certain scenarios, even when all current bounds are satisfied.

The other two eigenvectors are

$$\vec{\eta}_{1,3} = \frac{1}{\sqrt{\lambda_{1,3} - m_1^2 + |\hat{\delta}_{13}|^2 + |\hat{\delta}_{23}|^2}} \begin{pmatrix} \hat{\delta}_{13} \\ \hat{\delta}_{23} \\ \lambda_{1,3} - m_1^2 \end{pmatrix} \quad (2.34)$$

though, as stated above, their precision is not as good as for  $\eta_2$  due to the neglected LR mixing of the  $\tilde{\tau}$ . However, already another important fact can be noticed: the stau-component of the two sleptons  $\tilde{\ell}_1$  and  $\tilde{\ell}_3$  depends only on the difference between their mass and  $m_1$ . It specifically does not depend on the “stau-mixing parameters”  $\hat{\delta}_{13}$  or  $\hat{\delta}_{23}$ . This can be understood from the near mass degeneration of the lighter two sleptons, i. e.  $a$  is assumed to be small.

These analytical approximations can now be checked numerically. Indeed, the result for the second slepton is reproduced to very good accuracy. A direct consequence of this is the possibility of quite large flavour violating production cross sections for the production of the two  $\tilde{e}/\tilde{\mu}$ -like sleptons (in most cases  $\tilde{\ell}_2/\tilde{\ell}_3$  in the left and  $\tilde{\ell}_4/\tilde{\ell}_5$  in the right sector) provided that  $\hat{\delta}_{13} \approx \hat{\delta}_{23}$ . Additionally, these two sleptons in principle can be distinguished, as one of them, even in the case of LFV, cannot decay to a  $\tau$ . This results immediately from its vanishing  $\tilde{\tau}$ -component. The other slepton, however, does have this decay channel.

## 2.4 Sources of $CP$ -Violation

*This section discusses the possible sources of  $CP$  violation in the neutralino sector as far as it is relevant for the subsequent studies of this work.*

Supersymmetry allows several additional complex phases that result in  $CP$  violating effects [62, 89–91]. Relevant sources for  $CP$  violation in the process under consideration are phases from the higgsino mass parameter  $\mu = |\mu|e^{i\phi_\mu}$  and from the gaugino mass parameter  $M_1 = |M_1|e^{i\phi_{M_1}}$  [92].

Additionally, the slepton mass matrix can give rise to  $CP$  violation, e. g. by the trilinear scalar coupling parameter  $A_f = |A_f|e^{i\phi_{A_f}}$  for the sfermion  $\tilde{f}$ , though this should be suppressed by the smallness of the electron mass at least in mSUGRA-theories. This effect is taken into account in the analytical calculations, but not evaluated numerically.

$CP$  violating phases, however, are constrained by measurements of electric dipole moments (EDMs). An overview is given, e. g., in [93,94] and references therein. As supersymmetric contributions to these parameters arise at one loop level already (whereas the contributions from the quark sector of the SM arise only at two loop level) they are expected to be rather large. This introduces the so called *supersymmetric  $CP$ -problem*.

Strong limits on the supersymmetric phases were proposed [95–98] to solve this, as well as cancellations between SUSY contributions to the EDMs have been suggested. It was shown that in the constrained MSSM the phase  $\phi_{M_1}$  is not restricted, though the phase  $|\phi_\mu| \leq 0.1\pi$  [91,99,100]. Including lepton flavour violating terms, however, even this restriction on  $\phi_\mu$  may disappear [101].

$CP$  violation in the neutralino sector stems from the phases of  $M_1$  and  $\mu$ . This has recently been studied by means of neutralino production in the  $e^+e^-$  mode at the ILC [94,102–107]. The main  $CP$ -sensitive observables here are triple products of momenta [106,108] that can be constructed due to the coupling of the production and decay process by spin correlations [60,109–113].

However, it is not possible within the framework of this work since due to the scalar character of the sleptons, there are no spin correlations between production and decay. Instead, transverse polarisation allows to construct  $CP$ -sensitive observables. In this case, a triple product from the transverse component of the electron spin and two momentum vectors (e. g., the momentum vector of the incoming electron and that of the produced selectron) can be formed. A detailed description of the spin formalism can be found in [60,109,114,115]. The construction of a suitable  $CP$ -sensitive observable is shown in chapter 5.

Besides that, it might be possible to observe  $CP$  violating effects already in  $CP$ -even observables. Neglecting neutralino mixing, this has been studied by [22], showing rather large effects in the production of two L-selectrons. Including full neutralino mixing, the  $CP$ -even observables will also be subject of the numerical studies in chapter 5.



# Production Process

## 3.1 Feynman Graphs and Amplitudes

*This section gives the Feynman graphs for slepton production in  $e^-e^-$ -scattering in the most general form on tree level. This includes all effects from neutralino and slepton mixing as well as all possible modes of polarisation of the incoming beams. In addition, some general features of the process under consideration are discussed.*

In tree approximation, slepton pair production in  $e^-e^-$ -scattering proceeds via the exchange of neutralinos  $\tilde{\chi}_k^0$  ( $k = 1..4$ ) in the  $t$ - and  $u$ -channel, respectively. The relevant diagrams are shown in figure 3.1.

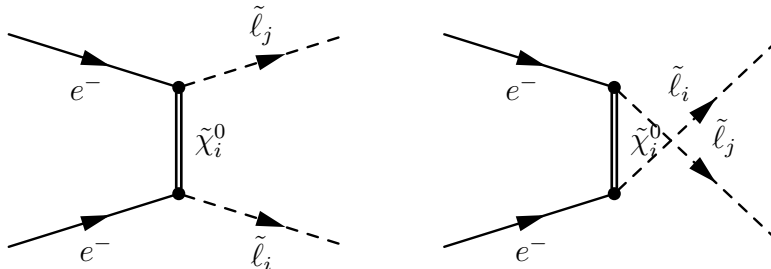


**Figure 3.1:** Production processes for two sleptons in  $e^-e^-$ -scattering.

From the interaction Lagrangian (2.24) and the couplings (2.25) amplitude for the production of slepton pairs  $\tilde{l}_i\tilde{l}_j$  ( $i, j = 1..6$  in case of flavour violation) can be calculated. The sleptons are ordered by their mass,  $\tilde{l}_1$  being the heaviest,  $\tilde{l}_6$  the lightest. This ordering follows from the conventional form of the slepton mass matrix (2.14). This is inverse to the mass ordering of the neutralinos, conventionally

$m_{\tilde{\chi}_1^0} < m_{\tilde{\chi}_2^0} < m_{\tilde{\chi}_3^0} < m_{\tilde{\chi}_4^0}$ . The amplitudes are

$$\begin{aligned} T_{ij}^{\lambda_1 \lambda_2}(\tilde{\chi}_k^0) &= g^2 \bar{v}(p_2, \lambda_2)(a_{ik}^* P_L + b_{ik}^* P_R) \\ &\quad \Delta_t^k(\not{q} + m_{\tilde{\chi}_k^0}) \\ &\quad (a_{jk}^* P_L + b_{jk}^* P_R) u(p_1, \lambda_1), \end{aligned} \quad (3.1)$$

$$\begin{aligned} U_{ij}^{\lambda_1 \lambda_2}(\tilde{\chi}_k^0) &= g^2 \bar{v}(p_2, \lambda_2)(a_{kj}^* P_L + b_{kj}^* P_R) \\ &\quad \Delta_u^k(\not{\phi} + m_k) \\ &\quad (a_{ki}^* P_L + b_{ki}^* P_R) \cdot u(p_1, \lambda_1) \end{aligned} \quad (3.2)$$

Here,  $T_{ij}^{\lambda_1 \lambda_2}(\tilde{\chi}_k^0)$  denotes the  $t$ -channel amplitude and  $U_{ij}^{\lambda_1 \lambda_2}(\tilde{\chi}_k^0)$  the associated  $u$ -channel amplitude. The helicities of the incoming electrons are given by  $\lambda_{1,2}$ . The neutralinos are heavy Majorana fermions. Thus, this process is one of the very rare cases with heavy fermion propagators on tree level in the production process. This leads to a very special structure of the polarisation dependence of this process. The propagators are

$$(\not{q}_1 + m_{\tilde{\chi}_k^0}) \Delta_t^k = (\not{q}_1 + m_{\tilde{\chi}_k^0}) \frac{i}{t - m_{\tilde{\chi}_k^0}^2}, \quad (3.3)$$

$$(\not{q}_2 + m_{\tilde{\chi}_k^0}) \Delta_u^k = (\not{q}_2 + m_{\tilde{\chi}_k^0}) \frac{i}{u - m_{\tilde{\chi}_k^0}^2} \quad (3.4)$$

with the neutralino index  $k = 1..4$ . Here, the momentum transfers are given by  $q_1 = p_1 - p_3$  and  $q_2 = p_1 - p_4$ .

In most scenarios the left selectron is the lightest left slepton, whereas the right selectron is the heaviest right one. This leads to the assignments  $\tilde{\tau}_2 = \tilde{\ell}_1$ ,  $\tilde{\mu}_L = \tilde{\ell}_2$ ,  $\tilde{e}_L = \tilde{\ell}_3$  and  $\tilde{e}_R = \tilde{\ell}_4$ ,  $\tilde{\mu}_R = \tilde{\ell}_5$  and  $\tilde{\tau}_1 = \tilde{\ell}_6$ .

However, the selectrons are nearly degenerated in mass with the smuons, so depending on the actual values of  $A$ ,  $\mu$  and  $\tan \beta$ , they might interchange, resulting in  $\tilde{\mu}_R = \tilde{\ell}_4$ ,  $\tilde{e}_R = \tilde{\ell}_5$  and  $\tilde{\tau}_1 = \tilde{\ell}_6$ . This has to be kept in mind for parameter scans. (The same goes for the left sector.)

For the calculation of the polarised cross section the amplitude squared has to be folded with the spin density matrices of the incoming electrons. The formalism of Bouchiat and Michel [109, 114, 115], taking all possible modes of polarisation into account, gives the following helicity projection operators for a spin- $\frac{1}{2}$  particle with mass  $m$  and momentum  $p^\mu$

$$u(p, \lambda') \bar{u}(p, \lambda) = \frac{1}{2} [\delta_{\lambda\lambda'} + \gamma_5 \not{s}^A \sigma_{\lambda\lambda'}^A] (\not{p} + m), \quad (3.5)$$

$$v(p, \lambda') \bar{v}(p, \lambda) = \frac{1}{2} [\delta_{\lambda\lambda'} + \gamma_5 \not{s}^A \sigma_{\lambda\lambda'}^A] (\not{p} - m) \quad (3.6)$$

in the basis of the Pauli matrices  $\sigma^A$ . The  $s^{A,\mu}$  ( $A = 1..3$ ) are the basis vectors for the polarisation. Together with  $p/m$  they form an orthonormal set of four-

vectors [109]:

$$p \cdot s^a = 0, \quad (3.7)$$

$$s^a \cdot s^b = -\delta^{ab}, \quad (3.8)$$

$$s_\mu^a \cdot s_\nu^b = -g_{\mu\nu} + \frac{p^\mu p^\nu}{m^2}. \quad (3.9)$$

$\vec{s}^{A=3}$  is oriented along the beam axis, whereas the two transverse vectors  $s^{A=1}$  and  $s^{A=2}$  are oriented perpendicular to it, forming a right-handed coordinate system. This system is not fixed on the production plane but to an external frame of reference, e. g., the laboratory. A detailed description for building this basis is given in [11, section 1.2.1].

For the cross section contributions are obtained

- for unpolarised or longitudinally polarised beams proportional to

$$(1 \pm P_1^L)(1 \pm P_2^L)$$

and

- for simultaneous transverse polarisation of both beams proportional to

$$P_1^T P_2^T$$

Due to the mass term in the neutralino propagators (3.3) and (3.4) one obtains contributions for proportional to

$$(1 \pm P_{1,2}^L)P_{2,1}^T,$$

even if the electron mass is neglected, if only one beam is transversely polarised. Since this last term is unique to processes beyond the SM [116], in the calculation of the amplitude all possible polarisations will be kept.

## 3.2 Squared Amplitude

*The squared amplitude for slepton production in  $e^-e^-$ -scattering is given in the manifest covariant form. Possible effects from LR mixing are discussed as well as possible contributions to CP-sensitive observables.*

The production process proceeds, in contrast to the  $e^+e^-$  mode, via both the  $t$ - and the  $u$ -channel. For this reason, writing the individual contributions in manifestly covariant form allows to limit oneself to, e. g. only the  $t$ -channel, whereas the

$u$ -channel can be obtained by simple substitutions. The same is true for the  $t - u$ -interference contributions. For this reason, this section gives the manifest covariant form of the squared amplitude of the production process. The translation of these equations into the laboratory system can be found in appendix, chapter B.

The squared amplitude is obtained from (3.1) and (3.2)

$$\begin{aligned} |\mathcal{M}_{ij}|^2 &= \sum_{k,l} \sum_{\lambda_i, \lambda'_i} \rho_{\lambda_1, \lambda'_1}(e_1^-) \rho_{\lambda_2, \lambda'_2}(e_2^-) \\ &\times \left[ T_{ij}^{\lambda_1 \lambda_2}(\tilde{\chi}_k^0) + U_{ij}^{\lambda_1 \lambda_2}(\tilde{\chi}_k^0) \right] \left[ T_{ij}^{\lambda'_1 \lambda'_2}(\tilde{\chi}_l^0) + U_{ij}^{\lambda'_1 \lambda'_2}(\tilde{\chi}_l^0) \right]^* \end{aligned} \quad (3.10)$$

$$= E_{t,ij} + E_{u,ij} + I_{ij} \quad (3.11)$$

The exchange terms  $E_{t,ij}$  and  $E_{u,ij}$  are given by the absolute squares

$$E_{t,ij} = \sum_{k,l} \sum_{\lambda_i, \lambda'_i} \rho_{\lambda_1, \lambda'_1}(e_1^-) \rho_{\lambda_2, \lambda'_2}(e_2^-) [T_{ij}^{\lambda_1 \lambda_2}(\tilde{\chi}_k^0)] \cdot [T_{ij}^{\lambda'_1 \lambda'_2}(\tilde{\chi}_l^0)]^* \quad (3.12)$$

$$E_{u,ij} = \sum_{k,l} \sum_{\lambda_i, \lambda'_i} \rho_{\lambda_1, \lambda'_1}(e_1^-) \rho_{\lambda_2, \lambda'_2}(e_2^-) [U_{ij}^{\lambda_1 \lambda_2}(\tilde{\chi}_k^0)] \cdot [U_{ij}^{\lambda'_1 \lambda'_2}(\tilde{\chi}_l^0)]^* \quad (3.13)$$

and the interference terms  $I_{ij}$  by

$$I_{ij} = \sum_{k,l} \sum_{\lambda_i, \lambda'_i} 2\Re \left\{ \rho_{\lambda_1, \lambda'_1}(e_1^-) \rho_{\lambda_2, \lambda'_2}(e_2^-) \cdot T_{ij}^{\lambda_1 \lambda_2}(\tilde{\chi}_k^0) \cdot U_{ij}^{\lambda'_1 \lambda'_2}(\tilde{\chi}_l^0)^* \right\}. \quad (3.14)$$

By means of (3.11) one obtains the total cross section

$$\sigma = \int \frac{1}{8(2\pi)^2} \frac{q}{s^{3/2}} |\mathcal{M}_{ij}|^2 d\Omega \quad (3.15)$$

with the solid angle element  $d\Omega = \sin \theta d\theta d\phi$ .

From the individual contributions given in the following sections in a systematic order,  $|\mathcal{M}_{ij}|^2$  can be constructed for the polarised case by

$$|\mathcal{M}_{ij}|^2 = \sum_{a=1}^4 E_{t,ij}^a + E_{u,ij}^a + I_{ij}^a \quad (3.16)$$

Here,  $E_{t,ij}^a$ ,  $E_{u,ij}^a$  and  $I_{ij}^a$  refer to the various polarisation combinations. The total contribution can be obtained by summation of all these

$$E_{t,ij} = \sum_a E_{t,ij}^a \quad (3.17)$$

(analogous equations hold for  $E_{u,ij}$  and  $I_{ij}$ ).



### 3.2.1 Exchange Terms

The *exchange terms*  $E_{t,ij}$  are defined to be the  $t$ - or  $u$ -channel contributions to  $|\mathcal{M}|^2$  (3.11). All the contributions in this section have a common pre factor:

$$X_t^{kl} = g^A \Delta_t^k \Delta_t^{l*} \quad (3.18)$$

for the  $t$ -channel and

$$X_u^{kl} = g^A \Delta_u^k \Delta_u^{l*} \quad (3.19)$$

for the  $u$ -channel.

The following sections give  $t$ -channel contributions only, suppressing the explicit sum over the neutralino indices  $k, l = 1..4$ . The  $u$ -channel can be obtained by the replacements  $i \leftrightarrow j, q_1 \leftrightarrow q_2$  and  $t \leftrightarrow u$ .

#### ■ *Longitudinal* $\otimes$ *Longitudinal Polarisation*

The contributions from unpolarised and longitudinally polarised electron beams to the total cross section are given by

$$E_{t,ij}^1 = 2X_t^{kl} \times \left\{ (1 + P_1^L)(1 - P_2^L) a_{ki}^* b_{kj}^* a_{li} b_{lj} [2(p_1 q_1)(p_2 q_1) - (p_1 p_2) q_1^2] \right. \quad (3.20a)$$

$$+ (1 - P_1^L)(1 + P_2^L) b_{ki}^* a_{kj}^* a_{lj} b_{li} [2(p_1 q_1)(p_2 q_1) - (p_1 p_2) q_1^2] \quad (3.20b)$$

$$+ (1 - P_1^L)(1 - P_2^L) m_k m_l a_{ki}^* a_{kj}^* a_{li} a_{lj} (p_1 p_2) \quad (3.20c)$$

$$\left. + (1 + P_1^L)(1 + P_2^L) m_k m_l b_{ki}^* b_{kj}^* b_{li} b_{lj} (p_1 p_2) \right\}. \quad (3.20d)$$

The terms are all  $CP$ -even and thus are not suitable to build  $CP$ -sensitive observables.

Introducing the LR mixing angle (2.16) of the produced sleptons one finds the dependences of (3.20) to this angle as given in table 3.1. Notice, that in associate ( $e^- e^- \rightarrow \tilde{e}_i \tilde{e}_j, i \neq j$ ) as well as in pair production ( $e^- e^- \rightarrow \tilde{e}_i \tilde{e}_i$ ) only one term dominates, whereas all other contributions are suppressed by at least a factor  $\sin^2 \theta_{\tilde{e}}$ , as this angle should be small, especially for the lighter two generations. The different dependence on  $\theta_{\tilde{e}}$  results in a different polarisation dependence of pair and associate production and will enhance one channel while simultaneously suppressing the other.

#### ■ *Longitudinal* $\otimes$ *Transverse Polarisation*

The terms proportional to the product of transverse and longitudinal beam polarisation are unique to theories beyond the SM [116]. As already discussed, they

	pair production	associate production
(3.20a)	$\cos^2 \theta_{\tilde{\ell}} \sin^2 \theta_{\tilde{\ell}}$	$\cos^4 \theta_{\tilde{\ell}}$
(3.20b)	$\cos^2 \theta_{\tilde{\ell}} \sin^2 \theta_{\tilde{\ell}}$	$\sin^4 \theta_{\tilde{\ell}}$
(3.20c)	$\cos^4 \theta_{\tilde{\ell}}$	$\cos^2 \theta_{\tilde{\ell}} \sin^2 \theta_{\tilde{\ell}}$
(3.20d)	$\sin^4 \theta_{\tilde{\ell}}$	$\sin^2 \theta_{\tilde{\ell}} \cos^2 \theta_{\tilde{\ell}}$

**Table 3.1:** Dependence of the exchange terms for longitudinally polarised beams on the LR mixing angle  $\theta_{\tilde{\ell}}$  of the produced sleptons.

result from the massive fermion exchanged in the  $t$ - and  $u$ -channel. There are two similar contributions of this kind, (3.21) and (3.22), because each electron beam can be transversely polarised, and each beam can have a different degree and direction of polarisation. The form given here is not yet contracted with the spin density matrix of the incoming transverse beam to give the most compact form. For this reason they include both  $x$  as well as  $y$  polarisation encoded in their respective Pauli matrix.

$$E_{t,ij}^2 = 2X_t^{kl} P_1^a \times \left\{ (1 - P_2^L) m_l a_{ki}^* b_{kj}^* a_{li} a_{lj} [-(p_2 p_1)(p_3 s^a) + \langle s^a p_1 p_2 q_1 \rangle] \right. \quad (3.21a)$$

$$\left. - (1 + P_2^L) m_l b_{ki}^* a_{kj}^* b_{lj} b_{li} [-(p_2 p_1)(p_3 s^a) - \langle s^a p_1 p_2 q_1 \rangle] \right. \quad (3.21b)$$

$$\left. - (1 - P_2^L) m_k a_{ki}^* a_{kj}^* b_{lj} a_{li} [(p_2 p_1)(s^a p_3) + \langle s^a p_1 p_2 q_1 \rangle] \right. \quad (3.21c)$$

$$\left. + (1 + P_2^L) m_k b_{ki}^* b_{kj}^* a_{lj} b_{li} [(p_2 p_1)(s^a p_3) - \langle s^a p_1 p_2 q_1 \rangle] \right\} \quad (3.21d)$$

$$E_{t,ij}^3 = 2X_t^{kl} P_2^b \times \left\{ - (1 - P_1^L) m_l a_{ki}^* b_{kj}^* b_{lj} b_{li} [(t^b p_3)(p_1 p_2) - \langle t^b p_1 p_2 q_1 \rangle] \right. \quad (3.22a)$$

$$\left. + (1 + P_1^L) m_l b_{ki}^* a_{kj}^* a_{lj} a_{li} [(t^b p_3)(p_1 p_2) + \langle t^b p_1 p_2 q_1 \rangle] \right. \quad (3.22b)$$

$$\left. - (1 - P_1^L) m_k a_{ki}^* a_{kj}^* a_{lj} b_{li} [-(t^b p_3)(p_2 p_1) + \langle t^b p_1 p_2 q_1 \rangle] \right. \quad (3.22c)$$

$$\left. + (1 + P_1^L) m_k b_{ki}^* b_{kj}^* a_{lj} b_{li} [-(t^b p_3)(p_2 p_1) - \langle t^b p_1 p_2 q_1 \rangle] \right\} \quad (3.22d)$$

Here the shorthand  $\langle abcd \rangle = i\varepsilon_{\mu\nu\rho\sigma} a^\mu b^\nu c^\rho d^\sigma$  is introduced where  $\varepsilon$  is defined in (A.2). These terms are equivalent to a  $CP$ -sensitive triple product and might be of interest for the study of  $CP$  violation.

Contracting these contributions with the spin density matrices of the incoming transversely polarised electrons results in a direct proportionality to the degree of

transverse polarisation. These contributions vanish, of course, in the total cross section, so they would only be visible in weighted or differential cross sections. They can be enhanced by suitable longitudinal polarisation of the second electron beam.

Introducing the slepton mixing angle  $\theta_{\tilde{\ell}}$ , their dependence on LR mixing as displayed in table 3.2 can be studied. Unfortunately all contributions are suppressed by at least  $\sin\theta_{\tilde{\ell}}$ , so they will not contribute for small LR mixing. This sensitivity, however, can probably be used to test the size of LR mixing in the slepton sector. Additionally, these terms may be used in case of flavour violation, as in many scenarios the  $\tilde{\tau}$  sector features large LR mixing.

	pair production	associate production
(3.21a)	$\cos^3\theta_{\tilde{\ell}}\sin\theta_{\tilde{\ell}}$	$-\cos^2\theta_{\tilde{\ell}}\sin^2\theta_{\tilde{\ell}}$
(3.21b)	$\sin^3\theta_{\tilde{\ell}}\cos\theta_{\tilde{\ell}}$	$-\cos^2\theta_{\tilde{\ell}}\sin^2\theta_{\tilde{\ell}}$
(3.21c)	$\cos^3\theta_{\tilde{\ell}}\sin\theta_{\tilde{\ell}}$	$-\cos^3\theta_{\tilde{\ell}}\sin\theta_{\tilde{\ell}}$
(3.21d)	$\sin^3\theta_{\tilde{\ell}}\cos\theta_{\tilde{\ell}}$	$-\sin^2\theta_{\tilde{\ell}}\cos^2\theta_{\tilde{\ell}}$
(3.22a)	$\sin^3\theta_{\tilde{\ell}}\cos\theta_{\tilde{\ell}}$	$\cos^2\theta_{\tilde{\ell}}\sin^2\theta_{\tilde{\ell}}$
(3.22b)	$\cos^3\theta_{\tilde{\ell}}\sin\theta_{\tilde{\ell}}$	$\sin^3\theta_{\tilde{\ell}}\cos\theta_{\tilde{\ell}}$
(3.22c)	$\cos^3\theta_{\tilde{\ell}}\sin\theta_{\tilde{\ell}}$	$\cos^3\theta_{\tilde{\ell}}\sin\theta_{\tilde{\ell}}$
(3.22d)	$\cos^3\theta_{\tilde{\ell}}\sin\theta_{\tilde{\ell}}$	$\sin^2\theta_{\tilde{\ell}}\cos^2\theta_{\tilde{\ell}}$

**Table 3.2:** Dependence of the exchange terms for one beam transversely polarised on the LR mixing angle  $\theta_{\tilde{\ell}}$  of the produced sleptons.

### ■ *Transverse* $\otimes$ *Transverse Polarisation*

The last of the exchange terms is proportional to the degrees of transverse polarisation of both beams. Similar contributions are also available in  $e^+e^-$  collisions [88, 116, 117].

$$\begin{aligned}
E_{t,ij}^4 &= 2X_t^{kl}P_1^aP_2^b \times \\
&\left\{ - (a_{ki}^*b_{kj}^*a_{li}b_{li} + b_{ki}^*a_{ki}^*b_{lj}a_{li}) \right. \\
&\times \left( + (t^bq_1)(p_2p_1)(s^aq_1) \right. \\
&\quad + (t^bs^a) [2(p_2q_1)(p_1q_1) - (p_2p_1)q_1^2] \\
&\quad \left. - (t^bp_1) [2(p_2q_1)(s^aq_1) - (p_2s^a)q_1^2] \right) \\
&\left. + (a_{ki}^*b_{kj}^*a_{lj}b_{li} - b_{ki}^*a_{kj}^*b_{lj}a_{li}) \right. \\
&\times \left[ -(t^bq_1)\langle s^ap_1p_2q_1 \rangle - (s^aq_1)\langle t^bp_1p_2q_1 \rangle \right]
\end{aligned} \tag{3.23a}$$

$$\begin{aligned}
&\times \left[ -(t^bq_1)\langle s^ap_1p_2q_1 \rangle - (s^aq_1)\langle t^bp_1p_2q_1 \rangle \right] \\
&\tag{3.23b}
\end{aligned}$$

$$+ (a_{ki}^* a_{kj}^* b_{li} b_{lj} + b_{ki}^* b_{kj}^* a_{lj} a_{li}) m_k m_l (t^b s^a) (p_1 p_2) \} \quad (3.23c)$$

As one can see, these terms also contain a  $CP$ -sensitive contribution via (3.23b), where the shorthand  $\langle abcd \rangle$  has again been used.

Introducing again the slepton mixing angle  $\theta_{\tilde{\ell}}$  one finds, however, that all contributions are suppressed by  $\sin^2 \theta_{\tilde{\ell}}$  and thus will not contribute for small LR mixing (table 3.3).

	pair production		associate production	
	1. term	2. term	1. term	2. term
(3.23a)	$\cos^2 \theta_{\tilde{\ell}} \sin^2 \theta_{\tilde{\ell}}$	$\cos^2 \theta_{\tilde{\ell}} \sin^2 \theta_{\tilde{\ell}}$	$-\cos^2 \theta_{\tilde{\ell}} \sin^2 \theta_{\tilde{\ell}}$	$-\cos^2 \theta_{\tilde{\ell}} \sin^2 \theta_{\tilde{\ell}}$
(3.23b)	$\cos^2 \theta_{\tilde{\ell}} \sin^2 \theta_{\tilde{\ell}}$	$-\cos^2 \theta_{\tilde{\ell}} \sin^2 \theta_{\tilde{\ell}}$	$-\cos^2 \theta_{\tilde{\ell}} \sin^2 \theta_{\tilde{\ell}}$	$\cos^2 \theta_{\tilde{\ell}} \sin^2 \theta_{\tilde{\ell}}$
(3.23c)	$\cos^2 \theta_{\tilde{\ell}} \sin^2 \theta_{\tilde{\ell}}$	$\cos^2 \theta_{\tilde{\ell}} \sin^2 \theta_{\tilde{\ell}}$	$-\cos^2 \theta_{\tilde{\ell}} \sin^2 \theta_{\tilde{\ell}}$	$-\cos^2 \theta_{\tilde{\ell}} \sin^2 \theta_{\tilde{\ell}}$

**Table 3.3:** Dependence of the doubly transverse exchange terms on the LR mixing angle  $\theta_{\tilde{\ell}}$  of the produced sleptons.

## 3.2.2 Interference Terms

The following section gives the  $t - u$ -interference terms for the production of sleptons in  $e^- e^-$  collisions. Again all possible polarisation modes are taken into account. Given here are the contributions  $I_{tu,ij}^a$ , stemming from  $T_{ij} U_{ij}^\dagger$ . As for the exchange terms, the explicit summation over the neutralino indices  $k, l = 1..4$  is suppressed. The actual interference terms  $I_{ij}^a$  in (3.16) are obtained by means of (3.14) as

$$I_{ij}^a = 2\Re\{I_{tu,ij}^a\}. \quad (3.24)$$

All the contributions in this section have a common pre factor

$$X_{tu}^{kl} = g^A \Delta_t^k \Delta_u^{l*}. \quad (3.25)$$

The individual contributions are given in a form which allows an easy comparison. This is not necessarily their shortest form.

### ■ *Longitudinal* $\otimes$ *Longitudinal Polarisation*

These terms are similar to the exchange terms (3.20) but show a slightly different dependence on LR mixing (table 3.4). From this follows that in case of negligible LR mixing, they contribute only in case of pair production. As was to be expected, they do not offer any option to construct a  $CP$ -sensitive observable.

$$I_{tu,ij}^1 = 2X_{tu}^{kl} \times \left\{ + (1 + P_1^L)(1 - P_2^L) a_{ki}^* b_{kj}^* b_{li} a_{lj} \right. \\ \left. \times [(p_2 q_1)(p_1 q_2) - (p_2 p_1)(q_1 q_2) + (p_2 q_2)(p_1 q_1)] \right. \quad (3.26a)$$

$$+ (1 - P_1^L)(1 + P_2^L) b_{ki}^* a_{kj}^* a_{li} b_{lj} \\ \left. \times [(p_2 q_1)(p_1 q_2) - (p_2 p_1)(q_1 q_2) + (p_2 q_2)(p_1 q_1)] \right. \quad (3.26b)$$

$$+ (1 - P_1^L)(1 - P_2^L) a_{ki}^* a_{kj}^* a_{li} a_{lj} m_k m_l (p_1 p_2) \quad (3.26c)$$

$$\left. + (1 + P_1^L)(1 + P_2^L) b_{ki}^* b_{kj}^* b_{li} b_{lj} m_k m_l (p_1 p_2) \right\} \quad (3.26d)$$

	pair production	associate production
(3.26a)	$\cos^2 \theta_{\tilde{\ell}} \sin^2 \theta_{\tilde{\ell}}$	$-\cos^2 \theta_{\tilde{\ell}} \sin^2 \theta_{\tilde{\ell}}$
(3.26b)	$\cos^2 \theta_{\tilde{\ell}} \sin^2 \theta_{\tilde{\ell}}$	$-\sin^2 \theta_{\tilde{\ell}} \cos^2 \theta_{\tilde{\ell}}$
(3.26c)	$\cos^4 \theta_{\tilde{\ell}}$	$\cos^2 \theta_{\tilde{\ell}} \sin^2 \theta_{\tilde{\ell}}$
(3.26d)	$\sin^4 \theta_{\tilde{\ell}}$	$\sin^2 \theta_{\tilde{\ell}} \cos^2 \theta_{\tilde{\ell}}$

**Table 3.4:** Dependence of the longitudinal interference terms on the LR mixing angle  $\theta_{\tilde{\ell}}$  of the produced sleptons.

### ■ Longitudinal $\otimes$ Transverse Polarisation

Also, in the interference terms, one finds contributions proportional to the transverse polarisation of only one of the electron beams. Like the exchange terms, they each contain a  $CP$ -sensitive part as well. As table 3.5 illustrates, even their dependence on LR mixing matches those of the exchange terms in table 3.2. From this follows however, that these terms are all suppressed by at least  $\sin \theta_{\tilde{\ell}}$  and offer no observables in case of negligible LR mixing.

$$I_{tu,ij}^2 = 2X_{tu}^{kl} P_T^a \times \left\{ (1 - P_2^L) a_{ki}^* b_{kj}^* a_{li} a_{lj} m_l [-(p_1 p_2)(s^a p_3) + \langle s^a p_1 p_2 q_1 \rangle] \right. \quad (3.27a)$$

$$- (1 + P_2^L) b_{ki}^* a_{kj}^* b_{li} b_{lj} m_l [-(p_1 p_2)(s^a p_3) - \langle s^a p_1 p_2 q_1 \rangle] \quad (3.27b)$$

$$- (1 - P_2^L) a_{ki}^* a_{kj}^* b_{li} a_{lj} m_k [(p_1 p_2)(s^a p_4) + \langle s^a p_1 p_2 q_2 \rangle] \quad (3.27c)$$

$$\left. + (1 + P_2^L) b_{ki}^* b_{kj}^* a_{li} b_{lj} m_k [(p_1 p_2)(s^a p_4) - \langle s^a p_1 p_2 q_2 \rangle] \right\} \quad (3.27d)$$

$$I_{tu,ij}^3 = 2X_{tu}^{kl}P_T^b \times \left\{ (1 - P_1^L) a_{ki}^* b_{kj}^* b_{li} b_{lj} m_l \left[ (t^b p_3)(p_1 p_2) - \langle t^b p_1 p_2 q_1 \rangle \right] \right. \quad (3.28a)$$

$$\left. - (1 + P_1^L) b_{ki}^* a_{kj}^* a_{li} a_{lj} m_l \left[ (t^b p_3)(p_2 p_1) + \langle t^b p_1 p_2 q_1 \rangle \right] \right. \quad (3.28b)$$

$$\left. - (1 - P_1^L) a_{ki}^* a_{kj}^* a_{li} b_{lj} m_k \left[ -(t^b p_4)(p_2 p_1) + \langle t^b p_1 p_2 q_2 \rangle \right] \right. \quad (3.28c)$$

$$\left. + (1 + P_1^L) b_{ki}^* b_{kj}^* b_{li} a_{lj} m_k \left[ -(t^b p_4)(p_1 p_2) - \langle t^b p_1 p_2 q_2 \rangle \right] \right\} \quad (3.28d)$$

	pair production	associate production
(3.27a)	$\cos^3 \theta_{\tilde{\ell}} \sin \theta_{\tilde{\ell}}$	$-\cos^2 \theta_{\tilde{\ell}} \sin^2 \theta_{\tilde{\ell}}$
(3.27b)	$\sin^3 \theta_{\tilde{\ell}} \cos \theta_{\tilde{\ell}}$	$-\cos^2 \theta_{\tilde{\ell}} \sin^2 \theta_{\tilde{\ell}}$
(3.27c)	$\cos^3 \theta_{\tilde{\ell}} \sin \theta_{\tilde{\ell}}$	$-\cos^3 \theta_{\tilde{\ell}} \sin \theta_{\tilde{\ell}}$
(3.27d)	$\sin^3 \theta_{\tilde{\ell}} \cos \theta_{\tilde{\ell}}$	$-\sin^2 \theta_{\tilde{\ell}} \cos^2 \theta_{\tilde{\ell}}$
(3.28a)	$\sin^3 \theta_{\tilde{\ell}} \cos \theta_{\tilde{\ell}}$	$\cos^2 \theta_{\tilde{\ell}} \sin^2 \theta_{\tilde{\ell}}$
(3.28b)	$\cos^3 \theta_{\tilde{\ell}} \sin \theta_{\tilde{\ell}}$	$\sin^3 \theta_{\tilde{\ell}} \cos \theta_{\tilde{\ell}}$
(3.28c)	$\cos^3 \theta_{\tilde{\ell}} \sin \theta_{\tilde{\ell}}$	$\cos^3 \theta_{\tilde{\ell}} \sin \theta_{\tilde{\ell}}$
(3.28d)	$\cos^3 \theta_{\tilde{\ell}} \sin \theta_{\tilde{\ell}}$	$\sin^2 \theta_{\tilde{\ell}} \cos^2 \theta_{\tilde{\ell}}$

**Table 3.5:** Dependence of the transverse interference terms on the LR mixing angle  $\theta_{\tilde{\ell}}$  of the produced sleptons.

### ■ *Transverse* $\otimes$ *Transverse Polarisation*

The following terms require both beams to be transversely polarised. Therefore, they do not contribute to the total cross section, but only to moments of those, or observables obtained by integrating only over ranges of the total solid angle.

$$I_{tu,ij}^4 = 2X_{tu}^{kl}P_T^a P_T^b \times \left\{ - (a_{ki}^* b_{kj}^* a_{li} b_{lj} + b_{ki}^* a_{kj}^* b_{li} a_{lj}) \right. \quad (3.29a)$$

$$\times \left[ + (t^b q_1)(p_1 p_2)(s^a q_2) \right. \quad (3.29b)$$

$$\left. + (t^b s^a) [(p_2 q_1)(p_1 q_2) - (p_2 p_1)(q_1 q_2) + (p_2 q_2)(q_1 p_1)] \right. \quad (3.29c)$$

$$\left. + (t^b q_2)(p_1 p_2)(q_1 s^a) \right]$$

$$\left. - (a_{ki}^* b_{kj}^* a_{li} b_{lj} - b_{ki}^* a_{kj}^* b_{li} a_{lj}) \right. \quad (3.29b)$$

$$\times \left[ + (t^b q_1) \langle s^a p_1 p_2 q_2 \rangle + (s^a q_2) \langle t^b p_1 p_2 q_1 \rangle \right] \quad (3.29b)$$

$$\left. - (a_{ki}^* a_{kj}^* b_{li} b_{lj} + b_{ki}^* b_{kj}^* a_{li} a_{lj}) m_k m_l (t^b s^a)(p_2 p_1) \right\} \quad (3.29c)$$

Of special importance for  $CP$  violation is (3.29b), as it can be used to construct a  $CP$ -sensitive observable. In fact, it offers the only  $CP$ -sensitive observable available in the production process. However, from the coupling structure of (3.29b), it is clear that this observable can be used only in the case of associate production, as LR mixing suppresses the term otherwise by a factor  $\sin^2 \theta_{\tilde{\ell}}$  (table 3.6). As this is the only  $CP$ -sensitive contribution in case of negligible LR mixing, one should also note, that the construction of a  $CP$ -odd observable from (3.29b) can not be obtained by integration over the whole solid angle. The construction of the respective observable is discussed in chapter 5.

	pair production		associate production	
	1. term	2. term	1. term	2. term
(3.29a)	$\cos^2 \theta_{\tilde{\ell}} \sin^2 \theta_{\tilde{\ell}}$	$+\cos^2 \theta_{\tilde{\ell}} \sin^2 \theta_{\tilde{\ell}}$	$\cos^4 \theta_{\tilde{\ell}}$	$+\sin^4 \theta_{\tilde{\ell}}$
(3.29b)	$\cos^2 \theta_{\tilde{\ell}} \sin^2 \theta_{\tilde{\ell}}$	$-\cos^2 \theta_{\tilde{\ell}} \sin^2 \theta_{\tilde{\ell}}$	$\cos^4 \theta_{\tilde{\ell}}$	$-\sin^4 \theta_{\tilde{\ell}}$
(3.29c)	$\cos^2 \theta_{\tilde{\ell}} \sin^2 \theta_{\tilde{\ell}}$	$+\cos^2 \theta_{\tilde{\ell}} \sin^2 \theta_{\tilde{\ell}}$	$-\cos^2 \theta_{\tilde{\ell}} \sin^2 \theta_{\tilde{\ell}}$	$-\cos^2 \theta_{\tilde{\ell}} \sin^2 \theta_{\tilde{\ell}}$

**Table 3.6:** Dependence of the doubly transverse interference terms on the LR mixing angle  $\theta_{\tilde{\ell}}$  of the produced sleptons.





---

## Chapter 4

# Scenarios

Without knowing how SUSY is realised in nature, one is left with well over a hundred parameters. These are masses, couplings, mixing angles and phases. Assuming a specific breaking scheme, however, together with the existence of a *Great Unified Theory* (GUT), which governs physics beyond a certain unification scale  $M_{\text{GUT}}$ , the number of parameters can be drastically reduced. Currently, the most popular of these schemes is “minimal Supergravity” (mSUGRA), where gravity mediates SUSY breaking. Other mechanisms include gauge mediated (GMSB) and anomaly mediated SUSY breaking (AMSB). While the main features of these models were qualitatively described in section 2.2.1, a more detailed introduction to these various mechanisms is given, e. g., in [8,32,57] and references therein. They will not be discussed in detail here, as the actual reconstruction of the mechanism of SUSY breaking is not subject of this study.

These schemes are quite different in their nature. Their common feature is, however, that one can retrieve the low scale parameters from only a few high scale parameters by means of renormalisation group equations (RGE). Using this approach, several sets of scenarios have been proposed to explore the potential of a future linear collider for the search of SUSY and the determination of the underlying model [118–121]. These so-called “benchmark scenarios” should serve here as a starting point. Currently, they are also used to estimate the potential of the LHC. Additionally, some points in parameter space deviating from these schemes will be investigated, assuming that all relevant low scale parameters are actually free parameters.

All scenarios considered here feature *R-parity* conservation. For this reason the lightest supersymmetric particle (LSP) is stable, offering a good candidate for cold dark matter. In this work the LSP is considered to be either the lightest neutralino,  $\tilde{\chi}_1^0$  or the gravitino,  $\tilde{G}$ . Both particles escape detection so that the typical experimental signatures include large amounts of missing-energy.

For the characterisation of the scenarios, conventionally the neutralino mixing with the definitions given in section 2.2.2 are being used. Together with the introduction of the parameters defining the scenarios, the neutralino and slepton sector is also

subject of studies in the following section. Finally, for all scenarios the total unpolarised cross sections for all selectron production channels are given. This should serve as a starting point for the subsequent chapters on  $CP$  violation and LFV.

The “typical” mSUGRA scenario SPS 1a' [122] was chosen as a basis for the investigation and construction of further representative scenarios, as it is one of the most studied scenarios today. This offers to view the results of this study within a broader framework. It is further discussed in section 4.1. Additionally, it defines the basis for Mixed SPS, section 4.2, which is derived from SPS 1a' by just lowering the higgsino mass parameter  $\mu$  yielding a mixed character for the neutralinos. Also, Scenario A, section 4.3, is inspired by SPS 1a': it is a GUT-scenario with somewhat higher gaugino mass parameters and a lower  $\mu$ -parameter. These parameters have been chosen to obtain a GUT-scenario with a strong higgsino-like neutralino sector. Due to current experimental bounds on the Higgs boson mass this is not possible with the parameters of SPS 1a'.

In Scenario B, section 4.4, with  $M_1 \gg M_2$  and  $\mu < M_1$  the GUT-relation (2.4) was dropped. First of all, this results in a mixed scenario with sizeable higgsino components in the lighter two neutralinos. Secondly, the inversion of the mass hierarchy in the gaugino sector leads to a wino-like character for  $\tilde{\chi}_3^0$ . This scenario features heavy neutralinos with  $\tilde{\chi}_2^0, \tilde{\chi}_3^0$ , and  $\tilde{\chi}_4^0$  in the range of 400-470 GeV, while  $\tilde{\chi}_1^0$  is still a light state of about 115 GeV.

Scenario C is a non-GUT-scenario with a normal mass hierarchy and a large mass difference between the lighter two, higgsino-like, and the heavier two, gaugino-like, neutralinos. The small value for  $\tan\beta = 3$  pronounces clean states. Due to the small mass for  $\tilde{\chi}_2^0$  of only 123 GeV, this particle can only decay via three-body decays  $\tilde{\chi}_2^0 \rightarrow \tilde{\chi}_1^0 f \bar{f}'$ . Scenarios of this type have been studied in the context of  $CP$  violation in the  $e^+e^-$  mode of a future linear collider [123]. The parameters for Scenario C are given in section 4.5.

Generally, the  $\tilde{\chi}_1^0$  does not have to be the LSP. In some regions of parameter space the LSP is the gravitino  $\tilde{G}$ . The corresponding scenarios feature special decay modes of the charged sleptons which might be exploited in the search for LFV. An mSUGRA-scenario of this type is Point  $\varepsilon$  [120], discussed in section 4.6. The neutralinos here are gaugino-like and, especially  $\tilde{\chi}_3^0$  and  $\tilde{\chi}_4^0$ , rather heavy.

SPS 7, section 4.7, finally, is not a mSUGRA scenario, but of the GMSB type. As for Point  $\varepsilon$ , the LSP is not the  $\tilde{\chi}_1^0$  but the  $\tilde{G}$ . SPS 7 should serve for comparison with Point  $\varepsilon$  and as an example for a non-mSUGRA scenario.  $\tilde{\chi}_1^0$  is of gaugino-like nature, while  $\tilde{\chi}_2^0$  already contains a sizeable higgsino component. The heavier two neutralinos are of higgsino-like nature with a sizeable  $\tilde{Z}$  component. The masses are generally lower than those in Point  $\varepsilon$ .

## 4.1 Gaugino-like mSUGRA: SPS 1a'

*This section gives a short introduction to the benchmark point SPS 1a', one of the most studied scenarios in SUSY today. It serves as a starting point for the numerical studies of this work. Besides the discussion of the scenario and its mass spectrum the total cross sections for selectron production are calculated.*

One of the most investigated benchmark scenarios is the so called SPS 1a scenario [118] and its descendant SPS 1a' [122]. For this reason it offers the option to compare the  $e^+e^-$  mode with the  $e^-e^-$  mode of a linear collider, and it should serve as a starting point of this work.

SPS 1a' is a “typical mSUGRA” scenario offering a pretty rich phenomenology at 500 GeV. It implies unification of couplings and masses at the GUT scale, and neither contains any additional  $CP$  violating phases beyond those of the SM nor flavour mixing elements. The lightest supersymmetric particle is a nearly pure bino-like neutralino. (For the nomenclature of the neutralinos see section 2.2.2.)

$$\begin{array}{lcl} M_{1/2} & = & 250 \text{ GeV} \\ M_0 & = & 70 \text{ GeV} \\ A_0 & = & -300 \text{ GeV} \end{array} \left| \begin{array}{lcl} \text{sign}(\mu) & = & +1 \\ \tan \beta & = & 10 \end{array} \right.$$

**Table 4.1:** SPS 1a' parameters at the GUT scale  $M_{\text{GUT}}$ .  $M_{1/2}$  is the universal gaugino mass,  $M_0$  the universal scalar mass, and  $A_0$  the universal trilinear coupling.

SPS 1a' is defined by the high scale parameters given in table 4.1. The resulting mass spectrum is given in table 4.2 [122]. It is obtained using SPHENO [124], which includes the full one-loop formulae for the masses together with the two-loop contributions of the neutral Higgs bosons for the  $\mu$ -parameter to solve the RGEs numerically. These values are only given for comparison, whereas all masses and couplings used in this work are consistently calculated on tree level, as no higher order calculations exist, including effects from LFV or  $CP$  violation, as well as for the non-GUT-models investigated.

The relevant low scale parameters serving as a starting point for further investigation are given in table 4.3. They are taken from the *SPA convention* [122]. Included is also the chargino mass calculated by diagonalisation of the chargino mass matrix using the formulae given in [125, appendix A]. This mass is of relevance for the decays of sleptons. It is already constrained to be  $m_{\tilde{\chi}_1} > 104 \text{ GeV}$  [126], giving a stringent bound on the allowed SUSY parameter space.

Using these low scale parameters, the neutralino masses and mixings on tree level shown in table 4.4 are obtained. These values deviate on the percent level from the

Particle	Mass [GeV]	Particle	Mass [GeV]
$h^0$	116.0	$\tilde{\tau}_1$	107.9
$H^0$	425.0	$\tilde{\tau}_2$	194.9
$A^0$	424.9	$\tilde{\nu}_\tau$	170.5
$H^\pm$	432.7	$\tilde{u}_R$	547.2
$\tilde{\chi}_1^0$	97.7	$\tilde{u}_L$	564.7
$\tilde{\chi}_2^0$	183.9	$\tilde{d}_R$	546.9
$\tilde{\chi}_3^0$	400.5	$\tilde{d}_L$	570.1
$\tilde{\chi}_4^0$	413.9	$\tilde{t}_1$	366.5
$\tilde{\chi}_1^\pm$	183.7	$\tilde{t}_2$	585.5
$\tilde{\chi}_2^\pm$	415.4	$\tilde{b}_1$	506.3
$\tilde{e}_R$	125.3	$\tilde{b}_2$	545.7
$\tilde{e}_L$	189.9	$\tilde{g}$	607.1
$\tilde{\nu}$	172.5		

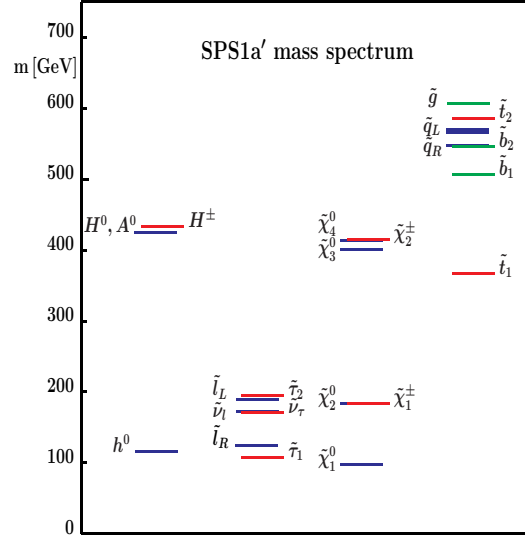


**Table 4.2:** Mass spectrum of supersymmetric particles and Higgs bosons in the reference point SPS 1a'. The masses of the second generation coincide with the first generation [122].

$M_1$	[GeV]	103.300	$\phi_{M_1}$	0.000
$\mu$	[GeV]	396.000	$\phi_\mu$	0.000
$M_2$	[GeV]	193.200	$\tan \beta$	10.000
$m_{\tilde{\chi}_1^\pm}$	[GeV]	179.993	$m_{\tilde{\chi}_2^\pm}$	[GeV] 417.943

**Table 4.3:** Low energy input parameters and  $\tilde{\chi}^\pm$ -masses for SPS 1a'.

ones including radiative corrections. This is the typical systematic error included in this study. SPS 1a' is a nearly pure gaugino scenario, i. e. the lightest two neutralinos contain almost no admixtures from the higgsinos.

Table 4.5 shows the mixing of the sleptons. As no flavour violation is present in this scenario, only the staus show sizeable mixing of their left and right states, which is suppressed by the small lepton masses in cases of  $\tilde{e}$  and  $\tilde{\mu}$ , see (2.15). Besides, the mixing table 4.5 also gives the masses and numbering of the sleptons. Figure 4.1 shows the total cross section as a function of the centre of mass energy  $\sqrt{s}$  for the production of selectrons with unpolarised beams in this scenario.

Due to the high cross sections reached in this scenario, all modes (i. e.  $\tilde{e}_R\tilde{e}_R$ ,  $\tilde{e}_R\tilde{e}_L$  and  $\tilde{e}_L\tilde{e}_L$ ) should be measurable at a collider energy of 500 GeV. However, the luminosity of the  $e^-e^-$  mode will be only  $\approx 20\%$  of the  $e^+e^-$  mode of the collider [127]. This is a result of the beam spread in the interaction point. To improve the statistics of the measurement, additional suitable longitudinal beam polarisations may be used to enhance the event rates by a factor of about 3.6 for pair production and 1.8 for associate production of the selectrons, assuming a degree of polarisation

	$\tilde{\chi}_1^0$	$\tilde{\chi}_2^0$	$\tilde{\chi}_3^0$	$\tilde{\chi}_4^0$
$\tilde{\gamma}$	0.843 0.000 <i>i</i>	-0.519 0.000 <i>i</i>	0.058 0.000 <i>i</i>	0.125 0.000 <i>i</i>
$\tilde{Z}$	-0.536 0.000 <i>i</i>	-0.799 0.000 <i>i</i>	0.152 0.000 <i>i</i>	0.228 0.000 <i>i</i>
$\tilde{H}_a^0$	0.000 0.007 <i>i</i>	0.000 -0.102 <i>i</i>	0.000 0.637 <i>i</i>	0.000 -0.764 <i>i</i>
$\tilde{H}_b^0$	0.037 0.000 <i>i</i>	0.287 0.000 <i>i</i>	0.754 0.000 <i>i</i>	0.590 0.000 <i>i</i>
Mass [GeV]	100.736	180.531	401.898	417.131

**Table 4.4:** Neutralino mixing and mass spectrum for SPS 1a'. Given is the diagonalisation matrix  $N$ .

	$\tilde{\ell}_1$	$\tilde{\ell}_2$	$\tilde{\ell}_3$	$\tilde{\ell}_4$	$\tilde{\ell}_5$	$\tilde{\ell}_6$
$\tilde{e}_L$	0.000	0.000	-1.000	0.000	0.000	0.000
$\tilde{\mu}_L$	0.000	1.000	0.000	0.000	0.021	0.000
$\tilde{\tau}_L$	-0.947	0.000	0.000	0.000	0.000	0.322
$\tilde{e}_R$	0.000	0.000	0.000	1.000	0.000	0.000
$\tilde{\mu}_R$	0.000	-0.021	0.000	0.000	1.000	0.000
$\tilde{\tau}_R$	0.322	0.000	0.000	0.000	0.000	0.947
Mass [GeV]	192.364	186.980	186.956	123.573	123.537	106.412

**Table 4.5:** Slepton mixing and mass spectrum for SPS 1a'. Given is the diagonalisation matrix  $U \equiv V \in \mathbb{R}$ .

of 90% is viable. Depending on the production channel under consideration, the optimal polarisation for enhancing the production cross section varies. Table 4.6 gives the various modes.

Using polarised beams, not only the cross section of the process under consideration can be enhanced. Another important feature of this process is that beam polarisation also decreases the main background, which stems from W-production. Here, besides W-pair production, also channels proceeding via only one W-boson are important (see section 8.1 for details). As the W-boson couples only to left particles, this production process is drastically reduced in case of right handed beam polarisation. This results in an overall gain in the signal to background ratio in case of the production of  $\tilde{e}_R\tilde{e}_R$  or  $\tilde{e}_R\tilde{e}_L$  (see also section 8.1, figure 8.5a). Only in the pair production of the left sleptons the background rises with the production cross section.

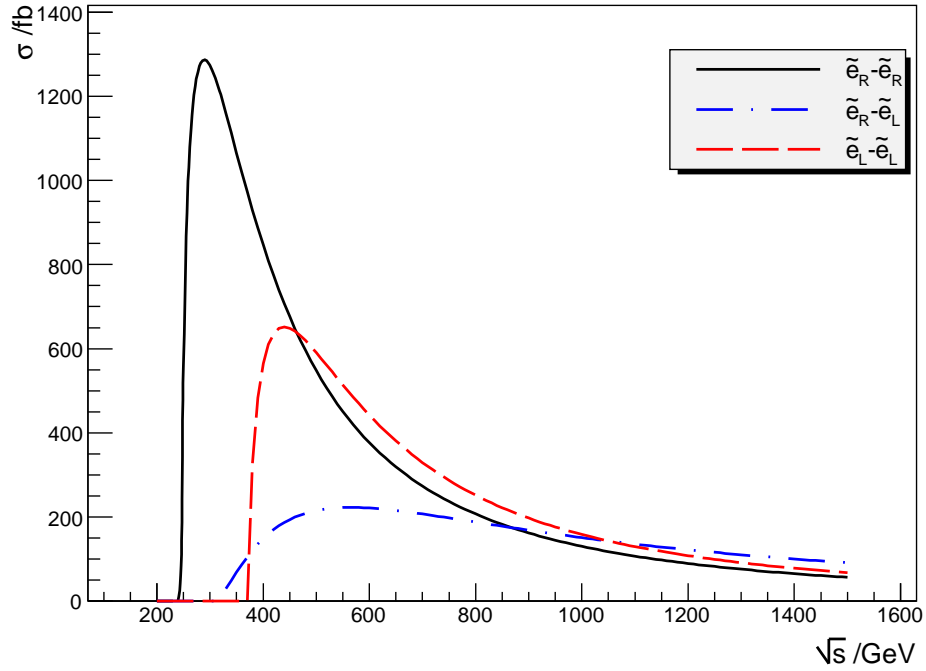


**Figure 4.1:** Total cross sections for the selectron production channels  $e^-e^- \rightarrow \tilde{e}_{R/L}\tilde{e}_{R/L}$  as a function of the centre of mass energy  $\sqrt{s}$  in the scenario SPS 1a'. Both beams are unpolarised.

1 <sup>st</sup> Beam	2 <sup>nd</sup> Beam	optimised Mode
+ or R	+ or R	$\tilde{\ell}_R^- \tilde{\ell}_R^-$
- or L	- or L	$\tilde{\ell}_L^- \tilde{\ell}_L^-$
		} pair production
+ or R	- or L	$\tilde{\ell}_R^- \tilde{\ell}_L^-$
- or L	+ or R	$\tilde{\ell}_R^- \tilde{\ell}_L^-$
		} associate production

**Table 4.6:** Suitable longitudinal polarisation to enhance the production cross section. “+” is equivalent for right handed, “-” for left handed polarisation of the incoming beams.

## 4.2 Small $|\mu|$ : Mixed SPS

*This scenario uses the same parameter points as SPS 1a' except for a much lower higgsino mass parameter  $\mu$ .  $\tilde{\chi}_1^0$  is the LSP which is still mainly a gaugino, but already the  $\tilde{\chi}_2^0$  contains a large higgsino component. For this reason one would call this a mixed scenario. This section discusses the mass spectrum and the production cross section for selectrons in Mixed SPS.*

As SPS 1a' features nearly pure gauginos for the lighter two neutralinos, it seems sensible to also study a scenario with the lightest neutralino, being a gaugino, whereas the second one is mainly a higgsino. Such a scenario is proposed in table 4.7. It is derived from SPS 1a' by lowering the value of the higgsino mass parameter to  $\mu = 140$  GeV to allow for comparison. As a consequence of this, all neutralinos in this scenario are quite light and could be studied in the  $e^+e^-$  mode of the collider.

Recent experimental data from WMAP, measuring the dark matter content of the universe [128, 129], seem to favour supersymmetric scenarios with a small  $\mu$  parameter. There are further, more theoretical, arguments supporting this idea [130, 131]. The favouring of small values of the higgsino mass parameter results in the lighter neutralinos to be of higgsino-like nature or at least have a strong higgsino component as can be seen from the general features for the mixing in table 2.2.

$M_1$	[GeV]	103.300	$\phi_{M_1}$	0.000
$\mu$	[GeV]	140.000	$\phi_\mu$	0.000
$M_2$	[GeV]	193.200	$\tan \beta$	10.000
$m_{\tilde{\chi}_1^\pm}$	[GeV]	106.527	$m_{\tilde{\chi}_2^\pm}$	[GeV] 241.888

**Table 4.7:** Low energy input parameters and  $\tilde{\chi}^\pm$ -masses for Mixed SPS.

Table 4.8 shows the mixing of the neutralinos in this scenario. One can see that  $\tilde{\chi}_1^0$  has a sizeable higgsino component but still contains strong gaugino parts, and  $\tilde{\chi}_2^0$  is mainly a higgsino with sizeable photino admixture. The two heavier neutralinos are of mixed nature without too much pronouncement of either component.

In the  $\tilde{\tau}$  sector the smaller  $\mu$  parameter (the  $A$ -parameter was fixed to the value of SPS 1a', section 4.1) results in a much smaller LR mixing, and consequently, in a different mass ordering of the sleptons. A direct effect is the near mass degeneracy in the left sector, with  $\tilde{\tau}_L$  being somewhat lighter than  $\tilde{e}_L$  and  $\tilde{\mu}_L$ . The resulting mass spectrum and ordering is given in table 4.9.

Due to the sizeable higgsino admixtures in the neutralinos, the total production cross sections are a bit lower than in SPS 1a', as the selectrons couple only to the

	$\tilde{\chi}_1^0$	$\tilde{\chi}_2^0$	$\tilde{\chi}_3^0$	$\tilde{\chi}_4^0$
$\tilde{\gamma}$	0.469 0.000 <i>i</i>	-0.577 0.000 <i>i</i>	0.407 0.000 <i>i</i>	0.531 0.000 <i>i</i>
$\tilde{Z}$	-0.846 0.000 <i>i</i>	-0.089 0.000 <i>i</i>	0.395 0.000 <i>i</i>	0.348 0.000 <i>i</i>
$\tilde{H}_a^0$	0.000 0.026 <i>i</i>	0.000 -0.188 <i>i</i>	0.000 0.656 <i>i</i>	0.000 -0.730 <i>i</i>
$\tilde{H}_b^0$	0.254 0.000 <i>i</i>	0.790 0.000 <i>i</i>	0.498 0.000 <i>i</i>	0.253 0.000 <i>i</i>
Mass [GeV]	77.408	128.063	151.071	242.100

**Table 4.8:** Neutralino mixing and mass spectrum for Mixed SPS. Given is the diagonalisation matrix  $N$ .

	$\tilde{\ell}_1$	$\tilde{\ell}_2$	$\tilde{\ell}_3$	$\tilde{\ell}_4$	$\tilde{\ell}_5$	$\tilde{\ell}_6$
$\tilde{e}_L$	0.000	-1.000	0.000	0.000	0.000	0.000
$\tilde{\mu}_L$	1.000	0.000	0.000	0.000	0.008	0.000
$\tilde{\tau}_L$	0.000	0.000	-0.988	0.000	0.000	0.155
$\tilde{e}_R$	0.000	0.000	0.000	1.000	0.000	0.000
$\tilde{\mu}_R$	-0.008	0.000	0.000	0.000	1.000	0.000
$\tilde{\tau}_R$	0.000	0.000	0.155	0.000	0.000	0.988
Mass [GeV]	186.959	186.956	186.700	123.573	123.569	116.062

**Table 4.9:** Slepton mixing and mass spectrum for Mixed SPS. Given is the diagonalisation matrix  $U \equiv V \in \mathbb{R}$ .

gaugino components of the neutralinos. As the neutralinos are all still containing large gaugino components though, the cross sections are in general comparable to SPS 1a' and will be accessible at the ILC at  $\sqrt{s} = 500$  GeV in the  $e^-e^-$  mode.



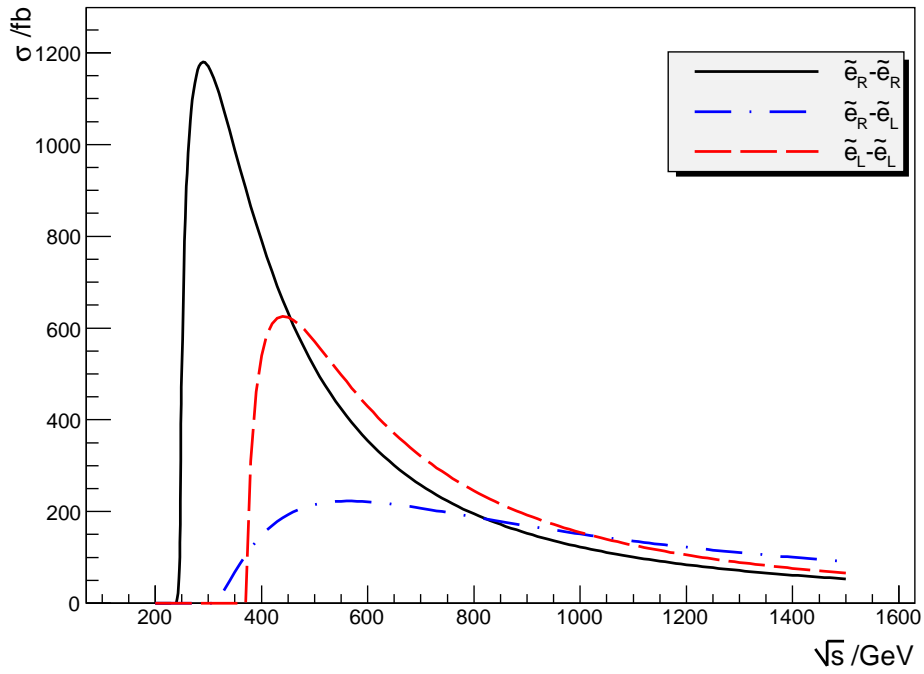


**Figure 4.2:** Total cross sections for the selectron production channels  $e^-e^- \rightarrow \tilde{e}_{R/L}\tilde{e}_{R/L}$  as a function of the centre of mass energy  $\sqrt{s}$  in the scenario Mixed SPS. Both beams are unpolarised.

### 4.3 Higgsino-like GUT: Scenario A

Similar to SPS 1a', this scenario features slightly higher gaugino mass parameters  $M_1$  and  $M_2$ , still connected by the GUT-relation (2.4). A small  $\mu$  parameter results in the LSP to be mainly a higgsino. This together with the mass spectrum, the production cross sections for selectrons are discussed.

The parameters of this scenario are given in table 4.10. The gaugino mass parameter  $M_2 = 500$  GeV is higher than in SPS 1a', and  $M_1$  is fixed by the GUT-relation (2.4). As the higgsino mass parameter  $\mu = 115$  GeV is almost at its lowest value allowed by the lower chargino mass limit, this scenario features nearly pure higgsinos for the lighter two neutralinos, whereas the heavier two neutralinos are gaugino-like, see table 4.11.

$M_1$	[GeV]	250.500	$\phi_{M_1}$	0.000
$\mu$	[GeV]	115.000	$\phi_\mu$	0.000
$M_2$	[GeV]	500.000	$\tan \beta$	5.000
$m_{\tilde{\chi}_1^\pm}$	[GeV]	106.923	$m_{\tilde{\chi}_2^\pm}$	[GeV] 514.513

**Table 4.10:** Low energy input parameters and  $\tilde{\chi}^\pm$ -masses for Scenario A.

	$\tilde{\chi}_1^0$	$\tilde{\chi}_2^0$	$\tilde{\chi}_3^0$	$\tilde{\chi}_4^0$
$\tilde{\gamma}$	0.118 0.000i	-0.239 0.000i	0.769 0.000i	0.581 0.000i
$\tilde{Z}$	0.000 -0.024i	0.000 0.098i	0.000 -0.578i	0.000 0.810i
$\tilde{H}_a^0$	-0.886 0.000i	0.407 0.000i	0.208 0.000i	0.073 0.000i
$\tilde{H}_b^0$	0.447 0.000i	0.876 0.000i	0.178 0.000i	0.034 0.000i
Mass [GeV]	96.192	119.997	259.866	514.440

**Table 4.11:** Neutralino mixing and mass spectrum for Scenario A. Given is the diagonalisation matrix  $N$ .

The higgsino components in the lighter two neutralinos are additionally emphasised by the lower value of  $\tan \beta = 5$  as lower values generally lead to purer states. This is easier to see if one writes the neutralino mass matrix (2.7) in the basis  $(\tilde{B}, \tilde{W}, \tilde{H}_1^0, \tilde{H}_2^0)$

	$\tilde{\ell}_1$	$\tilde{\ell}_2$	$\tilde{\ell}_3$	$\tilde{\ell}_4$	$\tilde{\ell}_5$	$\tilde{\ell}_6$
$\tilde{e}_L$	0.000	0.000	-1.000	0.000	0.000	0.000
$\tilde{\mu}_L$	0.000	1.000	0.000	0.000	0.005	0.000
$\tilde{\tau}_L$	-0.995	0.000	0.000	0.000	0.000	0.096
$\tilde{e}_R$	0.000	0.000	0.000	1.000	0.000	0.000
$\tilde{\mu}_R$	0.000	-0.005	0.000	0.000	1.000	0.000
$\tilde{\tau}_R$	0.096	0.000	0.000	0.000	0.000	0.995
Mass [GeV]	205.357	205.095	205.094	175.140	175.139	174.842

**Table 4.12:** Slepton mixing and mass spectrum for Scenario A. Given is the diagonalisation matrix  $U \equiv V \in \mathbb{R}$ .

$$\hat{Y} = \begin{pmatrix} M_1 & 0 & -m_Z c_\beta s_W & m_Z s_\beta s_W \\ 0 & M_2 & m_Z c_\beta c_W & -m_Z s_\beta c_W \\ -m_Z c_\beta s_W & m_Z c_\beta c_W & 0 & -\mu \\ m_Z s_\beta s_W & -m_Z s_\beta c_W & -\mu & 0 \end{pmatrix}. \quad (4.1)$$

Current experimental bounds suggest that  $\tan \beta \geq 3$ . This gives  $0.94 < \sin \beta < 1$ , resulting in only a small variation of  $\sin \beta$ , and only a minor change of the mixing due to the matrix elements  $\hat{Y}_{14}$  and  $\hat{Y}_{24}$ , while the change of  $\cos \beta$  is stronger in this region. Thus, it is apparent that lower values of  $\tan \beta$ , i. e. larger values of  $\cos \beta$ , enhance the off diagonal elements  $\hat{Y}_{13}$  and  $\hat{Y}_{23}$  of the mass matrix and hence lead to a stronger mixing between the gaugino and higgsino sector, while the elements  $\hat{Y}_{14}$  and  $\hat{Y}_{24}$  remain nearly unchanged.

The cross sections for this scenario are given in figure 4.3. From the higgsino-like character of the lighter neutralinos, one can already understand the lower cross sections compared to, e. g., SPS 1a'. As the selectron masses are of moderate values, all channels are kinematically accessible at  $\sqrt{s} = 500$  GeV. This scenario, however, is experimentally more challenging than those discussed so far, as the cross section for associate production at this energy reaches only  $\sigma_{RL} = 39$  fb. This channel is of special importance for the study of  $CP$  violation as it can be used to build a  $CP$ -sensitive observable (see chapter 5).

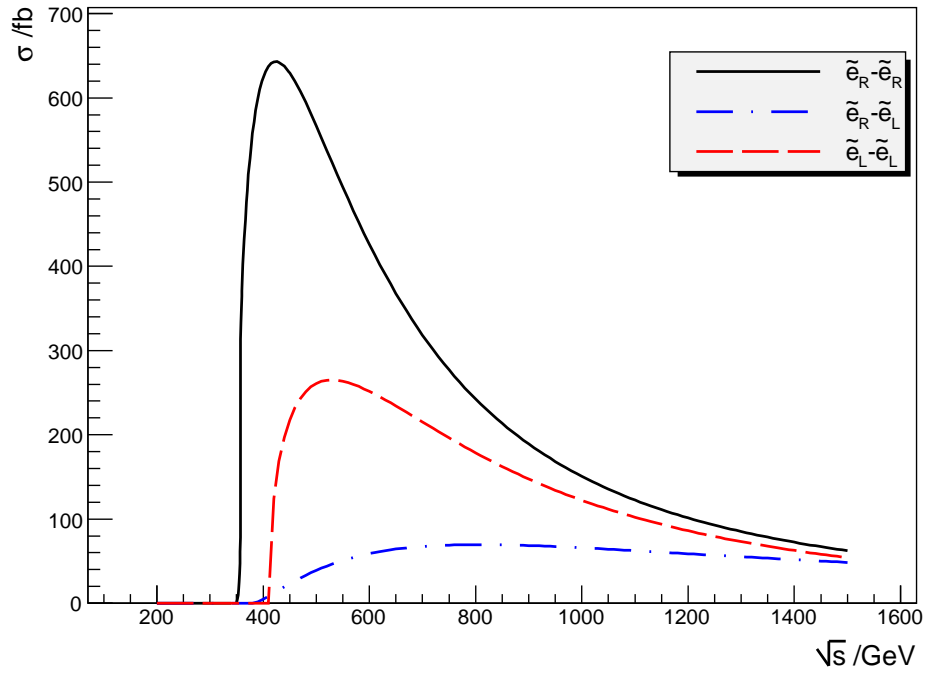


**Figure 4.3:** Total cross sections for the selectron production channels  $e^-e^- \rightarrow \tilde{e}_{R/L}\tilde{e}_{R/L}$  as a function of the centre of mass energy  $\sqrt{s}$  in the scenario Scenario A. Both beams are unpolarised.

## 4.4 Higgsino-like non-GUT: Scenario B

*In this scenario the GUT-relation (2.4) is given up treating  $M_1$  and  $M_2$  as independent parameters with reverted hierarchy ( $M_1 \gg M_2$ ). In contrast to the other scenarios Scenario B features a heavier higgsino-like neutralino sector. Additionally,  $\tilde{\chi}_3^0$  is mainly a wino and for that reason does not couple to right handed sleptons.*

Scenario B drops the GUT-relation and inverts the mass hierarchy in the gaugino sector:  $M_1 \gg M_2$  while  $\mu < M_1$ . It also features a low value for  $\tan\beta$ , see table 4.13. Consequently, the LSP  $\tilde{\chi}_1^0$  is of mixed nature with a sizeable higgsino component, while  $\tilde{\chi}_2^0$  is mainly a photino. The large mass splitting between  $M_1$  and  $M_2$  is also reflected in the mass splitting of the neutralinos: the LSP is very light ( $\approx 115$  GeV, comparable to the lighter chargino), whereas already  $m_{\tilde{\chi}_2^0} \approx \mu$  and as such comparable in mass with  $\tilde{\chi}_3^0$ . The latter is, as a result from the mass inversion, mainly a wino with strong higgsino components.  $\tilde{\chi}_4^0$ , finally, is mainly a  $\tilde{Z}$  but with a sizeable higgsino component. It is only about 60 – 70 GeV heavier than the  $\tilde{\chi}_2^0$  and  $\tilde{\chi}_3^0$ , resulting in a small mass splitting within these three states.

$M_1$	[GeV]	450.000	$\phi_{M_1}$	0.000
$\mu$	[GeV]	400.000	$\phi_\mu$	0.000
$M_2$	[GeV]	130.000	$\tan\beta$	3.000
$m_{\tilde{\chi}_1^\pm}$	[GeV]	114.466	$m_{\tilde{\chi}_2^\pm}$	[GeV] 420.392

**Table 4.13:** Low energy input parameters and  $\tilde{\chi}^\pm$ -masses for Scenario B.

	$\tilde{\chi}_1^0$	$\tilde{\chi}_2^0$	$\tilde{\chi}_3^0$	$\tilde{\chi}_4^0$
$\tilde{\gamma}$	-0.443 0.000i	-0.860 0.000i	0.189 0.000i	0.171 0.000i
$\tilde{Z}$	0.587 0.000i	-0.072 0.000i	0.719 0.000i	0.364 0.000i
$\tilde{H}_a^0$	0.000 -0.012i	0.000 -0.071i	0.000 0.452i	0.000 -0.889i
$\tilde{H}_b^0$	0.677 0.000i	-0.501 0.000i	-0.492 0.000i	-0.220 0.000i
Mass [GeV]	114.364	392.670	402.891	475.857

**Table 4.14:** Neutralino mixing and mass spectrum for Scenario B. Given is the diagonalisation matrix  $N$ .

The masses of the sleptons are given in table 4.15. The masses are quite light with nearly degenerated masses in the left and right sector, respectively. Only the stau

	$\tilde{\ell}_1$	$\tilde{\ell}_2$	$\tilde{\ell}_3$	$\tilde{\ell}_4$	$\tilde{\ell}_5$	$\tilde{\ell}_6$
$\tilde{e}_L$	0.000	0.000	-1.000	0.000	0.000	0.000
$\tilde{\mu}_L$	0.000	1.000	0.000	0.000	0.009	0.000
$\tilde{\tau}_L$	-0.989	0.000	0.000	0.000	0.000	0.145
$\tilde{e}_R$	0.000	0.000	0.000	1.000	0.000	0.000
$\tilde{\mu}_R$	0.000	-0.009	0.000	0.000	1.000	0.000
$\tilde{\tau}_R$	0.145	0.000	0.000	0.000	0.000	0.989
Mass [GeV]	176.112	175.185	175.181	126.244	126.240	124.956

**Table 4.15:** Slepton mixing and mass spectrum for Scenario B. Given is the diagonalisation matrix  $U \equiv V \in \mathbb{R}$ .

mass differs by about 1 GeV from the other sleptons due to a small mixing of the left and right stau states. Also the mass splitting between the left and right states is about 50 GeV, so all states are within the reach of a  $\sqrt{s} = 500$  GeV collider. Figure 4.4 shows the production cross section for selectron production. The cross sections for pair production are  $\sigma_{RR} = 490$  fb and  $\sigma_{LL} = 553$  fb at  $\sqrt{s} = 500$  GeV. Their maximum is reached at about  $\sqrt{s} \approx 400$  GeV. The associate production reaches a cross section of  $\sigma_{RL} = 14.1$  fb at  $\sqrt{s} = 500$  GeV, while its maximum of  $\sigma_{RL} = 26.7$  fb is reached at  $\sqrt{s} = 1$  TeV. Already at  $\sqrt{s} = 800$  GeV, however, it has reached  $\sigma_{RL} = 27.9$  fb. So, generally, for the study of  $CP$  violation a collider energy higher than  $\sqrt{s} = 500$  GeV would be desirable, while the gain is largest already for  $\sqrt{s} = 800$  GeV.

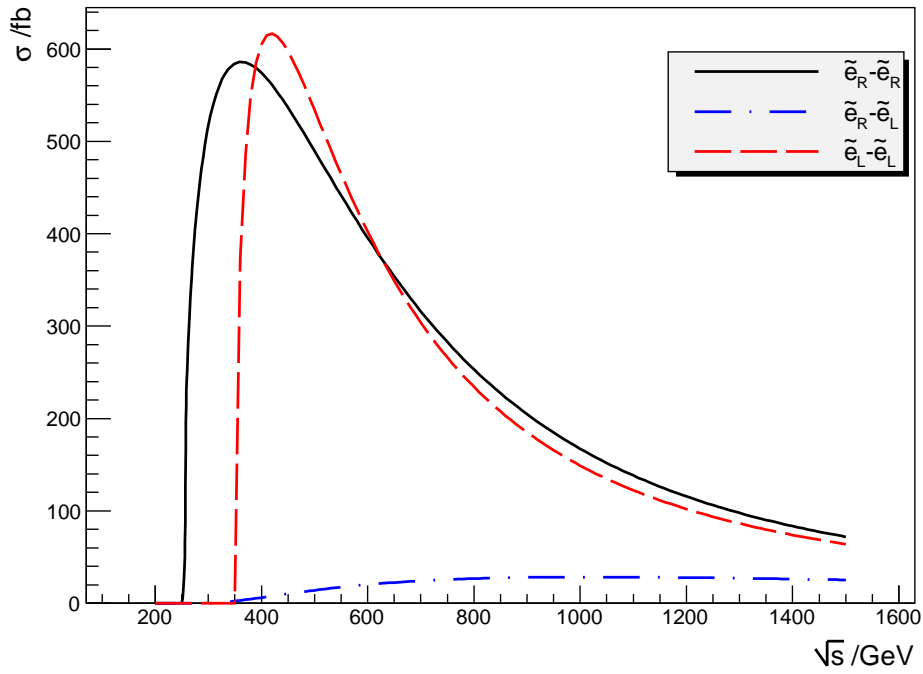


**Figure 4.4:** Total cross sections for the selectron production channels  $e^-e^- \rightarrow \tilde{e}_{R/L}\tilde{e}_{R/L}$  as a function of the centre of mass energy  $\sqrt{s}$  in the scenario Scenario B. Both beams are unpolarised.

## 4.5 Pure $\tilde{H}_a^0$ and $\tilde{H}_b^0$ : Scenario C

*This is again a higgsino-like scenario without the GUT-relation. In contrast to the former it features nearly pure  $\tilde{H}_a^0$  and  $\tilde{H}_b^0$  and a smaller mass splitting between the higgsinos on the one hand and the gauginos on the other.*

This scenario again does not use gaugino mass unification, i. e. the gaugino mass parameters  $M_1$  and  $M_2$  are treated as independent. They are assumed to be approximately equal in size with  $M_1 < M_2$ .

The small values  $\mu = 120$  GeV and  $\tan\beta = 3$  (see table 4.16) result in a pure higgsino character for both lighter neutralinos, whereas the heavier ones are nearly pure gauginos. The ordering of  $M_1$  and  $M_2$  leads to a wino-like  $\tilde{\chi}_3^0$ , whereas  $\tilde{\chi}_4^0$  is mainly a bino [132, table 2]. Both masses are of nearly equal size, though  $\tilde{\chi}_3^0$  contains a strong bino admixture. The mass splitting between the higgsino ( $\tilde{\chi}_1^0, \tilde{\chi}_2^0$ ) and the gaugino ( $\tilde{\chi}_3^0, \tilde{\chi}_4^0$ ) states is quite large. Whereas the former have masses of order  $\mu$ , the latter have masses of order  $M_1$  and  $M_2$ , respectively. The neutralino masses and mixing for this scenario are given in table 4.17.

$M_1$	[GeV]	430.000	$\phi_{M_1}$	0.000
$\mu$	[GeV]	120.000	$\phi_\mu$	0.000
$M_2$	[GeV]	440.000	$\tan\beta$	3.000
$m_{\tilde{\chi}_1^\pm}$	[GeV]	106.879	$m_{\tilde{\chi}_2^\pm}$	[GeV] 457.721

**Table 4.16:** Low energy input parameters and  $\tilde{\chi}^\pm$ -masses for Scenario C.

	$\tilde{\chi}_1^0$	$\tilde{\chi}_2^0$	$\tilde{\chi}_3^0$	$\tilde{\chi}_4^0$
$\tilde{\gamma}$	0.003 0.000 <i>i</i>	-0.230 0.000 <i>i</i>	0.851 0.000 <i>i</i>	0.473 0.000 <i>i</i>
$\tilde{Z}$	0.000 -0.001 <i>i</i>	0.000 0.076 <i>i</i>	0.000 -0.469 <i>i</i>	0.000 0.880 <i>i</i>
$\tilde{H}_a^0$	-0.990 0.000 <i>i</i>	0.138 0.000 <i>i</i>	0.037 0.000 <i>i</i>	0.007 0.000 <i>i</i>
$\tilde{H}_b^0$	0.143 0.000 <i>i</i>	0.960 0.000 <i>i</i>	0.236 0.000 <i>i</i>	0.042 0.000 <i>i</i>
Mass [GeV]	100.690	123.118	431.725	460.703

**Table 4.17:** Neutralino mixing and mass spectrum for Scenario C. Given is the diagonalisation matrix  $N$ .

The masses of the neutralino states open up rich decay channels for the heavier states.  $\tilde{\chi}_2^0$  is in this scenario the NLSP and can consequently only decay via three-body decays  $\tilde{\chi}_2^0 \rightarrow \tilde{\chi}_1^0 f f'$  to the LSP as  $R$ -parity is assumed to be conserved.



	$\tilde{\ell}_1$	$\tilde{\ell}_2$	$\tilde{\ell}_3$	$\tilde{\ell}_4$	$\tilde{\ell}_5$	$\tilde{\ell}_6$
$\tilde{e}_L$	0.000	0.000	-1.000	0.000	0.000	0.000
$\tilde{\mu}_L$	0.000	1.000	0.000	0.004	0.000	0.000
$\tilde{\tau}_L$	-0.998	0.000	0.000	0.000	0.000	0.070
$\tilde{e}_R$	0.000	0.000	0.000	0.000	1.000	0.000
$\tilde{\mu}_R$	0.000	-0.004	0.000	1.000	0.000	0.000
$\tilde{\tau}_R$	0.070	0.000	0.000	0.000	0.000	0.998
Mass [GeV]	165.926	165.496	165.495	136.455	135.785	135.625

**Table 4.18:** Slepton mixing and mass spectrum for Scenario C. Given is the diagonalisation matrix  $U \equiv V \in \mathbb{R}$ .

These types of scenarios have been studied for neutralino production at an  $e^+e^-$  collider with respect to the determination of the  $CP$  phases [123]. Scenario C will therefore be used to compare the  $e^+e^-$  and the  $e^-e^-$  mode.

The total unpolarised production cross sections shown in figure 4.5 are comparable with those in the other higgsino-like scenarios discussed. For pair production, cross sections of  $\sigma_{RR} = 489$  fb and  $\sigma_{LL} = 337$  fb are found at  $\sqrt{s} = 500$  GeV, respectively. In associate production, however, the total unpolarised cross section reaches only about  $\sigma_{RL} = 18$  fb, which slowly rises to about  $\sigma_{RL} \approx 32$  fb at much higher energies of  $\sqrt{s} \approx 1$  TeV.

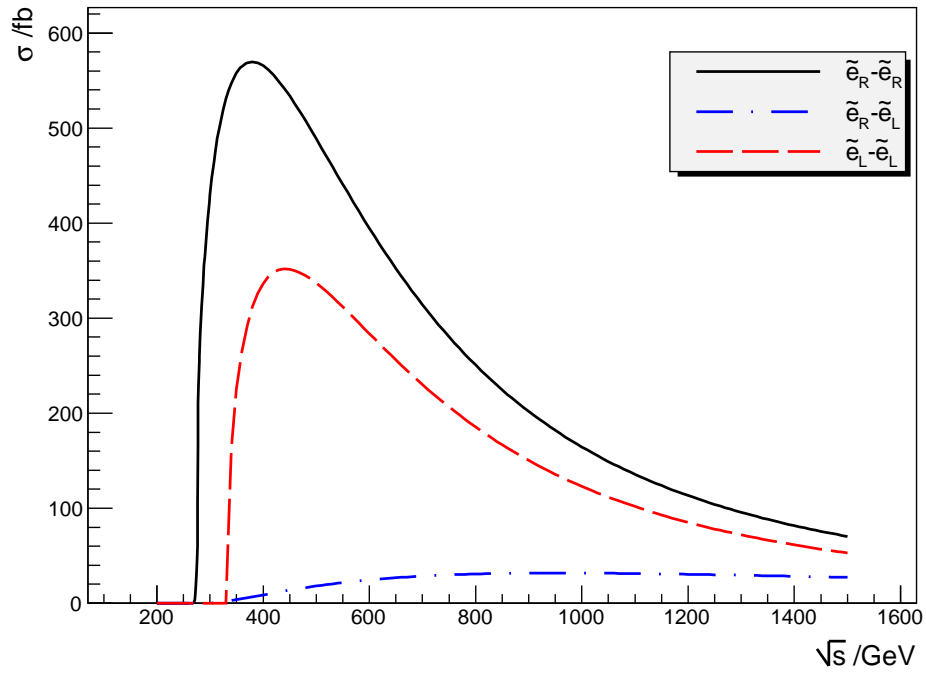


**Figure 4.5:** Total cross sections for the selectron production channels  $e^-e^- \rightarrow \tilde{e}_{R/L} \tilde{e}_{R/L}$  as a function of the centre of mass energy  $\sqrt{s}$  in the scenario Scenario C. Both beams are unpolarised.

## 4.6 Gaugino-like, $\tilde{G}$ LSP: Point $\varepsilon$

*The decay modes of the sleptons change drastically once a gravitino ( $\tilde{G}$ ) is the LSP. Such a scenario is discussed here together with the consequences for the observation of LFV, the mass spectrum and the production cross sections for selectrons.*

In the context of gravitino dark matter, scenarios were suggested that feature a *gravitino* as LSP (e. g., [120]). Here, the lighter  $\tilde{\tau}$  is often assumed to be the NLSP. As a consequence, the decay modes of the supersymmetric particles change considerably compared to the scenarios with a neutralino LSP discussed so far [133].

As in such scenarios the  $\tilde{\tau}_1$  as NLSP has to decay to the gravitino via  $\tilde{\tau}_1 \rightarrow \tau\tilde{G}$  a common feature of many of these models are long living staus due to the small coupling involved in this decay. This leads to unique detector signatures for the sleptons. Especially, if the two-body decay  $\tilde{\ell} \rightarrow \tilde{\chi}_1^0 \ell$  is kinematically forbidden (in most scenarios for the right sleptons), the sleptons will decay dominantly via three-body decays  $\tilde{\ell} \rightarrow \tau\tilde{\tau}\ell$ , whereas the direct decay to the LSP ( $\tilde{\ell} \rightarrow \ell\tilde{G}$ ) is strongly suppressed. In case of flavour conservation one would thus observe a  $\tilde{\tau}$  in association with a  $\tau$  from the selectron decay

$$\tilde{e} \rightarrow \tilde{\tau}^\pm \tau^\mp e \quad (4.2)$$

resulting in

$$e^- e^- \rightarrow \tilde{e}^- \tilde{e}^- \rightarrow \tilde{\tau}^\pm \tau^\mp e^- \quad \tilde{\tau}^\pm \tau^\mp e^-. \quad (4.3)$$

Thus, two electrons together with two taus and two staus would be observed, where the charge summed over the tau and stau states has to vanish. Then the following detector signatures arise

$$\begin{aligned} 2e^- 2\tilde{\tau}_1^+ 2\tau^-, \\ 2e^- 2\tilde{\tau}_1^- 2\tau^+, \\ 2e^- \tilde{\tau}_1^+ \tilde{\tau}_1^- \tau^- \tau^+. \end{aligned}$$

In flavour violating scenarios, however, one could observe one  $\tilde{\tau}$  directly resulting from the flavour violating production process

$$e^- e^- \rightarrow \tilde{\tau}_1 \tilde{e}.$$

Another  $\tilde{\tau}$  would then result from the three-body selectron decay (4.2), but this time with an associated  $\tau$  and an electron:

$$e^- e^- \rightarrow \tilde{\tau}_1 \tilde{e} \rightarrow \tilde{\tau}_1 + e \tilde{\tau}_1^\pm \tau^\mp. \quad (4.4)$$

This would yield the signatures

$$\begin{aligned} & 2\tilde{\tau}_1^- \tau^+ e^-, \\ & \tilde{\tau}_1^- \tilde{\tau}_1^+ \tau^- e^- \end{aligned}$$

giving the possibility to distinguish between the flavour conserving production of  $\tilde{\tau}_1$  via the decay of selectrons and the flavour violating scenario.

Due to the long lifetimes of the  $\tilde{\tau}$  it would be visible by an ionised track. Depending on its actual lifetime, the  $\tilde{\tau}$  could

- decay outside the detector and leave a track without a decay vertex
- decay within the detector for shorter lifetimes and resulting in a displaced vertex at the end of the track.

This clean signature gives a background free measurement of the flavour violating vertex in the  $e^- e^-$  mode [23].

The decay width of the  $\tilde{\tau}_1$ , being dominated by the two-body decay  $\tilde{\tau}_1 \rightarrow \tau \tilde{G}$ , is given by [134, 135]

$$\Gamma_{\tilde{\tau}_1} = \frac{(m_{\tilde{\tau}_1}^2 - m_{\tilde{G}}^2 - m_\tau^2)^4}{48\pi M_P^2 m_{\tilde{G}}^2 m_{\tilde{\tau}_1}^3} \left( 1 - \frac{4m_{\tilde{G}}^2 m_{\tilde{\tau}_1}^2}{(m_{\tilde{\tau}_1}^2 - m_{\tilde{G}}^2 - m_\tau^2)^2} \right)^{\frac{3}{2}} \quad (4.5)$$

$$= \frac{1}{48\pi M_P^2} \frac{m_{\tilde{\tau}_1}^5}{m_{\tilde{G}}^2} \left( 1 - \frac{m_{\tilde{G}}^2}{m_{\tilde{\tau}_1}^2} \right)^{\frac{3}{2}}. \quad (4.6)$$

Here,  $m_{\tilde{\tau}_1}$  is the mass of the  $\tilde{\tau}_1$ ,  $m_\tau \approx 1.77$  GeV is the  $\tau$ -mass, and  $m_{\tilde{G}}$  is the mass of the gravitino. With  $m_{\tilde{\tau}_1} = 150$  GeV (approximately the mass in Point  $\varepsilon$ ), this gives a lifetime for this particle of  $1/\Gamma_{\tilde{\tau}_1} = 7762$  s for  $m_{\tilde{G}} = 1$  GeV. For a gravitino mass of 100 GeV this lifetime increases to 25.9 years. It can be used to calculate the *mean decay length*  $L$  by

$$L = \frac{\beta\gamma}{\Gamma_{\tilde{\tau}_1}}. \quad (4.7)$$

From this follows, only if the gravitino mass is below 1 keV the stau can decay within the detector (assuming  $\beta\gamma = \mathcal{O}(1)$ ) [134]. However, it was shown that the staus can be stopped in the detector to allow the measurement of their decay [136]. The benchmark point Point  $\varepsilon$  is a mSUGRA scenario with the features just described [120]. As a typical GUT-scenario, it features mass unification and is defined by high scale parameters which can be found in table 4.19.

Evolving these parameters to the weak scale, using SPHENO [124] yields the low scale parameters of table 4.20. From these parameters, the resulting neutralino spectrum is calculated (table 4.21). The lighter two neutralinos are pure gauginos, which is a direct consequence of the large value of the  $\mu$  parameter compared to the gaugino masses. For this reason they have large couplings to the sleptons, which

$$\begin{array}{l|l} M_{1/2} = 440 \text{ GeV} & \text{sign}(\mu) = +1 \\ M_0 = 20 \text{ GeV} & \tan \beta = 15 \\ A_0 = -25 \text{ GeV} & \end{array}$$

**Table 4.19:** High scale input parameters of scenario Point  $\varepsilon$  [120].  $M_{1/2}$  is the universal gaugino mass,  $M_0$  the universal scalar mass, and  $A_0$  the universal trilinear coupling. All these are defined at the GUT-scale  $M_{\text{GUT}}$ .  $\tan \beta$  gives the ratio of the vacuum expectation values and  $\text{sign}(\mu)$  the sign of the higgsino mass parameter  $\mu$

results in high cross sections. As  $M_1 < M_2$ , the lighter neutralino is mainly a bino, and  $\tilde{\chi}_2^0$  mainly a wino. The heavier two neutralinos are nearly pure higgsinos with an almost equal mixture of  $\tilde{H}_a^0$  and  $\tilde{H}_b^0$  components. As they contain only negligible gaugino components, their contribution to the cross section is small. The pure nature of the neutralinos is supported by the larger value of  $\tan \beta = 15$ . Generally, the masses of the neutralinos are larger than in former scenarios:  $m_{\tilde{\chi}_1^0} \approx M_1$  and  $m_{\tilde{\chi}_2^0} \approx M_2$ , whereas the heavier two have masses of the order of  $\mu$ .

$M_1$	[GeV]	185.830	$\phi_{M_1}$	0.000
$\mu$	[GeV]	557.330	$\phi_\mu$	0.000
$M_2$	[GeV]	342.820	$\tan \beta$	15.000
$m_{\tilde{\chi}_1^\pm}$	[GeV]	330.030	$m_{\tilde{\chi}_2^\pm}$	[GeV] 576.328

**Table 4.20:** Low energy input parameters and  $\tilde{\chi}^\pm$ -masses for Point  $\varepsilon$ .

	$\tilde{\chi}_1^0$	$\tilde{\chi}_2^0$	$\tilde{\chi}_3^0$	$\tilde{\chi}_4^0$
$\tilde{\gamma}$	0.862 0.000 <i>i</i>	-0.497 0.000 <i>i</i>	0.042 0.000 <i>i</i>	0.090 0.000 <i>i</i>
$\tilde{Z}$	-0.504 0.000 <i>i</i>	-0.825 0.000 <i>i</i>	0.151 0.000 <i>i</i>	0.206 0.000 <i>i</i>
$\tilde{H}_a^0$	0.000 0.006 <i>i</i>	0.000 -0.070 <i>i</i>	0.000 0.660 <i>i</i>	0.000 -0.748 <i>i</i>
$\tilde{H}_b^0$	0.049 0.000 <i>i</i>	0.261 0.000 <i>i</i>	0.735 0.000 <i>i</i>	0.624 0.000 <i>i</i>
Mass [GeV]	183.969	330.326	561.531	575.886

**Table 4.21:** Neutralino mixing and mass spectrum for Point  $\varepsilon$ . Given is the diagonalisation matrix  $N$ .

The slepton sector is defined in table 4.22. Though  $\mu$  is much larger than in the former scenarios, this does not lead to a large LR mixing in the  $\tilde{\tau}$  sector due to the large A-parameter  $A_{\tilde{\tau}} = -34$ . As the masses of the particles in this scenario are not too heavy, it might be accessible at early stages of the LHC. Additionally,

	$\tilde{\ell}_1$	$\tilde{\ell}_2$	$\tilde{\ell}_3$	$\tilde{\ell}_4$	$\tilde{\ell}_5$	$\tilde{\ell}_6$
$\tilde{e}_L$	0.000	0.000	-1.000	0.000	0.000	0.000
$\tilde{\mu}_L$	0.000	1.000	0.000	0.000	0.014	0.000
$\tilde{\tau}_L$	-0.980	0.000	0.000	0.000	0.000	0.199
$\tilde{e}_R$	0.000	0.000	0.000	1.000	0.000	0.000
$\tilde{\mu}_R$	0.000	-0.014	0.000	0.000	1.000	0.000
$\tilde{\tau}_R$	0.199	0.000	0.000	0.000	0.000	0.980
Mass [GeV]	314.908	306.082	306.052	177.257	177.154	150.333

**Table 4.22:** Slepton mixing and mass spectrum for Point  $\varepsilon$ . Given is the diagonalisation matrix  $U \equiv V \in \mathbb{R}$ .

first measurements are already possible at a 500 GeV linear collider like the ILC, though some channels would require an energy upgrade.

The cross sections for the selectron production channels are shown in figure 4.6. Due to the masses of the selectrons a higher collider energy is required to access the LL-channel. Also the RL-channel only has a small cross section at 500 GeV. For this scenario an energy upgrade to 800 GeV would be desirable for the RL- and LL-channels. However, in the  $RR$ -channel a cross section of nearly 700 fb is reached at about  $\sqrt{s} = 500$  GeV.

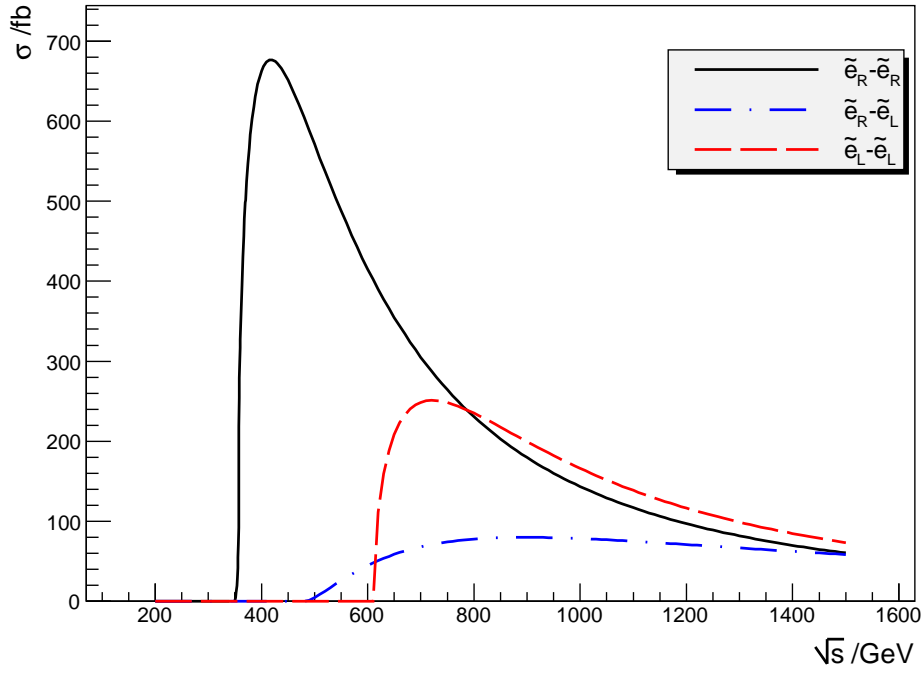


**Figure 4.6:** Total cross sections for the selectron production channels  $e^-e^- \rightarrow \tilde{e}_{R/L}\tilde{e}_{R/L}$  as a function of the centre of mass energy  $\sqrt{s}$  in the scenario Point  $\varepsilon$ . Both beams are unpolarised.

## 4.7 GMSB, $\tilde{G}$ -LSP: SPS 7

*SPS 7 again features a gravitino LSP. Additionally, it serves as an example for a scenario resulting from gauge mediated SUSY breaking. As in Point  $\varepsilon$ , the lighter stau is again the NLSP. This section gives the mass spectrum for SPS 7 and discusses the production cross section for selectrons in this scenario.*

The benchmark point SPS 7 [118] is, in contrast to the scenarios discussed so far, a supersymmetric scenario with gauge mediated SUSY breaking. Like the scenario Point  $\varepsilon$  discussed in section 4.6, it features a  $\tilde{\tau}$  as the NLSP. The three-body decays of the  $\tilde{e}$  and  $\tilde{\mu}$  to the NLSP are allowed and are thus their dominant decay modes. The GUT-scale parameters defining SPS 7 are given in table 4.23.

$$\begin{array}{lcl} \Lambda & = & 40 \text{ TeV} \\ M_{\text{mess}} & = & 80 \text{ GeV} \\ N_{\text{mess}} & = & 3 \end{array} \quad \left| \quad \begin{array}{lcl} \text{sign}(\mu) & = & +1 \\ \tan \beta & = & 15 \end{array} \right.$$

**Table 4.23:** High scale input parameters of scenario SPS 7 [118]. The ratio of the vacuum expectation values is given by  $\tan \beta$  and  $\text{sign}(\mu)$  is the sign of the higgsino mass parameter  $\mu$ . As this is a GMSB-type scenario  $M_{\text{mess}}$  gives the mass scale for the messengers and  $N_{\text{mess}}$  their number. Finally, the parameter  $\Lambda$  gives the scale of the hidden sector involved in SUSY breaking.

Evolving the high scale parameters to the electro-weak scale by means of SPHENO [124] gives the low scale parameters in table 4.24. As can be seen from table 4.25 the lightest neutralino is mainly a gaugino, but all others are of quite mixed nature. This had to be expected, as  $M_2$  is in the vicinity of  $\mu$ . The gaugino mass parameter  $M_2 \approx 325 \text{ GeV}$  yields a  $\tilde{\chi}_3^0$  of approximately this mass, hence most neutralino states will be accessible at a linear collider of  $\sqrt{s} = 500 \text{ GeV}$ .

$M_1$	[GeV]	173.600	$\phi_{M_1}$	0.000
$\mu$	[GeV]	315.700	$\phi_\mu$	0.000
$M_2$	[GeV]	325.400	$\tan \beta$	15.000
$m_{\tilde{\chi}_1^\pm}$	[GeV]	264.185	$m_{\tilde{\chi}_2^\pm}$	[GeV] 385.603

**Table 4.24:** Low energy input parameters and  $\tilde{\chi}^\pm$ -masses for SPS 7.

The slepton sector of this scenario features intermediate masses where at least in associate production all sleptons are kinematically accessible at an energy of



	$\tilde{\chi}_1^0$	$\tilde{\chi}_2^0$	$\tilde{\chi}_3^0$	$\tilde{\chi}_4^0$
$\tilde{\gamma}$	0.812 0.000 <i>i</i>	-0.526 0.000 <i>i</i>	0.140 0.000 <i>i</i>	0.209 0.000 <i>i</i>
$\tilde{Z}$	-0.527 0.000 <i>i</i>	-0.486 0.000 <i>i</i>	0.490 0.000 <i>i</i>	0.496 0.000 <i>i</i>
$\tilde{H}_a^0$	0.000 0.012 <i>i</i>	0.000 -0.100 <i>i</i>	0.000 0.663 <i>i</i>	0.000 -0.742 <i>i</i>
$\tilde{H}_b^0$	0.250 0.000 <i>i</i>	0.691 0.000 <i>i</i>	0.548 0.000 <i>i</i>	0.401 0.000 <i>i</i>
Mass [GeV]	167.244	267.717	321.740	385.779

**Table 4.25:** Neutralino mixing and mass spectrum for SPS 7. Given is the diagonalisation matrix  $N$ .

	$\tilde{\ell}_1$	$\tilde{\ell}_2$	$\tilde{\ell}_3$	$\tilde{\ell}_4$	$\tilde{\ell}_5$	$\tilde{\ell}_6$
$\tilde{e}_L$	0.000	0.000	-1.000	0.000	0.000	0.000
$\tilde{\mu}_L$	0.000	1.000	0.000	0.000	0.009	0.000
$\tilde{\tau}_L$	-0.990	0.000	0.000	0.000	0.000	0.144
$\tilde{e}_R$	0.000	0.000	0.000	1.000	0.000	0.000
$\tilde{\mu}_R$	0.000	-0.009	0.000	0.000	1.000	0.000
$\tilde{\tau}_R$	0.144	0.000	0.000	0.000	0.000	0.990
Mass [GeV]	273.735	269.391	269.374	138.111	138.071	126.528

**Table 4.26:** Slepton mixing and mass spectrum for SPS 7. Given is the diagonalisation matrix  $U \equiv V \in \mathbb{R}$ .

$\sqrt{s} = 500$  GeV. The pair production of the left states requires higher energies, though. Again, the LR mixing in the  $\tilde{\tau}$  sector is suppressed due to the smallness of the trilinear couplings in this scenario. Generally, the slepton spectrum is lighter than in case of Point  $\varepsilon$ .

As can be seen from figure 4.7, the production cross section for right pair production reaches about 1100 fb at  $\sqrt{s} = 500$  GeV, whereas for associate production, and even more for left pair production, a higher energy of about  $\sqrt{s} \approx 600$  GeV would be preferable. At this energy, right  $\tilde{e}_R - \tilde{e}_R$  pair production is still at about 400 fb, which is slightly more than the cross section for  $\tilde{e}_L - \tilde{e}_L$  production of about 300 fb. Associate production reaches 100 fb at this energy. These features are similar to Point  $\varepsilon$ , though the cross section for the right pair production is almost twice as large at its optimal energy in SPS 7. This results from the smaller right selectron mass.

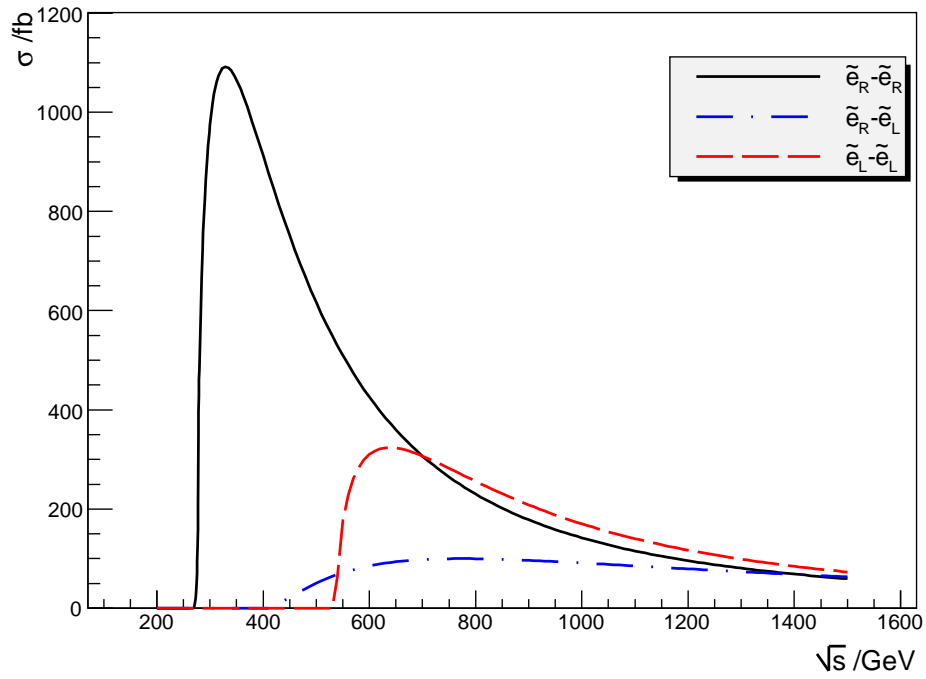


**Figure 4.7:** Total cross sections for the selectron production channels  $e^-e^- \rightarrow \tilde{e}_{R/L}\tilde{e}_{R/L}$  as a function of the centre of mass energy  $\sqrt{s}$  in the scenario SPS 7. Both beams are unpolarised.

---

## Chapter 5

# *CP* Violation

In this chapter the potential of an  $e^-e^-$ -collider for the determination of *CP* violating effects will be studied. This will be based on a *CP*-even as well as on a constructed *CP*-sensitive observable [132].

The total cross section, though of course a *CP*-even observable, shows a sensitive dependence on the *CP* phases in the neutralino sector, especially for the pair production of the left selectron. Extending the studies of [22] where the mixing of the neutralinos was neglected, the cross section as an observable for *CP* violation will be investigated in the scenarios introduced in chapter 4. Taking the full neutralino mixing into account, one finds a sensitive dependence of the total cross section to the phase  $\phi_{M_1}$  also for the associate production, though the effects are in general not as large as for  $\sigma_{LL}$ .

Exploiting transverse beam polarisation, the definition of a *CP*-sensitive observable based on triple product correlations in the process  $e^-e^- \rightarrow \tilde{e}_1\tilde{e}_2$  is possible. It is noteworthy that no *CP*-sensitive observables in the process  $e^+e^- \rightarrow \tilde{e}_i\tilde{e}_j$  can be constructed as all triple product correlations in question are proportional to the LR mixing of the selectrons which is generally negligible. This is true even if one could use transverse beam polarisation. However, a similar observable can be constructed in *neutralino production* with subsequent decay of the neutralinos to sleptons [123]. For this reason the process discussed here may be complementary to the studies in  $e^+e^- \rightarrow \tilde{\chi}_i^0\tilde{\chi}_j^0$  with subsequent decays [105, 108, 137–140]. Depending on the masses and decay modes of the neutralinos the new observable in the  $e^-e^-$  mode may give additional insight and may probably reveal *CP* violation in the neutralino system even if the effects in  $e^+e^-$  are too small.

## 5.1 Squared Amplitude

*In this section the squared amplitude is examined in the light of the construction of a suitable CP-sensitive observable. It is found that transverse polarisation is necessary to reach this goal.*

In order to define CP-sensitive observables, the squared amplitude for the production process has to be examined. Neglecting flavour violation, this is given for associate production  $e^-e^- \rightarrow \tilde{e}_i\tilde{e}_j$  ( $i, j = 1, 2, i \neq j$ ) of selectron mass eigenstates, (2.16), as

$$|M_{ij}|^2 = |M_{ij}^t|^2 + |M_{ij}^u|^2 + 2\Re\{M_{ij}^t M_{ij}^{u\dagger}\}. \quad (5.1)$$

The following discussion is also valid for non-vanishing LR mixing, but for the numerical evaluation only the associate production  $e^-e^- \rightarrow \tilde{e}_L\tilde{e}_R$  is taken into account, that is  $\tilde{e}_1 = \tilde{e}_R$  and  $\tilde{e}_2 = \tilde{e}_L$ .

To define the transverse polarisation four-vectors of the electron beams, a right handed coordinate system  $(x, y, z)$  is introduced with the  $z$ -axis along the momentum of the incoming electron  $e_1^-(p_1)$ . The  $x$ - and  $y$ -axes, however, are not defined with respect to the production plane, but fixed in the laboratory system [11]. In this coordinate system, the transverse beam polarisation four-vectors are

$$t^{1,2} = (0, \cos \phi_{1,2}, \sin \phi_{1,2}, 0), \quad (5.2)$$

with  $\phi_1$  and  $\phi_2$  the azimuthal angles of the polarisation vectors for electron  $e_1^-$  and  $e_2^-$ , respectively.

With this definition, the amplitude squared for the associate production process  $e^-e^- \rightarrow \tilde{e}_1\tilde{e}_2$  can be written as

$$|M_{12}^{t,u}|^2 = -\frac{g^4}{4}s(E_{\tilde{e}_2}^2 - q^2 \cos^2 \theta - m_{\tilde{e}_{2,1}}^2)c_{\pm\mp} \sum_{k,l=1}^4 f_k^{L*} f_l^L f_k^{R*} f_l^R \Delta_k^{t,u} \Delta_l^{t,u*}, \quad (5.3)$$

while the interference term of  $t$ - and  $u$ -channel yields

$$\begin{aligned} 2\Re\{M_{12}^t M_{12}^{u\dagger}\} &= \frac{g^4}{2} P_T^1 P_T^2 q^2 s \sin^2 \theta \sum_{k,l=1}^4 \Delta_k^t \Delta_l^{u*} \\ &\times \Re\{f_k^{L*} f_l^L f_k^{R*} f_l^R \\ &\quad [\cos(\eta - 2\phi) - i \sin(\eta - 2\phi)]\}, \end{aligned} \quad (5.4)$$

where  $c_{\pm\mp} = (1 \pm P_L^1)(1 \mp P_L^2)$ .  $P_L^i$  denotes the degree of longitudinal polarisation,  $q = \lambda^{1/2}(s, m_{\tilde{e}_1}^2, m_{\tilde{e}_2}^2)/(2\sqrt{s})$  the momentum transfer,  $m_{\tilde{e}_i}$  are the selectron masses,  $\eta = \phi_1 + \phi_2$ ,  $\theta$  and  $\phi$  being the polar and azimuthal angle of  $\tilde{e}_2$ . The energy of the second electron is  $E_{\tilde{e}_2} = (s + m_{\tilde{e}_2}^2 - m_{\tilde{e}_1}^2)/(2\sqrt{s})$ , and  $P_T^i$  denotes the degree of transverse polarisation for the electron  $e_i^-$  [132].

It should be noted that in case of a selectron mixing angle of  $\pi$  (i. e.  $\tilde{e}_1 = \tilde{e}_L$ ), the squared amplitude is obtained by replacing  $c_{\pm\mp} \rightarrow c_{\mp\pm}$  in (5.3), and by changing the overall sign in (5.4).

Using these equations, one finally arrives at the differential cross section for the production process:

$$\frac{d\sigma}{d\Omega} = \frac{1}{8(2\pi)^2} \frac{q}{s^{3/2}} |M_{12}|^2 \quad (5.5)$$

with  $d\Omega = \sin\theta d\theta d\phi$  and  $|M_{12}|^2$  as given in (5.1).

The  $CP$ -sensitive part of the cross section derived from (5.4) is proportional to

$$P_T^1 P_T^2 \sum_{k<l}^4 (\Delta_k^t \Delta_l^u - \Delta_l^t \Delta_k^u) \Im m\{f_k^{L*} f_l^L f_k^{R*} f_l^R\}. \quad (5.6)$$

This term vanishes due to symmetry of the propagators if integrated over the whole polar angle  $\theta$ . Therefore, in order to build a  $CP$ -sensitive observable, the integration over  $\theta$  has to be split into two regions amounting to a sign change of  $\cos\theta$ , which has to be incorporated into a projection function to be defined [123]. From (5.6) it is also clear that the transverse polarisation of both beams is necessary. This seems to favour the  $e^-e^-$  mode due to the higher polarisations possible for electrons. Here, beam polarisations of 0.9 seem possible yielding a prefactor of  $0.9^2 = 0.81$  [11, 141]. (Using the more conservative values of [10] it would still be  $0.8^2 = 0.64$ .) The polarisation of positrons conversely hand required in  $e^+e^-$  mode seems to be possible only to about 0.6 (0.4) without too much loss of luminosity. Thus, in this particular mode, a similar term would get a weight of only 0.54 (0.32) or about 66% (50%) compared to the  $e^-e^-$  mode, even if it would not be negligible.

## 5.2 Definition of the Observables

*This section discusses the possible observables suitable for the examination of  $CP$  violating effects in the production of selectrons in  $e^-e^-$ -scattering. After a short discussion of the use of the total cross section for the observation of  $CP$  violation, a new  $CP$ -odd observable is derived based upon triple products for transversely polarised beams.*

### 5.2.1 $CP$ -Even Observables

It has already been pointed out that the total cross section for selectron pair production can sensitively depend on the phase of  $M_1$ . This dependence is un-

suppressed in the case of LL-production, as it results from interferences of bino- and wino-like neutralino propagators in the  $t$ - and  $u$ -channel [22]. As right selectrons, however, couple only to the bino component of the neutralinos, these terms get strong suppressions in the case of LR production, and nearly vanish for the production of two right selectrons. (They vanish exactly in the pure bino limit of neutralino mixing.)

The total cross section of left selectron pair production itself might prove a useful observable in case all involved SUSY parameters, except the phases, are known. It then allows access to the phase of  $M_1$  by fitting the measured total cross section to the SUSY scenario. Being *CP*-even, on the other hand, makes this fit rather dependent on the precision of the SUSY parameters measured in other processes. It should also be stressed that the measurement of a specific value for the total cross section does not suffice to establish *CP* violation in the neutralino system without the knowledge of many other parameters.

## 5.2.2 *CP*-Sensitive Observables

The *CP*-sensitive part of the cross section (5.6) is proportional to the product  $P_1^T \cdot P_2^T$  of the transverse polarisation. To define the degrees of polarisation  $P_i^T$  ( $i = 1, 2$ ) with respect to the production plane it is necessary to reconstruct momentum vectors of the produced sleptons from their decays. Although these decays involve the production of the LSP, which will escape detection, it has been shown that this reconstruction is possible taking the decay of both sleptons into account. Generally, this reconstruction has a one- or two-fold ambiguity, which however, may be resolved if suitable decays are available [11, 123]. Then, it is possible to build a *CP*-sensitive observable for the production process. Due to the scalar character of the selectrons, there exist no spin correlations between production and decay. For this reason it is not possible to construct *CP*-sensitive triple product correlations of momenta as in the case of neutralinos and charginos [60, 109, 142]. In  $e^-e^- \rightarrow \tilde{e}_i\tilde{e}_j$ , a *CP*-sensitive observable has to exploit the  $t - u$ -interference term (5.4). To this end, one first defines a  $\theta$ -dependent asymmetry

$$A_{CP}(\theta) = \frac{N[\sin(\eta - 2\phi) > 0; \theta] - N[\sin(\eta - 2\phi) < 0; \theta]}{N[\sin(\eta - 2\phi) > 0; \theta] + N[\sin(\eta - 2\phi) < 0; \theta]} \quad (5.7)$$

$\eta$  denotes the relative angle of the two transverse polarisation vectors of the incoming electrons.  $\theta$  and  $\phi$  are the usual phase space angles. (Note the relative sign of the two spin coordinate systems with respect to the azimuthal angle  $\phi$ .)  $N[\sin(\eta - 2\phi) > 0 (< 0)]$  denotes the number of events with  $\sin(\eta - 2\phi) > 0 (< 0)$ . So, in integral form,  $A_{CP}(\theta)$  can be written as

$$A_{CP}(\theta) = \frac{1}{\sigma} \left[ - \int_{\frac{\eta}{2}}^{\frac{\pi}{2} + \frac{\eta}{2}} + \int_{\frac{\pi}{2} + \frac{\eta}{2}}^{\pi + \frac{\eta}{2}} - \int_{\pi + \frac{\eta}{2}}^{\frac{3\pi}{2} + \frac{\eta}{2}} + \int_{\frac{3\pi}{2} + \frac{\eta}{2}}^{2\pi + \frac{\eta}{2}} \right] \frac{d^2\sigma}{d\phi d\theta} d\phi. \quad (5.8)$$

The integration over  $\theta$  in two half spheres yields

$$A_{CP} = \left[ \int_0^{\pi/2} - \int_{\pi/2}^{\pi} \right] A_{CP}(\theta) d\theta. \quad (5.9)$$

This observable can be expressed as a moment of the total cross section [123]:

$$A_{CP} = \frac{1}{\sigma} \int d\phi d\theta \frac{d^2\sigma}{d\phi d\theta} \mathcal{F}_1(\theta, \phi). \quad (5.10)$$

With the projection function

$$\mathcal{F}_1 = \text{sign}(\cos \theta \sin 2\phi) \quad (5.11)$$

(5.7) can also be written as

$$A_{CP} = \frac{1}{N_{\text{tot}}} \left\{ N[s_{\eta'} > 0; c_\theta > 0] - N[s_{\eta'} > 0; c_\theta < 0] \right. \\ \left. + N[s_{\eta'} < 0; c_\theta < 0] - N[s_{\eta'} < 0; c_\theta > 0] \right\}$$

(where  $\eta' = \eta - 2\phi$ ). This observable has already been studied for neutralino production at the ILC where promising results have been found [123].

It can be shown that the observable (5.10) can be optimised using a more complicated projection function  $\mathcal{F}_2(\theta, \phi)$ , respecting the angular dependence of the differential cross section [143–147]. To this end, the relevant part of the squared amplitude is investigated which is given by

$$2\Re(M_{12}^t M_{12}^{u\dagger}) \propto \sin^2 \theta \sum_{k,l=1}^4 \Delta_k^t \Delta_l^{u*} \Re \left( f_k^{L*} f_l^L f_k^{R*} f_l^R \right. \\ \left. \times [\cos(\eta - 2\phi) - i \sin(\eta - 2\phi)] \right). \quad (5.12)$$

The optimal projection function would now be proportional to the angular dependence of this term including  $\cos \theta$  from the integration over  $d\Omega$ . For this reason, the most simple “optimised projection function” is defined as

$$\mathcal{F}_2 = \sin^2 \theta \cos \theta \sin(\eta - 2\phi). \quad (5.13)$$

This function could be further optimised by keeping the angular dependence stemming from the propagators  $\Delta_k^t$  and  $\Delta_l^{u*}$ ; but this would increase its complexity considerably, whereas (5.13) offers definite improvement compared to (5.11).

The  $CP$ -sensitive observable  $A_{CP}$  is given by the expectation values

$$A_{CP}[\mathcal{F}_i] = \frac{1}{\sigma} \langle \mathcal{F}_i \rangle = \frac{1}{\sigma} \int d\Omega \frac{d\sigma}{d\Omega} \mathcal{F}_i \quad (5.14)$$

of the projection functions  $\mathcal{F}_i$  from (5.11) and (5.13).

To construct the *final observable*, the statistical error has to be taken into account. It must not exceed the size of the observable itself, yielding the condition

$$\frac{\Delta\langle\mathcal{F}_i\rangle}{|\langle\mathcal{F}_i\rangle|} < 1 \quad (5.15)$$

with

$$\Delta\langle\mathcal{F}_i\rangle = \frac{\mathcal{N}_\sigma}{\sqrt{N}} \frac{1}{\sqrt{\langle\mathcal{F}_i^2\rangle - \langle\mathcal{F}_i\rangle^2}} \approx \frac{\mathcal{N}_\sigma}{\sqrt{N \cdot \langle\mathcal{F}_i^2\rangle}}. \quad (5.16)$$

Here,  $\mathcal{N}_\sigma$  are the standard deviations and  $N = \sigma\mathcal{L}$  the number of events obtained at the total cross section  $\sigma$  with an integrated luminosity  $\mathcal{L}$ . The effective *CP*-sensitive observable  $\hat{A}[\mathcal{F}_i]$  can now be given using the definition (5.16) of the error [132, 147]:

$$\hat{A}[\mathcal{F}_i] = \sqrt{\sigma} \frac{\langle\mathcal{F}_i\rangle}{\sqrt{\langle\mathcal{F}_i^2\rangle}}. \quad (5.17)$$

At a given integrated luminosity one can then estimate (5.16) being non-zero in standard deviations as

$$E_\sigma = |\hat{A}[\mathcal{F}_i]| \cdot \sqrt{\mathcal{L}}. \quad (5.18)$$

## 5.3 Numerical Results for *CP*-Violation

*This section evaluates the observables found numerically. The first part deals with general features, whereas subsequent sections evaluate the effects in the representative scenarios discussed in chapter 4. It is understood that especially in the higgsino like scenarios the new CP-sensitive observable might be helpful in the discovery of CP violation in the neutralino sector.*

### 5.3.1 General Features

#### ■ *GUT-Scenarios*

Within the study of the *CP*-sensitive observables for different neutralino mixtures one finds that the observable  $\hat{A}[\mathcal{F}_2]$  (and also  $\hat{A}[\mathcal{F}_1]$ ) rises with increasing higgsino component of the two lighter neutralinos. This results from the fact that



non- $CP$ -sensitive contributions to the total cross section decrease compared to the  $CP$ -sensitive parts when the higgsino component of the lighter two neutralinos increases. This corresponds to an increase of the relevant product of couplings  $\Im m\{f_k^{L*} f_l^L f_k^{R*} f_l^R\}$  resulting from neutralino mixing. The increase of the  $CP$ -sensitive observable with increasing higgsino components in the lighter two neutralinos, however, is accompanied by a decrease of the total production cross section of the selectrons. This results from the fact that the latter couple only to the gaugino component of the neutralinos.

Based on Scenario A defined in section 4.3, figure 5.1a shows the values of the effective optimised observable  $\hat{A}[\mathcal{F}_2]$ , (5.17) as a function of the higgsino mass parameter  $|\mu|$  and the gaugino mass parameter  $M_2$ . Here, the GUT-relation (2.4) between  $M_1$  and  $M_2$  is used. The corresponding production cross section is shown in figure 5.1b. It can be seen that the observable increases with the higgsino content of the lighter two neutralinos, reaching its largest absolute values of about  $\hat{A}[\mathcal{F}_2] = -0.1\sqrt{fb}$  in the higgsino region ( $\mu < M_2$ ), whereas the total cross section decreases to about 25% of its value in the gaugino region [132].

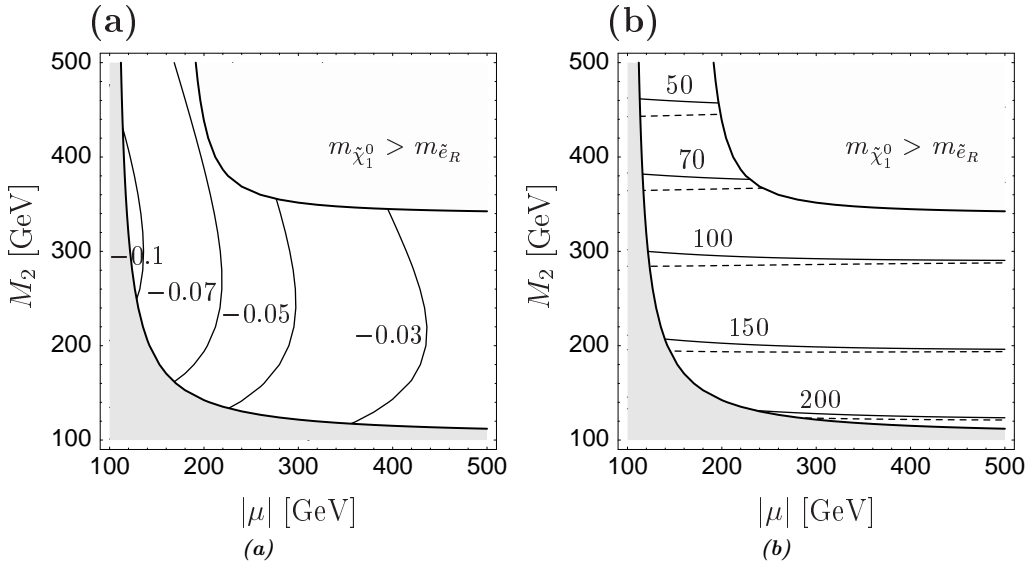


**Figure 5.1:** Contour lines of the effective observable  $\hat{A}[\mathcal{F}_2]$  in the  $|\mu| - M_2$  plane in units of  $\sqrt{fb}$  (figure 5.1a) and the corresponding production cross section in units of fb (figure 5.1b). The parameters which are not varied are from Scenario A defined in section 4.3. The shaded area is excluded by the chargino mass bound  $m_{\tilde{\chi}_1} < 104$  GeV, whereas the upper right corner would lead to  $m_{\tilde{\chi}^0} = m_{\text{LSP}} > m_{\tilde{e}_R}$  [132].

### ■ *Non-GUT-Scenarios*

non-GUT-scenarios an increase of the observable  $\hat{A}[\mathcal{F}_2]$  (as well as  $\hat{A}[\mathcal{F}_1]$ ) with an increase of the ratio  $|M_1|/M_2$  is also found. The increase of this ratio leads to a larger wino component in the lighter of the two gaugino-like neutralinos. For the GUT-relation, the lighter neutralino is always of bino-like nature, whereas it can become mainly a wino for  $|M_1|/M_2 > 1$ . The increase of the  $CP$ -sensitive observables in wino-like scenarios is again accompanied by a decrease of the total production cross section for the same reason as in higgsino like scenarios. As a representative example this is shown in figure 5.2a based on Scenario A for all parameters not varied.

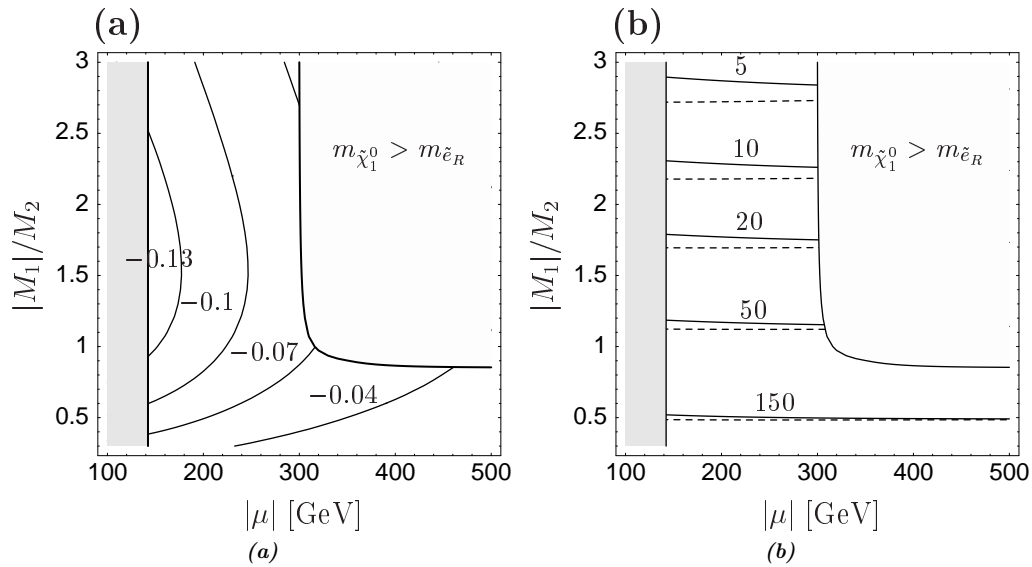


**Figure 5.2:** Contour lines of the effective observable  $\hat{A}[\mathcal{F}_2]$  in the  $|\mu| - |M_1|/M_2$  plane in units of  $\sqrt{fb}$  (figure 5.2a) and the corresponding production cross section in units of fb (figure 5.2b) with a fixed value of  $M_2 = 200$  GeV. All other parameters are from Scenario A defined in section 4.3. The shaded area is excluded by the chargino mass bound  $m_{\tilde{\chi}_1} < 104$  GeV, whereas the upper right corner would lead to  $m_{\tilde{\chi}_1^0} = m_{\text{LSP}} > m_{\tilde{e}_R}$  [132].

Above all, it can be concluded that the observables  $\hat{A}[\mathcal{F}_2]$  and  $\hat{A}[\mathcal{F}_1]$  are the largest in higgsino like scenarios where the lighter of the two gauginos has a dominant wino component.

### ■ *Dependence on $\tan \beta$ and $\phi_\mu$*

Different values of  $\tan \beta$  do not influence the  $CP$ -sensitive observable explicitly, but only via the mixing of the neutralinos. Larger values of  $\tan \beta$  lead to a stronger mix-

ing of the neutralino eigenstates, so for larger values, generally, gaugino-like neutralinos get a stronger higgsino component and vice versa. For the  $CP$ -sensitive observables  $\hat{A}[\mathcal{F}_1]$  and  $\hat{A}[\mathcal{F}_2]$ , this effect is two-fold. They decrease in the higgsino-like scenarios due to the stronger gaugino-admixture, whereas in gaugino-like scenarios they increase due to the stronger higgsino contribution. The effect is most pronounced for small values of  $\tan\beta$  and for gaugino-like scenarios. For example, going from  $\tan\beta = 5$  to  $\tan\beta = 10$  in SPS 1a' ( $\sqrt{s} = 500$  GeV,  $\phi_{M_1} = 0.5\pi, \phi_\mu = 0$ ), reduces the size of the observable by about 30%. At  $\tan\beta = 30$ , the observable  $\hat{A}[\mathcal{F}_2]$  is reduced by another 25% compared to  $\tan\beta = 10$ .

In higgsino-like scenarios, like Scenario C, the effect is less pronounced for larger values of  $\tan\beta$ . For  $\tan\beta = 10$ , again a reduction of  $\hat{A}[\mathcal{F}_2]$  of about 30% is found compared to  $\tan\beta = 5$ , but only about 10% comparing a scenario with  $\tan\beta = 10$  with one  $\tan\beta = 30$ . A general observation is that the size of the  $CP$ -sensitive observables strongly increases for small values of  $\tan\beta$ , whereas the dependence is weaker for large values. Generally,  $\hat{A}[\mathcal{F}_1]$  and  $\hat{A}[\mathcal{F}_2]$  show the same behaviour with respect to their  $\tan\beta$  dependence.

It can also be observed that the dependence of  $\hat{A}[\mathcal{F}_1]$  and  $\hat{A}[\mathcal{F}_2]$  on the phase  $\phi_\mu$  is much weaker than on the phase  $\phi_{M_1}$ . Investigating the relevant combination of couplings one finds  $\Im m\{f_k^{L*} f_l^L f_k^{R*} f_l^R\} \propto \sin\phi_{M_1}$ . This explains the strong dependence on  $\phi_{M_1}$  [132]. In most scenarios considered here, the dependence of  $\hat{A}[\mathcal{F}_1]$  and  $\hat{A}[\mathcal{F}_2]$  on the phase  $\phi_\mu$  is opposite to that on  $\phi_{M_1}$ . Although this sign difference is not a general feature, it should be kept in mind for scenarios where both phases are non-zero.

### 5.3.2 SPS 1a'

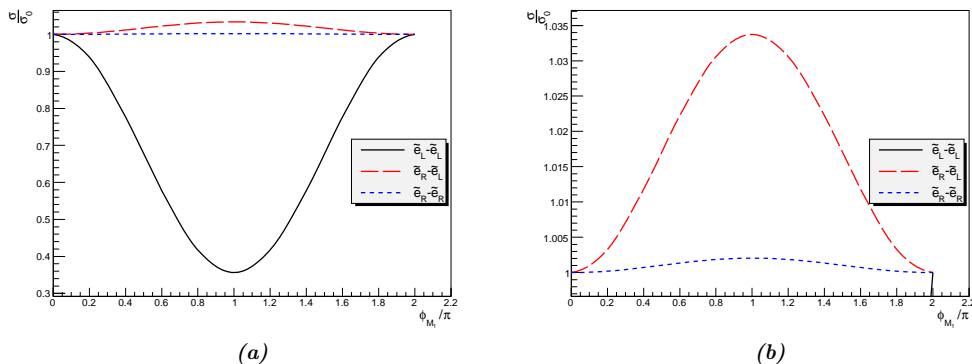


**Figure 5.3:** Dependence of the ratio  $\sigma/\sigma_0$  of the total cross section on the phase  $\phi_{M_1}$  for  $\phi_\mu = 0$  for selectron pair production at  $\sqrt{s} = 500$  GeV in scenario SPS 1a' (table 4.3). Figure 5.3a shows all possible channels, figure 5.3b only the RL and RR production. The  $CP$  violating cross sections are normalised to  $\sigma_0^{LL} = 590.9$  fb,  $\sigma_0^{RL} = 215.2$  fb and  $\sigma_0^{RR} = 548.1$  fb.

In this subsection, the effect of the  $CP$  violating phase  $\phi_{M_1}$  on the total cross sections in the various production channels, i. e. left and right selectron pair production, as well as associate production, is studied. In contrast to earlier studies [22], the effects from neutralino mixing are taken into account. To ease comparison, all total cross sections are normalised to their respective value  $\sigma_0$ , that is the total cross section at  $\sqrt{s} = 500$  GeV for vanishing phases  $\phi_{M_1} = 0$  and  $\phi_\mu = 0$ . The results for SPS 1a' are shown in figure 5.3.

From figure 5.3a it is clear that the sensitivity of left pair production to the phase is substantial and can lead to differences of up to 70% compared to a vanishing phase. On the other hand, it is also obvious that in right selectron pair production, kinematically the first accessible channel, the phase dependence is too weak for measurements. Figure 5.3b represents a detailed view of the right selectron pair production in comparison with the associate production channel. The effect amounts to about 3.5% in the second case, whereas it can be clearly seen that it nearly vanishes for right pair production as expected by the argument given in section 5.2.1.

The  $CP$ -sensitive observables  $\hat{A}[\mathcal{F}_1]$  and  $\hat{A}[\mathcal{F}_2]$  from (5.17) are shown in figure 5.4 for  $\sqrt{s} = 500$  GeV. Figure 5.4a shows their dependence on the gaugino phase  $\phi_{M_1}$ . For  $\phi_{M_1} = \pi/2$ , the observable  $\hat{A}[\mathcal{F}_1]$  is  $2.9\sqrt{\text{fb}}$ , whereas the optimised observable  $\hat{A}[\mathcal{F}_2]$  reaches  $3.2\sqrt{\text{fb}}$ . This results in a gain of about 10%, by matching the angular dependence of the sensitive term with the projection function (5.13).

The dependence on the phase of the higgsino mass parameter  $\phi_\mu$  is shown in

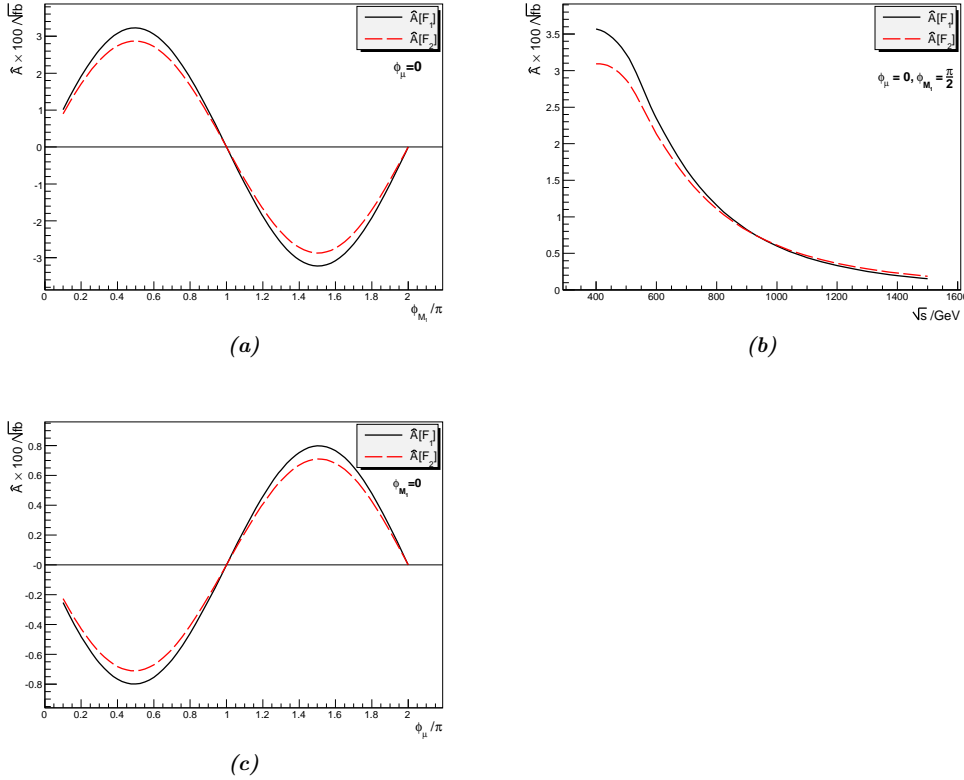


**Figure 5.4:**  $CP$ -sensitive observables in SPS 1a' (table 4.3) as a function of the phase  $\phi_{M_1}$  for  $\phi_\mu = 0$  (figure 5.4a) at 500 GeV, and their energy dependence for  $\phi_{M_1} = \pi/2$  (figure 5.4b). The dependence on  $\phi_\mu$  for  $\phi_{M_1} = 0$  for  $\sqrt{s} = 500$  GeV is displayed in figure 5.4c. For comparison, the simple observable  $\hat{A}[\mathcal{F}_1]$  as well as the optimised observable  $\hat{A}[\mathcal{F}_2]$  are shown.

figure 5.4c. Though, in principle the observables  $\hat{A}[\mathcal{F}_1]$  and  $\hat{A}[\mathcal{F}_2]$  are sensitive to the phase of  $\mu$ , their actual values are much smaller. It should be noted however, that the effect on the observables  $\hat{A}[\mathcal{F}_1]$  and  $\hat{A}[\mathcal{F}_2]$  resulting from  $\phi_\mu$  has an opposite sign compared to that stemming from  $\phi_{M_1}$ . This can lead to at least partial cancellation of the effect of  $CP$  violation for small  $\phi_{M_1}$  and large  $\phi_\mu$ , and can also limit the accuracy achievable for the determination of  $\phi_{M_1}$  ( $\phi_\mu$ ), if  $\phi_\mu$  ( $\phi_{M_1}$ ) is unknown.

In figure 5.4b the energy dependence of the observables is shown. It can be seen that their maximum value of about  $\hat{A}[\mathcal{F}_2] = 3.7\sqrt{\text{fb}}$  ( $\hat{A}[\mathcal{F}_1] = 3.3\sqrt{\text{fb}}$ ) is reached at about  $\sqrt{s} \approx 450$  GeV. Their sizes decrease strongly with the energy, as does the relative gain of the optimised observable  $\hat{A}[\mathcal{F}_2]$ .

Figure 5.5 shows  $\hat{A}[\mathcal{F}_1]$  and  $\hat{A}[\mathcal{F}_2]$ , respectively, in the  $\phi_{M_1}$ - $\phi_\mu$ -plane. From the maxima, the minimal luminosity required for a  $3\sigma$  deviation from the  $CP$ -conserv-

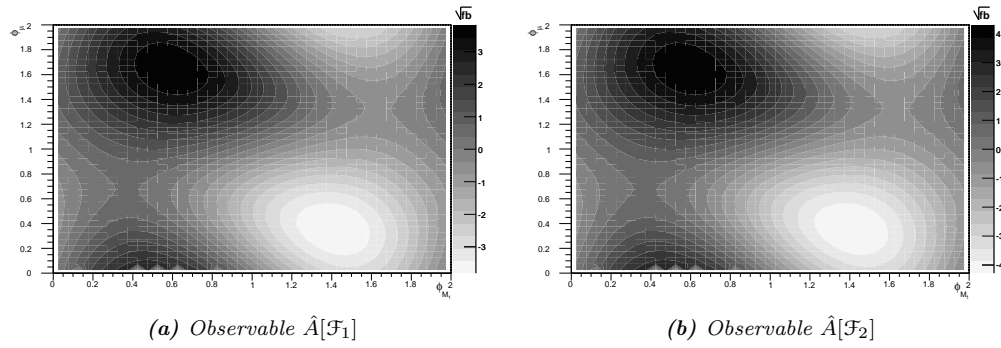


**Figure 5.5:**  $CP$ -sensitive observables  $\hat{A}[\mathcal{F}_1]$  (a) and optimised  $\hat{A}[\mathcal{F}_2]$  (b) for scenario SPS 1a' in the  $\phi_{M_1}$ - $\phi_\mu$  plane. The energy is set to  $\sqrt{s} = 500$  GeV.

ing scenario can be estimated by using (5.18). In SPS 1a', more than  $5000 \text{ fb}^{-1}$  would be required to establish the effect. Thus, it can be concluded, this effect will most likely not be measurable at an  $e^-e^-$ -collider, especially, when the considerably lower integrated luminosity of only 20 – 30% of the  $e^+e^-$  mode has to be kept in mind.

### 5.3.3 Mixed SPS

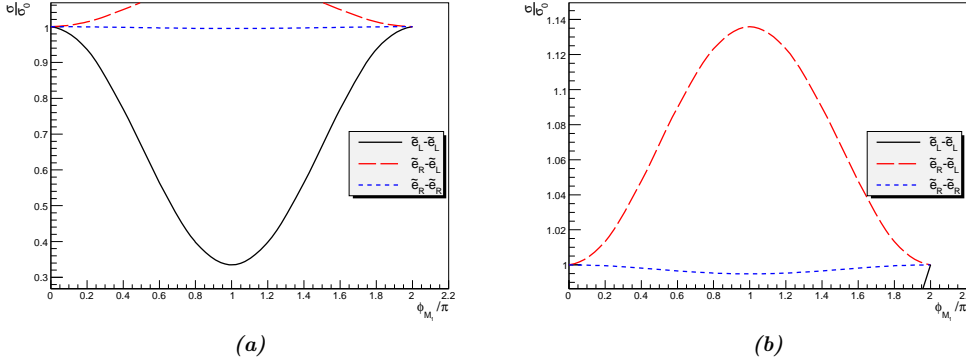


**Figure 5.6:** Dependence of the ratio  $\sigma/\sigma_0$  of the total cross section on the phase  $\phi_{M_1}$  for  $\phi_\mu = 0$  for selectron pair production at  $\sqrt{s} = 500$  GeV in scenario Mixed SPS (table 4.7). Figure 5.6a shows all possible channels, figure 5.6b only the RL and RR production. The  $CP$  violating cross sections are normalised to  $\sigma_0^{LL} = 570.7$  fb,  $\sigma_0^{RL} = 215.1$  fb and  $\sigma_0^{RR} = 514.3$  fb.

In this scenario, the effect of  $\phi_{M_1}$  on the total cross section is for left selectron pair production comparable to SPS 1a', again reaching nearly a difference of 70% for  $\phi_{M_1} = \pi$  compared to  $\phi_{M_1} = 0$ . However, due to the strong higgsino component in the lighter two neutralinos, this scenario is of a mixed character (see table 4.8) resulting in the cross section for associate production to show a pronounced dependence on  $\phi_{M_1}$  reaching a deviation of up to 14% for  $\phi_{M_1} = \pi$ , compared to the  $CP$ -conserving scenario. Still, no effect is observable in the  $RR$  production channel, which is to be expected from the vanishing coupling of right selectrons to the wino-component of the neutralino.

The larger higgsino admixture of the two lighter neutralinos in this scenario also increases the  $CP$ -sensitive observables up to  $\hat{A}[\mathcal{F}_2] \approx 9\sqrt{\text{fb}}$  ( $\hat{A}[\mathcal{F}_1] \approx 8\sqrt{\text{fb}}$ ) for maximal  $\phi_{M_1} = \pi/2$ , as seen in figure 5.7a. The gain from optimisation of the observable is comparable to SPS 1a'. The effect of  $\phi_\mu$  on the observable  $\hat{A}[\mathcal{F}_2]$  is nearly an order of magnitude smaller than of  $\phi_{M_1}$ , and may therefore not be measurable. On the other hand, it may partially cancel or enhance the effect of  $\phi_{M_1}$  depending on their relative sign.

Investigating the whole  $\phi_{M_1}$ - $\phi_\mu$ -plane, the  $CP$ -sensitive observable is generally much larger than for SPS 1a'. This can be seen in figure 5.8a and figure 5.8b. As the cross sections still are comparable to SPS 1a' (see figure 4.2), this results in much lower luminosities required for an actual test of this phase. From figure 5.8c follows, that a test of  $CP$  violation on the level of  $3\sigma$  is possible for integrated luminosities of about  $800 \text{ fb}^{-1}$ , if  $0.35\pi < \phi_{M_1} < 0.65\pi$  (or  $1.3\pi < \phi_{M_1} < 1.6\pi$ ,

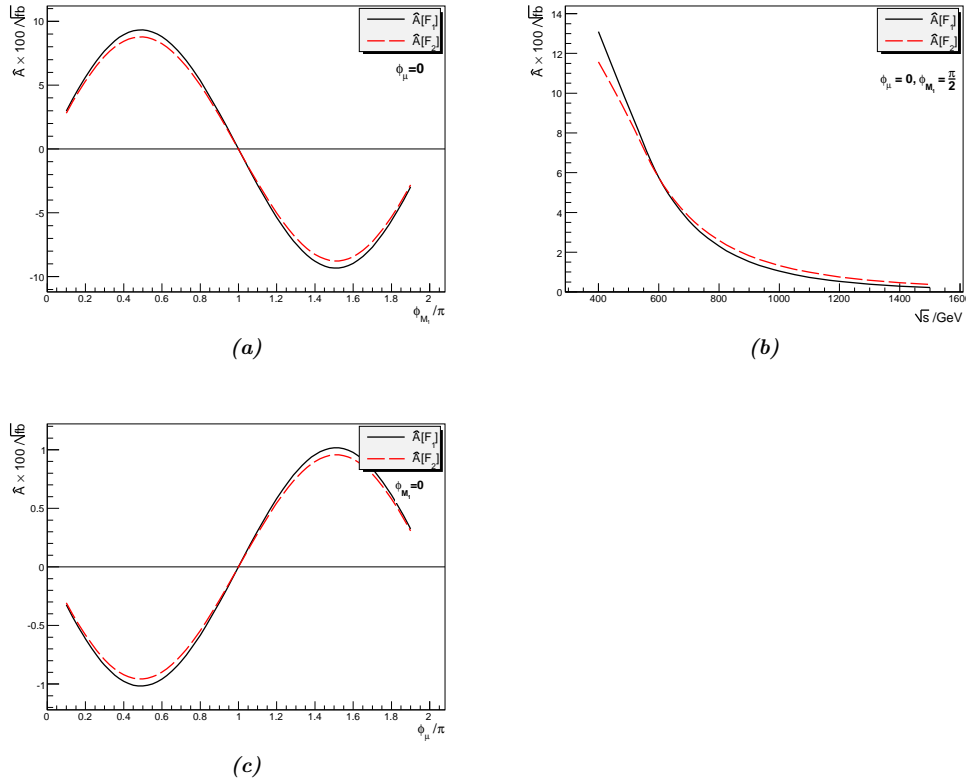


**Figure 5.7:**  $CP$ -sensitive observables in Mixed SPS (table 4.7) as a function of the phase  $\phi_{M_1}$  for  $\phi_\mu = 0$  (figure 5.7a) at 500 GeV, and their energy dependence for  $\phi_{M_1} = \pi/2$  (figure 5.7b). The dependence on  $\phi_\mu$  for  $\phi_{M_1} = 0$  for  $\sqrt{s} = 500$  GeV is displayed in figure 5.7c. For comparison, the simple observable  $\hat{A}[\mathcal{F}_1]$  as well as the optimised observable  $\hat{A}[\mathcal{F}_2]$  are shown.

respectively). Still, for establishing the effect experimentally at the  $5\sigma$ -level luminosities of at least  $2300 \text{ fb}^{-1}$  would be required, as can be seen from figure 5.8d. The largest effect is reached for  $\sqrt{s} \approx 400$  GeV (see figure 5.7b). At this energy the optimised observable reaches  $\hat{A}[\mathcal{F}_2] = 13.1\sqrt{\text{fb}}$ . To probe a phase  $\phi_{M_1} = \pi/2$  at the  $3\sigma$ - ( $5\sigma$ -)level an integrated luminosity  $\mathcal{L}_{3\sigma} = 525 \text{ fb}^{-1}$  ( $\mathcal{L}_{5\sigma} = 1458 \text{ fb}^{-1}$ ) would be required. This allows the test on the  $3\sigma$  ( $5\sigma$ ) level in 13 (35) years of running, if one assumes the current design parameters for the ILC [10,127], taking the lower integrated luminosity of the  $e^-e^-$  mode of only about  $42 \text{ fb}^{-1}$  per year into account. This is equivalent to a test of the observables on the level of  $1.65\sigma$  in one year, assuming an integrated luminosity of  $\mathcal{L} = 0.3 \cdot 500 \text{ fb}^{-1}$  can be collected.



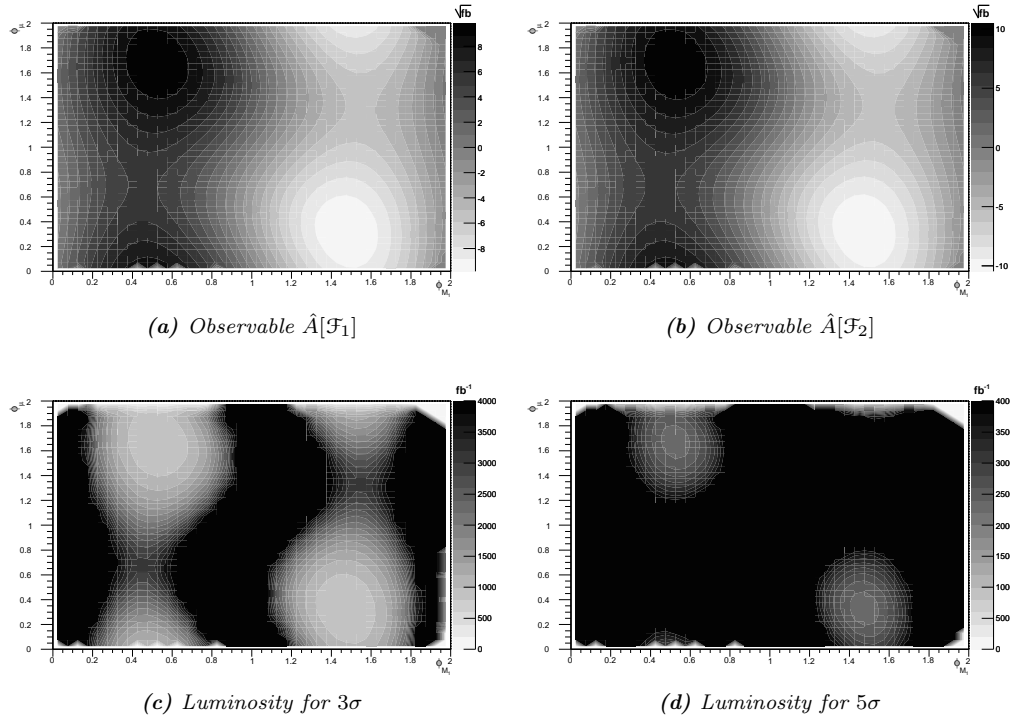


**Figure 5.8:**  $\hat{A}[\mathcal{F}_1]$  (a) and optimised  $\hat{A}[\mathcal{F}_2]$  (b)  $CP$ -sensitive observable for scenario Mixed SPS. (c) shows the luminosity required to establish  $CP$  violation at the  $3\sigma$ -level, (d) the luminosity required for a measurement of  $CP$  violation at the  $5\sigma$ -level in the  $\phi_{M_1}$ - $\phi_\mu$  plane. The energy is set to  $\sqrt{s} = 500$  GeV.

### 5.3.4 Scenario A

This scenario uses the GUT-relation (2.4) between  $M_1$  and  $M_2$  but, due to the smaller value of  $\mu = 115$  GeV, features higgsino-like lighter neutralinos. The production cross section for the pair production of left selectrons depends strongly on the phase  $\phi_{M_1}$ , figure 5.9a. Additionally though, in associate production also a rather strong dependence of  $\sigma$  on the phase  $\phi_{M_1}$  is found, resulting in an increase of up to 16% for  $\phi_{M_1} = \pi$  (see figure 5.9b) which is comparable to Mixed SPS.

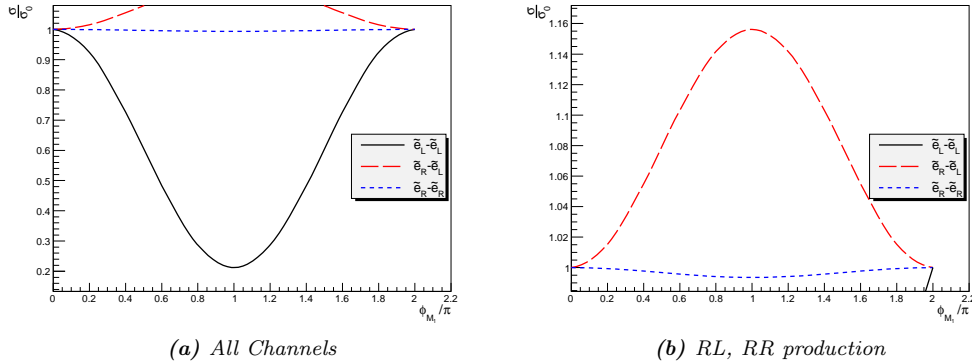


**Figure 5.9:** Dependence of the ratio  $\sigma/\sigma_0$  of the total cross section on the phase  $\phi_{M_1}$  for  $\phi_\mu = 0$  for selectron pair production at  $\sqrt{s} = 500$  GeV in scenario Scenario A (table 4.10). Figure 5.9a shows all possible channels, figure 5.9b only the RL and RR production. The  $CP$  violating cross sections are normalised to  $\sigma_0^{LL} = 260.8$  fb,  $\sigma_0^{RL} = 38.96$  fb and  $\sigma_0^{RR} = 566.9$  fb.

The  $\phi_{M_1}$  dependence of the  $CP$ -sensitive observables  $\hat{A}[\mathcal{F}_1]$  and  $\hat{A}[\mathcal{F}_2]$  is shown in figure 5.10a. Even though this is a higgsino-like scenario, the size of these observables is still comparable with Mixed SPS as, due to the GUT-relation between  $M_1$  and  $M_2$ ,  $\tilde{\chi}_3^0$  is still a bino. The value of  $\hat{A}[\mathcal{F}_2]$  reaches about  $\hat{A}[\mathcal{F}_2] = 8\sqrt{\text{fb}}$  at  $\phi_{M_1} = 0.5\pi$  as in Mixed SPS, but the difference between  $\hat{A}[\mathcal{F}_2]$  and  $\hat{A}[\mathcal{F}_1]$  is more pronounced in Scenario A. If the dependence on  $\phi_\mu$  in both scenarios is compared,  $\hat{A}[\mathcal{F}_2]$  is about 20% smaller at  $\phi_\mu = 0.5\pi$  in Scenario A.

The higher masses of the sleptons produced also shift the maximum total cross section to higher energies which is also true for  $\hat{A}[\mathcal{F}_1]$  and  $\hat{A}[\mathcal{F}_2]$  (figure 5.10b). From this follows the optimal energy to investigate this scenario to be  $\sqrt{s} \approx 500$  GeV. As can be seen from figure 5.11a and figure 5.11b, respectively, the size of the  $CP$ -sensitive observables  $\hat{A}[\mathcal{F}_1]$  and  $\hat{A}[\mathcal{F}_2]$  is slightly smaller but comparable to that in Mixed SPS over the whole  $\phi_{M_1}$ - $\phi_\mu$  plane. Considering the luminosity required to test  $CP$  violation at the  $3\sigma$ -level however, this slightly smaller observable already results in an integrated luminosity of about  $1000 \text{ fb}^{-1}$  for  $0.35\pi < \phi_{M_1} < 0.65\pi$  (or  $1.3\pi < \phi_{M_1} < 1.6\pi$  respectively). Luminosities of at least  $2800 \text{ fb}^{-1}$  would be

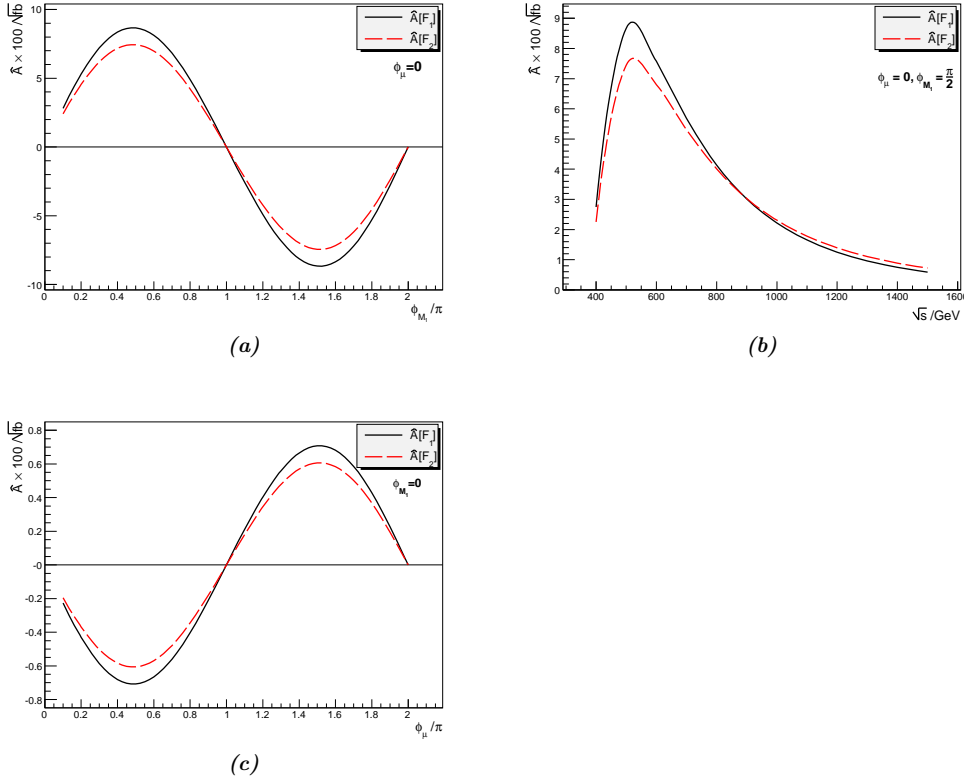


**Figure 5.10:**  $CP$ -sensitive observables in Scenario A (table 4.10) as a function of the phase  $\phi_{M_1}$  for  $\phi_\mu = 0$  (figure 5.10a) at 500 GeV, and their energy dependence for  $\phi_{M_1} = \pi/2$  (figure 5.10b). The dependence on  $\phi_\mu$  for  $\phi_{M_1} = 0$  for  $\sqrt{s} = 500$  GeV is displayed in figure 5.10c. For comparison, the simple observable  $\hat{A}[\mathcal{F}_1]$  as well as the optimised observable  $\hat{A}[\mathcal{F}_2]$  are shown.

required to establish the effect experimentally at the  $5\sigma$ -level, as can be seen from figure 5.11d. As these values are already valid at the optimal energy, this scenario is much more challenging than Mixed SPS.

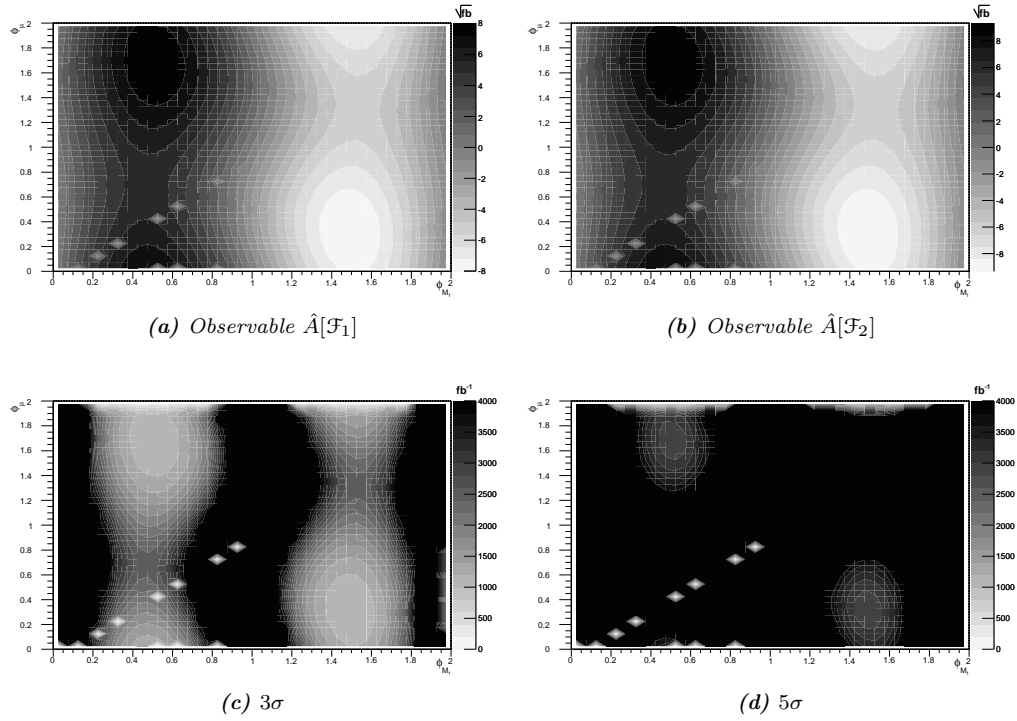


**Figure 5.11:**  $\hat{A}[\mathcal{F}_1]$  (a) and optimised  $\hat{A}[\mathcal{F}_2]$  (b)  $CP$ -sensitive observable for scenario Scenario A. (c) shows the luminosity required to establish  $CP$  violation at the  $3\sigma$ -level, (d) that required for a measurement of  $CP$  violation at the  $5\sigma$ -level in the  $\phi_{M_1}$ - $\phi_\mu$  plane. The energy is set to  $\sqrt{s} = 500$  GeV.

### 5.3.5 Scenario B

Evaluating figure 5.12a and figure 5.12b, the sensitivity of the  $CP$ -even observables on  $\phi_{M_1}$  is comparable in Scenario A and Scenario B. This also holds true for the dependence on  $\phi_{M_1}$  of the  $CP$ -sensitive observables  $\hat{A}[\mathcal{F}_1]$  and  $\hat{A}[\mathcal{F}_2]$ , as seen in figure 5.13a.

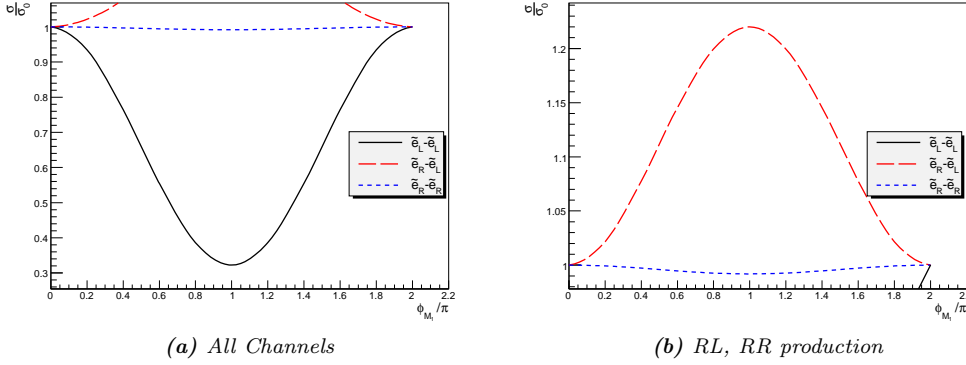


**Figure 5.12:** Dependence of the ratio  $\sigma/\sigma_0$  of the total cross section on the phase  $\phi_{M_1}$  for  $\phi_\mu = 0$  for selectron pair production at  $\sqrt{s} = 500$  GeV in scenario Scenario B (table 4.13). Figure 5.12a shows all possible channels, figure 5.12b only the RL and RR production. The  $CP$  violating cross sections are normalised to  $\sigma_0^{LL} = 351.8$  fb,  $\sigma_0^{RL} = 15.63$  fb and  $\sigma_0^{RR} = 487.7$  fb.

Concerning  $\phi_\mu$ , the dependence on this phase is much stronger in Scenario B than in Scenario A resulting in an increase by a factor of almost 5 for the observable  $\hat{A}[\mathcal{F}_2]$ . In Scenario B, the size of  $\hat{A}[\mathcal{F}_2] \approx 5\sqrt{\text{fb}}$  for  $\phi_\mu = 0.5\pi$  (figure 5.13c) is as well about 50% of  $\hat{A}[\mathcal{F}_2] \approx 11$  for  $\phi_{M_1} = 0.5\pi$  (figure 5.13a). Additionally, both the dependence on  $\phi_\mu$  and  $\phi_{M_1}$  of the observables  $\hat{A}[\mathcal{F}_1]$  and  $\hat{A}[\mathcal{F}_2]$  have the same sign in Scenario B, whereas it is of opposite sign in Scenario A. This has to be taken into account if both phases are non-vanishing. The optimal energy for the observation of  $\hat{A}[\mathcal{F}_2]$  is again  $\sqrt{s} = 500$  GeV.

The constructive interference of both phases can be seen in the  $\phi_{M_1}$ - $\phi_\mu$ -plane, figure 5.14a. Though the luminosity requirements for  $\phi_\mu = 0$  are comparable to Scenario A, the possible constructive interference leads to much larger areas in the  $\phi_{M_1}$ - $\phi_\mu$  plane that allow to establish  $CP$  violation on the  $3\sigma$ -level as seen in figure 5.14c. The minimal luminosity required for a measurement is reached for  $\phi_{M_1} \approx 0.6\pi$ ,  $\phi_\mu \approx 1.8\pi$  or  $\phi_{M_1} \approx 1.4\pi$ ,  $\phi_\mu \approx 0.2\pi$  and is approximately  $\mathcal{L} = 717 \text{ fb}^{-1}$ . For a measurement on the  $5\sigma$ -level in this region of parameter space, a luminosity of  $\mathcal{L} \approx 1990 \text{ fb}^{-1}$  would be required (see figure 5.14c and figure 5.14d, respectively).

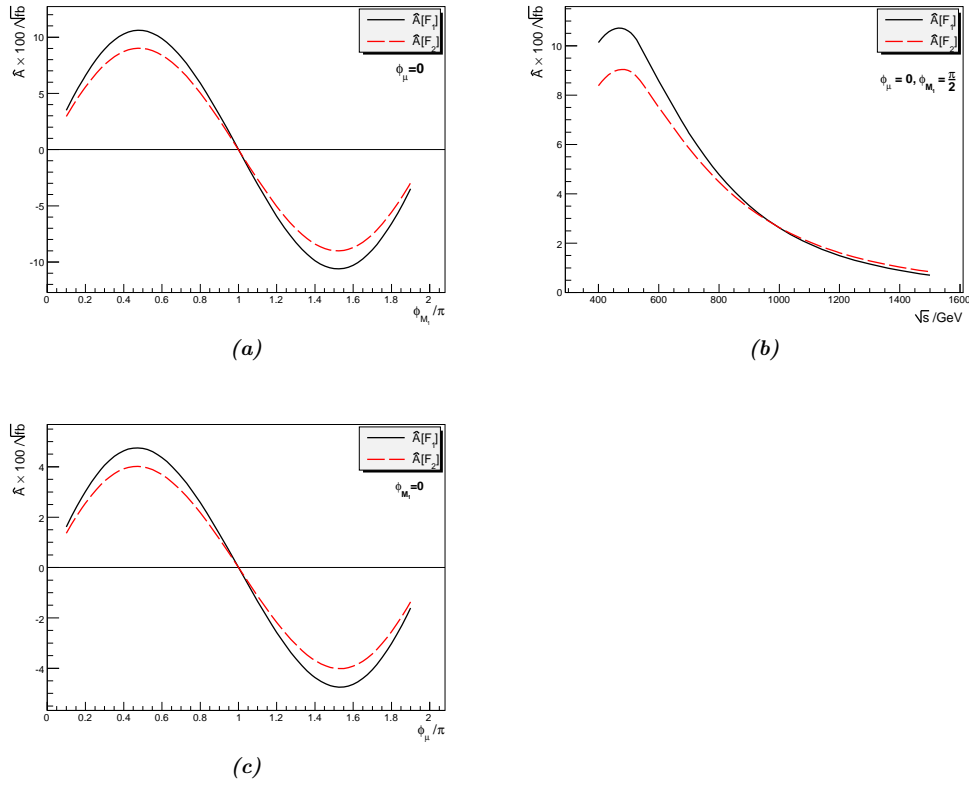


**Figure 5.13:**  $CP$ -sensitive observables in Scenario B (table 4.13) as a function of the phase  $\phi_{M_1}$  for  $\phi_\mu = 0$  (figure 5.13a) at 500 GeV, and their energy dependence for  $\phi_{M_1} = \pi/2$  (figure 5.13b). The dependence on  $\phi_\mu$  for  $\phi_{M_1} = 0$  for  $\sqrt{s} = 500$  GeV is displayed in figure 5.13c. For comparison, the simple observable  $\hat{A}[\mathcal{F}_1]$  as well as the optimised observable  $\hat{A}[\mathcal{F}_2]$  are shown.

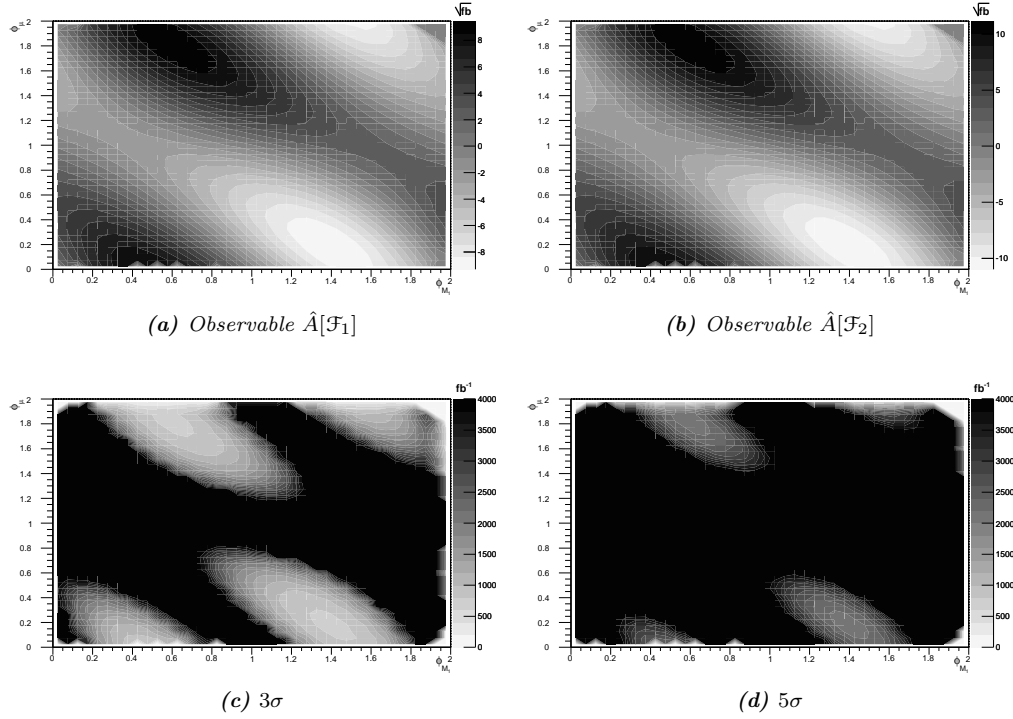


**Figure 5.14:**  $\hat{A}[\mathcal{F}_1]$  (a) and optimised  $\hat{A}[\mathcal{F}_2]$  (b)  $CP$ -sensitive observable for scenario Scenario B. (c) shows the luminosity required to establish  $CP$  violation at the  $3\sigma$ -level, (d) the luminosity required for a measurement of  $CP$  violation at the  $5\sigma$ -level in the  $\phi_{M_1}$ - $\phi_\mu$  plane. The energy is set to  $\sqrt{s} = 500$  GeV.

### 5.3.6 Scenario C

The small masses of neutralinos  $\tilde{\chi}_1^0$  (LSP) and  $\tilde{\chi}_2^0$  (NLSP) in this scenario should allow easy detection of these particles at the ILC. For this reason similar scenarios have been studied with respect to  $CP$  violation in the  $e^+e^-$  mode [123] allowing for comparison of both modes.

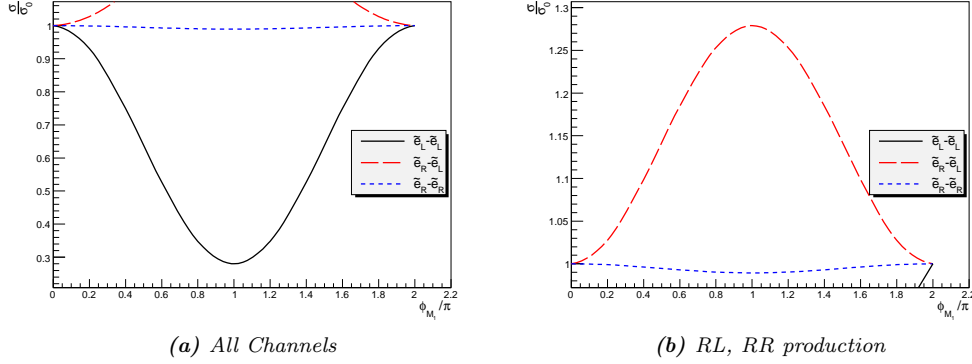


**Figure 5.15:** Dependence of the ratio  $\sigma/\sigma_0$  of the total cross section on the phase  $\phi_{M_1}$  for  $\phi_\mu = 0$  for selectron pair production at  $\sqrt{s} = 500$  GeV in scenario C (table 4.16). Figure 5.15a shows all possible channels, figure 5.15b only the RL and RR production. The  $CP$  violating cross sections are normalised to  $\sigma_0^{LL} = 336.9$  fb,  $\sigma_0^{RL} = 18.11$  fb and  $\sigma_0^{RR} = 488.9$  fb.

In Scenario C the effect of  $\phi_{M_1}$  on the unpolarised cross section (see figure 5.15) is pronounced, reaching a reduction of up to 70% for the LL channel at its minimum  $\phi_{M_1} = \pi$ . On the other hand, in the associate production process for  $\phi_{M_1} = \pi$  an enhancement of about 30% of the total cross section (figure 5.15b) is observed. So first hints may be gained by measuring the cross sections for various production modes, if the other supersymmetric parameters are known to a high precision from the  $e^+e^-$  mode of the ILC and complementary measurements at the LHC.

In this scenario however, the  $CP$ -sensitive observable  $\hat{A}[\mathcal{F}_1]$  proposed in [123] for  $e^+e^- \rightarrow \tilde{\chi}_1^0 \tilde{\chi}_2^0$  with the subsequent decay  $\tilde{\chi}_2^0 \rightarrow \tilde{\chi}_1^0 l \bar{l}$  reaches only about  $A = 1.2 \cdot 10^{-3} \sqrt{\text{fb}}$  at a collider energy of  $\sqrt{s} = 500$  GeV so that it will not be accessible. On the other hand, due to the large mass splitting in the neutralino sector, the production of  $\tilde{\chi}_3^0$  or  $\tilde{\chi}_4^0$  in association with the LSP is kinematically not possible for  $\sqrt{s} = 500$  GeV.

In the  $e^-e^- \rightarrow \tilde{e}_i^- \tilde{e}_j^-$  mode however, the  $CP$  violating vertex  $e^- \tilde{e}_i^- \tilde{\chi}_i^0$  can be tested with off-shell neutralinos. Here,  $\hat{A}[\mathcal{F}_1]$  and  $\hat{A}[\mathcal{F}_2]$  reach sizeable values as shown in figure 5.16a. Their dependence on  $\phi_\mu$ , however, is still about two orders of magnitude weaker as on  $\phi_{M_1}$  as can be seen from figure 5.16c. The energy



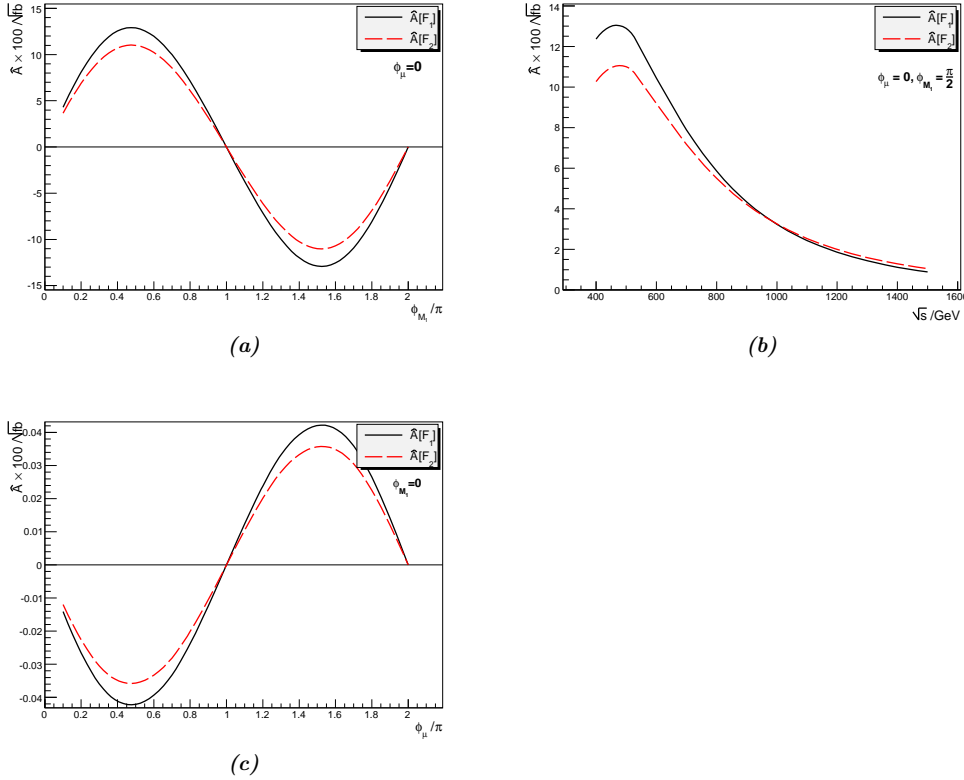


**Figure 5.16:**  $CP$ -sensitive observables in Scenario C (table 4.16) as a function of the phase  $\phi_{M_1}$  for  $\phi_\mu = 0$  (figure 5.16a) at 500 GeV, and their energy dependence for  $\phi_{M_1} = \pi/2$  (figure 5.16b). The dependence on  $\phi_\mu$  for  $\phi_{M_1} = 0$  for  $\sqrt{s} = 500$  GeV is displayed in figure 5.16c. For comparison, the simple observable  $\hat{A}[\mathcal{F}_1]$  as well as the optimised observable  $\hat{A}[\mathcal{F}_2]$  are shown.

dependence displayed in figure 5.16b shows that the maximal values for  $\hat{A}[\mathcal{F}_1]$  and  $\hat{A}[\mathcal{F}_2]$  in this scenario are reached for about  $\sqrt{s} = 500$  GeV.

In figure 5.17a and figure 5.17b again, the whole  $\phi_{M_1}$ - $\phi_\mu$ -plane is depicted. The observables reach sizeable values in large areas of the parameters space. These values are only somewhat reduced by the partial cancellation between the effect of  $\phi_{M_1}$  and that of  $\phi_\mu$ . The maximum of this cancellation is reached for  $\phi_\mu = 0.8\pi$  and  $\phi_{M_1} = 1.2\pi$ .

In this scenario the cross section for associate production is within the reach of a 500 GeV linear collider. Together with the large values of the  $CP$  violating observables,  $\hat{A}[\mathcal{F}_1]$  and  $\hat{A}[\mathcal{F}_2]$ ,  $CP$  violation in the neutralino system can be tested at the  $3\sigma$ -level in large parts of the parameter space if an integrated luminosity of  $\mathcal{L} \approx 500 \text{ fb}^{-1}$  can be accumulated. For  $0 < \phi_\mu < 0.5\pi$  and  $1.2\pi < \phi_\mu < 2\pi$  almost

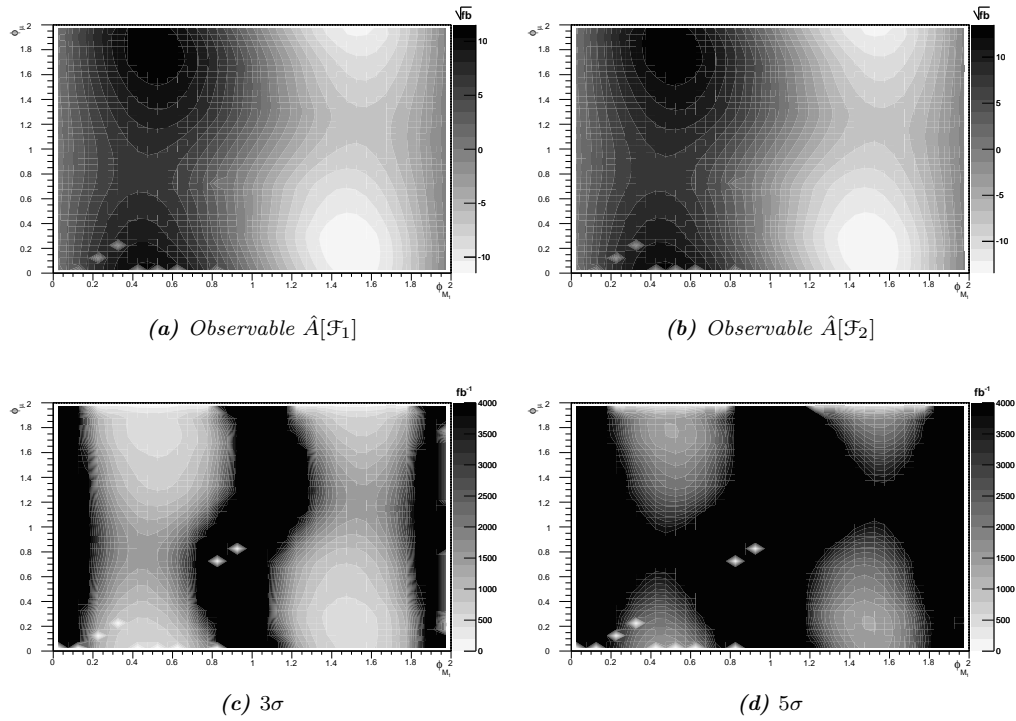


**Figure 5.17:**  $\hat{A}[\mathcal{F}_1]$  (a) and optimised  $\hat{A}[\mathcal{F}_2]$  (b)  $CP$ -sensitive observable for scenario Scenario C. (c) shows the luminosity required to establish  $CP$  violation at the  $3\sigma$ -level, (d) the luminosity required for a measurement of  $CP$  violation at the  $5\sigma$ -level in the  $\phi_{M_1}$ - $\phi_\mu$  plane. The energy is set to  $\sqrt{s} = 500$  GeV.

the whole regions of  $0.3 < \phi_{M_1} < 0.6$  and  $1.3 < \phi_{M_1} < 1.7$  would be accessible at this level (figure 5.17c). Compared to the  $e^+e^-$  mode, the  $e^-e^-$  mode would offer a clear improvement. Here, already an integrated luminosity of about  $\mathcal{L} = 167 \text{ fb}^{-1}$  (assuming the usual  $1/3$  of the luminosity as for  $e^+e^-$ ) would give a clue for  $CP$  violation at the  $2.5\sigma$ -level for  $\langle \mathcal{F}_2 \rangle$  and on the  $2.3\sigma$ -level for  $\langle \mathcal{F}_1 \rangle$ , respectively. The measurement on the  $5\sigma$ -level, however, seems at least possible in the regions of maximal phases,  $\phi_{M_1} \approx 0.5\pi$  ( $\phi_{M_1} \approx 1.5\pi$ ) and  $\phi_\mu \approx 0$  ( $\phi_\mu \approx 0.2\pi$ ) or  $\phi_\mu \approx 1.8$  ( $\phi_\mu \approx 2\pi$ ), if  $\mathcal{L} \approx 500 \text{ fb}^{-1}$  can be accumulated.

# Lepton Flavour Violation

In supersymmetric models, gauge- and Lorentz-invariance do not enforce total lepton number ( $L = L_e + L_\mu + L_\tau$ ) or individual lepton number ( $L_e, L_\mu, L_\tau$ ) to be conserved. Recent neutrino experiments actually establish individual lepton number to be violated (for a review see e. g. [4]). There exist, however, stringent experimental bounds on LFV in the charged lepton sector by various decay branching ratios (e. g. [78, 148–150]), so this is certain to be a small effect.

For this reason a clean environment is expected to be necessary, and it has already been pointed out that the  $e^-e^-$  mode of the ILC might be helpful [151]. Another advantage of the  $e^-e^-$  mode is the higher polarisation of the electron beams. At least 90% per  $e^-$ -beam seem feasible today, whereas for  $e^+$ -beams about 60% seem possible [11]. For longitudinal polarisation this results in up to 50% higher total cross section compared to the  $e^+e^-$  mode which could compensate the lower luminosity. This polarisation may be used to further suppress the background while at the same time enhancing the signals in various modes (e. g.  $\tilde{\ell}_R\tilde{\ell}_R$  final states). Additionally, in certain scenarios even a background free measurement may be obtained at the  $e^-e^-$ -collider [23] in contrast to the  $e^+e^-$  mode.

Recently it was also pointed out in phenomenological studies that, In recent phenomenological studies it has been pointed out, that even obeying stringent experimental bounds, the flavour violating phases do not have to be small. They can be sizeable once the full three generation mixing is taken into account [24–28].

Currently, most of the searches for LFV are done in low energy experiments like the search for rare decays, e. g.,  $\mu \rightarrow e\gamma$ . These experiments have already been able to pose stringent bounds on the size of LFV. Still, in case LFV is established, they won't be able to give any information whether the left or right sector is its source. Complementary to these experiments, this disentanglement could be achieved by high energy experiments. Together with the results from low energy experiments, this could lead to the identification of LFV in the charged sector and help in the exploration of the underlying soft-supersymmetry breaking Lagrangian.

## 6.1 Parametrisation

*The formalism used for the numerical studies in this work as well as the conventions utilised are introduced. Additionally, the experimental signature is discussed with the focus on scenarios with a gravitino LSP, offering a possible background free measurement. Finally, the current experimental bounds on LFV are summarised.*

Currently, several models for LFV exist but the actual mechanism realised in nature is still unknown [62, 152–157]. By parametrising the slepton mass matrix [86, 87] it is possible to study the effect of LFV in a model independent way. As long as there is no evidence for the realisation of a certain model, this approach seems to be a feasible way if one solely wants to study the potential of a specific collider mode like  $e^-e^-$ .

In this approach, the flavour violating off diagonal elements are inserted into the slepton mass matrix (2.14) as free parameters. Specific models then would just predict these values. LFV resulting from the neutrino sector and manifesting itself in the left sector of the slepton mass matrix has been studied extensively [68–76]. Contrasting that in this work, the flavour violating entries should be treated as free parameters. These off-diagonal elements are represented by hermitian matrices  $\hat{\delta}_{LL}$  and  $\hat{\delta}_{RR}$  parametrising flavour violation in the left and right sector, respectively. Additionally, the matrix  $\hat{\delta}_{RL}$  adds to the mixing of left and right particles together with the entries of  $M_{RL}^2$ , (2.15). Including flavour violation the mass matrices then read:

$$M_{LL}^2 = \begin{pmatrix} (m_L^{11})^2 + \hat{\delta}_{LL}^{11} & \hat{\delta}_{LL}^{12} & \hat{\delta}_{LL}^{13} \\ \hat{\delta}_{LL}^{21} & (m_L^{22})^2 + \hat{\delta}_{LL}^{22} & \hat{\delta}_{LL}^{23} \\ \hat{\delta}_{LL}^{31} & \hat{\delta}_{LL}^{32} & (m_L^{33})^2 + \hat{\delta}_{LL}^{33} \end{pmatrix} \quad (6.1)$$

$$M_{RR}^2 = \begin{pmatrix} (m_R^{11})^2 + \hat{\delta}_{RR}^{11} & \hat{\delta}_{RR}^{12} & \hat{\delta}_{RR}^{13} \\ \hat{\delta}_{RR}^{21} & (m_R^{22})^2 + \hat{\delta}_{RR}^{22} & \hat{\delta}_{RR}^{23} \\ \hat{\delta}_{RR}^{31} & \hat{\delta}_{RR}^{32} & (m_R^{33})^2 + \hat{\delta}_{RR}^{33} \end{pmatrix} \quad (6.2)$$

$$M_{LR}^2 = \begin{pmatrix} (m_{LR}^{11})^2 + \hat{\delta}_{LR}^{11} & \hat{\delta}_{LR}^{12} & \hat{\delta}_{LR}^{13} \\ \hat{\delta}_{LR}^{21} & (m_{LR}^{22})^2 + \hat{\delta}_{LR}^{22} & \hat{\delta}_{LR}^{23} \\ \hat{\delta}_{LR}^{31} & \hat{\delta}_{LR}^{32} & (m_{LR}^{33})^2 + \hat{\delta}_{LR}^{33} \end{pmatrix} \quad (6.3)$$

In literature no common scheme exists for the definition of the entries of the  $\hat{\delta}_{ij}$ -matrices. To simplify the comparison of the size of the LFV in different scenarios, in this work the values of the off-diagonal matrices  $\hat{\delta}_{ij}$  are given relative to their corresponding diagonal elements [158]. The actual off diagonal matrix element is obtained by multiplication of the given  $\delta_{ij}$  with the mass entries  $m_{ii} \times m_{jj}$ . The

matrices  $\hat{\delta}$  thus read:

$$\hat{\delta}_{LL} = \begin{pmatrix} \delta_{LL}^{11} (m_{11}^L)^2 & \delta_{LL}^{12} m_{11}^L m_{22} & \delta_{LL}^{13} m_{11}^L m_{33}^L \\ \delta_{LL}^{21} m_{22}^L m_{11}^L & \delta_{LL}^{22} (m_{22}^L)^2 & \delta_{LL}^{23} m_{22}^L m_{33}^L \\ \delta_{LL}^{31} m_{33}^L m_{11}^L & \delta_{LL}^{32} m_{33}^L m_{22} & \delta_{LL}^{33} (m_{33}^L)^2 \end{pmatrix} \quad (6.4)$$

$$\hat{\delta}_{RR} = \begin{pmatrix} \delta_{RR}^{11} (m_{11}^R)^2 & \delta_{RR}^{12} m_{11}^R m_{22}^R & \delta_{RR}^{13} m_{11}^R m_{33}^R \\ \delta_{RR}^{21} m_{22}^R m_{11}^R & \delta_{RR}^{22} (m_{22}^R)^2 & \delta_{RR}^{23} m_{22}^R m_{33}^R \\ \delta_{RR}^{31} m_{33}^R m_{11}^R & \delta_{RR}^{32} m_{33}^R m_{22}^R & \delta_{RR}^{33} (m_{33}^R)^2 \end{pmatrix} \quad (6.5)$$

$$\hat{\delta}_{LR} = \begin{pmatrix} \delta_{LR}^{11} m_{11}^L m_{11}^R & \delta_{LR}^{12} m_{11}^L m_{22}^R & \delta_{LR}^{13} m_{11}^L m_{33}^R \\ \delta_{LR}^{21} m_{22}^L m_{11}^R & \delta_{LR}^{22} m_{22}^L m_{22}^R & \delta_{LR}^{23} m_{22}^L m_{33}^R \\ \delta_{LR}^{31} m_{33}^L m_{11}^R & \delta_{LR}^{32} m_{33}^L m_{22}^R & \delta_{LR}^{33} m_{33}^L m_{33}^R \end{pmatrix} \quad (6.6)$$

### 6.1.1 Experimental Signatures

Many contributions to the cross section that are sensitive to lepton flavour violation also show a definite polarisation dependence. Unfortunately, for the same reasons as in case of  $CP$  violation (see chapter 5), it is not possible to exploit spin correlations between production and decay to construct observables. In scenarios with the  $\tilde{\tau}_1$  as NLSP, however, this particle can be long living and its production would give a clear signature itself. In other scenarios, however, the signature has to be derived from the decay of the sleptons produced. Considering leptonic decays as the dominant ones, as in the scenarios studied here, these decay products consist of an electron together with a  $\mu$  or a  $\tau$  plus – in case the  $\tilde{\chi}_1^0$  is the LSP – missing-energy from the neutralinos that escape detection.

The decoupling of production and decay together with the, compared to their mass, small total width of the sleptons results in the narrow width approximation to be valid for the scenarios considered here [27, 159]. In this approximation, the propagators of the sleptons are set on-shell and their decay is taken into account by means of the branching ratios.

The flavour conserving processes (e. g. single-W production) constitute the background to the signatures discussed here and will be considered in chapter 8. The dominant flavour violating contributions are those with a minimal number of flavour violating vertices

$$\begin{aligned} \sigma(e^- e^- \rightarrow e^- \ell_a^- \tilde{\chi}_1^0 \tilde{\chi}_1^0) &= \sigma(e^- e^- \rightarrow \tilde{e}_i \tilde{\ell}_a) \\ &\times \left\{ \text{BR}[\tilde{\ell}_a \rightarrow \ell_a \tilde{\chi}_1^0] \cdot \text{BR}[\tilde{e}_i \rightarrow e^- \tilde{\chi}_1^0] \right\} \end{aligned} \quad (6.7a)$$

$$\begin{aligned} &+ \sigma(e^- e^- \rightarrow \tilde{e}_i \tilde{e}_j) \\ &\times \left\{ \text{BR}[\tilde{e}_i \rightarrow \ell_a \tilde{\chi}_1^0] \cdot \text{BR}[\tilde{e}_j \rightarrow e^- \tilde{\chi}_1^0] \right\} \end{aligned} \quad (6.7b)$$

$$+ \text{BR}[\tilde{e}_i \rightarrow e^- \tilde{\chi}_1^0] \cdot \text{BR}[\tilde{e}_j \rightarrow \ell_a \tilde{\chi}_1^0] \}. \quad (6.7c)$$

(6.7a) constitutes the flavour violating production of one slepton and a selectron. The dominant contribution is achieved if the sleptons decay flavour conserving

as shown. (6.7b) and (6.7c) represent the flavour conserving production of two selectrons and their eventual flavour violating decay. As the latter contribution also consists of one flavour violating interaction, it is of the same order as the first contribution and has to be taken into account. The branching ratios used for this calculation thus have to be calculated with flavour violating couplings. Other processes yielding the same final state consist of more flavour violating interactions and are suppressed. Numerical checks reveal that they can be safely neglected as they are at least one order of magnitude smaller than the leading terms (6.7).

Some of the scenarios under investigation feature the possibility for a background free measurement of flavour violating interactions. This is the case if the gravitino is the LSP and the lighter stau is the NLSP. As the latter has to decay to the gravitino, it has a long lifetime resulting in a unique signature: a thick ionized track and a displaced vertex from the decay of the  $\tilde{\tau}$ , if its lifetime is short enough to allow a decay within the detector. The benchmark Point  $\varepsilon$  [120] described in section 4.6, as well as SPS 7 (section 4.7) are of this type. Of course, in these scenarios the decay of the sleptons do not have to be considered at all.

## 6.1.2 Bounds for LFV

The searches for LFV [78–82] give strong constraints on the entries of the flavour mixing matrices  $\delta_{ij}$ . Especially the bounds on  $\tilde{e}$ - $\tilde{\mu}$  mixing are already very strong. If, for sake of simplicity, only the mixing between two generations is considered, this results in very low cross sections for flavour violating processes at an  $e^-e^-$ -collider, especially for the  $\tilde{e}$ - $\tilde{\mu}$  channel. It changes drastically however, if full three generation mixing is taken into account [24–28].

Then, the relatively weak bounds on  $\tilde{e}$ - $\tilde{\tau}$  and  $\tilde{\mu}$ - $\tilde{\tau}$  mixing allow for a nearly equal mixture of  $\tilde{e}$  and  $\tilde{\mu}$  (see also section 2.3.3). In this case, high cross sections in  $e^-e^-$  collisions are possible, even in the  $\tilde{e}$ - $\tilde{\mu}$  channel. Additionally, one may then take advantage of the low background of this collider mode. Of special interest is the  $\tilde{e}$ - $\tilde{\tau}$  production channel due to the unique signature in scenarios with a long living  $\tilde{\tau}_1$ . The  $e^-e^-$ -collider may offer the opportunity to either establish flavour violation, or at least help in the exclusion of quite large parts of the parameter

Neutrino modes		Rare decays	
Observable	current limit	Observable	current limit
$\text{BR}(e \rightarrow \ell_b \nu \bar{\nu})$	0	$\text{BR}(\mu \rightarrow e \gamma)$	$< 1.2 \cdot 10^{-11}$
$\text{BR}(\mu \rightarrow e \nu \bar{\nu})$	$\approx 1.00$	$\text{BR}(\tau \rightarrow \mu \gamma)$	$< 4.5 \cdot 10^{-8}$
$\text{BR}(\tau \rightarrow \mu \nu \bar{\nu})$	$\approx 0.178$	$\text{BR}(\tau \rightarrow e \gamma)$	$< 1.1 \cdot 10^{-7}$
$\text{BR}(\tau \rightarrow e \nu \bar{\nu})$	$\approx 0.173$		

**Table 6.1:** Experimental constraints for lepton flavour violation. [56, 126, 160, 161].

space by means of direct searches.

To derive the exclusion regions for this rather complex interplay of parameters involved, numerical approximation formulae are used [158]. Included in this formulae are branching ratios for the rare radiative decays  $\ell_a \rightarrow \ell_b \gamma$  as well as  $\ell_a \rightarrow \ell_b \nu \bar{\nu}$ . The experimental bounds on these decays are given in table 6.1 [56, 126, 160, 161].

## 6.2 Observables

For the production of sleptons in  $e^-e^-$ -collisions one can consider as observables:

- Total cross sections,
- Polarisation asymmetries.

Without LFV in the slepton sector, the direct production of smuons and staus is forbidden in  $e^-e^-$ -scattering. For this reason, the production cross section of these particles is already a good observable. This, however, requires the possibility to distinguish between leptons stemming from a slepton decay and those, e. g., from W-decay, which is the main SM background in this collider mode. Another process faking the signal might be the supersymmetric version of this process, i. e. single-chargino-production. Both background processes will be discussed in chapter 8. This issue has already been studied in the case of LFV in the left sector, which features much lower flavour violating cross sections than the processes considered here [72]. There, the result has been, that the background is well enough under control for measurements.

If flavour is violated in the right sector, however, the main background, stemming from single W-boson production, can be strongly reduced by suitable longitudinal polarisation, as the W-boson couples only to left particles. Besides the reduction of the background, suitable polarisation also enhances the production cross section for right particles. Testing for LFV in the left sector with this polarisation mode does not help though, since this polarisation would also kill the signal.

An entirely background free measurement would be possible, if the gravitino is the LSP: the  $\tilde{\tau}_1$  (NLSP) then has to decay into the gravitino. This coupling however, is very weak and results in long lifetimes for the scalar. Depending on the exact parameters and the momentum of the  $\tilde{\tau}$ , it may possibly decay within the detector giving the clear signal of a *displaced vertex* at the end of an ionized track, or it may even traverse the detector and escape. Observations of such signatures would constitute a *smoking gun* for LFV at an  $e^-e^-$ -collider. Therefore,  $\tilde{\tau}$  production is of special interest. It should be noted that in  $e^+e^-$  collisions the staus can be directly produced. This signature hence does not establish LFV as easily there.

Investigating the squared amplitude, namely (3.21), (3.22), (3.27), (3.28), a unique feature of the production process  $e^-e^- \rightarrow \tilde{\ell}_a \tilde{\ell}_b$  is found: due to the exchange of

heavy Majorana fermions, i. e. the neutralinos, in the  $t$ - and  $u$ -channel, the amplitude squared contains contributions proportional to the transverse polarisation of one beam and the longitudinal polarisation of the other.

The Majorana character of the fermions, however, is only relevant in this specific process. Similar signatures might arise in other processes with the exchange of heavy fermions. It should be noted that no such process exists in the framework of the SM. A proof of this theorem is given in [116]. One might thus hope to exploit this feature to build an observable. These terms, however, are proportional to the LR mixing angle of the sleptons produced. For this reason, large LR mixing would be required, which is only expected in the  $\tilde{\tau}$ -sector of the MSSM. Unfortunately, numerical studies have revealed that the size of these observables is far too small to be measurable, and no polarisation based observable was found.

## 6.3 Slepton Mixing

*This section presents some general features of slepton mixing. Also, the case of vanishing direct mixing of the first two generations is discussed, and it is shown that even in this case nearly equal mixing of selectron and smuon is possible. It is shown that the analytical approximations made in section 2.3.3 are in good agreement with the numerical results and might offer a valuable tool to estimate the mixing of the sleptons analytically.*

Before studying observables for flavour violating processes, it is instructive to look at the slepton composition in various scenarios. This is of special interest as the direct mixing of selectron and smuon has already been proven to be small [56, 126, 160, 161]. In this study however, a general mixing of all three generations will be taken into account, and it was already shown in section 2.3 that this results in a quite complex pattern, even allowing for nearly equal selectron-smuon sleptons.

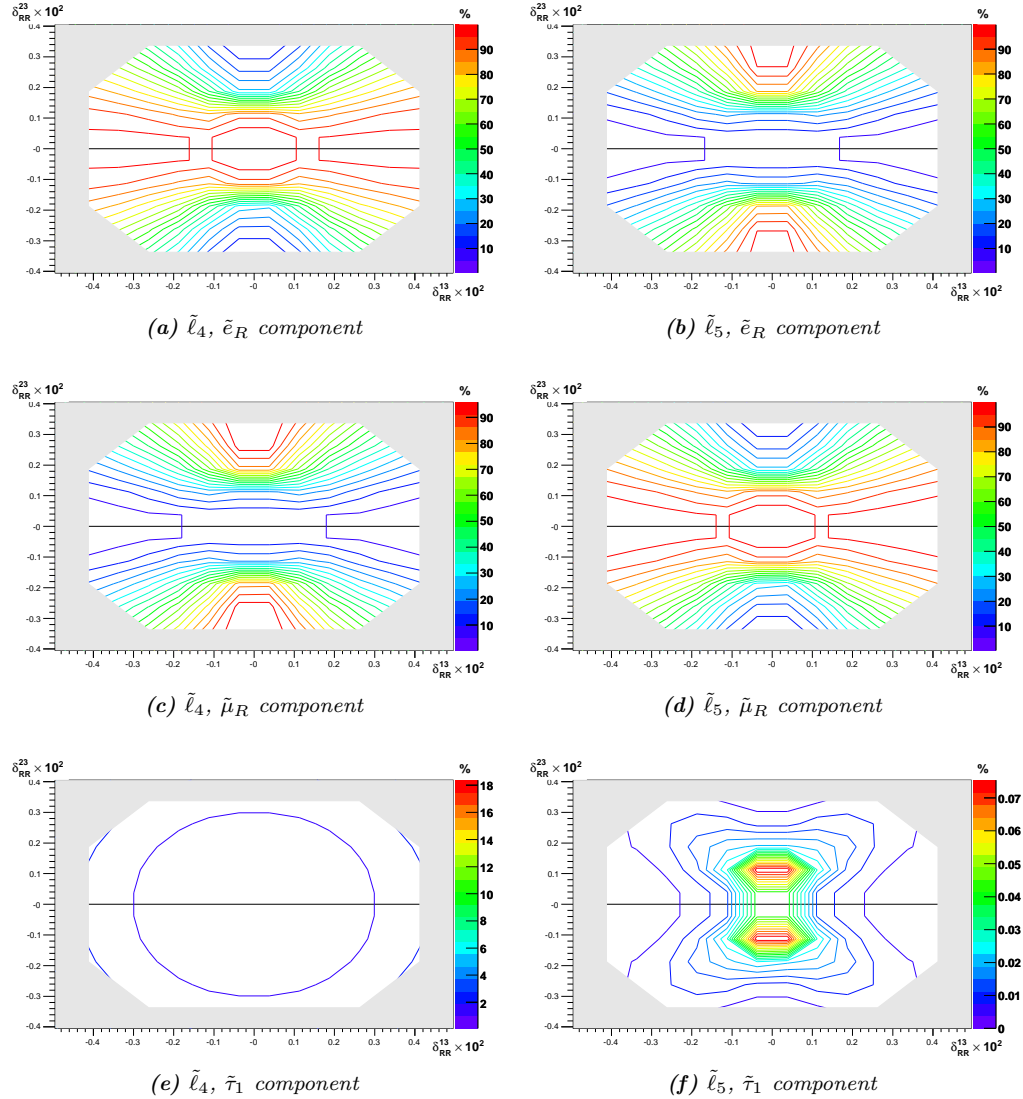
First of all, the lighter two right handed sleptons, namely  $\tilde{\ell}_4$  (“selectron R”) and  $\tilde{\ell}_5$  (“smuon R”), will be investigated. In section 2.3.3 it is predicted that even for vanishing direct mixing of these two states, i. e.  $\delta_{12}^R = 0$  sizeable mixing may result via  $\delta_{13}^R$  and  $\delta_{23}^R$ . Even an equal mixture of these two states is possible for suitable values. The numerical study depicted in figure 6.1, where all non-varied parameters are taken from SPS 1a’ (see section 4.1), clearly shows this effect. The shaded area corresponds to the limits from table 6.1. Similar results are found in all scenarios considered in this work. Noteworthy are the large regions with nearly equal mixing of the two states. These results are in agreement with earlier parameter scans which have estimated the size of LFV by picking random points in the parameter space [24, 25, 27, 28, 101].



Figure 6.1 shows that one of the lighter sleptons contains nearly no stau component. This is in perfect agreement with the analytical approximative prediction from (2.33). Taking the parameters of SPS 1a', this is  $\tilde{\ell}_5$ , as can be seen from figure 6.1f (note the colour scale, which is different to the other plots in this figure). On the other hand, it has been shown in (2.34) that one of the lighter two sleptons gets some  $\tilde{\tau}_1$  component which is proportional to  $\lambda_{1,3} - m_1^2$ . Due to the bounds on LFV only a small shift between the mass parameter and the physical mass is to be expected resulting in a small stau component. In the numerical example of SPS 1a' one observes this for  $\tilde{\ell}_4$  as seen from figure 6.1e. The size of this admixture reaches only about 4% with a weak dependence on  $\delta_{RR}^{13}$  and  $\delta_{RR}^{23}$ . Similar results are found in the other scenarios.

The final crucial result of section 2.3.3 is that the impact of  $\delta_{RR}^{12}$  on the mixing of the sleptons should be negligible as soon as  $\delta_{RR}^{13}, \delta_{RR}^{23} \gg \delta_{RR}^{12}$ . This is also established in the numerical studies. Taking SPS 1a' as an example, the comparison of figure 6.1 for  $\delta_{RR}^{12} = 0$  with figure 6.2 for  $\delta_{RR}^{12} = 1.5 \cdot 10^{-4}$  shows no visible difference. This also holds for all other scenarios considered. In this work, the current upper limit for  $\delta_{RR}^{12} = 1.5 \cdot 10^{-4}$  is used for all subsequent calculations to explore the maximal effects possible though the results will not change even for much lower values of  $\delta_{RR}^{12}$ .

Finally, keep in mind that for the analytical approximation in section 2.3.3 the LR mixing is entirely neglected, i. e.  $\delta_{RL}^{ij} = 0$ . In all numerical studies in the following sections however, the usual mSUGRA values for the diagonal elements of  $\delta_{RL}^{ii} = m_i(A_i - \mu \tan \beta)$  are being used. In the  $\tilde{\tau}$ -sector this leads to some mixing between the left and right states. It does not, however, affect the state without any stau admixture, which explains its very good agreement with the approximations. For the two states where the stau is involved, LR mixing results in a slight mass shift towards lower values. Additionally, it should be mentioned that a mixing of the left states is not taken into account, i. e.  $\delta_{LL}^{ij} = 0$ . The good validity of the analytical approximations, that assume a complete decoupling of the left and right handed sector, seems to justify this approach. Besides this, a mixing in the left sector would only affect the right handed part by means of the LR mixing.



**Figure 6.1:** Composition of slepton 4 (left column) and slepton 5 (right column) as a function of the flavour violating matrix entries  $\delta_{RR}^{13}$  and  $\delta_{RR}^{23}$ .  $\delta_{RR}^{12} = 0$  for all plots. The shaded area is already excluded experimentally, all non-varied parameters are from scenario SPS 1a' (section 4.1).

## 6.4 Numerical Results for LFV

*This section gives numerical results for the size of LFV for the scenarios SPS 1a', Point  $\varepsilon$  and SPS 7. For the latter two it is discussed whether a background free measurement is possible. This seems to be the case for Point  $\varepsilon$ , but is more difficult in SPS 7.*

After having studied of some general features of the slepton mixing in the previous section, the prospects to observe and establish LFV in the  $e^-e^-$  mode of a linear collider will now be discussed. Also in this context also the mixing in the different scenarios will be examined. The value of  $\delta_{RR}^{12}$  is always kept fixed at its upper limit of  $\delta_{RR}^{12} = 1.5 \cdot 10^{-4}$  unless stated otherwise.

Although in the context of LFV, there exists no such particle as a  $\tilde{e}_R$  in large parts of parameter space, one of the sleptons will contain a dominant  $\tilde{e}_R$  component. This particle can be thought of as a selectron with some small admixture of the other sleptons. To simplify the language in the following sections the particle with the largest  $\tilde{e}_R$  component will be called the  $\tilde{e}_R$  by convention. The other sleptons will be handled similarly, that is the  $\tilde{\mu}_R$  being the slepton with the largest  $\tilde{\mu}_R$  component and the  $\tilde{\tau}_1$  being the lighter of those two sleptons with the largest stau component.

### 6.4.1 SPS 1a'

First of all, the mixing of the sleptons will be considered in SPS 1a'. It is displayed in figure 6.2 by the  $\tilde{e}_R$  and  $\tilde{\tau}_1$  content of each slepton. The flavour mixing matrix elements  $\delta_{RR}^{13}$  and  $\delta_{RR}^{23}$  are varied, whereas the flavour mixing parameter  $\delta_{RR}^{12}$  was set to  $1.5 \cdot 10^{-4}$ , i. e. on the upper limit allowed by experimental data. The shaded area is excluded by the bounds given in table 6.1.

Without flavour violation the  $\tilde{\ell}_4$  would be the  $\tilde{e}_R$ , the  $\tilde{\ell}_5 \sim \tilde{\mu}_R$  and the  $\tilde{\ell}_6 \sim \tilde{\tau}_1$  (the  $\tilde{\tau}$  states show also some LR mixing, hence no strict right stau exists). The first observation is that the sleptons keep their characters in large regions of the allowed flavour violating parameter space. For  $\tilde{\ell}_4$  this means, that it is mainly a  $\tilde{e}_R$  for any allowed value  $-0.2 \cdot 10^{-2} < \delta_{RR}^{23} < 0.2 \cdot 10^{-2}$  (figure 6.2a). In the same region  $\tilde{\ell}_5$  is mainly a  $\tilde{\mu}_R$ . Its  $\tilde{\mu}_R$ -component can be deduced from figure 6.2c, keeping in mind that this particle is only a mixture of  $\tilde{e}_R$  and  $\tilde{\mu}_R$  due to its negligible  $\tilde{\tau}_1$  component (figure 6.2d).

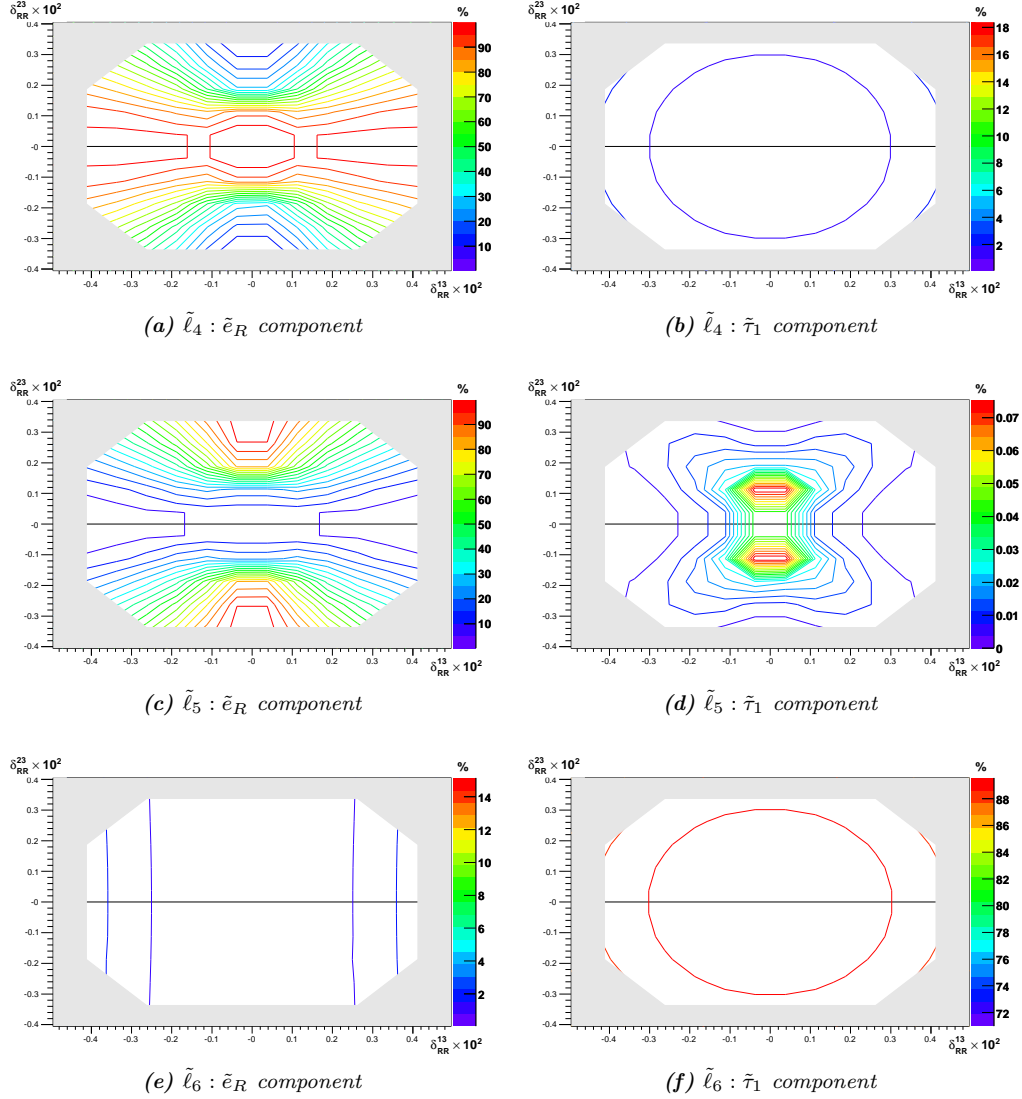


**Figure 6.2:** Selectron and stau content of  $\tilde{\ell}_4$  (first line),  $\tilde{\ell}_5$  (second line) and  $\tilde{\ell}_6$  (third line) as a function of the flavour violating matrix entries  $\delta_{RR}^{13}$  and  $\delta_{RR}^{23}$ .  $\delta_{RR}^{12} = 1.5 \cdot 10^{-4}$  for all plots. The shaded area is already excluded experimentally.

Studying the mixing of  $\tilde{\ell}_5$  one observes that, even despite the tiny value of  $\delta_{RR}^{12} = 1.5 \cdot 10^{-4}$  parametrising the direct mixing of the selectron and smuon compone, it contains a sizeable  $\tilde{e}_R$  component in large regions of parameter space (figure 6.2c). For  $-0.2 \cdot 10^{-2} < \delta_{RR}^{13} < 0.2 \cdot 10^{-2}$  and  $\delta_{RR}^{23} > 0.2 \cdot 10^{-2}$  (or  $\delta_{RR}^{23} < -0.2 \cdot 10^{-2}$ )  $\tilde{\ell}_5$  even turns into a mainly  $\tilde{e}_R$ -like particle whereas  $\tilde{\ell}_4$  gets a major  $\tilde{\mu}_R$  component. Here, the definition of the  $\delta$ s has to be kept in mind, as they are multiplied by the corresponding diagonal mass terms. The comparison with the selectron component of  $\tilde{\ell}_4$  in figure 6.2a reveals that the rise of the selectron component in  $\tilde{\ell}_5$  is directly related to the decrease of this component in  $\tilde{\ell}_4$ . So, even with a tiny (or even no, see figure 6.1) direct mixing of these two sleptons in this scenario nearly equal mixture of  $\tilde{e}_R$  and  $\tilde{\mu}_R$  in the  $\tilde{\ell}_4$  and the  $\tilde{\ell}_5$  can be found, provided  $\delta_{RR}^{13}$  and  $\delta_{RR}^{23}$  have suitable values. This is in agreement with the analytical approximations of section 2.3.3 as well as the earlier random parameter scans [24, 25, 27, 28, 101].

It should be stressed here that, although the direct mixing of  $\tilde{e}_R$  and  $\tilde{\mu}_R$  is negligible ( $\delta_{RR}^{12} = 1.5 \cdot 10^{-4}$ ), the largest mixing of the states is found between these two. At its maximum values, this mixing can lead to equal  $\tilde{e}_R$  and  $\tilde{\mu}_R$  components in  $\tilde{\ell}_4$  as well as in  $\tilde{\ell}_5$ , which results in large flavour violating production cross sections.

Another remarkable result, also in perfect agreement with the analytical approximations of section 2.3.3, is the already mentioned negligible  $\tilde{\tau}_1$  admixture in  $\tilde{\ell}_5$ . Note, that the colour scale in figure 6.2d is approximately three orders of magnitude smaller than in the other panels.

The second flavour violating vertex relevant in  $e^-e^-$  collision is the  $e-\tilde{\tau}-\tilde{\chi}^0$  vertex. The size of the coupling involved in this vertex depends crucially on the  $\tilde{e}_R$ - and the  $\tilde{\tau}_1$ -components of the sleptons. The first observation is that the stau component in  $\tilde{\ell}_4$  is at best at the percent level in (figure 6.2b), whereas it is entirely negligible for  $\tilde{\ell}_5$ . Compared to  $\tilde{e}_R$ - $\tilde{\mu}_R$  mixing, the maximum obtainable mixing with the  $\tilde{\tau}_1$ -state is suppressed by almost one order of magnitude. This is, once more, in agreement with the analytical approximations of (2.33) and (2.34).

From this very minute  $\tilde{\tau}$ -admixture to  $\tilde{\ell}_5$  it follows that the decay  $\tilde{\ell}_5 \rightarrow \tau\tilde{\chi}^0$  is negligible. For this reason  $\tau$ s observed from  $e^-e^- \rightarrow \tilde{\ell}_a\tilde{\ell}_b$  and the decays of the sleptons may only stem from the decay of  $\tilde{\ell}_4$  or the direct flavour violating production of a “ $\tilde{\tau}_1$ ” (i. e.  $\tilde{\ell}_6$ ) via  $e^-e^- \rightarrow \tilde{\ell}_{4,5}\tilde{\ell}_6$ , and the subsequent practically “flavour conserving” decay  $\tilde{\ell}_6 \rightarrow \tau\tilde{\chi}^0$ . This can also be observed in the relevant branching ratios  $\tilde{\ell}_4 \rightarrow \tau\tilde{\chi}_1^0$  and  $\tilde{\ell}_6 \rightarrow \tau\tilde{\chi}_1^0$ . The decays of  $\tilde{\ell}_4$  show a  $\tilde{\tau}$  final state in less than 5% of the entire allowed parameter space, even below 1% of the largest part of parameter space, while more than 95% fo the decays of  $\tilde{\ell}_6$  do so.

Finally, as already mentioned,  $\tilde{\ell}_6$  is mainly a  $\tilde{\tau}_1$  (figure 6.2f) in the entire allowed flavour violating parameter space. It only gains some  $\tilde{e}_R$ -contribution at the percent level (figure 6.2e). Its smuon component, on the other hand, is negligible, as is the  $\tilde{\tau}_1$  contributions to  $\tilde{\ell}_5$ . A parameter scan of the flavour violating process  $e^-e^- \rightarrow \tilde{\ell}_4\tilde{\ell}_5$  (i. e. “ $\tilde{e}_R$ - $\tilde{\mu}_R$ ” production) shows large total cross sections in sizeable regions of the parameter space, figure 6.3. In figure 6.3a, the flavour mixing parameter  $\delta_{RR}^{12}$  is set to  $1.5 \cdot 10^{-4}$ , whereas figure 6.3b shows the same for  $\delta_{RR}^{12} = 0$ . It

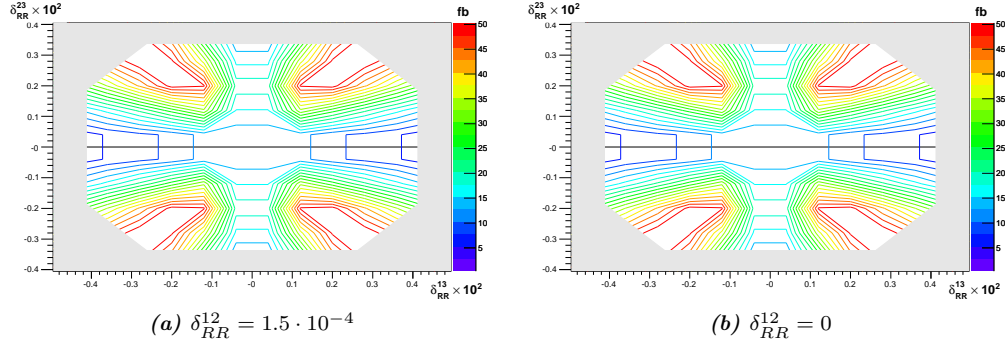


**Figure 6.3:** Total cross section for the production channel  $e^-e^- \rightarrow \tilde{e}_R\tilde{\mu}_R$  as a function of the flavour violating matrix entries  $\delta_{RR}^{13}$  and  $\delta_{RR}^{23}$  in the scenario SPS 1a' (section 4.1). The collider energy is set to  $\sqrt{s} = 500$  GeV.

can be seen that, within the current experimental bounds, the effect of  $\delta_{RR}^{12}$  is not visible in SPS 1a'. On the other hand, even if the direct mixing vanishes, sizeable cross sections up to  $\approx 50$  fb are possible due to the effect of three generation mixing discussed earlier. Here, the regions of maximum cross section coincide with the regions of maximum mixing between the  $\tilde{e}_R$  and  $\tilde{\mu}_R$  states. This can be seen in comparison of figure 6.3a with figure 6.2a, and figure 6.2c, respectively. It is also true for the decay branching ratios shown for the heavier two right sleptons in figure 6.4, for the decay of  $\tilde{\ell}_4$  to an  $e$  or a  $\mu$  and in figure 6.5, and for the decay of  $\tilde{\ell}_5$  in the same channels. It should be noted that, due to the slepton masses, only the leptonic decay channels are kinematically allowed.

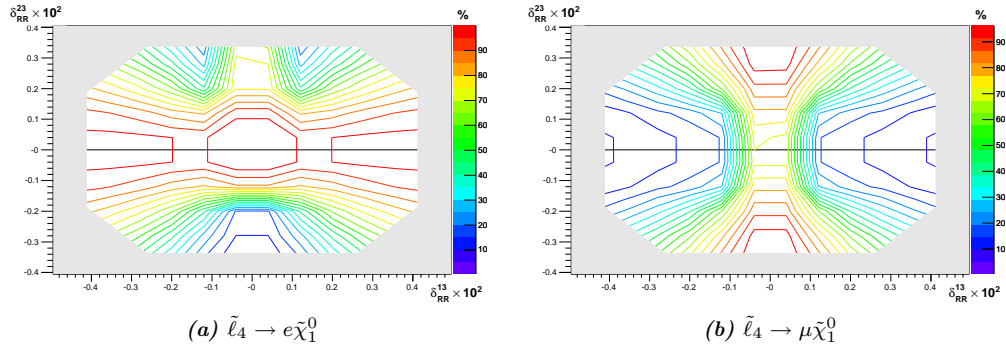


**Figure 6.4:** Branching ratio of the leptonic decays (a)  $\tilde{\ell}_4 \rightarrow e\tilde{\chi}_1^0$  (a) and (b)  $\tilde{\ell}_4 \rightarrow \mu\tilde{\chi}_1^0$  as a function of the flavour violating matrix entries  $\delta_{RR}^{13}$  and  $\delta_{RR}^{23}$  for  $\delta_{RR}^{12} = 1.5 \cdot 10^{-4}$  in the scenario SPS 1a' (section 4.1).

Compared to the flavour violating production of a “ $\tilde{\mu}_R$ ” in  $e^-e^-$  collision, the similar “ $\tilde{\tau}_1$ ” production is much more challenging. Figure 6.2 shows, that the  $\tilde{\tau}_1$

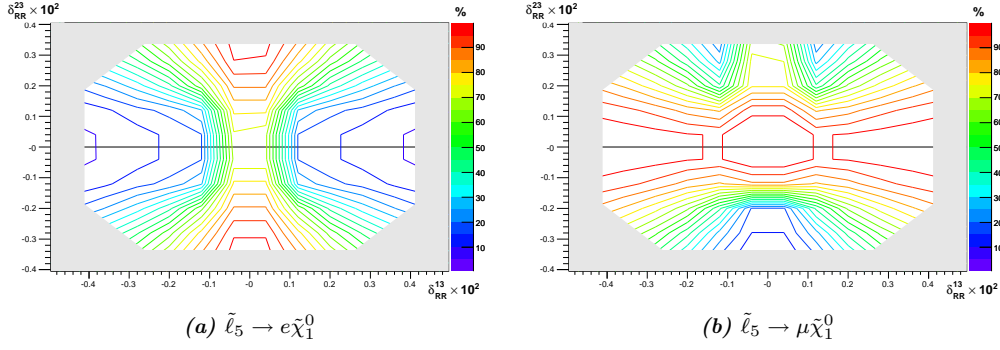


**Figure 6.5:** Branching ratio of the leptonic decays (a)  $\tilde{\ell}_5 \rightarrow e\tilde{\chi}_1^0$  and (b)  $\tilde{\ell}_5 \rightarrow \mu\tilde{\chi}_1^0$  as a function of the flavour violating matrix entries  $\delta_{RR}^{13}$  and  $\delta_{RR}^{23}$  for  $\delta_{RR}^{12} = 1.5 \cdot 10^{-4}$  in the scenario SPS 1a' (section 4.1).

component of  $\tilde{\ell}_4$  as well as the  $\tilde{e}_R$  component of  $\tilde{\ell}_6$  are much smaller than the equivalent  $\tilde{\mu}_R$  components, because the mixing with the stau sector is suppressed. This results in much lower flavour violating production cross sections, as seen from figure 6.6. The maximum cross sections reached are below 10 fb. Again, no difference for vanishing  $\delta_{RR}^{12}$  can be observed, figure 6.6b.

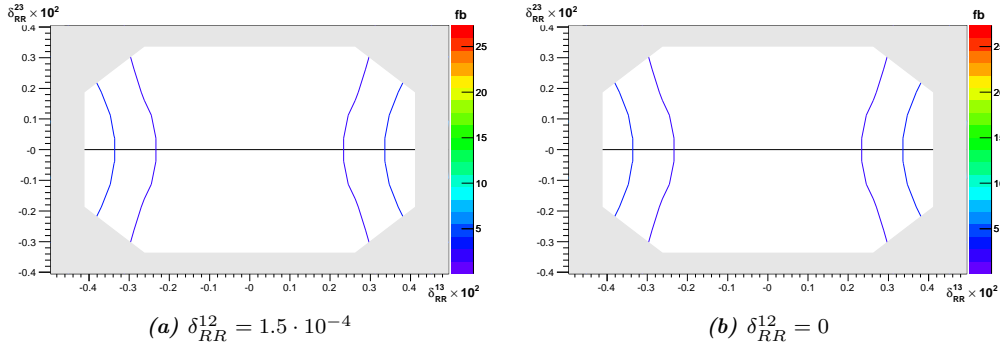


**Figure 6.6:** Total cross section for the production channel  $e^- e^- \rightarrow \tilde{e}_R \tilde{\tau}_1$  as a function of the flavour violating matrix entries  $\delta_{RR}^{13}$  and  $\delta_{RR}^{23}$  in the scenario SPS 1a' (section 4.1). The collider energy is set to  $\sqrt{s} = 500$  GeV.

## 6.4.2 Point $\varepsilon$

Before investigating Point  $\varepsilon$  in detail, the  $\tilde{e}_R$ - and the  $\tilde{\tau}_1$ -components of the sleptons are shown in figure 6.7. Again, in large regions of the parameter space  $\tilde{\ell}_4$  is found to be mainly a  $\tilde{e}_R$  and  $\tilde{\ell}_5$  mainly a  $\tilde{\mu}_R$ , whereas  $\tilde{\ell}_6$  plays the role of the  $\tilde{\tau}_1$ . It is noted immediately, that the experimentally allowed values for the flavour mixing parameters  $\delta_{RR}^{13}$  and  $\delta_{RR}^{23}$  are much larger in this scenario. Roughly speaking,  $|\delta_{RR}^{13}| < 0.55 \cdot 10^{-2}$  and  $|\delta_{RR}^{23}| < 0.4 \cdot 10^{-2}$ , which is nearly three times as large as the allowed range in SPS 1a'. An immediate consequence is, that in this scenario a much larger slepton mixing is in agreement with current experiments.

Considering, first of all, the  $\tilde{e}_R$ -components in  $\tilde{\ell}_4$  and  $\tilde{\ell}_5$  again a similar pattern as in SPS 1a' is found: in large parts of the allowed parameter space the sleptons keep the dominant character they would have in the flavour conserving case, but again the mixture of  $\tilde{\ell}_4$  and  $\tilde{\ell}_5$  can reach sizeable values. As already mentioned, due to the scaling of the flavour violating parameters with the proper diagonal matrix elements, the ranges are comparable in all scenarios.

As a larger part of the flavour violating parameter space is allowed in Point  $\varepsilon$  than in SPS 1a', the  $\tilde{\tau}_1$  component in  $\tilde{\ell}_4$  may reach much higher values of up to 5% (figure 6.7b). Nearly the same value can be reached for the  $\tilde{e}_R$ -component in  $\tilde{\ell}_6$ . The  $\tilde{\tau}_1$  contribution to  $\tilde{\ell}_5$  is negligible in the entire allowed parameter space, as seen from figure 6.7d, however, it can be about half an order of magnitude larger than in SPS 1a'.

For the flavour violating production process  $e^-e^- \rightarrow \tilde{\ell}_4\tilde{\ell}_5$  a similar pattern as in SPS 1a' is found. It is given in figure 6.8 for a collider energy of  $\sqrt{s} = 500$  GeV and longitudinally polarised beams to optimise the cross section. A degree of 90% is assumed for the polarisation, and production cross sections of up to  $\approx 50$  fb are reached in sizeable regions of the parameter space.

In this scenario, an important difference to SPS 1a' is, that the LSP is not the lightest neutralino, but the gravitino. For this reason, the decay of a right slepton is given by its decay to the  $\tilde{\ell}_6$ , which is the NLSP. The actual decay mode depends on the mass splitting of the right sleptons. For a sufficient large mass splitting, as realised in this scenario, the decay is mainly given by the three-body decay  $\tilde{\ell}_R \rightarrow \ell\tilde{\tau}_1\tau$ , and the subsequent decay of  $\tilde{\tau}_1$  to the gravitino. The latter is observable only, if the lifetime of  $\tilde{\tau}_1$  is short enough for it to decay within the detector [23, 120]. This results in the following process to be considered:

$$e^-e^- \rightarrow \tilde{\ell}_4^-\tilde{\ell}_5^- \rightarrow (\mu^-\tilde{\ell}_6^\pm\tau^\mp)(e^-\tilde{\ell}_6^\pm\tau^\mp). \quad (6.8)$$

$\tilde{\ell}_6$  in this case would be a long living particle, as it is the NLSP, and has to decay to the gravitino. For this reason the signal in the detector would consist of

- two ionised tracks from  $\tilde{\ell}_6$ ,
- two taus,
- one muon,



- one electron.

This signature can also result from the production process  $e^-e^- \rightarrow \tilde{\ell}_4\tilde{\ell}_4 \rightarrow (\mu\tilde{\ell}_6\tau)(e\tilde{\ell}_6\tau)$ , which is of the same flavour violating order. For the quantitative analysis using the decay products this has to be taken into account.

It should be stressed, that this signature allows for a background free measurement of flavour violation, if the mass splitting is  $\approx 15 - 20$  GeV. Otherwise the produced leptons are too soft and escape detection [23, 120]. The relevant mass differences are given in figure 6.9. Throughout the flavour violating parameter space, the mass splitting is sufficient to observe the leptons produced, as seen from the figure. This results in a unique identification of the flavour violating process  $e^-e^- \rightarrow \tilde{\ell}_4\tilde{\ell}_5$  to be possible.

Due to the long lifetime of the  $\tilde{\tau}_1$ , the production process  $e^-e^- \rightarrow \tilde{\ell}_4\tilde{\ell}_6^-$  is of special interest in this scenario. As in SPS 1a', the production cross section for this channel is much lower due to the generally smaller mixing of the states. The total production cross section for suitable longitudinal beam polarisation (assuming a polarisation of 90%) is given in figure 6.10 at  $\sqrt{s} = 500$  GeV. The collider signature for the process

$$e^-e^- \rightarrow \tilde{\ell}_4\tilde{\ell}_6^- \rightarrow (e^-\tilde{\ell}_6^\pm\tau^\mp)(\tau^-\tilde{\ell}_6^\pm\tau^\mp) \quad (6.9)$$

of production and decay would be

- two ionised tracks from  $\tilde{\ell}_6$ ,
- three taus,
- one electron.

Again, it could also stem from the flavour conserving production, and a subsequent flavour violating decay  $e^-e^- \rightarrow \tilde{\ell}_4\tilde{\ell}_4^- \rightarrow (\tau^-\tilde{\tau}_1^\pm\tau^\mp)(\tau^-\tilde{\tau}_1^\pm\tau^\mp)$ .

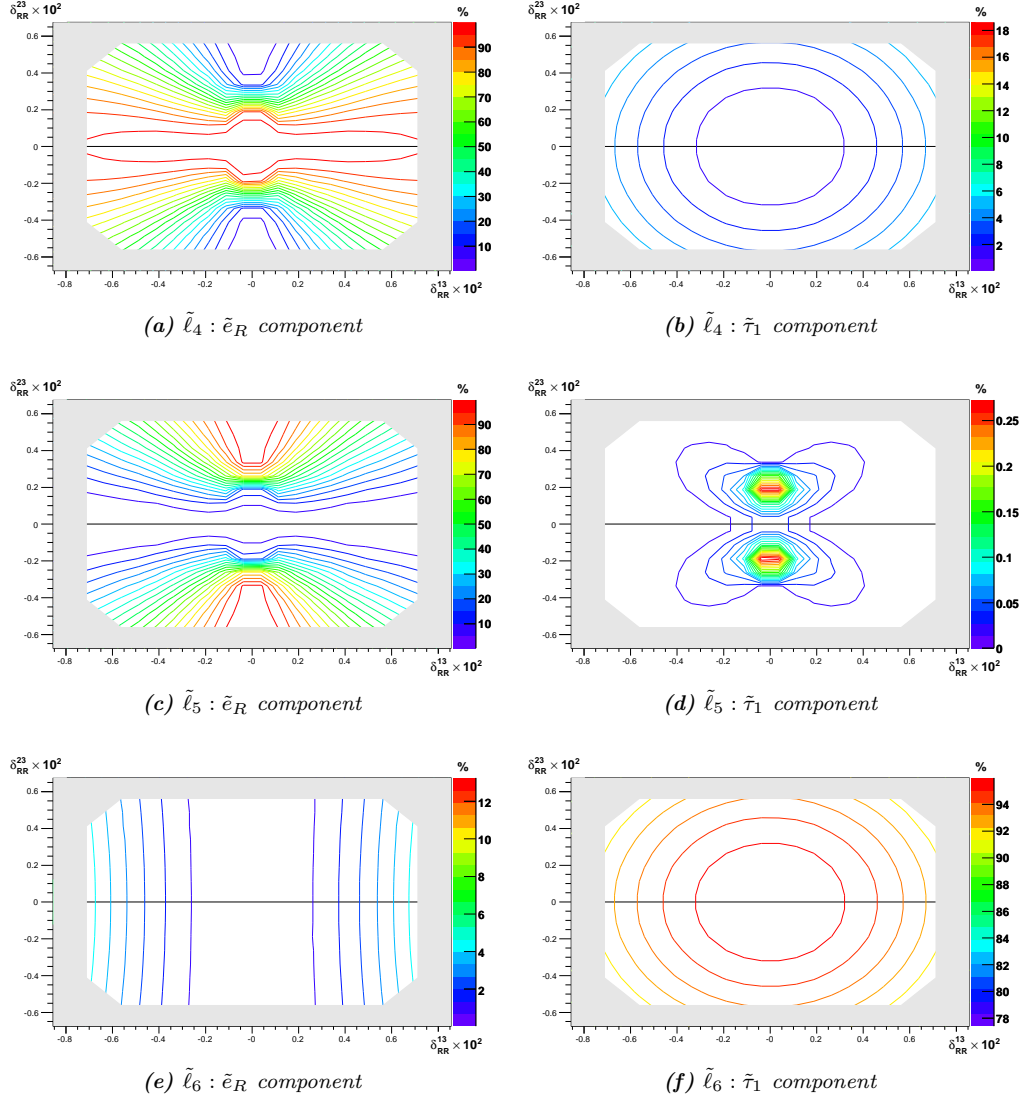


**Figure 6.7:** Selectron and stau content of  $slepton_4$  (first line),  $\tilde{\ell}_5$  (second line) and  $\tilde{\ell}_6$  (third line) as a function of the flavour violating matrix entries  $\delta_{RR}^{13}$  and  $\delta_{RR}^{23}$ .  $\delta_{RR}^{12} = 1.5 \cdot 10^{-4}$  for all plots. The shaded area is already excluded experimentally.

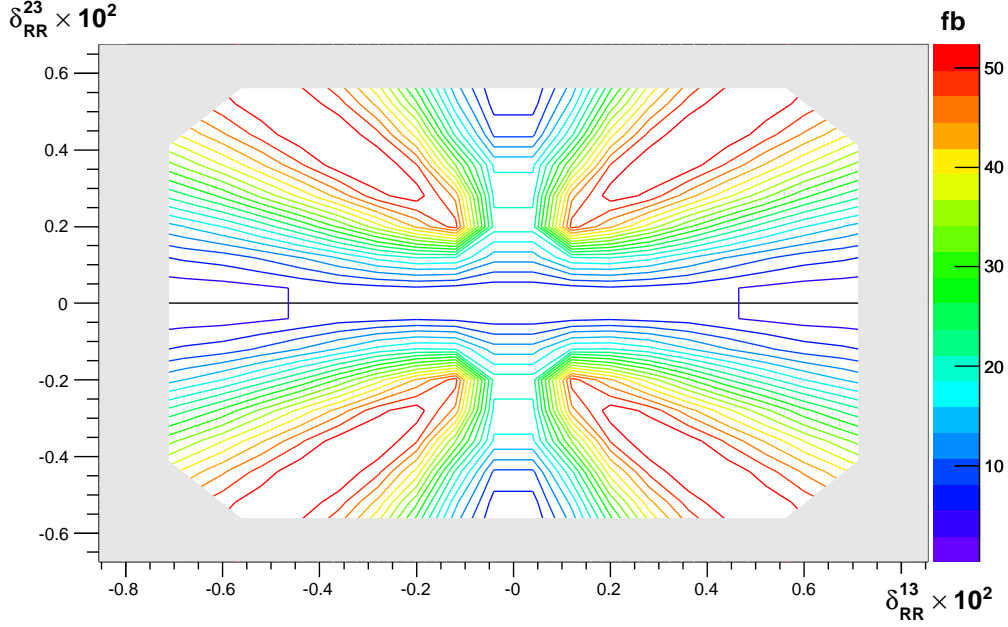


**Figure 6.8:** Total cross section for the production channel  $e^-e^- \rightarrow \tilde{e}_R \tilde{\mu}_R$  as a function of the flavour violating matrix entries  $\delta_{RR}^{13}$  and  $\delta_{RR}^{23}$  in the scenario Point  $\varepsilon$  (section 4.6). The shaded area is already excluded experimentally.  $\sqrt{s} = 500$  GeV and  $P_1^L = -P_2^L = 0.9$ .

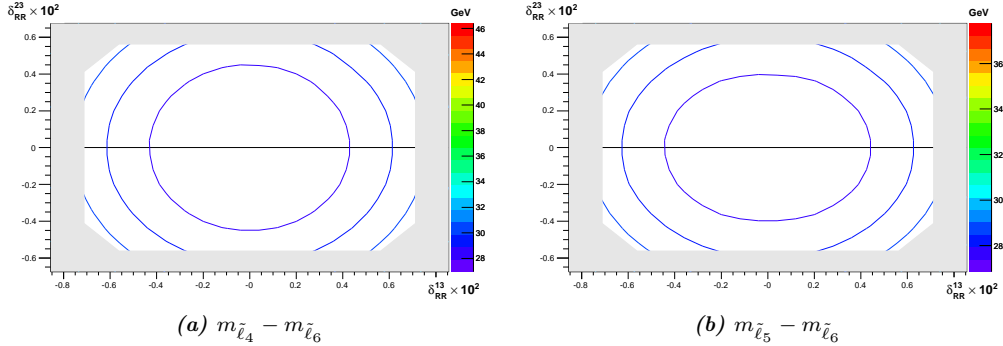


**Figure 6.9:** Mass splitting of the right sleptons in Point  $\varepsilon$ . (a) shows the difference between the masses of  $\tilde{\ell}_4$  and  $\tilde{\ell}_6$ , (b) that between the masses of  $\tilde{\ell}_5$  and  $\tilde{\ell}_6$ . The mass splitting is larger than 20 GeV throughout the allowed parameter space.

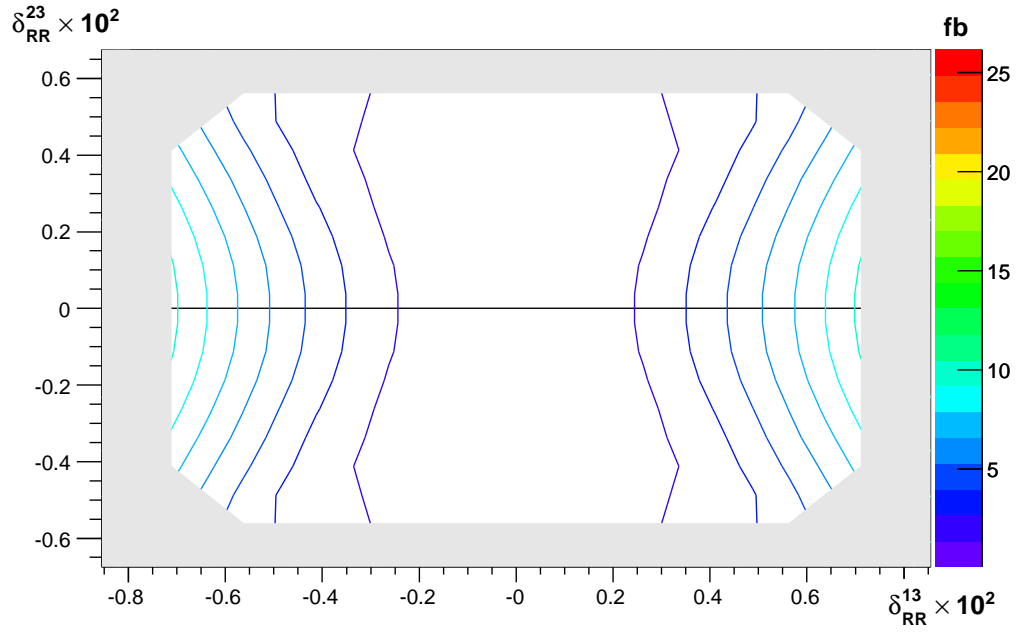


**Figure 6.10:** Total cross section for the production channel  $e^-e^- \rightarrow \tilde{e}_R\tilde{\tau}_1$  as a function of the flavour violating matrix entries  $\delta_{RR}^{13}$  and  $\delta_{RR}^{23}$  in the scenario Point  $\varepsilon$  (section 4.6). The shaded area is already excluded experimentally. The collider energy is set to  $\sqrt{s} = 500$  GeV. A right handed longitudinal polarisation of 90% was assumed for each beam.

### 6.4.3 SPS 7

The mixing of the slepton states for SPS 7 is given in figure 6.11. First of all, one finds great similarity to Point  $\varepsilon$  although the experimentally allowed region is a bit larger:  $|\delta_{RR}^{13}| < 0.6 \cdot 10^{-2}$  and  $|\delta_{RR}^{23}| < 0.4 \cdot 10^{-2}$ . Without flavour violation  $\tilde{\ell}_4$  would be the  $\tilde{e}_R$ ,  $\tilde{\ell}_5$  the  $\tilde{\mu}_R$  and finally  $\tilde{\ell}_6$  the lighter  $\tilde{\tau}_1$ , which is the NLSP in this scenario. As in Point  $\varepsilon$ , the LSP is the gravitino.

As seen from figure 6.11d the  $\tilde{\tau}$  component in  $\tilde{\ell}_5$  can reach only up to 0.2% in a still more confined region of the parameter space compared to Point  $\varepsilon$ . As in Point  $\varepsilon$ , this mixing is negligible, hence  $\tilde{\ell}_5$  is mainly a mixture of  $\tilde{e}_R$  and  $\tilde{\mu}_R$ . The  $\tilde{e}$ - $\tilde{\mu}$ -mixing however can be sizeable (figure 6.11a, figure 6.11c). The strong mixing of  $\tilde{\ell}_4$  and  $\tilde{\ell}_5$  can result in an inversion of their character. For  $|\delta_{RR}^{23}| > 0.25 \cdot 10^{-2}$   $\tilde{\ell}_4$  has a major  $\tilde{\mu}_R$  component, whereas  $\tilde{\ell}_5$  plays the role of the  $\tilde{e}_R$ .

Another important difference to Point  $\varepsilon$  is the larger mixing of  $\tilde{e}_R$  and  $\tilde{\tau}_1$ . In SPS 7 this mixing can be about twice as large as in Point  $\varepsilon$ . For  $|\delta_{RR}^{23}| > 0.3 \cdot 10^{-2}$  and  $|\delta_{RR}^{13}| > 0.5 \cdot 10^{-2}$  the  $\tilde{\tau}_1$  component in  $\tilde{\ell}_4$  is larger than 12% (figure 6.11b). On the other hand, for  $\tilde{\ell}_6$  a selectron component above 8% is found for  $|\delta_{RR}^{13}| > 0.55 \cdot 10^{-2}$  (figure 6.11e), while the dependence of this component on  $\delta_{RR}^{23}$  is only weak. This large selectron-stau mixing together with the possible inversion of the selectron and smuon states can also result in a large stau-smuon mixing. For  $|\delta_{RR}^{23}| > 0.3 \cdot 10^{-2}$  and  $|\delta_{RR}^{13}| > 0.5 \cdot 10^{-2}$  regions in parameter space with a large  $\tilde{\tau}_1$  component in  $\tilde{\ell}_4$  are found. Additionally, the selectron-smuon mixing in this region of parameter space results in  $\tilde{\ell}_4$  containing a dominant  $\tilde{\mu}_R$  component.

With the gravitino-LSP one might suspect the same background free measurements of flavour violation to be possible, as in Point  $\varepsilon$ . However, investigating the mass splitting of the sleptons given in figure 6.12a it is found to be very small. As seen from the thick dotted line in figure 6.12a, the mass difference  $m_4 - m_6$  is in almost the entire allowed parameter space smaller than 15 GeV, whereas the splitting  $m_5 - m_6$  is smaller than this limit throughout the allowed parameter space. At this limit, the collider signature for the decay of sleptons change, as the decay leptons might be too soft and escape detection [23, 120]. An immediate problem that would arise in this case is, that the intermediate state could not be reconstructed by the flavour of the primary decay leptons stemming from the decay  $\tilde{\ell}_a \rightarrow \ell_a \tilde{\tau}_1^\pm \tau^\mp$ . In this case the collider signature would then consist solely of

- two ionised tracks from  $\tilde{\ell}_6$ ,
- two  $\tau$ ,
- missing-energy from the soft leptons.

Another difficulty results from the fact, that the heavier right sleptons could decay directly to the gravitino via  $\tilde{\ell}_a \rightarrow \ell_a \tilde{G}$ , posing the problem of their identification. If their lifetime is short enough to decay within the detector, one could use the decay

leptons from  $\tilde{\ell}_a \rightarrow \ell_a \tilde{G}$ , together with the visible displaced vertex. Calculations done using SPHENO [124], as well as earlier simulations by SUSYGEN [162] indicate that this will be the case. As, on the other hand, calculations by ISAJET [163] show a dominant decay of the heavier states to  $\tilde{\tau}_1$ , it has to be concluded that the decay calculations are not yet under good control.

However, if by any means the character of the intermediate slepton states can be determined, flavour violation can be established in this scenario in the  $\tilde{\ell}_4 - \tilde{\ell}_5$ -channel in large regions of parameter space by a background free measurement. Total production cross sections are displayed in figure 6.13a, and they reach values larger than 50 fb. It should be kept in mind though, that the regions of maximal production cross sections in this channel coincide with those regions with minimal mass splitting as seen by comparison with figure 6.12. Still, about 30 – 40 fb are reached in regions where a larger mass splitting may allow the determination of the primary decay leptons.

Also, in the associate production of  $\tilde{\ell}_4$  with  $\tilde{\ell}_6$  cross sections up to  $\approx 30$  fb can be reached in this scenario, especially for small values of  $|\delta_{RR}^{23}| \leq 0.5 \cdot 10^{-2}$ , if a large direct mixing between  $\tilde{e}_R$  and  $\tilde{\tau}_1$  is realised ( $\delta_{RR}^{13} > 0.75 \cdot 10^{-2}$ ). This is displayed in figure 6.13b. The dependence on the value of  $\delta_{RR}^{23}$  in this scenario is more pronounced than in Point  $\varepsilon$ , and the cross sections can be up to about twice as large as those in, Point  $\varepsilon$ .

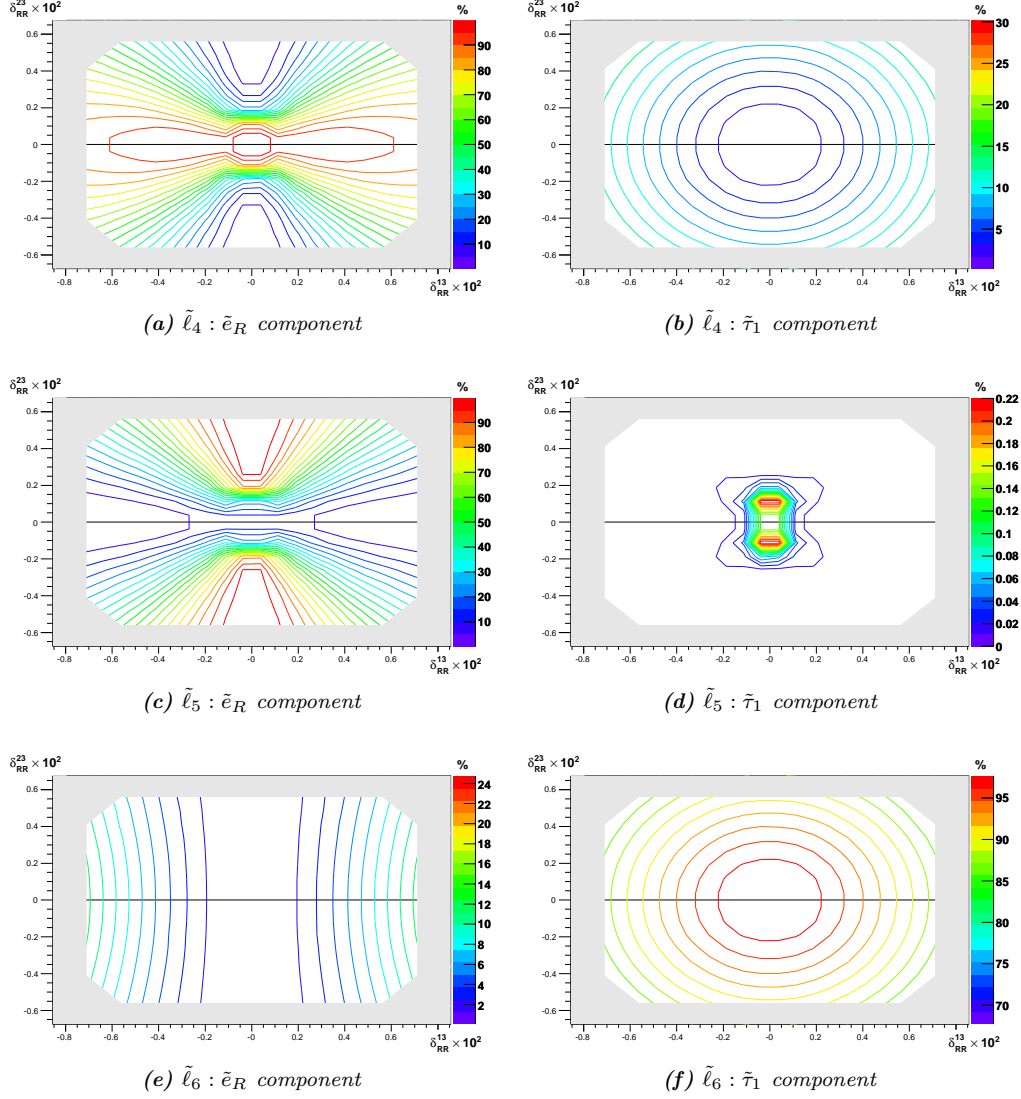


**Figure 6.11:** Selectron and stau content of  $\tilde{\ell}_4$  (first line),  $\tilde{\ell}_5$  (second line) and  $\tilde{\ell}_6$  (third line) as a function of the flavour violating matrix entries  $\delta_{RR}^{13}$  and  $\delta_{RR}^{23}$ .  $\delta_{RR}^{12} = 1.5 \cdot 10^{-4}$  for all plots. The shaded area is already excluded experimentally.

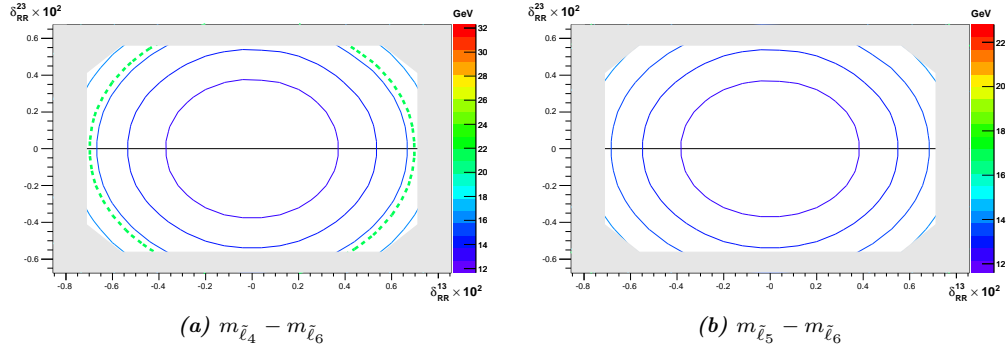


**Figure 6.12:** Mass splitting of the right sleptons in SPS 7. (a) shows the difference between the masses of  $\tilde{\ell}_4$  and  $\tilde{\ell}_6$ , (b) that between  $\tilde{\ell}_5$  and  $\tilde{\ell}_6$ . The thick dotted line marks a splitting of 15 GeV.

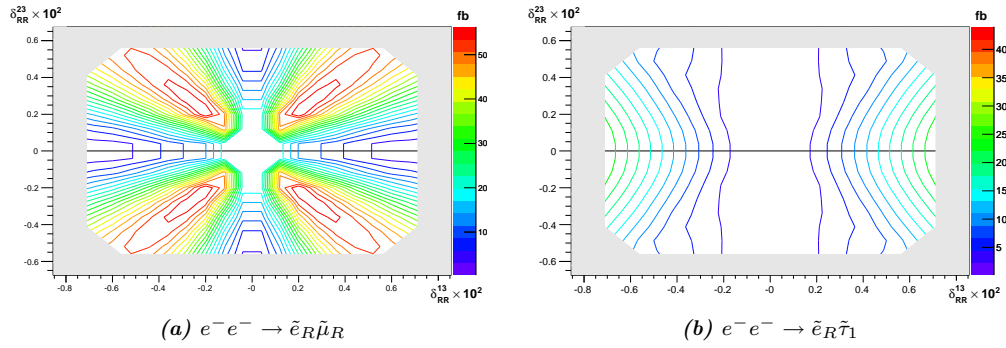


**Figure 6.13:** Total cross section for the production channels  $e^-e^- \rightarrow \tilde{e}_R \tilde{\mu}_R$  and  $e^-e^- \rightarrow \tilde{e}_R \tilde{\tau}_1$  as a function of the flavour violating matrix entries  $\delta_{RR}^{13}$  and  $\delta_{RR}^{23}$  in the scenario Point  $\varepsilon$  (section 4.6). The collider energy is set to  $\sqrt{s} = 500$  GeV.



# Muon Colliders: $\mu^- \mu^-$

For increasing the energy while still keeping the advantages of the clean environment of a circular lepton collider, it was already proposed in the 1960s to build a muon collider [164]. Recently, this opportunity has been discussed again mainly to investigate the electroweak symmetry breaking and the Higgs mechanism [165–175].

Like the  $e^- e^-$  mode is an option for the upcoming ILC, the  $\mu^- \mu^-$  mode would be a similar option at a future muon collider. (For the current status of this project see, e. g., [176]). The process under consideration here would be

$$\mu^- \mu^- \rightarrow \tilde{\ell}_i \tilde{\ell}_j. \tag{7.1}$$

The *First Muon Collider* (FMC), however, is currently planned to run at energies of  $\sqrt{s} = 100 - 500$  GeV and its design luminosity at  $\sqrt{s} = 500$  GeV is about  $10^{33}$  1/cm<sup>2</sup>s (see [176, table XIV]), an order of magnitude lower than the luminosity of the ILC. Additionally, the achievable degree of polarisation is only about 40%. From this follows, that a muon collider running in the  $\mu^- \mu^-$  mode would help only in scenarios where the sleptons are too heavy to be produced in  $e^- e^-$  collisions [177], and only if enough energy is available in a later stage of the project. Heavy sfermions are a common feature e. g., scenarios of split supersymmetry [178]. The *Next Muon Collider* (NMC) projected for 3-4 TeV would allow to study these scenarios [170].

The  $\mu^- \mu^-$  mode will be studied here briefly at  $\sqrt{s} = 500$  GeV for comparison. The general results could be transferred to higher energies. In all scenarios considered in this work, comparable results were found, hence only an illustrative example based upon SPS 1a' will be given.

Figure 7.1 shows the total cross sections for selectron and smuon production, respectively. The production cross sections are practically identical for selectron production in  $e^- e^-$  and smuon production in  $\mu^- \mu^-$ , as kinematic effects play no role, and the couplings are practically the same for both generations. From this follows an advantage of  $e^- e^-$  compared to  $\mu^- \mu^-$ , because the  $e^- e^-$ -collider operates at higher luminosities and allows for higher degrees of polarisation.

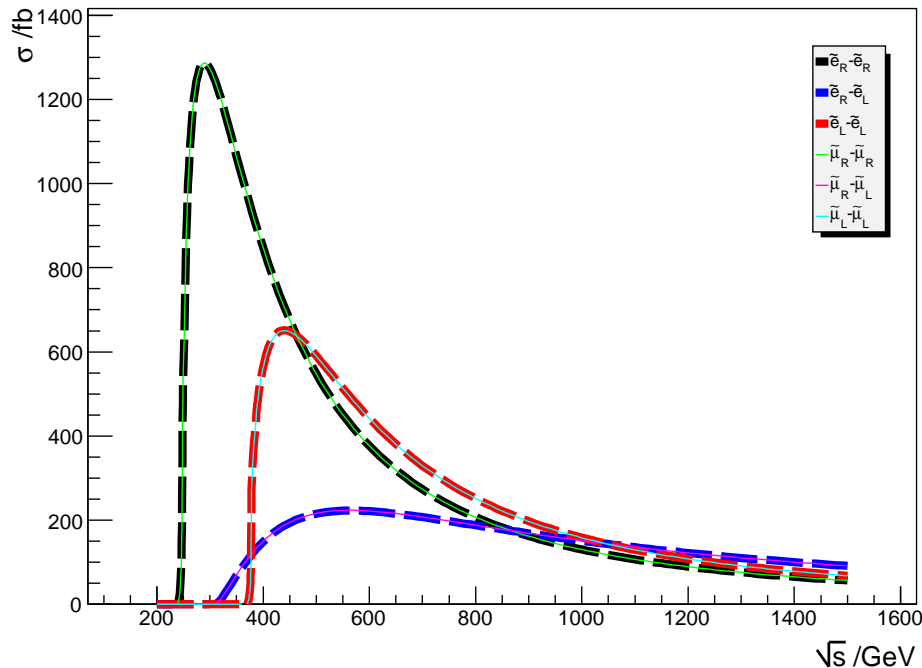


**Figure 7.1:** Total cross sections for selectron production channels  $e^-e^- \rightarrow \tilde{e}_{R/L}\tilde{e}_{R/L}$  (thick) and smuon production channels  $\mu^-\mu^- \rightarrow \tilde{\mu}_{R/L}\tilde{\mu}_{R/L}$  (thin) in the scenario SPS 1a' as a function of the centre of mass energy  $\sqrt{s}$ . Both beams are unpolarised.

## 7.1 $CP$ Violation

*The effect of  $CP$  violation in  $e^-e^-$ -scattering is compared to the  $\mu^-\mu^-$ -scattering case.*

The  $CP$  phase dependence of the total cross section is shown for the  $e^-e^-$  as well as  $\mu^-\mu^-$  collider in figure 7.2a and figure 7.2b. No difference is found for pair production and also the tiny difference for associate production, figure 7.2b, is negligible.

For the  $CP$ -sensitive observables in  $\mu^-\mu^-$ -scattering one also finds almost identical results as in  $e^-e^-$ . From this follows that the terms linear in the transverse polarisation, though containing  $CP$ -sensitive parts, are too small in  $\mu^-\mu^-$  to give any observable contribution. This is again a result from the tiny LR mixing, even in the smuon sector.

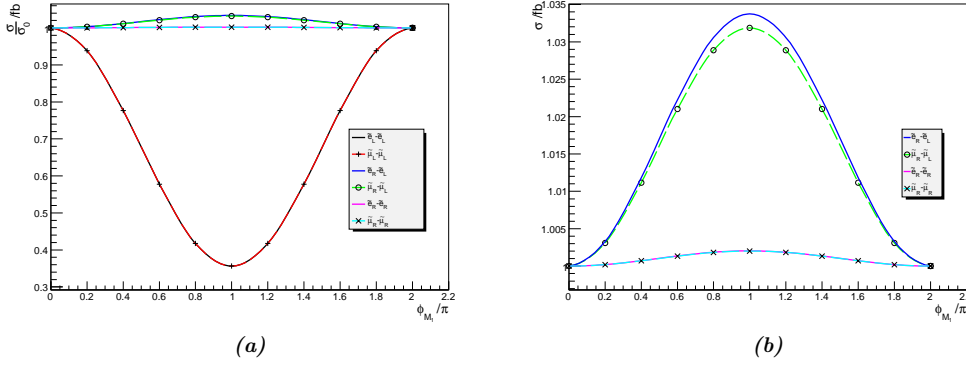


**Figure 7.2:** Dependence of the total cross section on the phase of  $M_1$  for selectron (lines) and smuon production (lines and markers). (a) shows all possible channels, (b) gives a close up of the RL and RR production.

## 7.2 LFV

*The effect of LFV investigated in chapter 6 for  $e^-e^-$ -scattering is compared to the  $\mu^-\mu^-$ -scattering case.*

For heavy sleptons, a muon collider could be advantageous as higher energies could be reached than in  $e^-e^-$  collisions. This would be relevant, if the sleptons are too heavy to be produced at significant rates at the  $e^-e^-$ -collider [177]. In the  $\mu^-\mu^-$  mode, the leading flavour violating processes would include the production of either a selectron or a stau together with a smuon. In the study of LFV at the muon collider one notices first of all that the bounds to selectron-stau mixing ( $\delta_{13}$ ) and to smuon-stau mixing ( $\delta_{23}$ ) are comparable, and one can find similar effects.

This holds also for the more complex three generation mixing, where nearly equal selectron and smuon components are possible for the sleptons of the first two generations. For this reason, all results from  $e^-e^-$  collisions can be transferred to the  $\mu^-\mu^-$  case.

Additionally, it should be noted that the muon collider at its first stage offers already the opportunity to study the rare decays of muons at the proton-driver [170, 179]. This front end physics could give stringent bounds on flavour violation. Its main advantage is that the muon source has a much higher luminosity compared to the one available for current low energy experiments. Therefore, it seems unlikely that a detailed study of flavour violation at the muon collider in the  $\mu^-\mu^-$  mode is useful, except for the disentangling of flavour violation in the left or right sector, which is not possible in low energy experiment. Generally, the results from chapter 6, however, can easily be translated to the  $\mu^-\mu^-$  case.

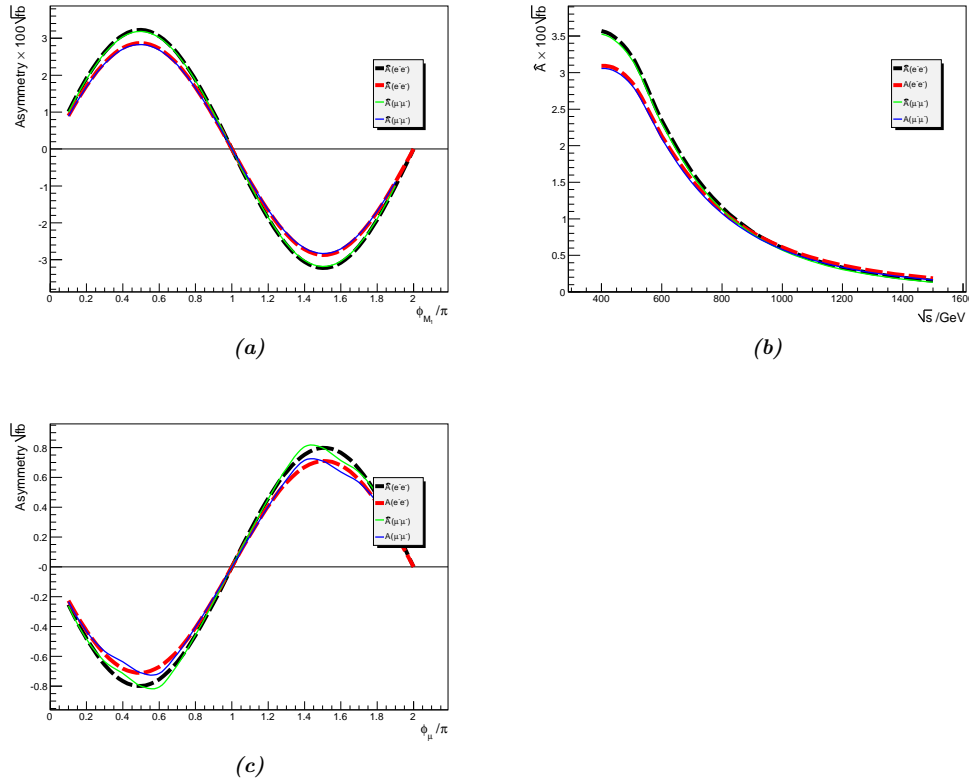


**Figure 7.3:**  $CP$ -sensitive observable as a function of the phase of  $M_1$   $\phi_{M_1}$  (figure 7.3a) at 500 GeV, and its energy dependence at constant phase  $\phi_{M_1} = \pi/2$  (figure 7.3b). For comparison the simple observable  $\hat{A}[\mathcal{F}_1]$  as well as the optimised observable  $\hat{A}[\mathcal{F}_2]$  are shown. The dependence on  $\phi_\mu$  is displayed in figure 7.3c. The thick lines give the  $e^-e^-$  observables, the thin lines those expected for smuon production in  $\mu^- \mu^-$  mode.

### 7.3 $\mu^- \mu^-$ versus $e^- e^-$

*The  $\mu^- \mu^-$ - and the  $e^- e^-$  mode are compared.*

From the preceding discussion, it follows that the  $\mu^- \mu^-$  mode will be advantageous only in scenarios with very heavy scalars. For this reason the  $\mu^- \mu^-$  mode will most likely not be useful in the case of the FMC, but only at the NMC. Here, the current efforts for the design of the *Compact Linear Collider* (CLIC), operating at energies of about 3 TeV in  $e^+e^-$  mode (with the option of an  $e^-e^-$  mode as well) have to be kept in mind. This electron collider is well in the energy range of the NMC [180]. For the case of the muon collider, the much lower luminosity would favour a project

like CLIC. Additionally, the achievable polarisation of only about 40% for muons compared to about 80-90% for electrons favours an electron collider, as a much better background reduction is possible by means of longitudinal polarisation of the beams. At a muon collider this reaches only about 20% of that for the  $e^-e^-$  case.

From all this follows, that a muon collider allows to perform the same studies as in  $e^-e^-$  collisions. However, the general performance of such a machine regarding the analysis of  $CP$  violation or LFV seems to be worse than in the  $e^-e^-$  case. The only region where one might gain from the  $\mu^-\mu^-$  mode is in scenarios with heavy scalars where the larger energy reach of this machine is of importance. Even there, projects like CLIC might offer better options, though. However, front end physics at the proton driver of the muon collider seems to offer some prospects for the study of LFV in the low energy domain.



---

## Chapter 8

# Background

Compared to hadron colliders like the LHC with their huge discovery potential for new physics, the background at lepton colliders is much smaller. Therefore they generally are considered a good environment for precision measurements [10, 11, 181, 182].

In the  $e^-e^-$  mode of the ILC, the relevant background is generally considered even lower than in the  $e^+e^-$  mode, which might be advantageous [13, 14, 20, 21, 183]. The goal of this section is to get an idea about the relevant background processes and the size of the background cross sections. This is not a full featured background analysis, and also will not include any detector simulations or the optimisation of cuts. This would require details about the final collider and detector layout, that are not available yet for the  $e^-e^-$  mode.

For the numerical evaluation of the processes, the program WHIZARD [184] together with the matrix element generator O'MEGA [185, 186] have been used. It has been found, that other tools like COMPHEP [187, 188] produce unphysical results due to numerical instabilities. The handling of the rather complex four particle phase space, necessary for the calculation of the total cross section, seems not under good control there, contrary to WHIZARD. Additionally, polarised cross sections are required to study the influence of polarisation on the background. This was possible by the use of the preview version of WHIZARD 1.43. Unfortunately, none of the tools available today allow flavour violating couplings by default. So the estimates given in this section are all calculated for the flavour conserving case.

## 8.1 Standard Model Background

*This section discusses the SM background relevant for the processes in this work. The aim of this section is not to give a complete quantitative background analysis, but only to present some estimates. A full study would be beyond the scope of this work, and would only make sense, if detailed machine parameters for the collider are already known. This is not the case today.*

Except for scenarios with a gravitino LSP, allowing for a background free measurement (see chapter 6), the signal to be observed for slepton production in  $e^-e^-$  is an electron  $e$ , a lepton  $\ell^-$  from the decay of the sleptons and missing-energy  $E_{\text{miss}}$ :

$$e^-e^- \rightarrow e^-\ell^- + E_{\text{miss}}.$$

Depending on the actual decay modes, the missing-energy may stem just from an escaping LSP (i.e.  $\tilde{\chi}_1^0$ ) or it may be composed of the escaping LSP and neutrinos (e.g., if the slepton decays dominantly to the lighter chargino).

The main background from the SM results from neutrino production by

$$e^-e^- \rightarrow e^-\nu_e\ell^-\bar{\nu}_\ell,$$

where the missing-energy  $E_{\text{miss}}$  is due to the neutrinos.

In the scenarios considered in this work, the right sleptons are not heavy enough to decay to heavy neutralinos  $\tilde{\chi}_3^0$  and  $\tilde{\chi}_4^0$ . This excludes processes like

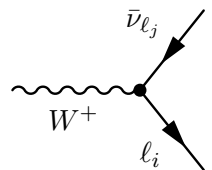
$$e^-e^- \rightarrow e^-e^-\ell^-\ell^+ + E_{\text{miss}}$$

stemming from the heavy neutralino decays. The right sleptons can only decay to  $\tilde{\chi}_2^0$  in some scenarios considered here, but compared to the decay to the LSP this is suppressed by at least an order of magnitude, and can thus be neglected.

### 8.1.1 Flavour Conserving Case

In the case of flavour conservation, the background consists of two electrons. In the SM in lowest order, the diagrams involving a W-boson and yielding the proper final state are shown in figure 8.1.

The leptonic decay vertex for the W-boson is given by



$$= i \frac{e\gamma_\mu}{\sqrt{2} \sin \theta_W} \delta_{ij} P_L, \quad (8.1)$$



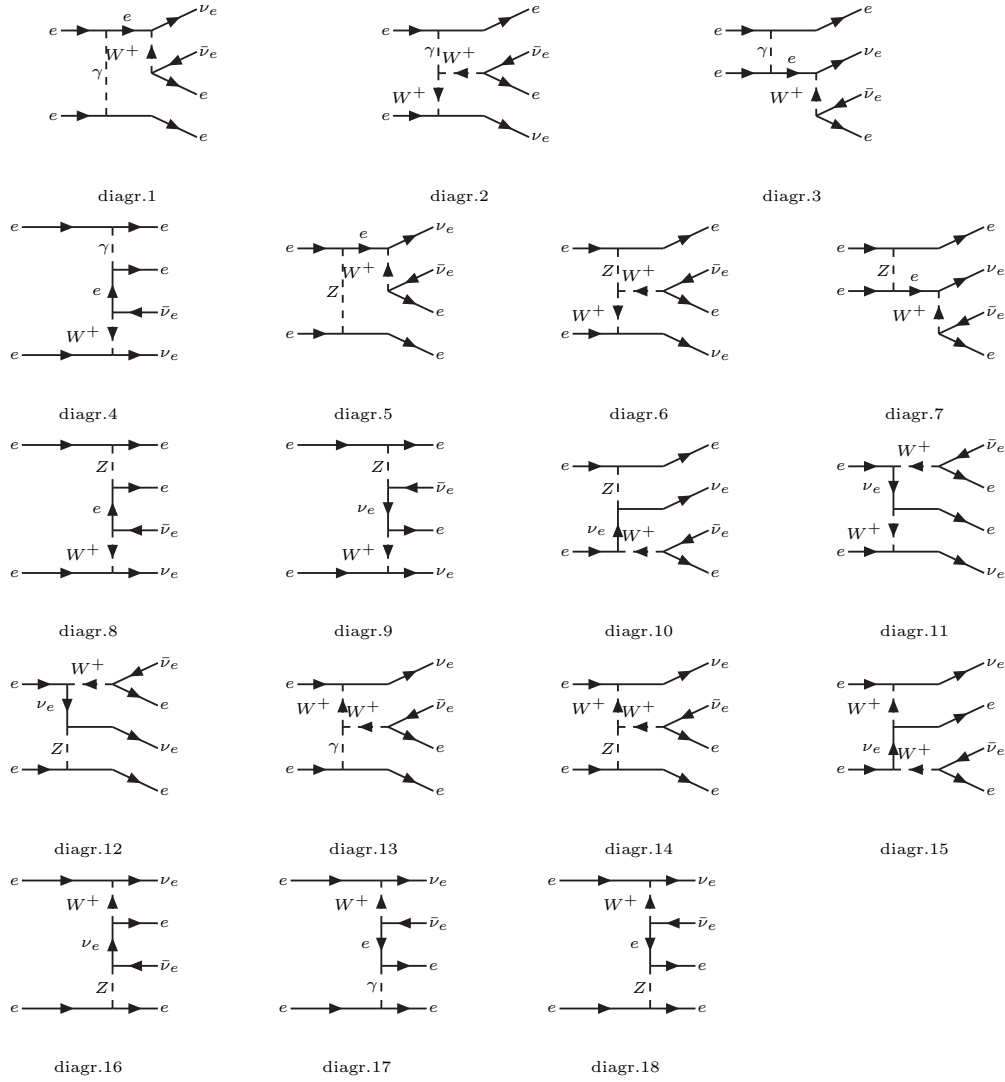


**Figure 8.1:** SM background diagrams for selectron pair production with subsequent decay to electrons (i. e. flavour conserving):  $e^-e^- \rightarrow e^-\nu_e e^-\bar{\nu}_e$ . These diagrams involve at least one  $W$ -boson.

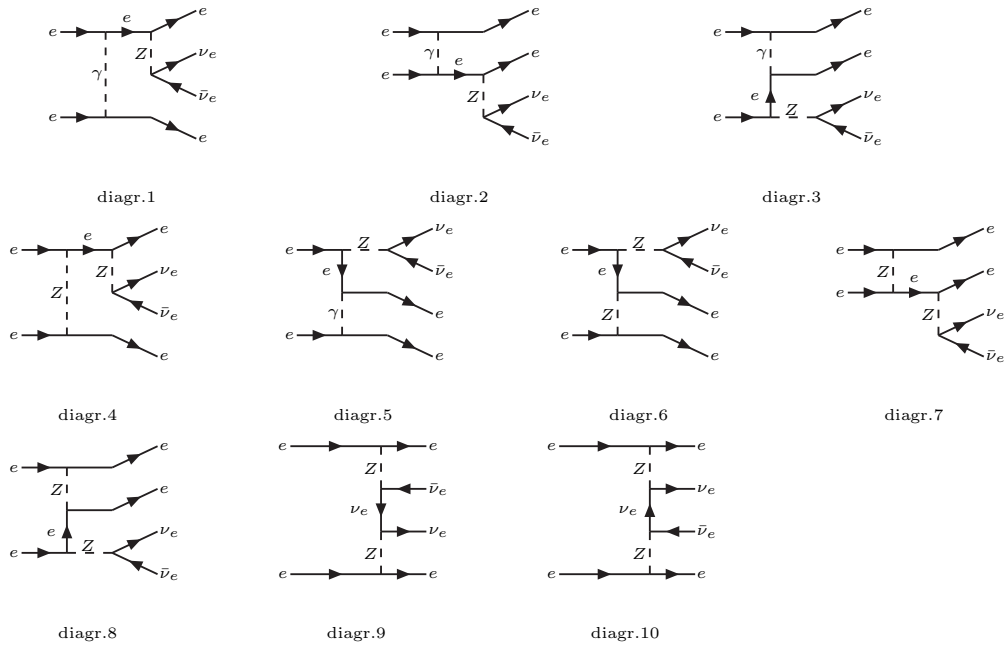


**Figure 8.2:** Diagrams contributing to the SM background for selection pair production with subsequent decay to electrons (i. e. flavour conserving):  $e^-e^- \rightarrow e^-\nu_e e^-\bar{\nu}_e$ . These diagrams do not involve any W-boson.

that is, the W-boson couples only to the left-handed part of the leptons, as can be seen clearly by the left projector  $P_L$  in the vertex. From this follows, that there is a strong polarisation dependence of the background. This gives the already mentioned handle to suppress the background by suitable polarisation.

However, besides the diagrams in figure 8.1, the same final state is also reached by the Z-boson and photon exchange diagrams shown in figure 8.2. From this follows immediately, that the background can not be switched off entirely, not even if 100% polarisation would be available.

### 8.1.2 Flavour Violating Case

In case of flavour violation, the final state under consideration consists of an electron and another lepton. This process proceeds in the SM in lowest order via the 18 diagrams given in figure 8.3.

In contrast to the flavour conserving background in the previous section, all these diagrams contain a W-boson at some point. This gives a strong dependence of the background on the polarisation of the incoming particles. If right sleptons are produced, the incoming polarisation chosen would not only enhance the production cross section, but also strongly suppress the SM background.

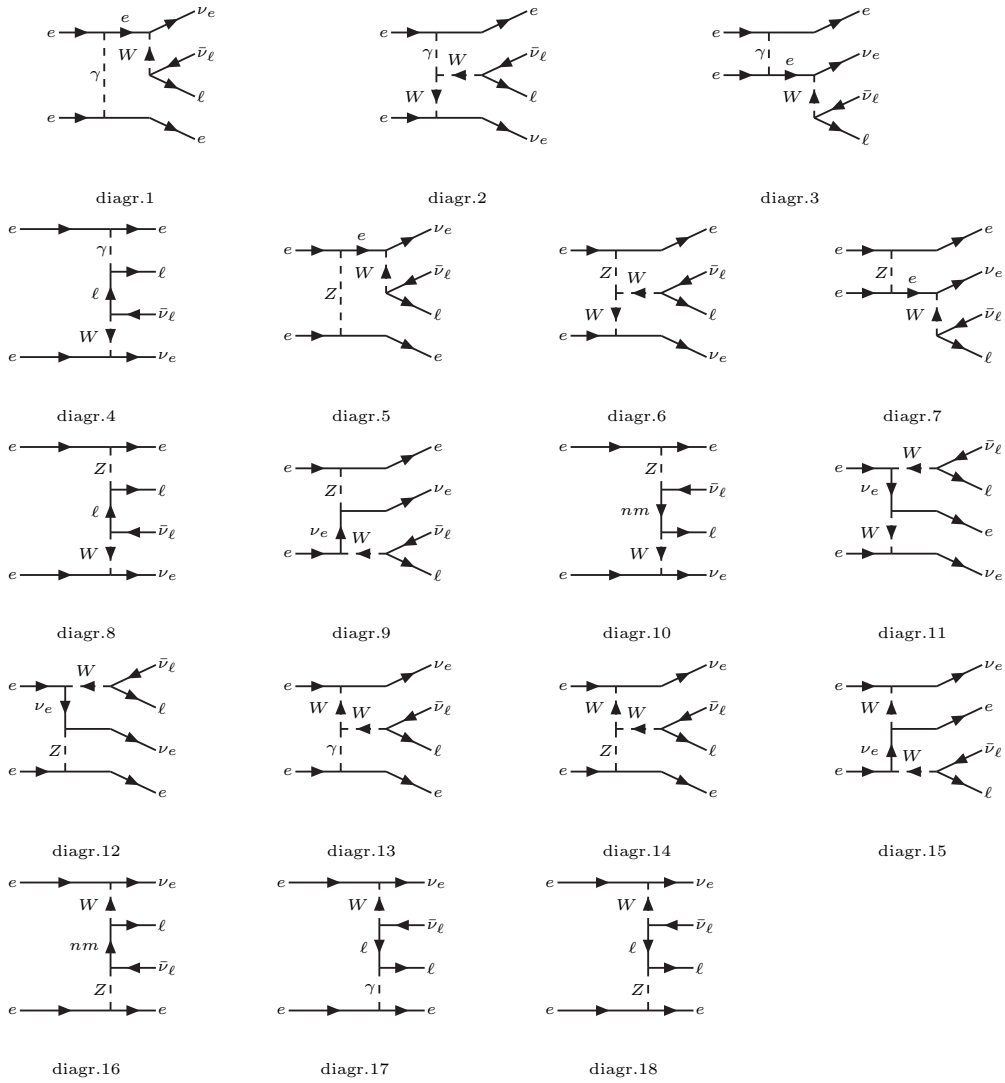


**Figure 8.3:** SM background diagrams for slepton production with subsequent decay to leptons (i.e. flavour violating):  $e^- e^- \rightarrow e^- \nu_e \ell^- \bar{\nu}_\ell$

### 8.1.3 Numerical Results

After generation of the contributing graphs within the SM by means of O'MEGA [185, 186], WHIZARD is used to calculate the total cross sections for various longitudinal polarisation modes, as well as the unpolarised case. It is assumed, that a polarisation of 80% is available according to the current design of the ILC [11, 189]. Additionally, the cuts in table 8.1 have been applied.

$$\left. \begin{array}{l} |\cos(\theta_{e^-, \nu_\ell})| < 0.90 \\ |\cos(\theta_{e^-, \ell})| < 0.90 \end{array} \right\} \begin{array}{l} E_{\bar{\nu}_\ell} > 10 \text{ GeV} \\ E_\ell > 10 \text{ GeV} \end{array}$$

**Table 8.1:** Cuts for the calculation of the SM background with WHIZARD.

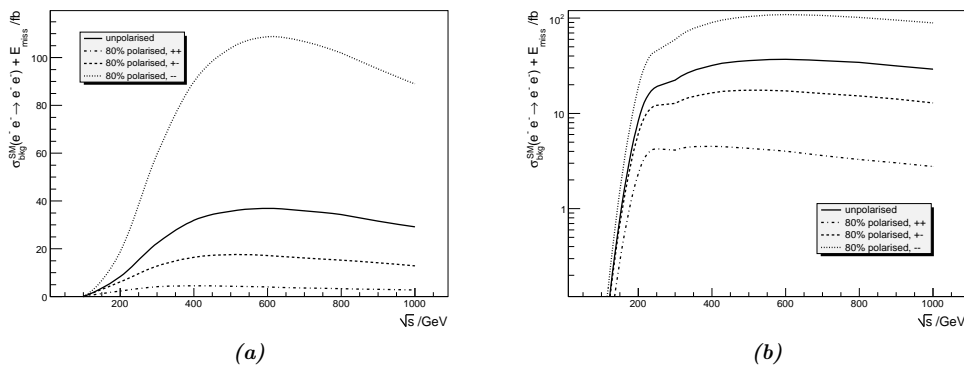


**Figure 8.4:** Polarisation dependence of the total cross sections of the SM background  $e^-e^- \rightarrow e^-e^- + E_{\text{miss}}$ . The missing-energy stems from an electron-neutrino-antineutrino pair escaping detection. For transverse polarisations, the background cross section coincides with the unpolarised one.

For flavour conserving selectron production, the background would consist of two electrons and missing-energy, which in the SM is given by an electron-neutrino-antineutrino pair that escapes detection. As can be seen from figure 8.4a, the production cross section is strongly dependent on polarisation. For unpolarised beams it reaches a maximum of about  $\approx 37$  fb at  $\sqrt{s} = 600$  GeV. This is also the value for transversely polarised beams, as they would be required for the  $CP$  violation studies in chapter 5.

The background can be reduced by almost an order of magnitude, if both beams can be longitudinally right-polarised, which is the optimal polarisation configuration for the production of right sleptons. In this case the background at  $\sqrt{s} = 600$  GeV is only about  $\approx 4$  fb, though its maximum now is reached at

$\sqrt{s} = 400$  GeV with  $\approx 4.5$  fb. It is also noteworthy, that the energy dependence of the background is much shallower than in the other polarisation modes. If one beam is right polarised, and the other one left polarised, the reduction of the background is not as strong. In this case one finds a maximum of  $\approx 18$  fb at  $\sqrt{s} = 500$  GeV, which is still only about half the size for unpolarised beams. With one beam left and one right polarisation, the associate production of one left and one right slepton would be enhanced.

On the other hand, for the production of left sleptons, left polarised electrons would be required. This also enhances the SM background considerably. It reaches a maximum of  $\approx 109$  fb at  $\sqrt{s} = 600$  GeV, about 3 times the value of unpolarised beams.

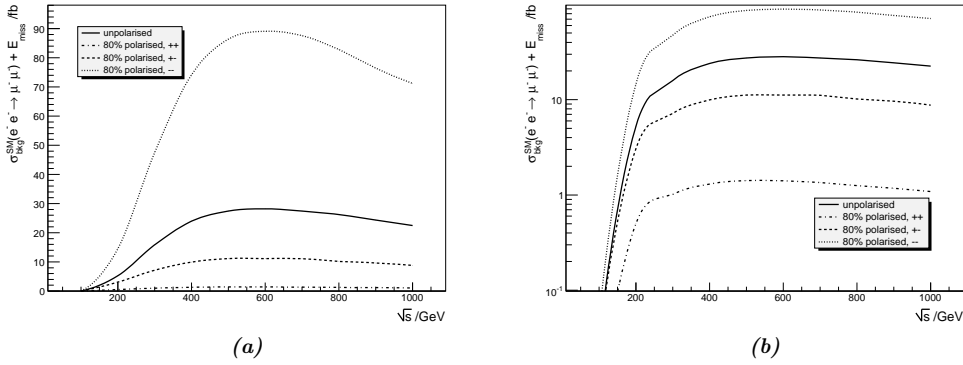


**Figure 8.5:** Polarisation dependence of the total cross sections of the SM background  $e^-e^- \rightarrow e^- \mu^- + E_{\text{miss}}$ . The missing-energy stems from an electron neutrino and a muon-antineutrino escaping detection. For transverse polarisations, the backgrounds cross section coincides with the unpolarised one.

For the study of flavour violation two channels are of relevance: the production of an electron together with a muon, or a tau together with missing-energy. In the SM the missing-energy amounts to an electron-neutrino and a muon- or tau-antineutrino escaping detection.

For the flavour violating production with subsequent leptonic decay, the relevant SM background is displayed in figure 8.5, the same is shown in figure 8.6 for the  $\tilde{e}\text{-}\tilde{\tau}$ -channel. At first, one notices that there are only minor differences in the cross sections for both background cross sections. This was expected, as the vertex (8.1) is independent of the actual lepton flavour, therefore the minimal differences are only due to the kinematics involved.

For both beams unpolarised, the background has a maximum of  $\approx 28$  fb at  $\sqrt{s} = 600$  GeV. For both beams right polarised, this value drops to  $\approx 1.4$  fb at maximum, reached at slightly higher energies as for the electron channel,  $\sqrt{s} = 500$  GeV in this case. For one left and one right polarised beam this maximum is  $\approx 18$  fb at

the same energy. The largest background is found for both beams left polarised, where it reaches  $\approx 89$  fb at  $\sqrt{s} = 600$  fb.

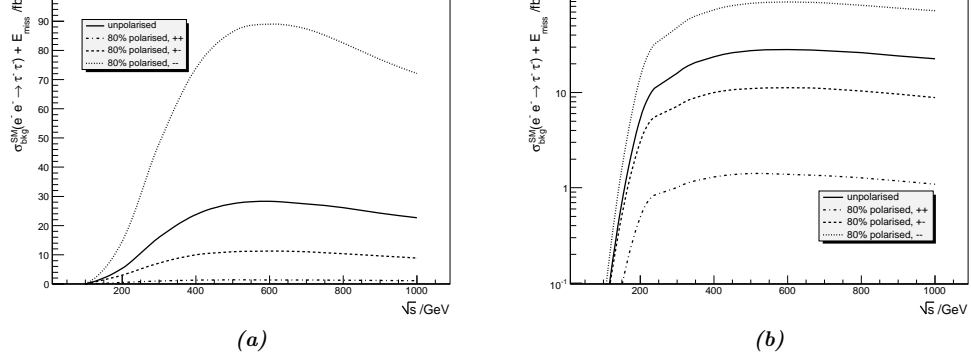


**Figure 8.6:** Polarisation dependence of the total cross sections of the SM background  $e^-e^- \rightarrow e^-\tau^- + E_{\text{miss}}$ . The missing-energy stems from an electron neutrino and a  $\tau$ -antineutrino escaping detection. For transverse polarisations, the background cross section coincides with the unpolarised one.

## 8.2 SUSY-Background

*This section summarises the relevant SUSY background, gives some estimate of its size, and compares it to the SM background on basis of the well known scenario SPS 1a'.*

In the  $R$ -parity conserving SUSY model, the following processes will contribute to the background

1.  $e^-e^- \rightarrow e^-\ell^-\tilde{\nu}_e\tilde{\nu}_\ell$
2.  $e^-e^- \rightarrow e^-\ell^-\tilde{e}_{1,2}^-\tilde{l}_{1,2}^+$
3.  $e^-e^- \rightarrow e^-\ell^-\tilde{e}_{1,2}^+\tilde{l}_{1,2}^-$
4.  $e^-e^- \rightarrow \tilde{\chi}_i^-\ell^-\tilde{\nu}_\ell$

Numerical estimates have been done with WHIZARD, and the scenario SPS 1a' serves as an example. Considering the first channel mentioned above, this mode gives a total production cross section of  $\mathcal{O}(10^{-4})$  fb, hence, it can safely be neglected. The contributions from processes 2 and 3 have been found to be of

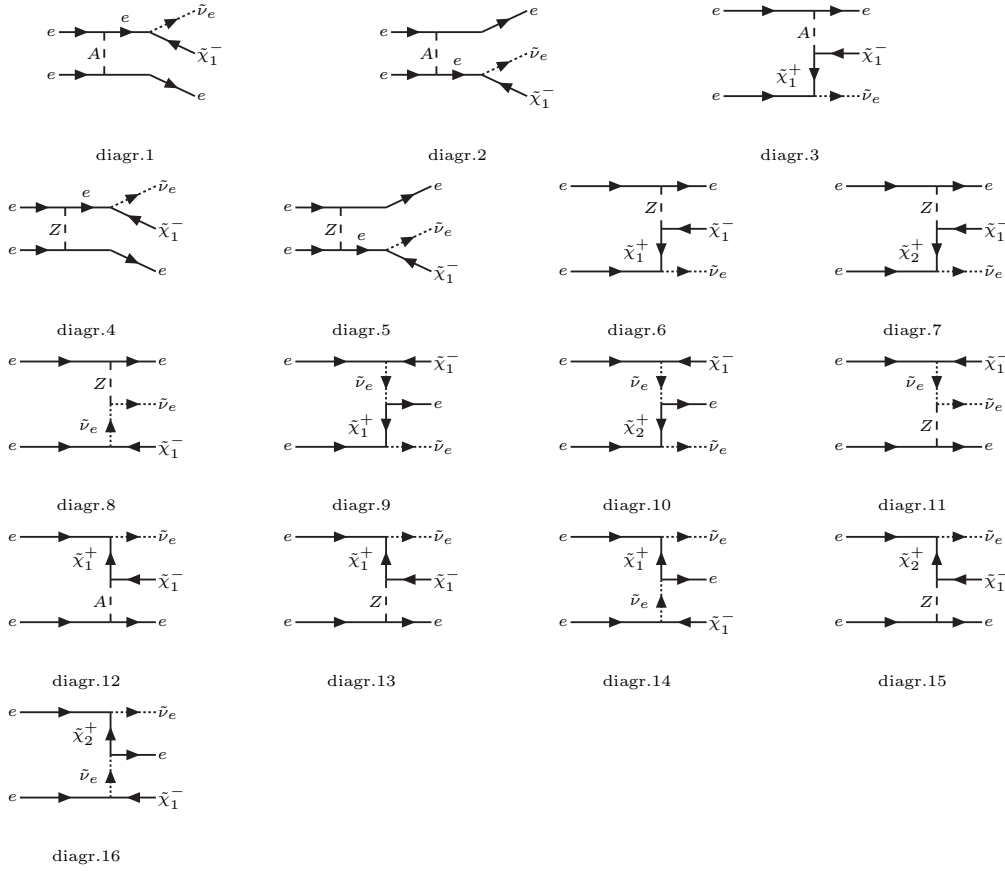


**Figure 8.7:** SUSY background diagrams for slepton production.

$\mathcal{O}(10^{-2})$  fb each, summed over all lepton channels. These contributions can also be safely neglected.

The dominant contribution to the supersymmetric background stems from the fourth channel. This is the supersymmetric version of the single- $W$ -processes in the SM. It consists of both, the production of the lighter chargino ( $\tilde{\chi}_1$ ), as well as the heavier one ( $\tilde{\chi}_2$ ). These charginos then subsequently decay to other particles which might not be distinguishable from the decay products of the sleptons, except in scenarios with metastable sleptons like Point  $\varepsilon$  or SPS 7. The production of the lighter chargino (similar for the heavier one) proceeds via the 16 diagrams shown in figure 8.7. These diagrams have been generated with COMPHEP [187,188].

The resulting production cross sections for both channels and the various polarisation modes are given in figure 8.8. From the comparison of figure 8.8a and figure 8.8b, one can see, that the contributions from  $\tilde{\chi}_2$  are about two orders of magnitude smaller than those from the lighter one. Nonetheless, general features are the same. One first notices the strong polarisation dependence of this back-

ground: for both incoming beams left polarised its contribution is almost  $36\times$  larger than for both beams right polarised. The second observation is that the background rises only slowly above the threshold (note that the scales in figure 8.8 are logarithmic). Even for unpolarised beams it stays below 10 fb, for energies  $\sqrt{s}$  up to 600 GeV, and if one beam is right polarised it is even below 5 fb in that region. Compared to the SM background it can be concluded that single-chargino production can not be neglected as a background process, as it can reach even half the size of the single-W background from the SM.

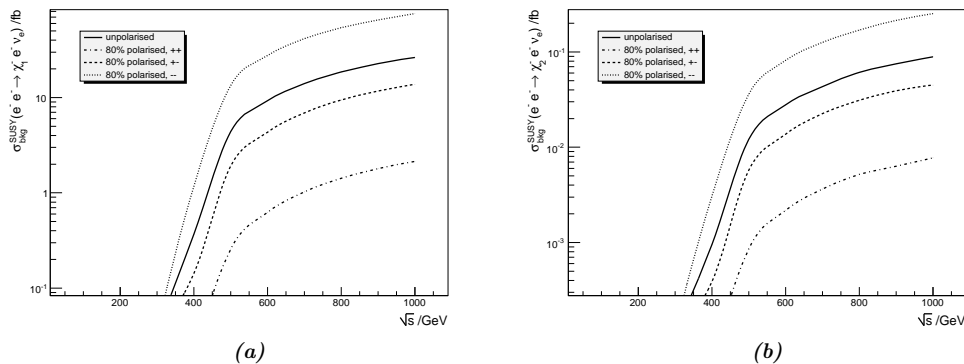


**Figure 8.8:** Polarisation dependence of the total cross sections of the SUSY background  $e^-e^- \rightarrow e^-\tilde{\chi}^- + \tilde{\nu}_e$ . For transverse polarisations, the background cross sections coincide with the unpolarised one.

For other scenarios featuring heavier sneutrinos or charginos, this background may be kinematically forbidden. In SPS 7 for example, the charginos and sneutrinos are about 100 GeV heavier each than in SPS 1a'. This will shift the production threshold for this process to higher energies. For this reason this background might not be relevant at the energies where LFV or  $CP$  violation is studied. In this sense SPS 1a' is a “worst case” scenario due to its rich phenomenology at low energies. Additionally, one can hope that once the  $e^-e^-$ -collider is running, the masses of the SUSY particles are known with sufficient precision, therefore better cuts than the simple ones applied here, may be available, resulting in this background to be under full control. The optimisation of the cuts and the separation of the signal from the background, however, will be the domain of experimental particle physics, and is clearly beyond the scope of this work.

Finally, at least the main background contribution for the processes considered here stems from single-W production processes within the SM, and its supersymmetric analogue the single-chargino production. The latter can reach the same order of magnitude as the SM process, and for that reason can not be neglected. The other SUSY processes adding up to the background, however, are at least two orders of magnitude smaller, as far as the selectron production processes are concerned.



---

## Chapter 9

# Summary

In this work, the use of an  $e^-e^-$ -collider for the search for  $CP$  violation and LFV has been studied. For this purpose the total production cross section for arbitrary sleptons in  $e^-e^-$ -scattering has been calculated on tree level, allowing for all possible polarisation modes, i. e. longitudinal and transverse polarisation of both incoming beams. Additionally, all possible mixings in the slepton sector, particularly LR mixing and LFV, have been taken into account, and the slepton mass matrix as well as the neutralino mass matrix have been treated as complex matrices allowing for  $CP$  violation in either sector. In an analytical approximation neglecting LR mixing in the slepton sector of the MSSM, it has been shown that, even by conforming to all current experimental bounds on LFV, it is possible to obtain a large slepton mixing. In particular, it has been found that the selectron and smuon states are allowed to form sleptons of equal admixtures of both components. Another result of the analytical calculation shows, that one of the sleptons only contains a negligible stau component, and that throughout, this slepton is determined to be the slepton of intermediate mass. These analytical results were supported by numerical calculations in various representative scenarios.

The squared amplitude for the production process  $e^-e^- \rightarrow \tilde{\ell}_a\tilde{\ell}_b$  has been calculated and presented in both the covariant form, as well as in the centre of mass system. All possible modes of polarisation have been taken into account. It has been possible to construct a  $CP$ -sensitive observable using transverse polarisation of both beams. The influence of the  $CP$ -violating phases  $\phi_{M_1}$  and  $\phi_\mu$  on the total production cross section has been investigated including full neutralino mixing, thus extending earlier works [22]. It has been shown, that in contrast to the pure bino limit of [22], measurable effects can be expected even in the associate production of a left and right selectron. For the  $CP$ -sensitive observables constructed, it has been shown that they might be useful especially in higgsino-like scenarios, whereas for mixed- and gaugino-like regions the asymmetries are minute. However, there they might prove useful in scenarios involving three-body decays  $\tilde{\chi}_2^0 \rightarrow \ell\tilde{\ell}\tilde{\chi}_1^0$ . In that case the  $CP$ -violating vertex is not accessible in the decay of neutralinos produced in the  $e^+e^-$  mode.

For the study of LFV the analytical approximations have been checked numerically and found to be congruent. It has been shown that the  $\tilde{e}\text{-}\tilde{\mu}$  as well as  $\tilde{e}\text{-}\tilde{\tau}$  processes should be accessible in large areas of the still allowed flavour violating parameter space, even allowing background free measurement in scenarios with a gravitino LSP, once the mass splitting of the slepton states is large enough.

For both  $CP$  violation as well as LFV, one representative scenario has shown that the same studies could also be performed at the  $\mu^-\mu^-$  mode of a future muon collider. However, it should be considered that a high energy  $e^-e^-$ -collider (like CLIC in the  $e^-e^-$  mode) might be more suitable for these studies due to the higher luminosity.

To estimate the background from the SM as well as SUSY, some numerical simulations have been performed based upon the benchmark point SPS 1a'. Due to its rather light sparticle spectrum, this can serve as a worst case scenario concerning the background. It has been shown, that the background will be well under control in the  $e^-e^-$  mode of the ILC, especially, since possible improvements on the cuts are to be expected.

In conclusion, the  $e^-e^-$  mode of the ILC appears to be an interesting option in certain areas of the parameter space, due to the benefit of the clean environment. However, it has not been found to be a general purpose machine that will generally improve the data in the slepton or neutralino sector. Furthermore, the much lower luminosity must be taken into account, and thus the long running time for the accumulation of enough events, e. g., for the study of  $CP$  violation. Although the process of slepton production offers some interesting theoretical features in its general form due to the exchange of a massive fermion, no measurably usable observable has been found to exploit these features for either  $CP$  violation or LFV. Generally these effects have been found to be too small to be measurable.

# Zusammenfassung

In dieser Arbeit wurde die Verwendung eines  $e^-e^-$ -Beschleunigers zur Suche nach  $CP$ - und Leptonflavourverletzung untersucht. Hierzu wurde der totale Wirkungsquerschnitt für die Produktion beliebiger Sleptonen in  $e^-e^-$ -Streuung auf Baumgraphenniveau berechnet, wobei alle möglichen Polarisationsmodi, also sowohl longitudinale- als auch transversale Polarisation beider einlaufender Strahlen, berücksichtigt wurden. Außerdem wurden alle möglichen Mischungen im Sleptonsektor, d. h. sowohl Links-Rechts- als auch Flaovurmischung, sowie die Mischung im Neutralinosektor in die Rechnung einbezogen wobei sowohl die Sleptonmassen- als auch die Neutralinomassenmatrix als komplex angenommen wurden. Dies erlaubt prinzipiell  $CP$ -Verletzung in jedem der beiden Sektoren zu untersuchen.

Durch eine analytische Näherungslösung unter Vernachlässigung der Links-Rechts-Mischung im Slepton-Sektor des MSSM konnte gezeigt werden, dass, auch unter Beachtung aller aktuellen experimentellen Schranken zur Sleptonflavourverletzung, dennoch große Mischungen in diesem Sektor möglich sind. Es konnte gezeigt werden, dass die Selektion- und Smuon-Zustände, unter Berücksichtigung aller drei Generationen bei der Mischung, Sleptonen mit je etwa gleicher Selektion- und Smuonkomponente bilden können. Ein weiteres Ergebnis dieser Näherung ist, dass eines der Sleptonen nur eine vernachlässigbare Stau-Komponente aufweisen sollte, und dass dies immer dasjenige Slepton sein wird, welches die mittlere Masse eines Sektors aufweist. Die Gültigkeit dieser analytischen Ergebnisse konnte durch numerische Berechnungen in einigen repräsentativen Szenarien bestätigt werden.

In dieser Arbeit wurde das Amplitudenquadrat des Produktionsprozesses  $e^-e^- \rightarrow \tilde{\ell}_a \tilde{\ell}_b$ , sowohl in manifest kovarianter Form, als auch im Schwerpunktsystem, berechnet und dargestellt. Der Einfluß der  $CP$ -verletzenden Phasen  $\phi_\mu$  und  $\phi_{M_1}$  auf den totalen Wirkungsquerschnitt wurde, unter Einbeziehung der kompletten Neutralinomischung, untersucht, was frühere Arbeiten [22] erweiterte. Es konnte gezeigt werden, dass auch bei assoziierter Produktion  $e^-e^- \rightarrow \tilde{e}_L \tilde{e}_R$  bereits meßbare Effekte zu erwarten sind. Durch Einbeziehung aller möglichen Polarisationsmodi in die Berechnung war es möglich, eine  $CP$ -sensitive Observable zu konstruieren, welche auf der Nutzung transversaler Polarisation für beide einlaufenden Elektronstrahlen

beruht. Diese Observable könnte vor allem in higgsinoartigen Szenarien nützlich sein, wohingegen gezeigt wurde, dass in gauginoartigen oder gemischten Szenarien nur sehr kleine Effekte zu erwarten sind. Eine ähnliche Observable wurde bereits für die Neutralinoproduktion an einem  $e^+e^-$  Beschleuniger untersucht [123]. Dort wurde gezeigt, dass diese Observable nur sehr kleine Effekte zeigt, wenn aus kinematischen Gründen ein Zweikörperzerfall der Neutralinos nicht möglich ist, und man auf den Dreikörperzerfall  $\tilde{\chi}_2^0 \rightarrow \ell\bar{\ell}\tilde{\chi}_1^0$  angewiesen ist. In diesen Szenarien mag der  $e^-e^-$ -Modus zur Studie der  $CP$ -Verletzung ebenfalls hilfreich sein.

Bei der Untersuchung der Leptonflavourverletzung wurden zunächst die analytischen Näherungen überprüft. Es wurde eine sehr gute Übereinstimmung zwischen numerischer und analytischer Rechnung gefunden. Auch konnte gezeigt werden, dass der Prozess  $e^-e^- \rightarrow \tilde{e}\tilde{\mu}$  ebenso wie  $e^-e^- \rightarrow \tilde{e}\tilde{\tau}$  in großen Bereichen des derzeit erlaubten Parameterraums zugänglich ist. In Szenarien mit einem Gravitino als LSP ist, eine hinreichend große Massendifferenz der Sleptonen vorausgesetzt, sogar eine hintergrundfreie Messung möglich.

In einem repräsentativen Szenario wurde schließlich sowohl  $CP$ - als auch Leptonflavourverletzung exemplarisch an einem Myon-Beschleuniger für den  $\mu^-\mu^-$ -Modus untersucht. Es konnte gezeigt werden, dass hier prinzipiell die selben Untersuchungen wie im  $e^-e^-$ -Modus eines Linearbeschleunigers möglich sind, dass aber ein  $e^-e^-$ -Beschleuniger höherer Energie (wie z. B. CLIC) aufgrund der höheren Luminosität hier mehr Vorteile bieten würde.

Zur Abschätzung des für die untersuchten Prozesse relevanten Hintergrundes sowohl aus Standardmodellprozessen als auch aus SUSY-Prozessen wurden auf Basis des Benchmark-Szenarios SPS 1a' einige Simulationen angestellt. Durch das relativ leichte Spektrum supersymmetrischer Teilchen diente dieses Szenario als „worst case test“. Es konnte hier gezeigt werden, dass der Hintergrund für die Messungen der hier untersuchten Prozesse im  $e^-e^-$ -Modus des ILC unter hinreichender Kontrolle ist, insbesondere da Verbesserungen in den verwendeten Cuts möglich sein sollten.

Zusammenfassend kann gesagt werden, dass der  $e^-e^-$ -Modus des ILC eine interessante Option in einigen Bereichen des Parameterraums darstellt, speziell wenn man vom niedrigen Hintergrund dieses Modus profitieren kann. Es konnte jedoch nicht gezeigt werden, dass dieser Modus generell zur Verbesserung der Daten des Slepton- oder Neutralinosektors geeignet ist. Es ist außerdem zu beachten, dass durch die niedrigere Luminosität des  $e^-e^-$ -Modus sehr lange Laufzeiten der Experimente nötig sein werden, um genügen Ereignisse z. B. zur Untersuchung der  $CP$ -Verletzung zu sammeln.

Auch wenn der Produktionsprozess die theoretisch sehr interessante Eigenschaft aufweist, ein massives Fermion im Austauschkanal zu besitzen konnte diese doch nicht zur Konstruktion von Observablen genutzt werden, da die resultierenden Effekte zu klein sind, um messbar zu sein.

## Danksagung

An dieser Stelle möchte ich mich bei all denen bedanken, die zur Fertigstellung dieser Arbeit beigetragen haben.

An erster Stelle sei hier natürlich mein „Doktorvater“ Prof. Dr. H. Fraas genannt. Ihm gebührt besonderer Dank nicht nur für die zahlreichen fachlichen Diskussionen und Anregungen sowie der hervorragenden Betreuung bei jederzeit geöffneter Tür, sondern auch für die im Laufe der Jahre doch zahlreichen „kulinarischen Veranstaltungen“. Weiterhin kann sein Engagement in der Lehre und für die Belange der Studenten sicherlich nie ausreichend gewürdigt werden. Auch sei erwähnt, dass diese Arbeit ohne seinen Einsatz kaum hätte beendet werden können.

Bei Prof. Dr. Alfred Bartl aus Wien möchte ich mich für die fachlichen Diskussionen und Hinweise bedanken, sowie die kritische Durchsicht dieser Arbeit und seine Bereitschaft das Zweitgutachten anzufertigen. Auch die Möglichkeit zum einen oder anderen wissenschaftlichen Austausch in Wien sei hier erwähnt.

Weiterhin möchte ich mich bei meinen ehemaligen Kollegen für die angenehme Atmosphäre in unserer Arbeitsgruppe und am gesamten Lehrstuhl für Theoretische Physik II bedanken. Genannt seien hier vor allem Ana Alboteanu, Gudrid Moortgat-Pick, Claus Blöchinger, Fabian Franke, Stefan Hesselbach, Olaf Kittel, Thorsten Ohl und Federico von der Pahlen.

Besonders möchte ich mich bei Brigitte Wehner, Christine Schmeißer und Bettina Spiegel für die zahlreichen dienstlichen (und nicht dienstlichen) „Kleinigkeiten“ vor allem auf der Verwaltungsseite, bedanken.

Gedacht sei an dieser Stelle aber insbesondere auch Ursula Eitelwein, die uns leider viel zu früh verlassen hat.

Gedankt sei weiterhin den Korrekturlesern dieser Arbeit, die das „eine oder andere“ Komma ergänzt und sicherlich zur sprachlichen Verbesserung beigetragen haben. Genannt seien hier Ana Alboteanu, Irene Ramoz, Judith Stahl und Thorsten Ratzka.

Ein sehr herzliches Danke schön geht auch an die Kollegen des `root`-Projekts am CERN (Genf), insbesondere Olivier Couet und Rene Brun die mehr als einmal

sehr schnell und stets unbürokratisch diverse Korrekturen an ihrer Software vorgenommen oder Funktionen in das `root`-Paket integriert haben, welche für die Abbildungen in dieser Arbeit erforderlich waren.

Dankend erwähnt sei weiterhin die finanzielle Unterstützung aus Projektmitteln von Prof. Dr. R. Rückl während einiger Phasen dieser Arbeit.

In diesem Zusammenhang gilt mein Dank auch der Universitätsbibliothek Würzburg, für die Möglichkeit durch flexible Gestaltung meiner Arbeitszeit, neben meiner Tätigkeit dort, die größten Teile dieser Arbeit zu verfassen.

Die Liste der Leute, die zum Gelingen einer solchen Arbeit auf die eine oder andere Weise beitragen, kann nahezu beliebig fortgesetzt werden. Es muß also genügen, zu versichern, dass ich keinen vergessen habe, auch wenn hier nicht ausreichend Platz ist um alle aufzuführen.

# Conventions and Definitions

This work uses natural units that is  $\hbar = c = 1$ .  
The metric is defined by the metric tensor:

$$(g_{\mu\nu}) = \begin{pmatrix} 1 & 0 & 0 & 0 \\ 0 & -1 & 0 & 0 \\ 0 & 0 & -1 & 0 \\ 0 & 0 & 0 & -1 \end{pmatrix} = (g^{\mu\nu}) \quad (\text{A.1})$$

with

$$\epsilon_{\mu\nu\sigma\tau} = \begin{cases} +1 & , \text{for } (\mu\nu\sigma\tau) \text{ an even permutation of } (0123) \\ -1 & , \text{for } (\mu\nu\sigma\tau) \text{ an odd permutation of } (0123) \\ 0 & , \text{otherwise.} \end{cases} \quad (\text{A.2})$$

Spinors are solutions to the Dirac equation:

$$(\not{p} - m) u(p) = 0, \quad (\text{A.3})$$

$$\bar{u}(p) (\not{p} - m) = 0. \quad (\text{A.4})$$

For spin- $\frac{1}{2}$  particles one gets two solutions [190]:

$$u(p, s) = \sqrt{p^0 + m} \begin{pmatrix} \chi_S \\ \frac{\vec{\sigma}\vec{p}}{p^0 + m} \chi_S \end{pmatrix}, \quad (\text{A.5})$$

$$v(p, s) = -\sqrt{p^0 + m} \begin{pmatrix} \frac{\vec{\sigma}\vec{p}}{p^0 + m} \epsilon \chi_S \\ \epsilon \chi_S \end{pmatrix}. \quad (\text{A.6})$$





# Laboratory Sytem

## B.1 Exchange Terms

In this section the formulae from section 3.2.1 are given in the laboratory system. The arguments for the individual contributions denote the degree of polarisation for the first and the second beam, where  $1 = x$  and  $2 = y$  denote the transverse and  $3 = z$  the longitudinal polarisations. The first argument refers to the first beam (i. e.  $(a)$  in section 3.2.1) the second to the second beam  $(b)$ .

### B.1.1 Longitudinal $\otimes$ Longitudinal Polarisation

$$\begin{aligned}
E_{t,ij}^1(3,3) &= 2X_t^{kl} \cdot 2E^2 \\
&\times \left\{ \begin{aligned} &[(1 + P_1^L)(1 - P_2^L)a_{ki}^*b_{kj}^*a_{li}b_{lj} + (1 - P_1^L)(1 + P_2^L)a_{kj}^*b_{ki}^*a_{lj}b_{li}] \\ &\times |\vec{p}_3|^2 \sin^2 \theta \\ &+ [(1 - P_1^L)(1 - P_2^L)a_{ki}^*a_{kj}^*a_{li}a_{lj} + (1 + P_1^L)(1 + P_2^L)b_{ki}^*b_{kj}^*b_{li}b_{lj}] \\ &\times m_k m_l \end{aligned} \right\} \tag{B.1}
\end{aligned}$$

Substitutions for the  $u$ -channel:

$$X_t^{kl} \rightarrow X_u^{kl} \quad i \leftrightarrow j \tag{B.2}$$

## B.1.2 Longitudinal $\otimes$ Transverse Polarisation

$$\begin{aligned}
E_{t,ij}^2(1,3) &= 2X_t^{kl}P_1^1 \cdot 2E^2|\vec{p}_3| \sin \theta \\
&\times \left\{ \begin{aligned}
&-(1 - P_2^L)m_l a_{ki}^* b_{kj}^* a_{li} b_{lj} e^{-i\phi} \\
&+(1 + P_2^L)m_l b_{ki}^* a_{kj}^* b_{li} b_{lj} e^{i\phi} \\
&-(1 - P_2^L)m_k a_{ki}^* b_{kj}^* a_{li} b_{lj} e^{i\phi} \\
&+(1 + P_2^L)m_k b_{ki}^* a_{kj}^* b_{li} b_{lj} e^{-i\phi} \end{aligned} \right\} \tag{B.3}
\end{aligned}$$

Substitutions for  $E_{t,ij}^2(2,3)$ :  $\phi \rightarrow -(\frac{\pi}{2} + \phi)$

To get the  $u$ -channel contributions the following substitutions have to be applied:

$$\begin{aligned}
E_{t,ij}^2(1,3) &\rightarrow E_{u,ij}^2(1,3) && \left\{ \begin{array}{l} i \leftrightarrow j \\ \phi \leftrightarrow -\phi \end{array} \right. \\
&\text{and} \\
E_{t,ij}^2(2,3) &\rightarrow -E_{u,ij}^2(2,3) && \left\{ \begin{array}{l} X_t^{kl} \rightarrow X_u^{kl} \end{array} \right. \tag{B.4}
\end{aligned}$$

$$\begin{aligned}
E_{t,ij}^3(3,1) &= 2X_t^{kl}P_2^1 \cdot 2E^2|\vec{p}_3| \sin \theta \\
&\times \left\{ \begin{aligned}
&+(1 - P_1^L)m_l a_{ki}^* b_{kj}^* b_{li} b_{lj} e^{-i\phi} \\
&-(1 + P_1^L)m_l b_{ki}^* a_{kj}^* a_{li} a_{lj} e^{i\phi} \\
&-(1 - P_1^L)m_k a_{ki}^* a_{kj}^* a_{lj} b_{li} e^{i\phi} \\
&+(1 + P_1^L)m_k b_{ki}^* b_{kj}^* a_{lj} b_{li} e^{i\phi} \end{aligned} \right\} \tag{B.5}
\end{aligned}$$

Substitutions for  $E_{t,ij}^3(3,2)$ :  $\phi \rightarrow \frac{\pi}{2} + \phi$

To get the  $u$ -channel contributions the following substitutions are required:

$$\begin{aligned}
E_{t,ij}^2(3,1) &\rightarrow E_{u,ij}^2(3,1) && \left\{ \begin{array}{l} i \leftrightarrow j \\ \phi \leftrightarrow -\phi \end{array} \right. \\
&\text{and} \\
E_{t,ij}^2(3,2) &\rightarrow -E_{u,ij}^2(3,2) && \left\{ \begin{array}{l} X_t^{kl} \rightarrow X_u^{kl} \end{array} \right. \tag{B.6}
\end{aligned}$$

## B.1.3 Transverse $\otimes$ Transverse Polarisation

$$\begin{aligned}
E_{t,ij}^4(1,1) &= 2X_t^{kl}P_1^1P_2^1 \cdot 2E^2 \\
&\times \left\{ \begin{aligned}
&-(a_{ki}^* b_{kj}^* a_{li} b_{lj} + b_{ki}^* a_{ki}^* b_{lj} a_{li})|\vec{p}_3|^2 \sin^2 \theta \sin^2 \phi \\
&-i(a_{ki}^* b_{kj}^* a_{lj} b_{li} - b_{ki}^* a_{kj}^* b_{lj} a_{li})|\vec{p}_3|^2 \sin^2 \theta \sin(2\phi) \\
&+(a_{ki}^* b_{kj}^* b_{li} b_{lj} + b_{ki}^* b_{kj}^* a_{li} a_{lj})m_k m_l \end{aligned} \right\} \tag{B.7}
\end{aligned}$$

This term is connected with  $E_{t,ij}^4(a=2, b=2)$  via the substitutions

$$-E_{t,ij}^4(1, 1) \rightarrow E_{t,ij}^4(2, 2) \begin{cases} \sin \phi \leftrightarrow \cos \phi \\ P_{1,2}^1 \leftrightarrow P_{1,2}^2 \end{cases} \quad (\text{B.8})$$

and

$$\begin{aligned} E_{t,ij}^4(1, 2) &= 2X_t^{kl} P_1^1 P_2^2 \cdot 2E^2 |\vec{p}_3|^2 \sin^2 \theta \\ &\times \left\{ (a_{ki}^* b_{kj}^* a_{li} b_{lj} + b_{ki}^* a_{ki}^* b_{lj} a_{li}) \sin(2\phi) \right. \\ &\quad \left. i(a_{ki}^* b_{kj}^* a_{lj} b_{li} - a_{ki}^* a_{kj}^* b_{li} a_{li}) \right\}. \end{aligned} \quad (\text{B.9})$$

The contribution  $E_{t,ij}^4(2, 1)$  is obtained by

$$E_{t,ij}^4(2, 1) = -E_{t,ij}^4(1, 2) \quad \text{with} \quad P_1 \leftrightarrow P_2. \quad (\text{B.10})$$

The  $u$ -channel contributions to the formulae in this section can be obtained by the substitution:

$$E_{t,ij}^4(\frac{1}{2}, \frac{1}{2}) \rightarrow E_{u,ij}^4(\frac{1}{2}, \frac{1}{2}) \begin{cases} i \leftrightarrow j \\ X_t^{kl} \rightarrow X_u^{kl} \end{cases} \quad (\text{B.11})$$

## B.2 Interference Terms

### B.2.1 Longitudinal $\otimes$ Longitudinal Polarisation

$$\begin{aligned} I_{tu,ij}^1(3, 3) &= 2X_{tu}^{kl} \cdot 2E^2 \\ &\times \left\{ -[(1 + P_1^L)(1 - P_2^L) a_{ki}^* b_{kj}^* b_{li} a_{lj} \right. \\ &\quad \left. + (1 - P_1^L)(1 + P_2^L) b_{ki}^* a_{kj}^* a_{li} b_{lj}] \times |\vec{p}_3|^2 \sin^2 \theta \right. \\ &\quad \left. + [(1 - P_1^L)(1 - P_2^L) a_{ki}^* a_{kj}^* a_{li} a_{lj} \right. \\ &\quad \left. + (1 + P_1^L)(1 + P_2^L) b_{ki}^* b_{kj}^* b_{li} b_{lj}] \right. \\ &\quad \left. \times m_k m_l \right\} \end{aligned} \quad (\text{B.12})$$

### B.2.2 Longitudinal $\otimes$ Transverse Polarisation

$$\begin{aligned} I_{tu,ij}^2(1, 3) &= 2X_{tu}^{kl} P_1^1 (-2E^2 |\vec{p}_3|^2 \sin \theta) \\ &\times \left\{ [(1 - P_2^L) a_{ki}^* b_{kj}^* a_{li} a_{lj} m_l \right. \\ &\quad \left. + (1 + P_2^L) b_{ki}^* b_{kj}^* a_{li} b_{lj} m_k] e^{-i\phi} \right. \\ &\quad \left. + [(1 + P_2^L) b_{ki}^* a_{kj}^* b_{li} b_{lj} m_l \right. \\ &\quad \left. + (1 - P_2^L) a_{ki}^* a_{kj}^* b_{li} a_{lj} m_k] e^{i\phi} \right\} \end{aligned} \quad (\text{B.13})$$

$$\begin{aligned}
I_{tu,ij}^2(2,3) &= 2X_{tu}^{kl}P_1^2(-2iE^2|\vec{p}_3|^2 \sin \theta) \\
&\times \left\{ \begin{aligned} &[(1 - P_2^L)a_{ki}^*b_{kj}^*a_{li}a_{lj}m_l \\ &+(1 + P_2^L)b_{ki}^*b_{kj}^*b_{li}a_{lj}m_k]e^{i\phi} \\ &+ [(1 + P_2^L)b_{ki}^*a_{kj}^*b_{li}b_{lj}m_l \\ &+(1 - P_2^L)a_{ki}^*a_{kj}^*b_{li}a_{lj}m_k]e^{-i\phi} \end{aligned} \right. \tag{B.14}
\end{aligned}$$

$$\begin{aligned}
I_{tu,ij}^3(3,1) &= 2X_{tu}^{kl}P_2^1(-2E^2|\vec{p}_3|^2 \sin \theta) \\
&\times \left\{ \begin{aligned} &[(1 - P_1^L)b_{ki}^*a_{kj}^*a_{li}a_{lj}m_l \\ &+(1 + P_1^L)b_{ki}^*b_{kj}^*b_{li}a_{lj}m_k]e^{-i\phi} \\ &- [(1 + P_1^L)a_{ki}^*b_{kj}^*b_{li}b_{lj}m_l \\ &+(1 - P_1^L)a_{ki}^*a_{kj}^*a_{li}b_{lj}m_k]e^{i\phi} \end{aligned} \right\} \tag{B.15}
\end{aligned}$$

$$\begin{aligned}
I_{tu,ij}^3(3,2) &= 2X_{tu}^{kl}P_2^2i(-2E^2|\vec{p}_3|^2 \sin \theta) \\
&\times \left\{ \begin{aligned} &[-(1 - P_2^L)b_{ki}^*a_{kj}^*a_{li}a_{lj}m_l \\ &+(1 + P_1^L)b_{ki}^*b_{kj}^*b_{li}a_{lj}m_k]e^{i\phi} \\ &+ [(1 + P_1^L)a_{ki}^*b_{kj}^*b_{li}b_{lj}m_l \\ &-(1 - P_1^L)a_{ki}^*a_{kj}^*a_{li}b_{lj}m_k]e^{-i\phi} \end{aligned} \right\} \tag{B.16}
\end{aligned}$$

### B.2.3 Transverse $\otimes$ Transverse Polarisation

$$\begin{aligned}
I_{tu,ij}^4(\frac{1}{2}, \frac{1}{2}) &= P_1^2P_2^2 \cdot 2X_{tu}^{kl} \cdot 2E^2 \\
&\times \left\{ \begin{aligned} &-(a_{ki}^*b_{kj}^*a_{li}b_{lj} + b_{ki}^*a_{kj}^*b_{li}a_{lj})|\vec{p}_3|^2 \sin^2 \theta \cos(2\phi) \\ &\pm i(a_{ki}^*b_{kj}^*a_{li}b_{lj} - b_{ki}^*a_{kj}^*b_{li}a_{lj})|\vec{p}_3|^2 \sin^2 \phi \sin(2\phi) \\ &\mp (a_{ki}^*a_{kj}^*b_{li}b_{lj} + b_{ki}^*b_{kj}^*a_{li}a_{lj})m_k m_l \end{aligned} \right\} \tag{B.17}
\end{aligned}$$

$$\begin{aligned}
I_{tu,ij}^4(a = \frac{1}{2}, b = \frac{2}{1}) &= P_1^2P_2^2 \cdot 2X_{tu}^{kl} \cdot 2E^2|\vec{p}_3|^2 \sin^2 \theta \\
&\times \left\{ \begin{aligned} &\mp (a_{ki}^*b_{kj}^*a_{li}b_{lj} + b_{ki}^*a_{kj}^*b_{li}a_{lj}) \sin(2\phi) \\ &\pm i(a_{ki}^*b_{kj}^*a_{li}b_{lj} - b_{ki}^*a_{kj}^*b_{li}a_{lj}) \end{aligned} \right\} \tag{B.18}
\end{aligned}$$

## Bibliography

- [1] S. L. Glashow.  
**A Modell of Leptons.**  
*Nuclear Physics*, 22:579, 1961.
- [2] S. Weinberg.  
**Partial-Symmetries of Weak Interactions.**  
*Physical Review Letters*, 19:1264, 1967.
- [3] A. Salam.  
**Weak and Electromagnetic Interactions**, page 367ff.  
Elementary Particle Theory. Almqvists & Wiksell, Stockholm, 1968.
- [4] M. Maltoni, T. Schwetz, M. A. Tortola, and J. W. F. Valle.  
**Status of global fits to neutrino oscillations.**  
*New Journal of Physics*, 6:122, 2004.  
*[hep-ph/0405172]*
- [5] P. W. Higgs.  
**Broken symmetries, massless particles and gauge fields.**  
*Physics Letters*, 12:132–133, 1964.  
*doi: 10.1016/0031-9163(64)91136-9*
- [6] P. W. Higgs.  
**Broken Symmetries and the Masses of Gauge Bosons.**  
*Physical Review Letters*, 13:508–509, 1964.  
*doi: 10.1103/PhysRevLett.13.508*
- [7] P. W. Higgs.  
**Spontaneous Symmetry Breakdown without Massless Bosons.**

- Physical Review*, 145:1156–1163, 1966.  
*doi: 10.1103/PhysRev.145.1156*
- [8] D. J. H. Chung et al.  
**The Soft Supersymmetry-Breaking Lagrangian: Theory and Applications.**  
*Physics Reports*, 407:1–203, 2005.  
*[hep-ph/0312378]*
- [9] G. Bhattacharyya.  
**Supersymmetry as a physics model beyond the Standard Model.**  
*Indian Journal of Physics*, Special Issue:83–106, 2001.  
*[hep-ph/0108267]*
- [10] **TESLA "The Superconducting Electron-Positron Linear Collider with an Integrated X-Ray Laser Laboratory" – Technical Design Report.**  
Technical Report, Deutsches Elektronen Synchrotron, 2001.
- [11] G. Moortgat-Pick et al.  
**The role of polarized positrons and electrons in revealing fundamental interactions at the Linear Collider.**  
*[hep-ph/0507011]*
- [12] W. Y. Keung and L. Littenberg.  
**Test of supersymmetry in  $e^-e^-$  collisions.**  
*Physical Review D*, 28(5):1067–1070, 1983.  
*doi: 10.1103/PhysRevD.28.1067*
- [13] F. Cuypers.  
**Selectron Searches in  $e^-e^-$ ,  $e^- \gamma$  and  $\gamma\gamma$  Scattering.**  
In A. Miyamoto, Y. Fujii, T. Matsui, and S. Iwata, editors, *Physics and Experiments with Linear Colliders: Proceedings*, pages 549–556, Singapore, 1995. World Scientific.  
3rd Workshop On Physics And Experiments With  $e^+e^-$  Linear Colliders (LCWS 95), Iwate, Japan, 8-12 Sep 1995.  
*[hep-ph/9603243]*
- [14] F. Cuypers, G. J. van Oldenborgh, and R. Rückl.  
**Supersymmetric Signals in  $e^-e^-$  Collisions.**  
*Nuclear Physics B*, 409:128–143, 1993.  
*[hep-ph/9305287]*
- [15] J. L. Feng.

- Supersymmetry at Linear Colliders: The Importance of Being  $e^-e^-$ .**  
*International Journal of Modern Physics A*, 13:2319–2328, 1998.  
[[hep-ph/9803319](#)]
- [16] M. E. Peskin.  
**Systematics of Slepton Production in  $e^+e^-$  and  $e^-e^-$  Collisions.**  
*International Journal of Modern Physics A*, 13:2299–2306, 1998.  
[[hep-ph/9803279](#)]
- [17] J. L. Feng.  
**Physics at  $e^-e^-$  Colliders.**  
*International Journal of Modern Physics A*, 15:2355–2364, 2000.  
[[hep-ph/0002055](#)]
- [18] J. L. Feng and M. E. Peskin.  
**Selectron Studies at  $e^-e^-$  and  $e^+e^-$  Colliders.**  
*Physical Review D*, 64:115002, 2001.  
doi: 10.1103/PhysRevD.64.115002 [[hep-ph/0105100](#)]
- [19] A. Freitas, H. U. Martyn, U. Nauenberg, and P. M. Zerwas.  
**Sleptons: Masses, Mixings, Couplings.**  
In H. Videau and J.-C. Brient, editors, *International Conference On Linear Colliders: Proceedings*, Paris, France, 2004. Ecole Polytechnique.  
Paris, France, 19-24 Apr 2004.  
[[hep-ph/0409129](#)]
- [20] C. Blochinger, H. Fraas, G. Moortgat-Pick, and W. Porod.  
**Selectron Pair Production at  $e^-e^-$  and  $e^+e^-$  Colliders with Polarized Beams.**  
*European Physical Journal C*, 24:297–310, 2002.  
[[hep-ph/0201282](#)]
- [21] C. Blochinger, H. Fraas, and T. Mayer.  
**Selectron Pair Production in Electron-Electron-Scattering.**  
In D. Kazakov and A. Gladyshev, editors, *Supersymmetry and unification of fundamental interactions*, pages 217–220, Singapore, 2001. World Scientific.  
9th International Conference On Supersymmetry And Unification Of Fundamental Interactions (SUSY01), Dubna, Russia, 11-17 Jun 2001.  
[[hep-ph/0109182](#)]
- [22] S. Thomas.  
**CP-odd Phases in Slepton Pair Production.**

- International Journal of Modern Physics A*, 13:2307–2318, 1998.  
[hep-ph/9803420]
- [23] A. Ibarra and S. Roy.  
**Lepton flavour violation in future linear colliders in the long-lived stau NLSP scenario.**  
*Journal of High Energy Physics*, 0705:059, 2007.  
[hep-ph/0606116]
- [24] W. Porod and W. Majerotto.  
**Large lepton flavor violating signals in supersymmetric particle decays at future  $e^+e^-$  colliders.**  
*Physical Review D*, 66:015003, 2002.  
doi: 10.1103/PhysRevD.66.015003 [hep-ph/0201284]
- [25] W. Porod and W. Majerotto.  
**Large lepton flavour violating signals in supersymmetric particle decays.**  
In Nath et al. [194].  
DESY Hamburg, Germany, 17-23 Jun 2002.  
[hep-ph/0210326]
- [26] A. Bartl et al.  
**CP Phases, LFV, RpV & all that.**  
In J. Kang and S. O. Seoul, editors, *Physics and Experiments with Future Electron-Positron Linear Colliders: Proceedings*, pages 212–218. Korean Physical Society, 2002.  
International Workshop on Linear Colliders (LCWS 2002), Jeju Island, Korea, 26-30 Aug 2002.  
[hep-ph/0301027]
- [27] A. Bartl et al.  
**Test of lepton flavour violation at LHC.**  
*European Physical Journal C*, 46:783–789, 2006.  
[hep-ph/0510074]
- [28] W. Porod.  
**Lepton Number Violation in Decays of Supersymmetric Particles.**  
*Czech Journal of Physics*, 55:B233–B240, 2005.  
[hep-ph/0410318]
- [29] U. Amaldi, W. de Boer, and H. Fürstenau.  
**Comparison of Grand Unified Theories with Electroweak and Strong Coupling Constants Measured at LEP.**



*Physics Letters B*, 260:447, 1997.

- [30] J. R. Ellis, S. Kelley, and D. V. Nanopoulos.  
**Probing the desert using gauge coupling unification.**  
*Physics Letters B*, 260:131–137, 1991.  
*doi: 10.1016/0370-2693(91)90980-5*
- [31] C. Giunti, C. W. Kim, and U. W. Lee.  
**Running coupling constants and grand unification models.**  
*Modern Physics Letters A*, 6:1745–1755, 1991.
- [32] S. P. Martin.  
**Perspectives in Supersymmetry**, chapter A Supersymmetry  
Primer, pages 1–98.  
In Kane [195], 1998.  
Updated version 2006.  
*[hep-ph/9709356]*
- [33] J. Ellis.  
**Supersymmetry for Alp Hikers.**  
In N. Ellis and J. March-Russell, editors, *Proceedings: 2001 Euro-  
pean School for High-Energy Physics (ESHEP 2001)*, pages 157–203,  
Geneva, Switzerland, 2003. CERN.  
*[hep-ph/0203114]*
- [34] The Super-Kamiokande Collaboration.  
**Evidence for oscillation of atmospheric neutrinos.**  
*Physical Review Letters*, 81:1562–1567, 1998.  
*doi: 11.1103/PhysRevLett.81.1562 [hep-ex/9807003]*
- [35] The Super-Kamiokande Collaboration.  
**Measurement of the solar neutrino energy spectrum using  
neutrino-electron scattering.**  
*Physical Review Letters*, 82:2430–2434, 1999.  
*doi: 11.1103/PhysRevLett.82.2430 [hep-ex/9812011]*
- [36] T. Kajita and Y. Totsuka.  
**Observation of atmospheric neutrinos.**  
*Review of Modern Physics*, 73:85–118, 2001.
- [37] S. Dimopoulos, S. Raby, and F. Wilczek.  
**Supersymmetry and the Scale of Unification.**

- Physical Review D*, 24:1681–1683, 1981.  
*doi: 10.1103/PhysRevD.24.1681*
- [38] S. Dimopoulos and H. Georgi.  
**Softly Broken Supersymmetry and SU(5).**  
*Nuclear Physics B*, 193:150, 1981.  
*doi: 10.1016/0550-3213(81)90522-8*
- [39] P. Langacker and M. Luo.  
**Implications of precision electroweak experiments for  $M(t)$ ,  $\rho(0)$ ,  $\sin^2\theta(W)$  and grand unification.**  
*Physical Review D*, 44:817–822, 1991.  
*doi: 10.1103/PhysRevD.44.817*
- [40] S. Dawson.  
**SUSY and Such.**  
*NATO Advanced Study Institute Series B: Physics*, 365:33–80, 1997.  
*[hep-ph/9612229]*
- [41] G. L. Kane.  
**Tasi lectures: weak scale supersymmetry - a top-motivated-bottom-up approach.**  
In S. S. Gubser and J. D. Lykken, editors, *Strings, Branes and Extra Dimensions: TASI 2001: Proceedings*, pages 273–333, River Edge, N.J., 2001. World Scientific.  
Boulder, Colorado, 3-29 Jun 2001.  
*[hep-ph/0202185]*
- [42] B. Pendleton and G. G. Ross.  
**Mass and Mixing Angle Predictions from Infrared Fixed Points.**  
*Physics Letters B*, 98:291, 1981.  
*doi: 10.1016/0370-2693(81)90017-4*
- [43] L. E. Ibanez and G. G. Ross.  
**Towards a Realistic SUGRA GUT.**  
*Physics Letters B*, 131:335, 1983.  
*doi: 10.1016/0370-2693(83)90511-7*
- [44] G. L. Kane, C. Kolda, and J. D. Wells.  
**Calculable Upper Limit on the Mass of the Lightest Higgs Boson in Any Perturbatively Valid Supersymmetric Theory.**  
*Physical Review Letters*, 70:2686–2689, 1993.  
*doi: 10.1103/PhysRevLett.70.2686 [hep-ph/9210242]*
- [45] J. R. Espinosa and M. Quirós.

**Upper Bounds on the Lightest Higgs Boson Mass in General Supersymmetric Standard Models.**

*Physics Letters B*, 302:51–58, 1993.

[*hep-ph/9212305*]

- [46] ALEPH Collaboration.  
**Observation of an excess in the search for the Standard Model Higgs boson at ALEPH.**  
*Physics Letters B*, 495:1–17, 2000.

- [47] DELPHI Collaboration.  
**Search for the Standard Model Higgs boson at LEP in the year 2000.**  
*Physics Letters B*, 499:23, 2001.

- [48] L3 Collaboration.  
**Higgs candidates in  $e^+e^-$  interactions at  $\sqrt{s} = 206$  GeV.**  
*Physics Letters B*, 495:18, 2000.

- [49] OPAL Collaboration.  
**Search for the Standard Model Higgs boson in  $e^+e^-$  collisions at  $\sqrt{s} = 192 - 209$  GeV.**  
*Physics Letters B*, 499:38, 2001.

- [50] A. Sopczak.  
**Complete LEP Data: Status of Higgs Boson Searches.**  
*Physics of Atoms and Nuclei*, 65:2116–2124, 2002.  
[*hep-ph/0112082*]

- [51] J. F. Gunion and H. E. Haber.  
**Higgs Bosons in Supersymmetric Models (I).**  
*Nuclear Physics B*, 272:1–76, 1986.  
*doi: 10.1016/0550-3213(86)90340-8*

- [52] J. F. Gunion and H. E. Haber.  
**Higgs Bosons in Supersymmetric Models (II). Implications for Phenomenology.**  
*Nuclear Physics B*, 278:449–492, 1986.  
*doi: 10.1016/0550-3213(86)90050-7*

- [53] H. E. Haber and G. L. Kane.

**The Search for Supersymmetry: Probing Physics Beyond the Standard Model.**

*Physics Reports*, 117:75, 1985.

doi: 10.1016/0370-1573(85)90051-1

- [54] I. J. R. Aitchison.  
**Supersymmetry and the MSSM: An Elementary Introduction.**  
Notes of Lectures for Graduate Students in Particle Physics. Oxford, May 2004.  
[hep-ph/0505105]
- [55] M. Drees.  
**An Introduction to Supersymmetry.**  
[hep-ph/9611409]
- [56] W.-M. Yao et al.  
**Review of Particle Physics.**  
*Journal of Physics G: Nuclear and Particle Physics*, 33(1):1–1232, 2006.  
doi: 10.1088/0954-3899/33/1/001
- [57] P. Roy.  
**Mechanisms of Supersymmetry Breaking in the MSSM.**  
*Pramana*, 60:169–182, 2003.  
[hep-ph/0207293]
- [58] H. P. Nilles.  
**Supersymmetry, supergravity and particle physics.**  
*Physics Reports*, 110(1-2):1–162, August 1984.
- [59] A. Bartl, H. Fraas, W. Majerotto, and N. Oshimo.  
**Neutralino Mass Matrix in the Minimal Supersymmetric Model.**  
*Physical Review D*, 40(5):1594–1605, 1989.  
doi: 10.1103/PhysRevD.40.1594
- [60] G. Moortgat-Pick.  
**Spineffekte in Chargino-/Neutralino-Produktion und -Zerfall.**  
Dissertation, Universität Würzburg, 1999.
- [61] S. Y. Choi, J. Kalinowski, G. Moortgat-Pick, and P. M. Zerwas.  
**Analysis of the Neutralino System in Supersymmetric Theories.**

- European Physical Journal*, C22:563–579, 2001.  
[hep-ph/0108117]
- [62] N. Arkani-Hamed, H.-C. Cheng, J. L. Feng, and L. J. Hall.  
**CP Violation from Slepton Oscillations at the LHC and NLC.**  
*Nuclear Physics B*, 505:3–39, 1997.  
[hep-ph/9704205]
- [63] A. Bartl, H. Fraas, and W. Majerotto.  
**Production and decay of selectrons and squarks in ep collisions.**  
*Nuclear Physics B*, 297(3):479–497, February 1988.  
doi: 10.1016/0550-3213(88)90314-8
- [64] A. Bartl, H. Fraas, and W. Majerotto.  
**Gaugino-Higgsino mixing in selectron and sneutrino pair production.**  
*Zeitschrift für Physik C Particles and Fields*, 34(3):411–417, September 1987.  
doi: 10.1007/BF01548825
- [65] R. N. Mohapatra and G. Senjanovic.  
**Neutrino mass and spontaneous parity nonconservation.**  
*Physical Review Letters*, 44:912, 1980.  
doi: 10.1103/PhysRevLett.44.912
- [66] R. N. Mohapatra and G. Senjanovic.  
**Neutrino Masses and Mixings in Gauge Models with Spontaneous Parity Violation.**  
*Physical Review D*, 23:165, 1981.  
doi: 10.1103/PhysRevD.23.165
- [67] M. Gell-Mann, P. Ramond, and R. Slansky.  
**Complex Spinors and Unified Theories.**  
In *Stony Brook Workshop*, 1979.  
Print-80-0576 (CERN).
- [68] A. Redelbach.  
**Calculation of cross sections and distributions for lepton flavor violating slepton pair production at  $e^-e^-$ -collisions.**  
Diplomarbeit, Universität Würzburg, 2000.
- [69] F. Deppisch, H. Päs, A. Redelbach, R. Rückl, and Y. Shimizu.

- Probing the Majorana mass scale of right-handed neutrinos in mSUGRA.**  
*European Physical Journal C*, 28:365–374, 2003.  
[hep-ph/0206122]
- [70] F. Deppisch, H. Päs, A. Redelbach, R. Rückl, and Y. Shimizu.  
**LFV Constraints on the Majorana Mass Scale in mSUGRA.**  
In Nath et al. [194], pages 1012–1017.  
DESY Hamburg, Germany, 17–23 Jun 2002.  
[hep-ph/0210407]
- [71] F. Deppisch, H. Päs, A. Redelbach, R. Rückl, and Y. Shimizu.  
**Neutrino Oscillations, SUSY See-Saw Mechanism and Charged Lepton Flavor Violation.**  
*Nuclear Physics Proceedings Supplement*, 116:316–320, 2003.  
[hep-ph/0211138]
- [72] F. Deppisch, H. Päs, A. Redelbach, R. Rückl, and Y. Shimizu.  
**The SUSY seesaw model and lepton-flavor violation at a future electron-positron linear collider.**  
*Physical Review D*, 69:054014, 2004.  
doi: 10.1103/PhysRevD.69.054014 [hep-ph/0310053]
- [73] F. Deppisch, J. Kalinowski, H. Päs, A. Redelbach, and R. Rückl.  
**Supersymmetric Lepton Flavour Violation at the LHC and LC.**  
Work performed for the LHC/LC study group.  
[hep-ph/0401243]
- [74] F. Deppisch, H. Päs, A. Redelbach, and R. Rückl.  
**Lepton flavor violation in the SUSY seesaw model: an update.**  
*Springer Proceedings in Physics*, 98:27–38, 2005.  
[hep-ph/0403212]
- [75] F. Deppisch and J. W. F. Valle.  
**Enhanced lepton flavour violation in the supersymmetric inverse seesaw model.**  
*Physical Review D*, 72:036001, 2005.  
doi: 10.1103/PhysRevD.72.036001 [hep-ph/0406040]
- [76] F. Deppisch, H. Päs, R. Rückl, and A. Redelbach.  
**Constraints on SUSY Seesaw Parameters from Leptogenesis and Lepton Flavor Violation.**  
*Physical Review D*, 73:033004, 2006.  
doi: 10.1103/PhysRevD.73.033004 [hep-ph/0511062]

- [77] F. Deppisch.  
**Towards a reconstruction of the SUSY seesaw model.**  
Dissertation, Universität Würzburg, 2004.
- [78] M. L. Brooks et al.  
**New Limit for the Family-Number Non-conserving Decay**  
 $\mu^+ \rightarrow e^+\gamma$ .  
*Physical Review Letters*, 83:1521–1524, 1999.  
doi: 11.1103/PhysRevLett.83.1521 [hep-ex/9905013]
- [79] U. Bellgardt et al.  
**Search for the Decay**  $\mu^+ \rightarrow e^+e^+e^-$ .  
*Nuclear Physics B*, 299:1, 1988.  
doi: 10.1016/0550-3213(88)90462-2
- [80] B. Aubert et al.  
**Search for lepton flavor violation in the decay**  $\tau^\pm \rightarrow e^\pm\gamma$ .  
*Physical Review Letters*, 96:041801, 2005.  
doi: 10.1103/PhysRevLett.96.041801 [hep-ex/0508012]
- [81] B. Aubert et al.  
**Search for lepton flavor violation in the decay**  $\tau \rightarrow \mu\gamma$ .  
*Physical Review Letters*, 95:041802, 2005.  
doi: 10.1103/PhysRevLett.95.041802 [hep-ex/0502032]
- [82] Y. Yusa et al.  
**Search for neutrinoless decays**  $\tau \rightarrow 3\ell$ .  
*Physics Letters B*, 589:103–110, 2004.  
doi: 10.1016/j.physletb.2004.04.002 [hep-ex/0403039]
- [83] N. Cabibbo.  
**Unitary Symmetry and Leptonic Decays.**  
*Physical Review Letters*, 10:531–532, 1963.  
doi: 10.1103/PhysRevLett.10.531
- [84] M. Kobayashi and T. Maskawa.  
**CP violation in the renormalizable theory of weak interaction.**  
*Progress in Theoretical Physics*, 49:652–657, 1973.
- [85] L. Chau and W. Keung.  
**Comments on the Parametrization of the Kobayashi-Maskawa Matrix.**  
*Physical Review Letters*, 53:1802, 1984.  
doi: 10.1103/PhysRevLett.53.1802

- [86] L. J. Hall, V. A. Kostelecky, and S. Raby.  
**New Flavor Violations in Supergravity Models.**  
*Nuclear Physics B*, 267:415, 1986.  
*doi: 10.1016/0550-3213(86)90397-4*
- [87] F. Gabbiani and A. Masiero.  
**FCNC in Generalized Supersymmetric Theories.**  
*Nuclear Physics B*, 322:235, 1989.  
*doi: 10.1016/0550-3213(89)90492-6*
- [88] K.-I. Hikasa.  
**Transverse Polarization Effects in  $e^+e^-$  Collisions: The Role of Chiral Symmetry.**  
*Physical Review D*, 33:3203, 1986.  
*doi: 10.1103/PhysRevD.33.3203*
- [89] A. Masiero and L. Silvestrini.  
**Perspectives in Supersymmetry**, chapter CP Violation in Low-Energy SUSY, pages 423–441.  
In Kane [195], 1998.  
*[hep-ph/9709242]*
- [90] S. Khalil.  
**CP violation in supersymmetric theories.**  
*International Journal of Modern Physics A*, 18:1697–1732, 2003.  
*[hep-ph/0212050]*
- [91] V. Barger et al.  
**CP-Violating Phases in SUSY, Electric Dipole Moments, and Linear Colliders.**  
*Physical Review D*, 64:056007, 2001.  
*doi: 10.1103/PhysRevD.64.056007 [hep-ph/0101106]*
- [92] M. Dugan, B. Grinstein, and L. J. Hall.  
**CP Violation in The Minimal  $n=1$  Supergravity Theory.**  
*Nuclear Physics B*, 255:413, 1985.  
*doi: 10.1016/0550-3213(85)90145-2*
- [93] A. Masiero and O. Vives.  
**Flavour and CP violation in supersymmetry.**  
*New Journal of Physics*, 4:4, 2002.
- [94] O. Kittel.  
**CP Violation in Production and Decay of Supersymmetric Particles.**



- Dissertation, Universität Würzburg, 2004.  
[*hep-ph/0504183*]
- [95] S. Abel, S. Khalil, and O. Lebedev.  
**EDM Constraints in Supersymmetric Theories.**  
*Nuclear Physics B*, 606:151–182, 2001.  
[*hep-ph/0103320*]
- [96] J. R. Ellis, S. Ferrara, and D. V. Nanopoulos.  
**CP Violation and Supersymmetry.**  
*Physics Letters B*, 114:231, 1982.  
*doi: 10.1016/0370-2693(82)90484-1*
- [97] W. Buchmuller and D. Wyler.  
**CP Violation and R Invariance in Supersymmetric Models of Strong and Electroweak Interactions.**  
*Physics Letters B*, 121:321, 1983.  
*doi: 10.1016/0370-2693(83)91378-3*
- [98] J. Polchinski and M. B. Wise.  
**The Electric Dipole Moment of the Neutron in Low-Energy Supergravity.**  
*Physics Letters B*, 125:393, 1983.  
*doi: 10.1016/0370-2693(83)91310-2*
- [99] A. Bartl, T. Gajdosik, W. Porod, P. Stockinger, and H. Stremnitzer.  
**Electron and Neutron Electric Dipole Moments in the Constrained MSSM.**  
*Physical Review D*, 60:073003, 1999.  
*doi: 10.1103/PhysRevD.60.073003* [*hep-ph/9903402*]
- [100] A. Bartl et al.  
**General Flavor Blind MSSM and CP Violation.**  
*Physical Review D*, 64:076009, 2001.  
*doi: 10.1103/PhysRevD.64.076009* [*hep-ph/0103324*]
- [101] A. Bartl, W. Majerotto, W. Porod, and D. Wyler.  
**Effect of supersymmetric phases on lepton dipole moments and rare lepton decays.**  
*Physical Review D*, 68:053005, 2003.  
*doi: 10.1103/PhysRevD.68.053005* [*hep-ph/0306050*]
- [102] A. Bartl, H. Fraas, O. Kittel, and W. Majerotto.  
**CP sensitive observables in  $e^+e^- \rightarrow \tilde{\chi}_i^0 \tilde{\chi}_j^0$  and neutralino decay into the Z boson.**

- European Physical Journal C*, 36:233–243, 2004.  
*doi: 10.1140/epjc/s2004-01893-2 [hep-ph/0402016]*
- [103] A. Bartl et al.  
**Impact of CP phases on SUSY particle production and decays.**  
In Valle et al. [192].  
Valencia, Spain, 14-18 Oct 2003.  
*[hep-ph/0312306]*
- [104] O. Kittel.  
**CP violation in production of neutralinos in  $e^+e^-$  collisions.**  
In Valle et al. [192].  
Valencia, Spain, 14-18 Oct 2003.  
*[hep-ph/0311169]*
- [105] A. Bartl, T. Kernreiter, and O. Kittel.  
**A CP asymmetry in  $e^+e^- \rightarrow \tilde{\chi}_i^0 \tilde{\chi}_j^0 \rightarrow \tilde{\chi}_j^0 \tau \tilde{\tau}_k$  with tau polarization.**  
*Physics Letters B*, 578:341–348, 2004.  
*[hep-ph/0309340]*
- [106] A. Bartl, H. Fraas, O. Kittel, and W. Majerotto.  
**CP asymmetries in neutralino production.**  
In *Extended Joint ECFA/DESY Study on Physics and Detectors for a Linear Electron-Positron Collider* [193].  
Amsterdam, The Netherlands, 1-4 Apr 2003.  
*[hep-ph/0308143]*
- [107] A. Bartl, H. Fraas, T. Kernreiter, and O. Kittel.  
**T-odd Correlations in the Decay of Scalar Fermions.**  
*European Physical Journal C*, 33:4–442, 2004.  
*[hep-ph/0306304]*
- [108] A. Bartl, H. Fraas, O. Kittel, and W. Majerotto.  
**CP asymmetries in neutralino production in  $e^+e^-$  collisions.**  
*Physical Review D*, 69:035007, 2004.  
*doi: 10.1103/PhysRevD.69.035007 [hep-ph/0308141]*
- [109] G. Moortgat-Pick.  
**Neutralino-Produktion und -Zerfall bei Elektron-Positron Kollisionen.**  
Diplomarbeit, Universität Würzburg, 1996.
- [110] G. Moortgat-Pick, H. Fraas, A. Bartl, and W. Majerotto.

- Polarization and Spin Effects in Neutralino Production and Decay.**  
*European Physical Journal C*, 9:(1)521–534; Erratum–*ibid.*C(1)54, 1999.  
[*hep-ph/9903220*]
- [111] G. Moortgat-Pick, H. Fraas, A. Bartl, and W. Majerotto.  
**Spin Effects in Neutralino Production in  $e^+e^-$  Annihilation with polarized beams.**  
*Acta Physica Polonia B*, 29:1497–1504, 1998.  
[*hep-ph/9803304*]
- [112] G. Moortgat-Pick and H. Fraas.  
**Angular and Energy Distribution in Neutralino Production and Decay with complete Spin Correlations.**  
*Acta Physica Polonia B*, 28:2395–2400, 1997.  
[*hep-ph/9712354*]
- [113] G. Moortgat-Pick and H. Fraas.  
**Spin Correlations in Production and Subsequent Decay of Neutralinos.**  
*Physical Review D*, 59:015016, 1999.  
*doi: 10.1103/PhysRevD.59.015016* [*hep-ph/9708481*]
- [114] C. Bouchiat and L. Michel.  
**Mesure de la Polarisation des Electrons Relativistes.**  
*Nuclear Physics*, 5:416, 1958.  
(in French).
- [115] H. E. Haber.  
**Spin Formalism and Applications to New Physics Searches.**  
In *Proceedings of the 21<sup>st</sup> SLAC Summer Institute on Particle Physics*, 1994.
- [116] K.-I. Hikasa.  
**Effects of transverse polarization in electron-positron collisions.**  
*Physics Letters B*, 143(1-3):266–268, 1984.  
*doi: 10.1016/0370-2693(84)90847-5*
- [117] F. M. Renard.  
**Basis of Electron Positron Collisions.**  
Dreux, 1981.

- [118] B. C. Allanach et al.  
**The Snowmass Points and Slopes: Benchmarks for SUSY Searches.**  
*European Physical Journal C*, 25:113–123, 2002.  
[hep-ph/0202233]
- [119] M. Battaglia et al.  
**Updated Post-WMAP Benchmarks for Supersymmetry.**  
*European Physical Journal C*, 33:273–296, 2004.  
[hep-ph/0306219]
- [120] A. De Roeck et al.  
**Supersymmetric Benchmarks with Non-Universal Scalar Masses or Gravitino Dark Matter.**  
*European Physical Journal C*, 49:1041–1066, 2007.  
[hep-ph/0508198]
- [121] W. Kilian and P. M. Zerwas.  
**ILC: Physics Scenarios.**  
Talk given at 2005 International Linear Collider Physics and Detector Workshop and 2nd ILC Accelerator Workshop, Snowmass, Colorado, 14-27 Aug 2005, 2006.  
[hep-ph/0601217]
- [122] J. A. Aguilar-Saavedra et al.  
**Supersymmetry Parameter Analysis: SPA Convention and Project.**  
*European Physical Journal C*, 46:43–60, 2006.  
[hep-ph/0511344]
- [123] A. Bartl et al.  
**CP-odd observables in neutralino production with transverse  $e^+$  and  $e^-$  beam polarization.**  
*Journal of High Energy Physics*, 0601:170, 2006.  
[hep-ph/0510029]
- [124] W. Porod.  
**SPheno, a program for calculating supersymmetric spectra, SUSY particle decays and SUSY particle production at  $e^+e^-$  colliders.**  
*Computational Physics Communications*, 153:275–315, 2003.  
[hep-ph/0301101]
- [125] A. Bartl, K. Hidaka, T. Kernreiter, and W. Porod.  
**Tau-Sleptons and Tau-Sneutrino in the MSSM with Complex Parameters.**

- Physical Review D*, 66:115009, 2002.  
*doi: 10.1103/PhysRevD.66.115009 [hep-ph/0207186]*
- [126] S. Eidelman et al.  
**Review of Particle Physics.**  
*Physics Letters B*, 592, 2004.
- [127] M. Woods et al.  
**Luminosity, Energy and Polarization Studies for the Linear Collider: Comparing  $e^+e^-$  and  $e^-e^-$  for NLC and TESLA.**  
In *5th International Workshop on Electron-Electron Interactions at TeV Energies*, 2003.  
*[physics/0403037]*
- [128] C. L. Bennett et al.  
**First Year Wilkinson Microwave Anisotropy Probe (WMAP) Observations: Preliminary Maps and Basic Results.**  
*Astrophysical Journal Supplement*, 148:1, 2003.  
*[astro-ph/0302207]*
- [129] D. N. Spergel et al.  
**First Year Wilkinson Microwave Anisotropy Probe (WMAP) Observations: Determination of Cosmological Parameters.**  
*Astrophysical Journal Supplement*, 148:175, 2003.  
*[astro-ph/0302209]*
- [130] R. Kitano and Y. Nomura.  
**A Solution to the Supersymmetric Fine-Tuning Problem within the MSSM.**  
*Physics Letters B*, 631:58–67, 2005.  
*doi: 10.1016/j.physletb.2005.10.003 [hep-ph/0509039]*
- [131] R. Kitano and Y. Nomura.  
**Supersymmetry with Small  $\mu$ : Connections between Naturalness, Dark Matter, and (Possibly) Flavor.**  
*[hep-ph/0606134]*
- [132] A. Bartl et al.  
**Selectron production at an  $e^-e^-$  linear collider with transversely polarized beams.**  
*Physics Letters B*, 644:165–171, 2007.  
*doi: 10.1016/j.physletb.2006.11.038 [hep-ph/0610431]*
- [133] S. Ambrosanio, G. D. Kribs, and S. P. Martin.

- Three-body decays of selectrons and smuons in low-energy supersymmetry breaking models.**  
*Nuclear Physics B*, 516:55–69, 1998.  
[hep-ph/9710217]
- [134] O. Cakir, I. T. Cakir, J. R. Ellis, and Z. Kirca.  
**Measurements of Metastable Staus at Linear Colliders.**  
[hep-ph/0703121]
- [135] M. Kawasaki, K. Kohri, and T. Moroi.  
**Big-Bang Nucleosynthesis with Long-Lived Charged Slepton.**  
*Physics Letters B*, 649:436–439, 2007.  
[hep-ph/0703122]
- [136] H. U. Martyn.  
**Detecting metastable staus and gravitinos at the ILC.**  
*European Physical Journal C*, 48:15–24, 2006.  
[hep-ph/0605257]
- [137] S. Y. Choi, M. Drees, B. Gaissmaier, and J. Song.  
**Analysis of CP Violation in Neutralino Decays to Tau Sleptons.**  
*Physical Review D*, 69:035008, 2004.  
[hep-ph/0310284]
- [138] A. Bartl, H. Fraas, O. Kittel, and W. Majerotto.  
**CP violation in chargino production and decay into sneutrino.**  
*Physics Letters B*, 598:76–82, 2004.  
[hep-ph/0406309]
- [139] O. Kittel, A. Bartl, H. Fraas, and W. Majerotto.  
**CP sensitive observables in chargino production and decay into a W boson.**  
*Physical Review D*, 70:115005, 2004.  
[hep-ph/0410054]
- [140] S. Y. Choi et al.  
**Reconstructing the Chargino System at  $e^+e^-$  Linear Colliders.**  
*European Physical Journal C*, 14:535–546, 2000.  
[hep-ph/0002033]
- [141] G. Moortgat-Pick.  
**A Future Linear Collider with polarised beams: Searches for New Physics.**  
*AIP Conference Proceedings*, 675:206–216, 2003.  
[hep-ph/0303234]

- [142] O. Kittel.  
**CP Violation in Production and Decay of Supersymmetric Particles.**  
PhD thesis, Universität Würzburg, 2004.  
[*hep-ph/0504183*]
- [143] D. Atwood and A. Soni.  
**Analysis for magnetic moment and electric dipole moment form factors of the top quark via  $e^+e^- \rightarrow t^+t^-$ .**  
*Physical Review D*, 45(7):2405–2413, 1992.  
doi: 10.1103/PhysRevD.45.2405
- [144] M. Diehl and O. Nachtmann.  
**Optimal observables for the measurement of three gauge boson couplings in  $e^+e^- \rightarrow W^+W^-$ .**  
*Zeitschrift für Physik C*, 62(3):397–411, 1994.  
doi: 10.1007/BF01555899
- [145] M. Daviera, L. Duflota, F. L. Diberdera, and A. Rougeb.  
**The optimal method for the measurement of tau polarization.**  
*Physics Letters B*, 306:411–417, 1993.  
doi: 10.1016/0370-2693(93)90101-M
- [146] J. F. Gunion, B. Grzadkowski, and X.-G. He.  
**Determining the  $tt$  and  $ZZ$  Couplings of a Neutral Higgs Boson of Arbitrary  $CP$  Nature at the Next Linear Collider.**  
*Physical Review Letters*, 77(26):5172–5175, 1996.  
doi: 10.1103/PhysRevLett.77.5172
- [147] S. Y. Choi, M. Drees, and J. Song.  
**Neutralino Production and Decay at an  $e^+e^-$  Linear Collider with Transversely Polarized Beams.**  
*Journal of High Energy Physics*, 0609:064, 2006.  
[*hep-ph/0602131*]
- [148] Y. Yusa.  
**Search for neutrinoless decays  $\tau \rightarrow 3\ell$ .**  
*Physics Letters B*, 589:103–110, 2004.  
[*hep-ex/0403039*]
- [149] B. Aubert and The BABAR Collaboration.  
**Search for Lepton Flavor Violation in the Decay  $\tau \rightarrow \mu\gamma$ .**  
*Physical Review Letters*, 95:041802, 2005.  
doi: 10.1103/PhysRevLett.95.041802 [*hep-ex/0502032*]
- [150] B. Aubert and The BABAR Collaboration.

- Search for Lepton Flavor Violation in the Decay  $\tau \rightarrow e^- \gamma$ .**  
*Physical Review Letters*, 96:041801, 2006.  
*doi: 10.1103/PhysRevLett.96.041801 [hep-ex/0508012]*
- [151] N. Arkani-Hamed, H. C. Cheng, J. L. Feng, and L. J. Hall.  
**Probing Lepton Flavor Violation at Future Colliders.**  
*Physical Review Letters*, 77:1937–1940, 1996.  
*doi: 10.1103/PhysRevLett.77.1973 [hep-ph/9603431]*
- [152] S. Weinberg.  
**Baryon- and Lepton-Nonconserving Processes.**  
*Physical Review Letters*, 43(21):1566–1570, 1979.  
*doi: 10.1103/PhysRevLett.43.1566*
- [153] F. Borzumati and A. Masiero.  
**Large Muon- and Electron-Number Nonconservation in Supergravity Theories.**  
*Physical Review Letters*, 57(8):961–964, 1986.  
*doi: 10.1103/PhysRevLett.57.961*
- [154] J. L. Feng.  
**Theoretical Overview: Motivations for Lepton Flavor Violation.**  
In Y. Kuno, W. R. Molzon, and S. Pakvasa, editors, *New Initiatives on Lepton Flavour Violation and Neutrino Oscillations with High Intense Muon and Neutrino Sources*, pages 18–29, Singapore, 2002. World Scientific.  
Joint U.S. / Japan Workshop on New Initiatives in Muon Lepton Flavor Violation and Neutrino Oscillation with High Intense Muon and Neutrino Sources, Honolulu, Hawaii, 2-6 Oct 2000.  
*[hep-ph/0101122]*
- [155] A. Rossi.  
**Supersymmetric Seesaw without Singlet Neutrinos: Neutrino Masses and Lepton-Flavour Violation.**  
*Physical Review D*, 66:075003, 2002.  
*doi: 10.1103/PhysRevD.66.075003 [hep-ph/0207006]*
- [156] A. Dedes, J. Ellis, and M. Raidal.  
**Higgs-Mediated  $B_{s,d}^0 \rightarrow \mu\tau, e\tau$  and  $\tau \rightarrow 3\mu, e\mu\mu$  Decays in Supersymmetric Seesaw Models.**  
*Physics Letters B*, 549:159–169, 2002.  
*doi: 10.1016/S0370-2693(02)02900-3 [hep-ph/0209207]*
- [157] A. Masiero, S. K. Vempati, and O. Vives.



- Massive Neutrinos and Flavour Violation.**  
*New Journal of Physics*, 6:202, 2004.  
[*hep-ph/0407325*]
- [158] I. Masina and C. A. Savoy.  
**Sleptonarium (Constraints on the CP and Flavour Pattern of Scalar Lepton Masses).**  
*Nuclear Physics B*, 661:365–393, 2003.  
[*hep-ph/0211283*]
- [159] H. Pilkuhn.  
**The Interaction of Hadrons.**  
North-Holland Publishing Company, 1967.
- [160] K. Hagiwara et al.  
**Review of particle physics.**  
*Physical Review D*, 66:010001, 2002.  
*doi: 10.1103/PhysRevD.66.010001*
- [161] K. The Belle Collaboration: Abe.  
**A New Search for  $\tau \rightarrow \mu\gamma$  and  $\tau \rightarrow e\gamma$  Decays at Belle.**  
Presented at 33rd International Conference on High Energy Physics (ICHEP 06), 2006.  
[*hep-ex/0609049*]
- [162] N. Ghodbane.  
**Susygen3, an Event Generator for Linear Colliders.**  
In E. Fernandez and A. Pacheco, editors, *4th International Workshop On Linear Colliders: Proceedings*, pages 745–749, Barcelona, 1999. Universitat Autònoma.  
Sitges, Barcelona, Spain, 28 Apr - 5 May 1999.  
[*hep-ph/9909499*]
- [163] H. Baer, F. E. Paige, S. D. Protopopescu, and X. Tata.  
**ISAJET 7.48: A Monte Carlo Event Generator for  $pp$ ,  $\bar{p}p$ , and  $e^+e^-$  Interactions.**  
[*hep-ph/0001086*]
- [164] G. I. Budker.  
**Accelerators and Colliding Beams.**  
*AIP Conference Proceedings*, 4:33, 1969.
- [165] V. Barger et al.  
**Physics Goals of a  $\mu^+\mu^-$  Collider.**

- AIP Conference Proceedings*, 352:55–69, 1996.  
[*hep-ph/9503258*]
- [166] J. F. Gunion.  
**Higgs Physics at a Muon Collider.**  
In B. A. Kniehl, editor, *The Higgs Puzzle*, pages 142–151, Singapore, 1997. World Scientific.  
Ringberg Workshop: The Higgs Puzzle - What Can We Learn From LEP2, LHC, NLC, And FMC? Ringberg, Germany, 8-13 Dec 1996.  
[*hep-ph/9703203*]
- [167] J. F. Gunion.  
**Muon Colliders: The Machine and The Physics.**  
*AIP Conference Proceedings*, 415:234–251, July 1997.  
[*hep-ph/9707379v2*]
- [168] V. Barger, M. S. Berger, J. F. Gunion, and T. Han.  
**Higgs Boson Physics in the s-channel at  $\mu^+\mu^-$  colliders.**  
*Physics Reports*, 286:1, 1997.
- [169] M. Demarteau and T. Han.  
**Higgs Boson and Z Physics at the First Muon Collider.**  
*AIP Conference Proceedings*, 435:177–192, 1998.  
[*hep-ph/9801407*]
- [170] V. Barger.  
**Overview of Physics at a Muon Collider.**  
*AIP Conference Proceedings*, 441:3–17, 1998.  
[*hep-ph/9803480*]
- [171] B. Autin, A. Blondel, and J. Ellis, editors.  
**Prospective Study of Muon Storage Rings at CERN.** CERN, 1999.  
[*CERN Yellow Report CERN 99-02, ECFA 99-197*]
- [172] M. S. Berger.  
**Higgs Bosons at a Muon Collider.**  
In Graf [191].  
Snowmass, Colorado, 30 Jun - 21 Jul 2001.  
[*hep-ph/0110390*]
- [173] M. S. Berger, J. F. Gunion, and T. Han.  
**The Physics of Higgs Factories.**  
In Graf [191].

- Snowmass, Colorado, 30 Jun - 21 Jul 2001.  
[*hep-ph/0110340*]
- [174] T. Ratzka.  
**Heavy Quark Production at a Muon Collider.**  
Diplomarbeit, Universität Würzburg, 2001.
- [175] A. Wagner.  
**Neutralinoproduktion an einem Muon-Collider.**  
Diplomarbeit, Universität Würzburg, 2002.
- [176] M. M. Alsharo'a.  
**Recent Progress in Neutrino Factory and Muon Collider Research within the Muon Collaboration.**  
*Physical Review Special Topics Accelerators and Beams*, 6:081001, 2003.  
*doi: 10.1103/PhysRevSTAB.6.081001* [*hep-ex/0207031*]
- [177] F. Cuyppers and C. A. Heusch.  
**Physics with Like-Sign Muon Beams.**  
*AIP Conference Proceedings*, 352:219–231, 1996.  
[*hep-ph/9508230*]
- [178] N. Arkani-Hamed, S. Dimopoulos, G. F. Giudice, and A. Romanino.  
**Aspects of Split Supersymmetry.**  
*Nuclear Physics B*, 709:3–46, 2005.  
[*hep-ph/0409232*]
- [179] J. F. Gunion.  
**Physics at a Muon Collider.**  
*AIP Conference Proceedings*, 435:37–57, 1998.  
[*hep-ph/9802258*]
- [180] J. Ellis, E. Keil, and G. Rolandi.  
**Options for Future Colliders at CERN.**  
1998.  
[*CERN-SL-98-004*]
- [181] J. Kalinowski.  
**Supersymmetry Working Group: Summary Report.**  
In *Extended Joint ECFA/DESY Study on Physics and Detectors for a Linear Electron-Positron Collider* [193].  
Amsterdam, The Netherlands, 1-4 Apr 2003.  
[*hep-ph/0309235*]

- [182] LHC/LC Study Group: Weiglein, G. et al.  
**Physics Interplay of the LHC and the ILC.**  
*Physics Reports*, 426:47–358, 2006.  
[hep-ph/0410364]
- [183] J. A. Aguilar-Saavedra.  
**Study of selectron properties in the  $\tilde{e}\tilde{e} \rightarrow e^-X_1^0e^-X_2^0$  decay channel.**  
In *1st ECFA Study of Physics and Detectors for a Linear Collider*, Montpellier, 2003. ECFA.  
Montpellier, France, 11-16 Nov 2003.  
[hep-ph/0312140]
- [184] W. Kilian.  
**WHIZARD 1.0: A generic Monte-Carlo integration and event generation package for multi-particle processes. Manual.**  
LC-TOOL-2001-039, Updated for Whizard 1.42.
- [185] T. Ohl.  
**O'Mega: An Optimizing Matrix Element Generator.**  
In *Seventh International Workshop on Advanced Computing and Analysis Technics in Physics Research, ACAT 2000*, pages 173–175, Batavia, 2000. American Institute of Physics.  
[hep-ph/0011243]
- [186] M. Moretti, T. Ohl, and J. Reuter.  
**O'Mega: An Optimizing Matrix Element Generator.**  
In *Workshop On Physics At TeV Colliders*, pages 1981–2009, Les Houches, France, 2001.  
Les Houches, France, 7-18 Jun 1999.  
[hep-ph/0102195]
- [187] A. Pukhov, E. Boos, M. Dubinin, and V. Edneral.  
**CompHEP: A package for evaluation of Feynman diagrams and integration over multi-particle phase space. User's manual for version 33**, 1999.  
[hep-ph/9908288]
- [188] E. Boos et al.  
**CompHEP 4.4 - Automatic Computations from Lagrangians to Events.**  
*Nuclear Instruments and Methods A*, 534:250–259, 2004.  
[hep-ph/0403113]

- [189] K. Desch.  
**Supersymmetry at LHC and ILC.**  
In *Proceedings of 32nd SLAC Summer Institute on Particle Physics (SSI 2004): Natures Greatest Puzzles*, 2004.  
[hep-ph/0501096]
- [190] O. Nachtmann.  
**Phänomene und Konzepte der Elementarteilchenphysik.**  
Friedr. Vieweg & Sohn Verlagsgesellschaft mbH, Braunschweig, 1986.
- [191] N. Graf, editor.  
**APS/DPF/DPB Summer Study on the Future of Particle Physics (Snowmass 2001)**, Snowmass, Colorado, 2001.  
Snowmass, Colorado, 30 Jun - 21 Jul 2001.
- [192] J. Valle, M. Hirsch, M. Maltoni, and S. Pastor, editors.  
**International Workshop On Astroparticle And High-Energy Physics (AHEP-2003)**, Trieste, 2003. SISSA.  
Valencia, Spain, 14-18 Oct 2003.
- [193] **4th ECFA/DESY Workshop On Physics And Detectors For A 90-GeV To 800-GeV Linear e+ e- Collider**, number 2004-01  
in DESY-PROC, Hamburg, 2004. DESY.  
Amsterdam, The Netherlands, 1-4 Apr 2003.
- [194] P. Nath, P. M. Zerwas, and C. Grosche, editors.  
**10th International Conference on Supersymmetry and Unification of Fundamental Interactions (SUSY02)**, Hamburg, 2002.  
DESY, DESY.  
DESY Hamburg, Germany, 17-23 Jun 2002.
- [195] G. L. Kane, editor.  
**Perspectives in Supersymmetry.**  
Number 18 in Advanced series on directions in high energy physics.  
World Scientific, Singapore, 1998.



## List of Tables

2.1	Particle spectrum of the MSSM . . . . .	12
2.2	Neutralino character . . . . .	15
3.1	$P_L \otimes P_L$ exchange terms and LR mixing angle . . . . .	30
3.2	$P_L \otimes P_T$ exchange terms and LR mixing angle . . . . .	31
3.3	$P_T \otimes P_T$ exchange terms and LR mixing angle . . . . .	32
3.4	$P_L \otimes P_L$ interference terms and LR mixing angle . . . . .	33
3.5	$P_L \otimes P_T$ interference terms and LR mixing angle . . . . .	34
3.6	$P_T \otimes P_T$ interference terms and LR mixing angle . . . . .	35
4.1	Parameters for SPS 1a' at $M_{\text{GUT}}$ . . . . .	39
4.2	Mass spectrum of SPS 1a' . . . . .	40
4.3	Low energy input parameters and $\tilde{\chi}^\pm$ -masses for SPS 1a'. . . . .	40
4.4	Neutralino mixing in SPS 1a' . . . . .	41
4.5	Slepton mixing in SPS 1a' . . . . .	41
4.6	Suitable polarisation modes . . . . .	42
4.7	Low energy input parameters and $\tilde{\chi}^\pm$ -masses for Mixed SPS. . . . .	43
4.8	Neutralino mixing in Mixed SPS . . . . .	44
4.9	Slepton mixing in Mixed SPS . . . . .	44
4.10	Low energy input parameters and $\tilde{\chi}^\pm$ -masses for Scenario A. . . . .	46
4.11	Neutralino mixing in Scenario A . . . . .	46
4.12	Slepton mixing in Scenario A . . . . .	47
4.13	Low energy input parameters and $\tilde{\chi}^\pm$ -masses for Scenario B. . . . .	49
4.14	Neutralino mixing in Scenario B . . . . .	49
4.15	Slepton mixing in Scenario B . . . . .	50
4.16	Low energy input parameters and $\tilde{\chi}^\pm$ -masses for Scenario C. . . . .	52
4.17	Neutralino mixing in Scenario C . . . . .	52
4.18	Slepton mixing in Scenario C . . . . .	53

---

4.19	Parameters for Point $\varepsilon$ at $M_{\text{GUT}}$ . . . . .	57
4.20	Low energy input parameters and $\tilde{\chi}^{\pm}$ -masses for Point $\varepsilon$ . . . . .	57
4.21	Neutralino mixing in Point $\varepsilon$ . . . . .	57
4.22	Slepton mixing in Point $\varepsilon$ . . . . .	58
4.23	Parameters for SPS 7 at $M_{\text{GUT}}$ . . . . .	60
4.24	Low energy input parameters and $\tilde{\chi}^{\pm}$ -masses for SPS 7. . . . .	60
4.25	Neutralino mixing in SPS 7 . . . . .	61
4.26	Slepton mixing in SPS 7 . . . . .	61
6.1	Experimental constraints for lepton flavour violation. [56,126, 160,161]. . . . .	90
8.1	Cuts for the calculation of the SM background with WHIZARD. . . . .	120



## List of Figures

2.1	Unification in SUSY and SM . . . . .	11
3.1	Production processes for two sleptons in $e^-e^-$ -scattering. . . . .	25
4.1	Total cross sections in SPS 1a' . . . . .	42
4.2	Total cross sections in Mixed SPS . . . . .	45
4.3	Total cross sections in Scenario A . . . . .	48
4.4	Total cross sections in Scenario B . . . . .	51
4.5	Total cross sections in Scenario C . . . . .	54
4.6	Total cross sections in Point $\varepsilon$ . . . . .	59
4.7	Total cross sections in SPS 7 . . . . .	62
5.1	Contour lines for $\hat{A}[\mathcal{F}_2]$ in the $ \mu  - M_2$ -plane . . . . .	69
5.2	Contour lines of $\hat{A}[\mathcal{F}_2]$ in the $ \mu  -  M_1 /M_2$ plane . . . . .	70
5.3	Dependence of $\sigma$ on $\phi_{M_1}$ in SPS 1a' . . . . .	72
5.4	$CP$ -sensitive observables in SPS 1a' . . . . .	73
5.5	$\hat{A}[\mathcal{F}_1]$ and $\hat{A}[\mathcal{F}_2]$ in SPS 1a' in the $\phi_{M_1}-\phi_\mu$ plane . . . . .	74
5.6	Dependence of $\sigma$ on $\phi_{M_1}$ in Mixed SPS . . . . .	75
5.7	$CP$ -sensitive observables in Mixed SPS . . . . .	76
5.8	$\hat{A}[\mathcal{F}_1]$ and $\hat{A}[\mathcal{F}_2]$ in Mixed SPS in the $\phi_{M_1}-\phi_\mu$ plane . . . . .	77
5.9	Dependence of $\sigma$ on $\phi_{M_1}$ in Scenario A . . . . .	78
5.10	$CP$ -sensitive observables in Scenario A . . . . .	79
5.11	$\hat{A}[\mathcal{F}_1]$ and $\hat{A}[\mathcal{F}_2]$ in Scenario A in the $\phi_{M_1}-\phi_\mu$ plane . . . . .	80
5.12	Dependence of $\sigma$ on $\phi_{M_1}$ in Scenario B . . . . .	81
5.13	$CP$ -sensitive observables in Scenario B . . . . .	82
5.14	$\hat{A}[\mathcal{F}_1]$ and $\hat{A}[\mathcal{F}_2]$ in Scenario B in the $\phi_{M_1}-\phi_\mu$ plane . . . . .	83
5.15	Dependence of $\sigma$ on $\phi_{M_1}$ in Scenario C . . . . .	84
5.16	$CP$ -sensitive observables in Scenario C . . . . .	85

5.17	$\hat{A}[\mathcal{F}_1]$ and $\hat{A}[\mathcal{F}_2]$ in Scenario C in the $\phi_{M_1}$ - $\phi_\mu$ plane . . . . .	86
6.1	Slepton composition in SPS 1a' . . . . .	94
6.2	$\tilde{e}$ and $\tilde{\tau}$ content of the sleptons . . . . .	96
6.3	$\sigma(e^-e^- \rightarrow \tilde{e}_R\tilde{\mu}_R)$ in SPS 1a' . . . . .	98
6.4	Branching ratio for leptonic decays of Slepton 4 in SPS 1a' . . . . .	98
6.5	Branching ratio for leptonic decays of Slepton 5 in SPS 1a' . . . . .	99
6.6	$\sigma(e^-e^- \rightarrow \tilde{e}_R\tilde{\mu}_R)$ in SPS 1a' . . . . .	99
6.7	Slepton components . . . . .	102
6.8	$\sigma(e^-e^- \rightarrow \tilde{e}_R\tilde{\mu}_R)$ in Point $\varepsilon$ . . . . .	103
6.9	Mass splitting of the right sleptons in Point $\varepsilon$ . . . . .	103
6.10	$\sigma(e^-e^- \rightarrow \tilde{e}_R\tilde{\tau}_1)$ in Point $\varepsilon$ . . . . .	104
6.11	Slepton components in SPS 7 . . . . .	107
6.12	Mass splitting of the right sleptons in SPS 7 . . . . .	108
6.13	$\sigma(e^-e^- \rightarrow \tilde{e}_R\tilde{\mu}_R)$ and $\sigma(e^-e^- \rightarrow \tilde{e}_R\tilde{\tau}_1)$ in SPS 7 . . . . .	108
7.1	Total cross sections in $\mu^-\mu^-$ and $e^-e^-$ . . . . .	110
7.2	Dependence of $\sigma$ on $\phi_{M_1}$ in $e^-e^-$ and $\mu^-\mu^-$ . . . . .	111
7.3	$CP$ -sensitive observables in $\mu^-\mu^-$ and $e^-e^-$ . . . . .	112
8.1	SM single-W-boson diagrams . . . . .	117
8.2	SM background without W-bosons . . . . .	118
8.3	SM background diagrams for LFV . . . . .	119
8.4	Flavour conserving SM background for various polarisations. . . . .	120
8.5	Polarisation dependence of the LFV SM background ( $\mu$ -channel). . . . .	121
8.6	Polarisation dependence of the LFV SM background ( $\tau$ -channel). . . . .	122
8.7	SUSY background diagrams . . . . .	123
8.8	Polarisation dependence of the SUSY background . . . . .	124

# Index

## Symbols

- $A$ , 26, 61
- $B$ -boson, 13
- $CP$ 
  - conservation, 14
  - phase, 63
  - violating effect, 22, 63
  - violating phase, 13, 15, 19, 72
    - $\phi_{M_1}$ , 63, 71–86, 112, 125, 127
    - $\phi_\mu$ , 23, 70–86, 112, 125, 127
  - violating vertex, 84
  - violation
    - neutralino mixing, 63
    - neutralino sector, 7, 68
    - pair production, 63
    - polarisation, 63
    - slepton sector, 7
    - transverse polarisation, 63
- $CP$ -even, 29, 66
  - observable, 8, 23, 63
  - neutralino mixing, 66
- $CP$ -odd observable, 35, 65
- $CP$ -sensitive, 32
  - observable, 8, 23, 27, 29, 30, 32, 35, 47, 63–68, 125
  - $\phi_\mu$ , 71
  - $\tan\beta$ , 71
    - , 72, 75, 78, 81
  - definition, 68
  - effective, 68
  - GUT-scenario, 68
  - non-GUT-scenario, 70
  - optimisation, 67
- $M_1$ , 14
- $M_2$ , 14
- $R$ -parity, 37, 122
- $W^0$ , 13
- $Z$ -boson, 13
- $\delta_{ij}$ 
  - bounds, 90
  - definition, 97
- $\tilde{\chi}_1^0$ , 37
- $\langle abcd \rangle$ , 30
- $\hat{\delta}_{ij}$ , 88
- $\hat{\delta}_{12} = 0$ , 21
- $\hat{\delta}_{12} \neq 0$ , 21
- $\hat{\delta}_{ij}$ , 20, 88
- $\mathcal{L}_{\ell\tilde{\ell}\tilde{\chi}_i^0}$ , 17
- $\mu$ , 13, 14
- $\mu$  parameter, 44
- $\mu$ , 26
- $\tilde{\chi}_3^0$ 
  - wino like, 52
- $\tilde{\chi}_4^0$ 
  - bino like, 52
- $\phi_{M_1}$ , 23
- $\sin^2\theta_w$ , 10
- $\tan\beta$ , 14, 26, 47, 49
- $\sigma^A$ , 26
- $\tan\beta$ , 14
- $\theta_{\tilde{\ell}}$ , 17, 30–35
- $e^+e^-$ 
  - comparison to  $e^-e^-$ , 87
- $e^-e^-$ 
  - comparison to  $e^+e^-$ , 87
- $e^-\tilde{e}^-\tilde{\chi}_i^0$ , 84

- $t$ -channel, 25, 29
  - pre factor, 29
- $t$ -channel amplitude, 26
- $t - u$ -interference, 28, 32
- $u$ -channel, 25, 29
  - pre factor, 29
- $u$ -channel amplitude, 26
- $z$ -axis, 64
- $\tilde{\ell}_R \rightarrow \ell \tilde{\tau}_1 \tau$ , 100
- $\tilde{e}_R - \tilde{\mu}_R$  mixing, 97
- LFV
  - bounds, 90
  - cross section, 100
    - , 100
  - restrictions, 90
  - $CP$ -sensitive observable, 72, 75, 78, 81
  - $\tilde{\tau}$  sector, 44, 61
    - associate production, 72, 75, 78, 81, 84
    - cross section, 43, 44, 46, 47, 50, 53, 58, 61
    - $\tilde{\mu}$ , 98, 100, 106
    - $\tilde{\tau}$ , 99, 101, 106
    - decay branching ratio, 98
    - decay channel, 98, 100
    - gaugino sector, 49
    - high scale
      - parameters, 39
    - high scale parameters, 56, 60
  - LFV
    - cross section, 98, 100
    - low scale parameters, 56, 60
    - mass degeneracy, 44
    - mass spectrum, 43, 46
    - mass splitting, 101, 105
    - mixed scenario, 60
    - mSUGRA, 56
    - neutralino sector, 44, 46, 47, 49, 52, 56
    - neutralino spectrum, 57, 60
      - pair production, 72, 75, 78, 81, 84
      - slepton mixing, 95, 100, 105
      - slepton sector, 44, 50, 57, 60, 61
  - SUSY
    - parameter space, 39
    - parameters, 37
    - phases, 66
  - $\tilde{\chi}$ 
    - SUSY background, 123
  - $\tilde{G}$ , 37
  - $\phi_{M_1}$ , 63, 71–86, 112, 125, 127
  - $\phi_\mu$ , 23, 70–86, 112, 125, 127
  - $e^+e^-$  collider, 7
  - $\tilde{e} - \tilde{\mu}$  channel
    - cross section, 90
  - $\tilde{e} - \tilde{\tau}$  mixing, 90
  - $\tilde{\tau}$ 
    - sector, 17
  - $\tilde{\tau}$  sector
    - , 44, 57, 61
    - x  $\tilde{\tau}$  sector, 57
  - $\tilde{\mu} - \tilde{\tau}$  mixing, 90
  - $\tilde{\tau}$  admixture, 22
  - $\tilde{\tau}$  sector, 16, 20, 31, 44
  - $\tilde{e} - \tilde{\mu}$  channel, 90
  - $\tilde{e} - \tilde{\mu}$  mixing, 90
  - $\tilde{e} - \tilde{\tau}$ -channel, 121
  - $e - \tilde{\tau} - \tilde{\chi}^0$  vertex, 97

## A

  - A-parameter, 57
  - ambiguity, 66
    - production
      - plane, 66
  - amplitude, 25, 26, 64
    - production, 26
    - squared, 26–28, 64, 91
  - AMSB, 13, 37
  - analytical approximation, 8, 125
    - justification, 97
    - numerical justification, 93

slepton mixing, 92, 93  
 antineutrino, 120  
   muon, 116, 121  
   tau, 116, 121  
 approximation, 21  
 associate production, 60, 64, 72, 125  
   , 72, 75, 78, 81, 84

## B

background, 18, 41, 56, 87, 89–91,  
   118, 121, 126  
   cross section, 115  
   decrease, 41  
   energy dependence, 121  
   flavour conserving, 89, 116  
   flavour violating, 118  
   left slepton sector, 91  
   photon, 118  
   polarisation, 41  
   polarisation dependence, 118, 121  
   right slepton sector, 91  
   single-W, 116, 124  
   SM, 91  
   SM processes, 116  
   suppression, 87, 91, 118  
   SUSY, 122  
   SUSY processes, 122  
   W-boson, 118  
   Z-boson, 118  
 background free, 18  
   measurement, 8, 87, 90, 95, 101,  
   105, 106, 126  
 baryon asymmetry, 10  
 basis vectors, 26  
 beam axis, 27  
 beam spread, 40  
 benchmark point, 90, 126  
 benchmark scenarios, 37  
 bino, 57  
 bino like  $\tilde{\chi}_4^0$ , 52  
 boson

Higgs, 9, 10, 12, 38  
 W, 12, 91, 118  
 Z, 12  
 bounds  
    $\delta_{ij}$ , 90  
 branching ratio, 8, 90, 91

## C

Cabbibo-Kobayashi-Maskawa-Matrix,  
   19  
 CDM, 10  
 chargino, 12, 14, 116  
   SUSY background, 123  
 chiral symmetry, 20  
 clean environment, 109  
 CLIC, 112, 113, 126  
 cold dark matter, 10, 37  
 collider  
   muon, 109, 111, 112, 126  
 Compact Linear Collider, 112  
 CompHEP, 115, 123  
 convention  
   LFV, 88  
 coordinate system, 27, 64  
   polarisation, 64  
 Cosmology, 10  
 coupling, 19  
   flavour violating, 90  
   slepton neutralino, 25  
   trilinear, 13, 17, 22  
 covariant form, 27  
 cross section, 39, 57, 69, 125  
   , 40, 43, 44, 46, 47, 50, 53, 58, 61  
    $\tilde{\mu}$   
   , 98, 100, 106  
    $\tilde{\tau}$   
   , 99, 101, 106  
   background, 115  
   differential, 31, 65  
   enhancement, 91  
   flavour violating, 90, 97

- LFV, 98, 100
- low, 90
- moment, 67
- polarisation optimisation, 41
- production, 91, 118, 120
- selectron production, 38
- SUSY background, 124
- total, 31, 66, 67, 87, 90, 91
- unpolarised, 38
- weighted, 31
- cuts, 120
- D**
- dark matter, 43
- decay
  - branching ratio, 87
    - , 98
  - channel
    - , 98, 100
  - flavour conserving, 19
  - flavour violating, 18, 22, 90
  - lepton, 105, 106
  - leptonic, 121
  - leptonic vertex, 116
  - mode, 100
  - radiative, 91
  - rare, 87, 91
  - slepton, 91
  - stau to gravitino, 90
  - three-body, 38, 52, 55, 60, 100, 125
  - two-body, 55, 56
  - vertex
    - displaced, 56
    - none, 56
  - W-boson, 91, 116, 118
- degree of polarisation, 66
- detector, 91
  - signal, 100, 101, 105, 116
  - signature, 100, 101, 105, 116
- detector signature
  - flavour violation, 55
  - long living stau, 55
- diagonalisation, 19, 20
  - $CP$ -conservation, 19
  - $CP$  violation, 19
  - neutralino mass matrix, 15
  - slepton mass matrix, 19
- differential cross section, 65
- dipole moment
  - electric, 18
  - magnetic, 18
- direct mixing, 20, 92, 106
  - vanishing, 20
- discovery potential, 115
- displaced vertex, 56, 90, 91, 105
- E**
- EDM, 23
- effect
  - flavour violating, 16, 18
- eigenstate
  - interaction, 14, 16
  - mass, 14, 16
  - neutralino, 71
  - slepton, 16
- eigenvalue equation, 20
- eigenvector, 21
- electric dipole moment, 23
- electron
  - mass, 17
  - transverse polarised, 30
- electron-neutrino, 120, 121
- electroweak
  - precision data, 10
  - symmetry breaking, 9, 109
- energy
  - upgrade, 58
- energy dependence
  - background, 121
- environment
  - clean, 109

equal mixing, 92  
 exchange term, 28, 29  
   beyond SM, 30  
   longitudinal, 29  
   longitudinal-transverse, 30  
   transverse-transverse, 31  
   unpolarised, 29  
 experiment  
   high energy, 87  
   low energy, 87  
   neutrino, 87  
 experimental bound, 21, 87  
 experimental bounds, 8  
   LFV, 88  
 external frame of reference, 27  
 extra dimension, 13  
**F**  
 family structure, 9  
 fermion field, 11  
   chiral, 11  
 Feynman graphs, 25  
 fine-tuning, 9, 10  
 First Muon Collider, 109  
 flavour conservation  
   background, 116  
 flavour conserving  
   background, 89  
   decay, 19  
   process, 89  
 flavour mixing parameters, 20  
 flavour violating  
   coupling, 90  
   cross section, 90, 97  
   decay, 18, 22, 90  
   effect, 16, 18  
   interaction, 90  
   order, 101  
   phase, 87  
   production, 22, 89  
   vertex, 89, 97

flavour violation, 16–18, 31  
   background, 118  
   detector signature, 55  
   slepton production, 19  
 FMC, 109, 112  
 free parameters, 14  
 front end physics, 111  
 fundamental theory, 9

## G

gauge  
   boson, 12, 14  
   coupling unification, 9, 10  
   field, 11  
   interaction, 12  
   invariance, 87  
   structure, 11  
 gaugino, 12  
   -like, 14, 39  
   component, 14  
   interaction, 12  
   mass parameter, 13, 14, 22, 38, 46  
   mass unification, 14  
   sector  
     , 49  
 gluino, 12  
 gluon, 12  
 GMSB, 12, 37, 38, 60  
   scenario, 60  
 Grand Unified Theory, *see* GUT, 9  
 gravitino, 10, 37, 38, 55, 90, 91, 100, 105  
   LSP, 60, 90, 100, 116  
 gravity, 10, 37  
 Great Unified Theory, 37  
 GUT, 18, 39, 46, 49, 52, 56, 57, 60, 69, 70, 78  
   relation, 46, 49, 52  
   scale, 39  
   scenario, 38

**H**

heavy fermion, 92  
 helicity projection operator, 26  
 hidden sector, 12  
 hierarchy, 21  
   mass, 21  
   problem, 9, 10  
 Higgs  
   boson, 9, 10, 12, 38  
   field, 7  
   mass, 9, 10, 38  
   mechanism, 7, 9, 109  
   sector, 12  
 higgsino, 12, 14  
   -like, 14  
   component, 43, 46, 49  
   mass parameter, 13, 14, 22, 38,  
     43, 46  
   mass term, 13  
 higgsino-like scenario, 52  
 high scale, 13  
   parameters, 37  
     , 39, 56, 60

**I**

ILC, 7, 8, 18, 23, 44, 58, 67, 76, 84,  
   87, 109, 115, 120, 126, 128  
 individual lepton number, 87  
 integrated luminosity, 68  
 interaction  
   flavour violating, 90  
 interaction point, 40  
 interference term, 28, 64  
   beyond SM, 33  
   longitudinal, 32  
   longitudinal-transverse, 33  
   pre factor, 32  
   transverse-transverse, 34  
   unpolarised, 32  
 International Linear Collider, *see* ILC,  
   7

ionized track, 91

Isajet, 106

**K**

kinematics, 121

**L**

laboratory system, 64  
 Lagrangian, 17, 19, 25, 87  
   interaction, 25  
   lepton-slepton-neutralino interac-  
     tion, 17  
   MSSM, 13  
 language  
   simplification, 95  
 Large Hadron Collider, *see* LHC, 7  
 left-right mixing, *see* LR mixing  
 LEP, 10  
 lepton, 12  
   charged sector, 87  
   flavour, 18, 121  
   flavour violation, 18  
   mass, 13, 16, 17  
   number  
     individual, 87  
     total, 87  
 Lepton Flavour Violation, *see* LFV,  
   7  
 lepton-slepton-neutralino interaction,  
   15, 17  
 lepton-slepton-neutralino interaction  
   Lagrangian, 17  
 leptonic decay, 121  
 leptonic decay vertex, 116  
 LFV, 7, 8, 16–20, 22, 38, 39, 55, 87,  
   88, 90–93, 95, 111, 113, 124–  
   126  
   convention, 88  
   cross section, 98  
     , 98  
   direct search, 91



- experimental bound, 88
- left slepton sector, 88, 91
- neutrino sector, 88
- observable, 91
- off-diagonal element, 88
- parametrisation, 88
- right slepton sector, 91
- slepton mass matrix, 88
- LHC, 7, 18, 37, 57, 84, 115
- lifetime, 100, 105
- lighter chargino, 123
- lightest supersymmetric particle, *see* LSP
- LL-production, 66
- long living particle, 100
- long living stau, 55
  - detector signature, 55
- loop effects, 13
- Lorentz-invariance, 87
- low energy experiment, 87
- low scale parameters, 37
  - , 56, 60
- LR mixing, 16, 17, 19–22, 27, 31–33, 35, 44, 57, 61, 63, 64, 92, 93, 95, 110, 125
- LR mixing angle, 29–35
- LSP, 10, 37, 38, 46, 49, 52, 55, 66, 69, 70, 84, 88–91, 100, 105, 116, 126
  - gravitino, 55, 60, 90, 100, 116
  - neutralino, 89
- luminosity, 40, 65, 68, 76, 81, 85–87, 126
  - design, 109
  - integrated, 68
- M**
- Majorana
  - fermion, 8, 26, 92
  - spinor, 15
- mass
  - degeneracy, 12
    - , 44
  - degeneration, 21, 22
  - difference, 21, 101
  - eigenstate, 14, 16
  - electron, 17
  - hierarchy, 21
  - Higgs, 9, 10, 38
  - inversion, 38, 49
  - muon, 17
  - neutrino, 10, 17
  - parameter
    - gaugino, 14, 22, 38, 46
    - higgsino, 13, 14, 22, 38, 43, 46
  - slepton, 13
  - spectrum
    - , 39, 43, 46
  - splitting, 10, 21, 49, 52, 84, 100, 101, 105, 106, 126
    - , 101, 105
  - unification, 14, 18, 21, 56
- mass matrix
  - neutralino, 15, 125
  - slepton, 13, 16, 18–20, 26, 125
    - $CP$  violation, 22
    - general, 16
    - LFV, 18
- mean decay length, 56
- measurement
  - background free, 8, 56, 90, 95, 101, 105, 106, 126
- messengers, 12
- minimal Supergravity, 37
- Minimal Supersymmetric Standard Model, *see* MSSM, 10
- missing-energy, 37, 89, 105, 116, 120
- mixed scenario, 43
  - , 60
- mixing
  - neutralino, 23, 69, 72, 125
  - selectron-smuon, 92, 105

- selectron-stau, 105
- smuon-stau, 105
- three generation, 8
- mixing angle, 17
  - slepton, 29, 31–35
- momentum transfer, 26, 64
- momentum vector, 66
- MSSM, 10–12, 125
  - Lagrangian, 13
  - particle spectrum, 12
- mSUGRA, 12, 17, 22, 37–39, 56, 93
  - , 56
- muon
  - antineutrino, 116, 121
  - collider, 109, 111, 112, 126
  - mass, 17

## N

- narrow width approximation, 89
- neutralino, 8, 10, 12, 14, 25
  - decay to sleptons, 63
  - eigenstate, 71
  - exchange, 25
  - index, 26, 29
  - lightest, 14, 37
  - LSP, 89
  - mass matrix, 15, 46, 125
    - diagonalisation, 15
  - mass order, 26
  - mixing, 11, 23, 69, 72, 125
    - $CP$  violation, 63
    - $CP$ -even observable, 66
  - propagator, 27, 66
  - sector, 23, 38, 63, 68
    - , 44, 46, 47, 49, 52, 56
  - spectrum
    - , 57, 60
  - system, 63
- neutralino mixing, 8
- neutrino, 12, 116
  - electron, 116, 121

- experiment, 87
- mass, 10, 17
- oscillation, 7, 10, 17
- sector, 18, 88
- neutrino sector
  - LFV, 88
- new physics, 10, 17, 115
- Next Muon Collider, 109
- Next-to-lightest SUSY particle, *see* NLSP
- NLSP, 18, 52, 55, 60, 84, 89–91, 100, 105
- NMC, 109, 112
- non-GUT-model, 39
- non-GUT-scenario, 38
- non-mSUGRA, 38
- numerical studies, 8

## O

- O’Mega, 115, 120
- observable, 66
  - $CP$ -even, 8
  - $CP$ -sensitive, 8, 23, 27, 29, 30, 32, 35, 47, 63–68, 125
  - LFV, 91
- off-diagonal element
  - LFV, 88
- off-shell neutralino, 84
- optimised projection function, 67

## P

- pair production, 61, 72
  - $CP$  violation, 63
  - , 72, 75, 78, 81, 84
- parameter space, 37, 39, 95
  - SUSY, 39
- parameters
  - SUSY, 37
  - high scale, 37
  - low scale, 37
  - , 39
- parametrisation

LFV, 88  
 particle spectrum, 11  
 Pauli matrices, 26  
 phase  
    $CP$  violating, 13, 15, 19  
   flavour violating, 87  
   supersymmetric, 23  
 photino, 12, 15, 49  
 photon, 12, 13, 118  
   background, 118  
 polar angle, 65  
 polarisation, 87, 120  
    $CP$  violation, 63  
   asymmetry, 91  
   azimuthal angle, 64  
   combination, 28  
   configuration, 120  
   coordinate system, 64  
   degree, 66  
   dependence, 29  
     background, 118, 121  
     process, 26  
     SUSY background, 124  
   electron, 65  
   formalism, 26  
   four-vector, 64  
   longitudinal, 64, 91, 92  
     , 40  
   modes, 25, 26  
   muon, 113  
   positron, 65  
   transverse, 7, 8, 20, 27, 30, 31, 33,  
     34, 63–66, 92, 125  
    $CP$  violation, 23  
   vector, 64  
 polarised cross section, 26  
 pre factor, 29, 32  
 precision measurements, 115  
 process  
   beyond SM, 27  
 product of couplings, 69

production, 64  
   cross section, 91, 118, 120  
   flavour violating, 22, 89  
   plane, 27, 66  
     ambiguity, 66  
     reconstruction, 66  
   process, 8  
   single- $\tilde{\chi}$ , 91, 124  
   single-W, 89, 91, 123, 124  
   slepton, 25, 27  
 production process, 18, 66  
   differential cross section, 65  
 projection function, 65, 67, 68  
   optimal, 67  
   optimisation, 67  
   optimised, 67  
 projector, 118  
 propagator, 26  
 proton-driver, 111

## Q

quantum field theory, 7  
 quark, 12

## R

R-Parity, 10  
 radiative decay, 91  
 rare decay, 18, 87, 91, 111  
 reconstruction  
   production  
   plane, 66  
 renormalisation group equations, *see*  
   RGE, 37  
 replacement  
    $t \rightarrow u$ -channel, 29  
 RGE, 37, 39  
 right sector, 20  
 rotation matrix, 19

## S

scenario

- $\varepsilon$ , 38, 55–61, 90, 95, 100, 103–106, 108, 123
- A, 38, 46–48, 69, 70, 78–81
- B, 38, 49–51, 81–83
- C, 38, 52–54, 71, 84–86
- characterisation, 37
- GMSB, 60
- higgsino, 46
- higgsino-like, 52
- mixed, 43
- Mixed SPS, 38, 43–45, 75–79
- neutralino mixing, 37
- non-GUT, 52
- SPS7, 38, 60–62, 90, 95, 105, 108, 123, 124
- SPS 1a, 39
- SPS 1a', 8, 38–44, 46, 47, 71–75, 92–95, 98–101, 109, 110, 122, 124, 126, 128
- seesaw mechanism, 18
- selectron
  - left, 26
  - mixing angle, 65
  - pair production, 66
    - $CP$ -even observable, 66
    - cross section, 66
  - production
    - cross section, 38
  - right, 26
- sfermion, 11, 16
- signal
  - detector, 100, 101, 105, 116
  - enhancement, 87
- signal to background ratio, 41
- signature, 91
  - detector, 100, 101, 105, 116
- single- $\tilde{\chi}$ 
  - production, 91, 124
- single-W
  - background, 124
  - production, 89, 91, 123, 124
- slepton, 12, 13, 22
  - composition, 16, 92
  - decay, 91
  - decay mode, 55
  - eigenstates, 16
  - mass, 13
  - mass matrix, 13, 16, 18–20, 26, 88, 125
    - $CP$  violation, 22
    - diagonal term, 97
    - diagonalisation, 19
    - LFV, 88
  - mass order, 26
  - mixing, 7, 16, 95
    - , 40
  - mixing angle, 29, 31–35
  - nomenclature, 95
  - numbering, 26, 40
  - production, 25, 27
  - sector, 13, 16, 18, 31, 37, 91, 125
    - $CP$  violation, 8
      - , 44, 50, 57, 60, 61
      - left, 88, 91
    - Yukawa coupling, 13
- slepton mixing, 20, 125
  - , 95, 100, 105
    - analytical approximation, 92, 93
    - general features, 92
- SM, 7–13, 16–19, 23, 27, 29, 39, 91, 92, 116–124, 126
- SM processes
  - background, 116
- small  $\mu$ , 43
- sneutrino, 12
- Software
  - CompHEP, 115, 123
  - Isajet, 106
  - O'Mega, 115, 120
  - SPheno, 39, 56, 60, 106
  - SusyGen, 106
  - Whizard, 115, 120, 122

- SPA convention, 39  
 sparticle spectrum, 126  
 SPheno, 39, 56, 60, 106  
 spin  
   coordinate system, 66  
   correlation, 23, 66, 89  
   density matrix, 26, 30  
   electron, 23  
   formalism, 23  
   superpartner, 12  
 split supersymmetry, 109  
 squared amplitude, 26–28, 64, 91  
 squark, 12  
 standard deviation, 68  
 Standard Model, *see* SM, 7  
 statistical error, 68  
 stau  
   component, 93, 95, 97, 125  
   decay  
     to gravitino, 90  
   decay length, 56  
   decay measurement, 56  
   decay to gravitino, 91  
   decay width, 56  
   decay within detector, 56  
   lifetime, 56, 91  
   long lifetime, 90  
   long living, 89, 91  
   NLSP, 89  
   sector, 16, 17, 99  
   signature, 91  
 string theory, 10, 13  
 SUGRA, 10  
 superfield, 11  
   chiral, 11  
   vector, 11  
 Supergravity, *see* SUGRA  
 supergravity  
   minimal, 12, 17, 22, 37–39, 56, 93  
 supergravity models, 12  
 superpartner, 11  
 supersymmetric  $CP$ -problem, 23  
 supersymmetric framework, 9  
 Supersymmetry, *see* SUSY, 7  
 supersymmetry  
   breaking, 12, 14  
     anomaly mediated, 13, 37  
     gauge mediated, 12, 37, 38, 60  
     gravity mediated, 12, 17, 22, 37–39, 56, 93  
   global, 12  
   local, 12  
 SUSY, 7, 8, 10–15, 18, 23, 37, 39, 60, 66, 122–124, 126  
   background, 122  
      $\tilde{\chi}$ , 123  
     chargino, 123  
     cross section, 124  
     dominant contribution, 123  
     negligible contribution, 123  
     polarisation dependence, 124  
     threshold, 124  
   background processes, 122  
   breaking  
     gauge mediated, 60  
     particle mixing, 16  
 SUSYGen, 106  
 symmetry, 65  
 systematic error, 40
- ## T
- tau  
   antineutrino, 116, 121  
 term  
   exchange, 28  
   interference, 28  
 TESLA, *see* ILC  
 three generation mixing, 8, 18, 20, 87, 90, 92, 98, 111  
 three-body decay, 38, 52, 55, 60, 100, 125  
 threshold

SUSY background, 124  
top quark, 10  
total cross section, 66, 67, 87, 90, 91  
tree level, 39  
trilinear coupling, 13, 17, 22, 61  
triple product, 23, 30, 63, 65, 66  
    correlation, 63  
two generation mixing, 90  
two-body decay, 55, 56

## U

unification, 39  
    gauge coupling, 9, 10, 14  
    mass, 14, 56  
    scale, 10, 37

## V

vacuum expectation values, 14  
vector superfield, 11  
vertex, 121  
     $CP$  violating, 84  
    decay, 56  
    displaced, 90, 91, 105  
    flavour violating, 18, 56, 89, 97  
    leptonic decay, 116  
    W-boson, 116  
    W-boson decay, 118

## W

W-boson, 12, 14, 41, 91, 116, 118  
    background, 118  
    decay, 91  
    decay vertex, 118  
    pair production, 41  
    single production, 41  
Weyl spinor, 15  
Whizard, 115, 120, 122  
Wilkinson Microwave Anisotropy Probe,  
    *see* WMAP  
wino, 12, 14, 49, 57  
wino like  $\tilde{\chi}_3^0$ , 52  
WMAP, 43

## Y

Yukawa coupling  
    Slepton, 13

## Z

Z-boson, 12, 118  
    background, 118  
zino, 12, 15

# Publikationen

## Vorträge

- **Slepton pair production in  $e^-e^-$  Collisions**,  
Universität Wien, Wien 2004
- **Selektronpaarproduktion an einem  $e^-e^-$  Linearbeschleuniger**,  
DPG Frühjahrstagung, Aachen 2003
- **Slepton pair production at an  $e^-e^-$  Linear Collider**,  
ECFA DESY Linear Collider Workshop, Prag 2002
- **Neutralinoproduktion an einem Muoncollider**,  
DPG Frühjahrstagung, Leipzig 2002

## Veröffentlichungen

- A. Bartl, H. Fraas, K. Hohenwarter-Sodek, T. Kernreiter, G. Moortgat-Pick, A. Wagner:  
**Selectron production at an  $e^-e^-$  linear collider with transversely polarized beams.**  
*Physics Letters B*, 644:165–171, 2007.  
<http://nbn-resolving.de/10.1016/j.physletb.2006.11.038> [*hep-ph/0610431*]
- POWER Working Group Report:  
**The role of polarized positrons and electrons in revealing fundamental interactions at the Linear Collider.**  
[*hep-ph/0507011*]
- H. Fraas, F. Franke, G. Moortgat-Pick, F. v. d. Pahlen, A. Wagner:  
**Precision Measurement of Higgs-Chargino Couplings in chargino pair production at a muon collider**  
*European Physical Journal C*, 2003, 29, 587
- A. Wagner:  
**Neutralinoproduktion an einem Muon-Collider.** Diplomarbeit,  
Universität Würzburg, 2002.







